

Durham E-Theses

*The application of sedimentological analysis and
luminescence dating to waterlain deposits from
archaeological sites*

Parish, Romola

How to cite:

Parish, Romola (1992) *The application of sedimentological analysis and luminescence dating to waterlain deposits from archaeological sites*, Durham theses, Durham University. Available at Durham E-Theses Online: <http://etheses.dur.ac.uk/5866/>

Use policy

The full-text may be used and/or reproduced, and given to third parties in any format or medium, without prior permission or charge, for personal research or study, educational, or not-for-profit purposes provided that:

- a full bibliographic reference is made to the original source
- a [link](#) is made to the metadata record in Durham E-Theses
- the full-text is not changed in any way

The full-text must not be sold in any format or medium without the formal permission of the copyright holders.

Please consult the [full Durham E-Theses policy](#) for further details.

**THE APPLICATION OF
SEDIMENTOLOGICAL ANALYSIS
AND LUMINESCENCE DATING
TO WATERLAIN DEPOSITS FROM
ARCHAEOLOGICAL SITES**

Romola Parish

The copyright of this thesis rests with the author.
No quotation from it should be published without
his prior written consent and information derived
from it should be acknowledged.

**Thesis submitted for the degree of
Ph.D. at the University of Durham,
September, 1992.**



25 MAR 1993

THE APPLICATION OF SEDIMENTOLOGICAL ANALYSIS AND LUMINESCENCE DATING TO WATERLAIN DEPOSITS FROM ARCHAEOLOGICAL SITES

Romola Parish

The thesis follows an interdisciplinary approach combining sediment analysis and luminescence dating of sediments from selected archaeological sites. The work aims to assess the role of sediment analysis for luminescence dating, and the potential of TL and IRSL for dating waterlain material of Holocene age.

A comparative chronology based on radiocarbon, stratigraphic and archaeological grounds is important. However, the viability of comparing different dating techniques is considered in the light of the dating results.

The novel IRSL and established TL techniques were shown to be successful for dating waterlain sediments, provided that a suitable light source is used for laboratory bleaching. Age comparisons between the luminescence techniques was excellent. Disparities between luminescence and C-14 ages is largely explained on a sedimentological basis.

The role of sediment analysis is shown to be of great importance for luminescence dating. Certain sedimentological and luminescence characteristics are shown to be closely linked. The relationship between undated sediments affected by instability or low intensity of signals, and weathering in the strata from which the samples were taken is tested by experiment. This demonstrates that weathering of feldspars in the stratum severely affects the luminescence signals and therefore the potential for dating these samples. This represents a step towards the recognition of problematic samples in the field.

In conclusion, it is shown that luminescence is suitable as an absolute dating technique for a wide variety of inorganic sedimentary material between 0-200 000 years old. This exceeds the C-14 technique both in range of material and in age limits. The main source of error is associated with variations in water content, which with the recognition of the significance of weathering, demonstrates the importance of sediment analysis in support of luminescence dating studies.

TABLE OF CONTENTS

List of Figures

List of Tables

Acknowledgements

Declaration

CHAPTER 1 INTRODUCTION	Page 1
1.1 Sediment Dating	1
1.2 Luminescence Dating	2
1.3 Sedimentary Processes and Luminescence Dating	4
1.4 Chronological Control	6
1.5 Aims and Outline of the thesis	8
1.6 Site Selection Criteria	9
CHAPTER 2 THE SITES	11
2.1 East Anglian Fenland	11
2.1.1 Quaternary History	11
2.1.2 Archaeology	13
2.1.3 Flag Fen	15
2.1.4 Chronological Control	16
2.1.5 Summary	17
2.2 Eskmeals, Cumbria	17
2.2.1 Quaternary History	18
2.2.2 Archaeology	19
2.2.3 Williamson's Moss	20
2.2.3.1 Archaeology	21
2.2.3.2 Chronological Control	22
2.2.3.3 Summary	23
2.2.4 Stubb Place	24
2.2.4.1 Chronological Control	24
2.2.4.2 Summary	25
2.3 Hartlepool Bay, Cleveland	25
2.3.1 Quaternary History	26
2.3.2 Archaeology	27
2.3.3 Chronological Control	28
2.3.4 Summary	28
2.4 The River dune area of the Western Netherlands	29
2.4.1 Quaternary History	29

2.4.2 Perimarine area and the Donken	31
2.4.3 Archaeology	32
2.4.4 Hazendonk and Slingeland	34
2.4.5 Chronological Control	35
2.4.6 Hazendonk and Slingeland; summary	35
2.5 Summary	36

CHAPTER 3 THE FORMATION OF SEDIMENTARY DEPOSITS, AND IMPLICATIONS FOR THE APPLICATION OF LUMINESCENCE DATING

3.1 Formation of Sedimentary deposits	38
3.1.1 Transport and Deposition	39
3.1.1.1 Fluvial Environments	41
3.1.1.2 Intertidal Environments	42
3.1.1.3 Lagoonal and Lacustrine Environments	43
3.1.1.4 Estuarine and Marine Environments	44
3.1.2 Post-Depositional Change	45
3.1.2.1 Compaction and Diagenesis	45
3.1.2.2 Water Content	47
3.1.2.3 Pedogenesis	47
3.1.2.4 Weathering	47
3.1.3 Summary	51
3.2 Techniques of Sedimentary Analysis	52
3.2.1 Sampling	52
3.2.2 Dosimetry	53
3.2.3 Water Content	53
3.2.4 Particle Size Analysis	54
3.2.5 Mineralogy	56
3.2.6 Elemental Composition	57
3.2.7 Weathering Indices	58
3.2.8 Physical Appearance of the Grains	59
3.2.9 Feldspar Identification	59
3.2.10 Organic Carbon Content	60
3.2.11 Summary	60

CHAPTER 4 RESULTS OF SEDIMENTOLOGICAL ANALYSES

4.1 Preliminary Considerations	62
4.2 Sedimentological Analysis by Site	62
4.2.1 Flag Fen	62

4.2.1.1	Stratigraphy	62
4.2.1.2	Sample Descriptions	63
4.2.1.3	Summary	66
4.2.2	Williamsons Moss	67
4.2.2.1	Stratigraphy	67
4.2.2.2	Sample Descriptions	68
4.2.2.3	Summary	71
4.2.3	Stubb Place	72
4.2.3.1	Stratigraphy	72
4.2.3.2	Sample Descriptions	73
4.2.3.3	Summary	76
4.2.4	Hartlepool Bay	77
4.2.4.1	Stratigraphy	77
4.2.4.2	Sample Descriptions	78
4.2.5	Hazendonk	79
4.2.5.1	Stratigraphy	79
4.2.5.2	Sample Descriptions	81
4.2.6	Slingeland	82
4.2.6.1	Stratigraphy	82
4.2.6.2	Sample Descriptions	83
4.3	Discussion	85
CHAPTER 5 LUMINESCENCE TECHNIQUES		89
5.1	Introduction	89
5.2	Luminescence Techniques	90
5.2.1	TL Measurements	90
5.2.2	IRSL Measurements	92
5.2.3	Relationship between TL and IRSL	96
5.2.4	Other OSL Techniques	98
5.2.5	ED Evaluation and the Age Equation	98
5.2.6	Irradiation	100
5.2.7	Dosimetry	101
5.2.7.1	Alpha Radiation	101
5.2.7.2	Beta Radiation	102
5.2.7.3	Gamma Radiation	103
5.2.7.4	Cosmic Radiation	104
5.2.7.5	Calcium Fluoride Dosimetry	104
5.3	Additional Aspects relevant to Dating	105

5.3.1	Sample Preparation	105
5.3.2	Normalization	106
5.3.3	Stability of the Luminescence Signal	108
5.3.4	Anomalous fading in Feldspars	110
5.3.4.1	Mechanisms of fading	112
5.3.4.2	Tests for fading	113
5.3.5	Preheating	113
5.4	Contributions of this Study	115
5.4.1	Bleaching studies	115
5.4.1.1	Laboratory Bleaching	118
5.4.2	Sensitivity changes in the luminescence signal	120
5.4.3	Water Content	122
5.5	Summary of the dating procedure	124
CHAPTER 6 LUMINESCENCE DATING RESULTS		127
6.1.1	Flag Fen	127
6.1.2	Williamsons Moss	128
6.1.3	Stubb Place	129
6.1.4	Hartlepool Bay	131
6.1.5	Hazendonk	132
6.1.6	Slingeland	132
6.2	Discussion	133
6.2.1	TL versus IRSL versus C-14	133
6.2.2	Accuracy of luminescence dates	137
6.3	Conclusions	138
CHAPTER 7 SIGNIFICANCE OF CHEMICAL WEATHERING OF FELDSPARS AND IRSL		
7.1	Relationships between luminescence and sedimentology	140
7.1.1	Group 1	141
7.1.2	Group 2	141
7.1.3	Group 3	141
7.1.4	Significance of categories	142
7.2	Structure of feldspars	143
7.3	Weathering of feldspars	143
7.4	Weathering Experiment	145
7.4.1	Results	146
7.4.2	Conclusions	147

7.4.3 Implications for dating	147
CHAPTER 8 SUMMARY AND CONCLUSIONS	149
8.1 Summary of work undertaken	149
8.2 Justification of luminescence methodology	152
8.3 Role of Sedimentological analysis in luminescence dating	152
8.4 The future of luminescence dating	157
BIBLIOGRAPHY	
APPENDIX A Radiocarbon data	
APPENDIX B B.1 Key to stratigraphic diagrams	
B.2 Key to sedimentological analysis diagrams	
APPENDIX C C.1 Dosimetry data for all samples	
C.2 Measurement data for all samples	

LIST OF FIGURES

	following page....
2.1 Map of East Anglian Sites	11
2.2 Map of Cumbrian sites	17
2.3 Stubb Place stratigraphic correlation	24
2.4 Map of Hartlepool Bay	25
2.5 Hartlepool Bay stratigraphic correlation	27
2.6 Map of Dutch sites	29
2.7 Hazendonk stratigraphic sequence	34
2.8 Slingeland stratigraphic sequence	35
4.2.1 Flag Fen stratigraphy	62
4.2.2 SEM photographs; FF1	63
4.2.3 SEM photographs; FF3	65
4.2.4 Williamsons Moss stratigraphy	67
4.2.5 SEM of WM1	68
4.2.6 SEM of WM1	68
4.2.7 SEM of WM1	68
4.2.8 SEM of WM 3	69
4.2.9 SEM of WM 3	69
4.2.10 SEM of WM 3	70
4.2.11 SEM of WM 3	70
4.2.12 SEM of WM5	71
4.2.13 Stubb Place stratigraphy	72
4.2.14 SEM of SP3	73
4.2.15 SEM of SP3	73
4.2.16 SEM of SP5	74
4.2.17 SEM of SP5	74
4.2.18 Hartlepool Bay stratigraphy	77
4.2.19 SEM of WH1	78
4.2.20 SEM of WH1	78
4.2.21 Hazendonk stratigraphy	79
4.2.22 SEM of HAZ1	81
4.2.23 SEM of HAZ1	81
4.2.24 SEM of HAZ1	81
4.2.25 Slingeland stratigraphy	82

5.1	Flow chart of dating methodology	89
5.2.1	Diagram of the luminescence process	89
5.2.2	TL Filter transmission	91
5.2.3	ED evaluation methods	98
5.3.1	Initial IRSL signals for different preheat times at 160°C	113
5.4.1	Transmission of light through water and BG-39 filters	117
5.4.2	TL and IRSL bleaching under sunlight and filtered white light	119
5.4.3	Bleaching-induced TL sensitivity changes	120
5.4.4	IRSL decay curve changes in form with bleaching	120
5.4.5	Water content; saturated value versus fractional uptake	123
5.5.1	TL plateaux	124
5.5.2	TL growth curves	124
5.5.3	IRSL decay curves	124
6.1.1	Stratigraphy and dates; Flag Fen	127
6.1.2	Stratigraphy and dates; Williamsons Moss	128
6.1.3	Stratigraphy and dates; Stubb Place	129
6.1.4	Stratigraphy and dates; Hartlepool Bay	131
6.1.5	Stratigraphy and dates; Hazendonk	132
6.1.6	Stratigraphy and dates; Slingeland	132
6.2.1	TL versus IRSL dates	133
6.2.2	TL versus C-14 dates	133
6.2.3	IRSL versus C-14 dates	133
6.2.4	Error versus water content	137
7.1.1	SEM of Group1 sample	141
7.1.2	SEM of Group 3 sample	142
7.3.1	SEM of heavily weathered feldspar	144
7.3.1	SEM of heavily weathered feldspar	144
7.4.1	XRD before and after weathering	146
7.4.2	SEM before weathering	146
7.4.3	SEM after weathering	146
7.4.4	Initial IRSL signal intensities and weathering	146
7.4.5	Changes in TL peak shape after weathering	146
7.4.6	Fading loss induced by weathering	147

LIST OF TABLES

	page...
2.1 Transgression sequence of the Western Netherlands and associated archaeology	30
2.2 Chronology of clay deposition in the Molenaarsgraaf area	34
3.1 Comparison of the effectiveness of bleaching of different sedimentary environments	40
4.1 XRF results	62
5.2.1 Comparison of initial IRSL intensity stimulated by different IRSL wavelengths	94
5.2.2 Effect of voltage on initial intensity and signal:noise ratio of the IRSL of FF3	96
5.2.3 Beta radiation sources and dose-rates	100
5.3.1 IRSL normalization as % of total natural emission	107
5.3.2 Trap depths and lifetimes for TL of K-feldspars at 15°C	109
5.3.3 Loss by fading observed in three samples; FF1, FF2, HAZ1	110
5.3.4 Comparison of initial IRSL signal from preheated and stored samples	115
5.4.1 Bleaching residuals after exposure to sunlight and filtered white light	118
5.5.1 Summary of dating procedures used	124
6.1 Comparison of luminescence and independent age ranges for all samples	127

This research was sponsored by a SERC research studentship between October 1988 to September 1991, and was completed during the tenure of a temporary lectureship at Sussex. I wish to thank my three supervisors, Anthony Harding, Ian Bailiff and Michael Tooley, for their patience and encouragement and for their diversity of ideas.

I also wish to thank, for their technical assistance and encouragement; Christine Doel, Ken Durose, Ron Hardy, Jim Innes, Martin Jones, Mark Kirkland, Paul Larson, Anthony Long, Helen Rendell, Sue Rowland, Sue Stallibrass and Maurice Tucker. There are numerous others, at Durham, Sussex and elsewhere who unknowingly inspired the work during its darker days.

I also wish to thank my father and Martin Millett, who have had much to put up with over the last four years.

I hereby declare that no part of this work has been submitted for any degree at this or any other University.

CHAPTER 1 INTRODUCTION

This thesis comprises an interdisciplinary study of the relationships between sedimentological analysis and luminescence dating of selected waterlain sediments taken from archaeological contexts. The project aims to test the viability of luminescence dating of waterlain sediments of Holocene age, and explore the ways in which sedimentary analysis of the strata being dated can aid the selection of samples of greatest potential for dating. Sections 1.1 and 1.2 are general introductory summaries outlining the context of the research. Detailed discussions and references are given in later chapters.

1.1 Sediment Dating.

The establishment of absolute chronologies in Quaternary studies and archaeology is vital for the accurate interpretation and correlation of events of environmental change and anthropogenic activity. The advent of radiocarbon dating in 1955 enabled absolute dating (based on a calibrated method) to be applied to organic materials within the archaeological timescale up to c.60 000 years ago. Radiocarbon dating has also facilitated the construction of curves of sea-level rise during the post-glacial period as in the East Anglian Fenland, (Shennan, 1985a,b) and 'tied down' floating chronologies based on archaeological artefact typology. Radiocarbon is still the most common method of dating both in archaeology and in more recent Quaternary studies. However, luminescence dating of sediments has the potential to rival radiocarbon in importance in the future. This is due to two main reasons: luminescence dating techniques can be applied to a wide range of inorganic sedimentary deposits which are unsuitable for radiocarbon dating, and the techniques cover a much greater timespan, up to 200 000 years at present.

In addition to the reasons stated above, luminescence dating can potentially be of greatest value to archaeology during the ~~last millennium~~ ^{last 10 000 years} BC, where the radiocarbon calibration curve is at its flattest. Here, luminescence can replace radiocarbon dating, and provide a more accurate chronology. The accuracy of luminescence dates is generally around 10% of the age, but in certain sediments, as discussed in Chapter 5, accuracies of 20% of the age may still be acceptable. The development of other scientific dating techniques has enabled an increasing range of sediments and contexts to be dated, such as U-Th on calcite over timespans of 50-500 000 years with accuracies of $\pm 10\%$ (Edwards et al, 1987) and K-Ar on volcanic material over timespans of 1000-30 000 years, ± 1000 years (Gillot and Cornette, 1986). To this suite of absolute dating techniques, luminescence can provide a valuable contribution.

Luminescence dating can be applied to most inorganic sediments, provided they have been exposed to heat (eg. tephra) or light (eg. loess) before burial. The techniques most commonly date the quartz and feldspar minerals in deposits, whose luminescence behaviour is relatively well understood. The almost ubiquitous presence of these minerals in sedimentary deposits and on archaeological sites means that most inorganic materials are potentially suitable candidates for dating.

Luminescence dating has approximate age limits of 0 to c. 200 000 years although claims ~~have~~ recently been made for dating back to 1 Ma (Berger, 1992), depending on the radioactivity in the local environment. Luminescence techniques therefore overlap the whole radiocarbon age range, and also overlap the ranges of other absolute techniques applied to the earlier Quaternary, such as Electron Spin Resonance (ESR) which is related to luminescence in that it measures the electric charge that has accumulated in crystals, usually of calcite and tooth enamel; K-Ar and magnetic polarity methods. These techniques are applied to the oldest sites of human evolution in Africa, where the application of luminescence dating would potentially be of great value as an additional absolute dating technique. Of primary concern in this project is the contribution of luminescence to the Holocene (last 10 ka) as an additional technique to radiocarbon and to replace it where appropriate.

All absolute dating techniques have problems in terms of the accuracy of dates and sources of error. In order to assess the value of luminescence in the dating of sediments of Holocene age when other archaeological and radiocarbon techniques are more firmly established, a comparative chronology is needed to determine the accuracy of the newer techniques. This project tests the viability of luminescence against established chronologies for a selection of sites. Below, a brief outline is given of luminescence dating in order to introduce the aspects which are most relevant to this study.

1.2 Luminescence Dating

Luminescence dating techniques were first established for burnt clay materials, particularly pottery. The techniques are based on the measurement of trapped electrons derived from the decay of naturally occurring radioisotopes. Natural sources of radiation include U, Th and K-40 which occur naturally within the soil or sediment environment. These isotopes emit ionizing radiation and electrons as products of decay which are trapped in defects in the crystal structure of the minerals in the sedimentary environment.

The trapped electrons are evicted when the sediment is heated, as in the process of firing pottery or as a result of volcanic activity, or exposed to light, eg. during the transport and deposition of

sediments. The crystals are then said to be 'zeroed' with respect to trapped electric charge, as following evicton, the electrons recombine with 'holes' in the crystal structure (see Chapter 5) giving rise to the emission of light (the luminescence signal).

The rate of accumulation of electrons in the crystals of the minerals is controlled largely by the degree of radioactivity in the soil and the length of time in which the crystal has been exposed to that radiation field. The age of the sediment is estimated from the amount of trapped charge. This is measured by the intensity of the luminescence signal and determined by the Equivalent Dose (ED), which is then divided by the dose-rate (DR); ie. $AGE = ED/DR$. The ED represents the amount of artificial radiation dose given to the sample which gives rise to a signal of the same intensity as that in the natural samples. The dose-rate is the annual radiation dose from the sedimentary environment.

Laboratory measurements of the accumulated radiation dose since zeroing are made by heating the sample (TL or thermoluminescence) or exposing the sample to artificial light sources (OSL, or Optically Stimulated Luminescence). In OSL, the light sources used are generally either a green argon-ion laser (514.5 nm) or infra-red diodes (880Δ80 nm). The latter is known an Infra-red stimulated luminescence (IRSL) and was used in conjunction with TL in this study. Both TL and optical signals are sensitive to optical bleaching and are suitable for sediment dating.

There are, however, problems in the application of luminescence dating to sediments, which affect the accuracy of age determination. Those problems which most concern this project are those related to the bleaching of the luminescence signal by sunlight prior to burial of the sediment; to the past water-content of the sample and to the effects of post-depositional change on the stability and intensity of the luminescence signal over the timespans involved. The first and second problems have been investigated to some extent during the development of luminescence dating of sediments, and are discussed fully in chapters 3 and 5; the final problem has not been subjected to such detailed investigation, and is an important part of this study. These elements are outlined briefly below.

In the dating of sediments by luminescence the bleaching of the signal by sunlight during transport and deposition is fundamental to the technique. For windblown sediments the particles have usually received sufficient light exposure to be well-bleached at deposition, leading to the success of the luminescence dating of loess and dune sands. For waterlain material, however, the sunlight spectrum may be attenuated by water depth, turbulence or suspended sediment load. This may result in some particles not receiving sufficient exposure to light to have bleached the total sunlight sensitive signal. Such sediments are referred to as being 'partially bleached'.

The identification of partially bleached sediments in the laboratory is difficult. The level to which the sample was bleached before deposition cannot be determined from the luminescence signal measured in the laboratory. The determination of the degree of bleaching is important as it may lead to inaccurate ED evaluation. This phenomenon is particularly relevant to waterlain material such as that sampled in this study, and is discussed fully in Chapter 5. The use of appropriate sources of light for laboratory bleaching experiments, which reflects the conditions under which the sample was bleached at deposition is important in the determination of the correct ED. This is also investigated in Chapter 5.

Additional problems in luminescence dating which are investigated here include the effect of water content on the dose-rate to the sample. The presence of water in the pores of soil or sediment has an attenuating effect on the paths of the electrons emitted as a product of radioactive decay, and therefore on the dose-rate to the crystals. The correction for water-content is a major component in the error of the age, and is likely to be a significant problem for sediments which lie at or below the present water-table, and which are likely to have been saturated for much of their burial history. This is typical of the samples investigated here.

Finally, the effects of post-depositional change on the sediment during the period of burial are important. These include compaction, which will reduce the pore-space in which water can be held; soil formation processes and chemical weathering which may have an effect on the stability of the luminescence signal through time. These effects are relatively unknown and are a major part of this study. The relationships between sedimentary processes and the potential and accuracy of TL and IRSL dating therefore require some investigation in order to increase the accuracy of luminescence dates, and the range of materials to which the techniques can be applied.

1.3 Sedimentary Processes and Luminescence Dating.

Very few studies involving integrated sedimentological analysis with luminescence dating have been performed, with a few exceptions, such as that of Pye and Johnson (1988). The sedimentary environment has received some attention with respect to the problems associated with bleaching of waterlain material and of different sediment fractions in different depositional environments (Berger, 1990; Rendell, 1992; Stokes, 1992). However, less attention has been given to pedogenic and weathering processes and their effect on luminescence signals.

The dating of soils has exposed some problems, particularly with respect to bleaching of the crystals (Wintle and Catt, 1985b) and bioturbation was evoked as the mechanism of bleaching. However, problems remain in relation to the dating of soil B horizons, as dates on these deposits may reflect the age of the parent material rather than the phase of soil formation. This is potentially

disappointing as palaeosols are often important stratigraphic markers in the Quaternary and are ubiquitous in most archaeological sites. They can be dated relatively by dating the material above and below. This has been done successfully for loess sequences (eg. Stremme, 1989), but this may not be possible on many archaeological sites. A number of pedogenic horizons are sampled in this project. It is therefore important to identify strata in which pedogenesis has occurred in order to eliminate them, as these layers may be subject to erroneous ED evaluation due to insufficient bleaching.

Detailed sedimentary analysis can also give important indicators of the depositional environment within which particular strata were laid down. The particle size distribution of the sample indicates the conditions of water velocity and depth, which may enable an assessment to be made regarding the potential bleaching efficiency of the environment. These conditions will also depend on the source and distance travelled by the sediment, which may be determined from wider environmental interpretations of available data. These effects are discussed in Chapter 3.

The sites selected were subjected to detailed sedimentary analysis, in order to assess the value of such analysis for luminescence dating applications. An integrated approach to dating the sediments by TL and IRSL, and observations of the sedimentological characteristics of the material allows such an assessment to be made. Three main aspects are of primary importance arising from the detailed sedimentary analyses; first, the value of such detailed study in the selection and identification of the most suitable sediment samples for dating; second, the effects of weathering of feldspars on the luminescence signal, and finally, the effects and identification of compaction of sediments on the past water content of the sample.

The effects of weathering of feldspars, which was the main mineral group dated in this project (see Chapter 5) is considered to be of some importance. Chemical weathering operates by ion exchange and dissolution at specific points in the crystal, which include the defects in which the traps and luminescence centres occur which give rise to the signal. Any disruption of the chemical nature of the crystal can therefore potentially affect the luminescence signal. This has not been investigated before, and serves to test the conclusions drawn from the observed relationships between sedimentological and luminescence characteristics for the samples in this study and is discussed in Chapter 7.

In addition, the effects of compaction and the recognition of compacted deposits with respect to the evaluation of the past water content of the deposits is considered which is a major source of error in the age evaluation. The correction of the dose-rate for water content gives rise to a significant proportion of the total error on the luminescence age, and is likely to be of greater

relevance to 'wet' sediments such as those sampled in this study, than for 'dry' sediments such as loess and dune sands.

1.4 Chronological Control.

In order to assess the accuracy of these relatively new dating techniques, it is necessary to compare the luminescence dates with an established chronology. In most cases, this is based on radiocarbon dates, which immediately arouses questions concerning the viability of the comparison between different dating techniques, which the user needs to be aware of. Additional stratigraphic control is given by archaeological material stratified between sediment samples, and from stratigraphic correlations of deposits which have been dated elsewhere. The archaeological component of the chronological control is therefore an important part of the assessment of the success of the luminescence dating, and also demonstrates the potential value of luminescence techniques for archaeological horizons within the Holocene.

Different absolute dating techniques relate to specific events which are dated. In the case of radiocarbon, the event dated is that of the death of the organism, when C-14 ceases to be in equilibrium with the environment and the C-14 content falls with time as a result of radioactive decay. In the case of luminescence dating of sediments, the event dated for sediments is the last exposure to sunlight before burial. The comparison of C-14 and luminescence ages for a sedimentary deposit may therefore not agree because they relate to different events. For example, organic material associated with prehistoric occupation and dated by radiocarbon may not match a chronology based on the luminescence dating of sediments which are related to the last exposure to sunlight of the samples. These samples may not have been bleached immediately before deposition in their present context. In the case of U-Th dating direct comparisons of U-Th on secondary minerals cannot be made with the TL on the host minerals (Nanson et al, 1991). The last exposure to sunlight of the sediment may not relate to its present depositional environment.

Radiocarbon dating is based on the calibration of measurements of activity against a standard reference or against a dendrochronological curve. The calibration curve is non-linear and in the flat regions of the curve can produce the same calibrated age range for different C-14 ages. This increases the error on the age determination, particularly in specific regions of the calibration curve, such as around 1000 BC. However, C-14 is still the most common dating technique with which luminescence dates are compared and to a large extent, comparisons are good and disparities between dating techniques can often be accounted for on the basis of the events to which each technique is related, cf. Nanson and Young (1987), although careful studies of the agreement between different dating methods are rare.

Standardisation of the radiocarbon ages, in terms of the source of calibration is therefore important to retain the same level of accuracy in the comparison between techniques. In this study, the radiocarbon dates upon which the chronological control for each site is based are generally quoted in the literature as uncalibrated dates in C-14 years BP. In order to overcome the problems associated with the comparisons of absolute luminescence ages with uncalibrated radiocarbon ages, all the radiocarbon dates have been calibrated. This was done using the 'CALIB' programme produced by the University of Washington Quaternary Isotope Laboratory in 1987. This programme is based on a 20 year atmospheric record extending back to 7210 cal BC (c. 8100 C-14 BP). All dates quoted in the text are the calibrated ranges followed by a number in brackets. This number refers to the location of the date in Appendix A where the uncalibrated dates, laboratory numbers and sources are listed.

Both luminescence and radiocarbon techniques are affected by error of measurement and counting statistics, and the age determination of C-14 is further affected by contamination effects and other sample conditions; in the case of luminescence, the age range of a sample is affected by uncertainties associated with the water content correction, signal stability and dose-rate evaluation. The importance in the archaeological element in the project lies in its role as an additional independent source of comparative chronology.

The luminescence dating of different grain-size fractions in the sediment, and dating the fractions by both optical and TL techniques may be used to gain some degree of internal consistency, despite the fact that the TL and OSL techniques are based on different, but related, physical principles. This needs to be justified on sedimentological grounds, as the different size fractions in a waterlain sediment may have been subject to different methods of transport (eg. suspension as opposed to saltation) and so have been exposed to different wavelengths and intensities of sunlight bleaching. This is discussed in Chapter 3.

Finally, it is important to remember the potential of luminescence in dating inorganic sequences which cannot be dated by other relative or absolute methods within the Holocene timespan. Luminescence provides potentially valuable methods of dating which have been proven for aeolian material and which is applicable to a very wide variety of sediment types, and to acceptable degrees of accuracy (c. 10% of the age). In cases where the error on the age determination is greater than 20%, the luminescence age may still be better than no age at all, where there is no other means of dating the sediment.

1.5 Aims of the thesis.

The aim of the thesis is primarily to address some of the problems outlined above, primarily the bleaching of waterlain sediments, and the effects of post-depositional change (in particular, the weathering of feldspars and past water content) on the stability of the luminescence signal over the timespan of interest. The work also tests the viability of the technique as applied to waterlain sediments of Holocene age, following an interdisciplinary approach. The selection of suitable sites is of great importance and is discussed in section 1.6 below. The approach of the project combines the investigation of the sedimentary and luminescence characteristics of selected deposits and dating of the coarse and fine grain fractions by TL and IRSL where appropriate.

The luminescence behaviour of the samples is considered in the light of their sedimentary characteristics and conclusions are drawn relating to the observed relationships. The conclusions regarding the effects of weathering of feldspars are tested in the laboratory. Finally, the role of sedimentary analysis in luminescence dating is assessed, with a view to defining a series of criteria which may be applied to select the sediments which are potentially more suitable for dating.

The accuracy of the dates is compared to established chronologies based on radiocarbon and archaeology, and the viability of the luminescence dates is evaluated with respect to the dating of Holocene waterlain and archaeological sediments.

An outline of the thesis is given below:

Chapter 1; Introduction to the role of luminescence in dating sediments and sedimentary analysis, comparative chronologies, and some of the major problems the thesis seeks to address; site selection criteria.

Chapter 2; The sites selected for study; their Quaternary histories, archaeology and chronological control.

Chapter 3; Processes in the formation of sedimentary deposits, and how these affect the luminescence stability and bleaching of samples; sedimentological techniques adopted in this study.

Chapter 4; Results of sedimentological analysis; SEM studies; characteristics of samples selected for dating.

Chapter 5; Luminescence dating techniques; the luminescence process; investigations into bleaching and water content; methods adopted in the study.

Chapter 6; Results of dating; accuracy of dates; success of TL versus IRSL dating.

Chapter 7; Relationships between luminescence dating and sedimentary analysis; effects of weathering of feldspars on the luminescence signal, and its implications for dating.

Chapter 8; Summary and Conclusions; evaluation of the exercise; assessment of the role of sedimentary analysis; identification of 'datable' samples'; future research.

1.6 Site Selection Criteria.

The selection of sites was based on a number of essential criteria, outlined below:

1. Chronological Control

The sites were required to have an established chronological control against which to compare the luminescence dates. This was primarily based on radiocarbon, but in most sites, additional control was provided by archaeological horizons correlated with the sequences sampled, as at Williamsons Moss. In the case of Flag Fen, the radiocarbon chronology is based on very large numbers of dates, and is considered to be secure and reliable. In addition to this, sites were sought which had an archaeological dating context, and relevance to sea-level changes during the later Quaternary.

2. Sedimentary Environment

Waterlain sediments were selected for a number of reasons. Until recently, problems associated with incomplete bleaching of waterlain material rendered them less attractive for TL dating. However, with the advent of the recently developed optical dating techniques, waterlain material has been less affected by partial-bleaching problems, and research has extended into this area. Waterlain sediments also proved to be the most abundant in the sedimentary sequence of lowlying areas, and contained additional environmental information relating to depositional environments.

3. Environmental Reconstruction

The availability of material relating to the changing environment in the Quaternary was deemed to be of value in order to add weight to the interpretations regarding depositional environments of the sediments. Regional environmental changes, reflected in changes in vegetation, sea-levels and soil formation and erosion are reflected in the sedimentary sequence. The presence of diatoms, ~~was a~~ useful indicator of conditions of water depth etc. but these were rare in the samples dated and so were not an important consideration of the environmental analysis.

4. Accessibility

Access to the site was needed in order not only to take the samples, but to return to retrieve the dosimetry monitoring equipment left in the ground for one year. This proved to be a significant element in the final selection of sites.

Those sites which were finally selected as meeting all the criteria comprised Flag Fen (East Anglia), Williamsons Moss and Stubb Place (Eskmeals, Cumbria), Hartlepool Bay (Cleveland) and the

Hazendonk and Slingeland in the Netherlands. With the exception of Stubb Place, all these sites have a good chronological control. The inclusion of Stubb Place, which lacks a chronological control, is based on the selection of a test site for the application of luminescence to deposits of relatively 'unknown' age. This site, therefore, tests the viability of 'blind' applications and the internal consistency of luminescence techniques.

CHAPTER 2 THE SITES

The selection of sites for this study was based on the criteria discussed in Chapter 1. The selected sites are all located in areas extensively affected by Holocene sea-level changes. These have controlled both coastal development and opportunities for human occupation and activity. Chronologies for the sites are based on radiocarbon dating and associated archaeological material, either on site or adjacent to the sampling site. Samples were taken where the stratigraphy represented the most complete sequences of both archaeological and geomorphological sediments. The sites are discussed in turn below, outlining an environmental history and chronological control during the period of relevance to this study ie. the last 12, 000 years.

The key to stratigraphic figures is located in Appendix B.

2.1 EAST ANGLIAN FENLAND.

The Fenland of East Anglia lies in the eastern part of Britain, south of the Wash (figure 2.1). The site sampled in this study is located to the east of Peterborough near the fen-edge. The Fens have been extensively affected by sea-level changes during the Holocene, and this has affected the depositional environments and human activity in the area. The Fens have been intensively studied both with respect to the construction of an absolutely dated curve of relative sea-level change based on stratigraphic interpretation and radiocarbon dating, and for the rich archaeological remains buried in the peat.

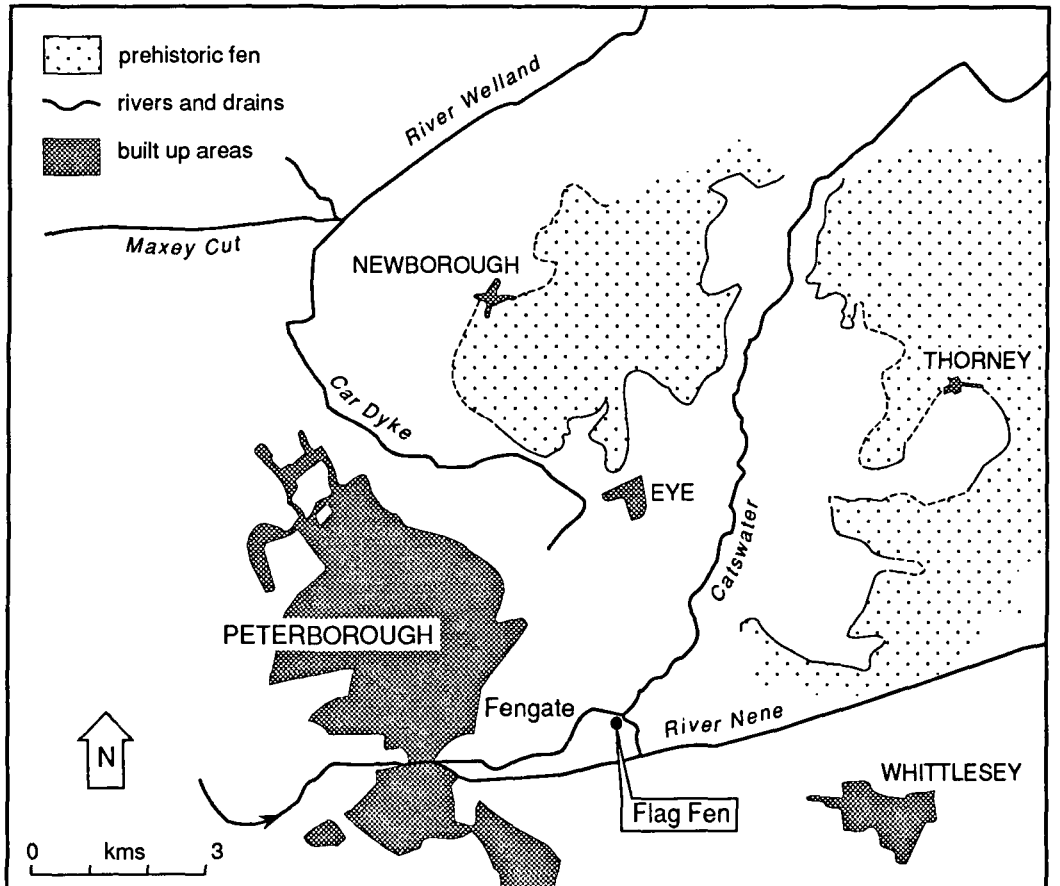
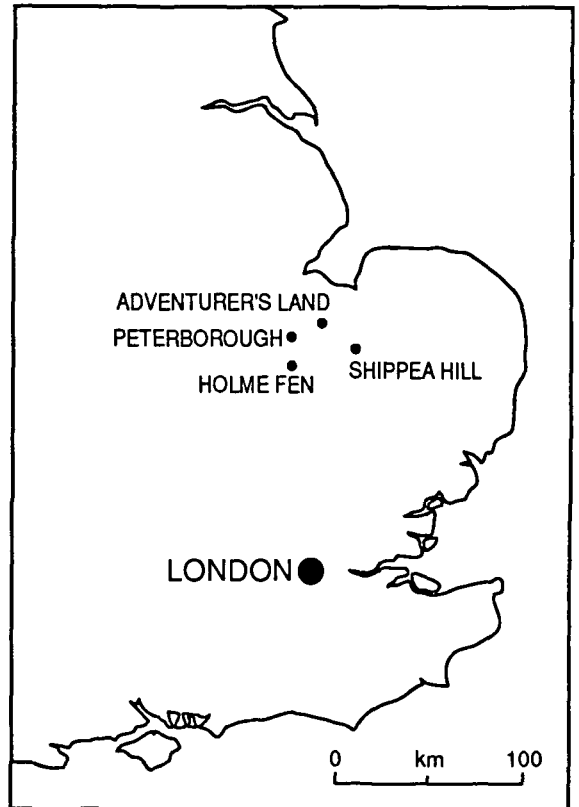
2.1.1 Quaternary History

The main stratigraphic units deposited during the Quaternary in the Fens were described by Skertchly (1877) and Godwin (1978). They comprise Lower Peat, Fen Clay, Upper Peat and Upper Silt. These basic stratigraphic units still apply to present interpretations although complexities relating to local topographic and geomorphologic processes can cause problems in the correlation of sequences. Correlations of the major transgressions and regressions have been drawn with deposits in NW England and the Netherlands (eg. Tooley, 1978a; Shennan et al, 1983).

Work by Shennan (1985a,b) has made a significant contribution to the establishment of an absolute chronology for sea-level changes in the Fens, based on 112 radiocarbon dates. This chronology is therefore related to the sequences of deposits observed at Flag Fen and provides, with the archaeological evidence, a dating control for the application of luminescence dating. Supporting evidence from pollen and diatom analysis allow an estimation of contemporary

Figure 2.1

Location of East Anglian sites
(after French, 1988)



depositional environments relevant to the bleaching of sediment samples. His work forms the basis of the chronology outlined below. For individual radiocarbon dates on which this chronology is based, the reader is referred to Shennan (1985a, b).

Since c.4500 BC sea-level changes have been the major factor affecting the rates and patterns of sedimentation in the Fenland (Shennan 1985a). Alternating phases of freshwater fen and intertidal marine sedimentation are reflected in changes in vegetation and deposition over a wide area. Marine and brackish water sediments are recorded up to 45 km inland. Transgressions and regressions reflect positive and negative tendencies of sea-level. Evidence for these tendencies is found in stratigraphic sequences, which develop under the influence of sea-levels and coastal processes (Shennan et al 1983). These changes are not synchronous and local and regional factors may dominate at different times.

Shennan's (1985b) sequence of events recognises 7 cycles of transgression (Wash) and regression (Fenland) phases from 4000 BC onwards. Wash 1 (pre 4500 BC) comprised a transgression which was confined by local topographic and hydrologic conditions. This is recorded at -8m OD at Adventurers Fen (see figure 2.1 for locations), and represents a low energy marine sedimentary environment. The succeeding regression phase (Fenland 1) is represented by continued peat formation at Holme Fen and Shippea Hill between 4350 and 4250 BC. Wash 2 represents a phase of rising water tables and low energy tides between 4050 and 3650 BC, and Fenland 2 a phase of peat formation between 3650 and 3450 BC.

The Wash 3 and 4 phases represent the deposition of Fen Clay over much of the southern Fens. The Fen Clay deposit is a fine silty-clay loam, and is overlain by the Upper Peat formed during the Fenland 4 phase (2550-2250 BC). This peat formation is controlled by local hydrologic conditions, demonstrated by the change of fen woodland to raised bog (Godwin, 1978). Further transgression and regression cycles (Wash 5, Fenland 5, Wash 6 and Fenland 6) occurred before the deposition of the Upper Silt. During Fenland 6 local silting up of channels occurred which led to partial abandonment of land in the 3-4C AD (Hallam, 1970). During Wash 7, the Romano-British transgression deposited the Upper Silt between 400-800 AD. This transgression was responsible for the silting up of the drainage system with clastic deposits which are now in places upstanding above the shrinking peat surface as roddons, and can be traced by aerial photography over much of the Fens.

The agricultural development of the Upper Silt deposits seems to have occurred, on archaeological evidence, around AD 50 (Salway, 1970; Potter, 1981). Two further cycles of transgression and regression (Wash and Fenland 7 and 8) were expressed as changes in water tables and fluvial clastic sedimentation and flooding from AD 800-1000 and AD 1000 onwards.

The sedimentary environments represented by the deposits of Fen Clay and Upper Silt have been described by Shennan (1985b). Fen Clay is characterised by 55% clay, 45% silt and <5% sand. In the roddons and creeks, the deposit is a finely laminated silty loam or sandy silt. The Upper Silt is characterised by 50% silt, 47% clay, 3% sand, but contains over 70% sand in channels. Clastic sedimentation is characteristic of low energy environments dominating much of the deposition processes of these major units. The freshwater fen was protected by tidal flats and salt marsh which would have dispersed much of the energy of the tides. Silty clay deposits indicate quiet water deposition on and behind natural levees. High Spring tides would have been the greatest cause of flooding. Local sedimentation rates were not evaluated in Shennan's study, as local trends and processes would have exerted a significant influence which is difficult to evaluate.

The deposition of the four main stratigraphic units, as recognised by Godwin (1978) and Shennan (1985a,b) are therefore constrained by a chronology based on the means of a significant set of radiocarbon dates. The transgression and regression phases would not have been synchronous all over the Fens, and local topographic features, eg. the sand islands of Whittlesey and Thorney, and hydrologic factors are recognised as being of great significance. However, the age limits for the Wash-Fenland cycle illustrated above give a chronological control for the transgression-related deposits identified in the samples from Flag Fen. Archaeological material gives an additional control for the upper part of the sequence.

2.1.2 Archaeology

The Fen-edge has significant evidence of occupation from the Mesolithic but sites of Mesolithic, Neolithic and Early Bronze Ages are relatively rare (Pryor, 1985). The location of the settlements would have been largely determined by the prevailing conditions with respect to sea-levels and local ground water tables. The area has been subject to much archaeological investigation, and the reconstruction of the ancient landscape by analysis of pollen, soils and archaeological remains allows a reasonably detailed picture to be drawn of the human occupation, resource use and environment through time.

The upper fen-edge, is located just to the east of Peterborough, and would have been exposed as higher, drier land on the edge of swampy fen carr. Isolated sandy 'islands' such as those of Whittlesey and Thorney existed as the upstanding remnants of the undulating Pleistocene till surface. Occupation would have concentrated on these drier areas, near the rich resources of the swampy fen. The peat fen area was not occupied permanently, but was used as grazing land (Pryor, 1986; 1988) in a similar situation to the Somerset Levels (Coles and Coles, 1986) and the Dutch River-dune area (Louwe Kooijmans, 1974).

The Pleistocene terraces of the Welland and Nene valleys draining into the fen at the fen-edge have also been foci of occupation. The extensive area of managed landscape of the Fengate site (see figure 2.1b) is located on the first of the Welland terraces and comprises extensive field systems. The site at Fengate represents several phases of occupation from mid-Neolithic onwards (Pryor, 1986). There is a phase of abandonment during the Bronze Age, demonstrated by localised silting of the site, and reoccupation in the Romano-British period. This was ended by the 3rd Century transgression, during which ditches were largely filled with clay, and the site partially covered.

Prehistoric occupation of the Fens occurred over a variety of environments within the Fenland. At Maxey, continuity of occupation has been demonstrated from Neolithic to Romano-British times on areas of drier land without alluvial covers (Pryor and French, 1985; Crowther et al, 1985). In areas where significant alluvial deposition has occurred, as at Etton and Borough Fen, Neolithic occupation dominates, as the landscape became too wet for later occupation except on the sandy islands. An extensive Neolithic buried soil survives below the alluvial cover on the Fen-edge and islands (Hall, 1987).

The investigation of the soils buried under alluvium on the sandy islands has contributed to the picture of human activity. French (1988a, b, 1992) investigated the micromorphology of the soils at the Eye gravel peninsula north of the Flag Fen site. Four phases of pedogenesis were identified; first under the Boreal-Atlantic forest where soils developed under the woodland; secondly under a phase of less dense woodland cover, marked by increased incorporation of organic material in clay coatings, indicating minor disturbance; this may be related to local clearance by Mesolithic cultures. The third phase is one of partial truncation of the horizons relating to a period of clearance and erosion, and finally burial by freshwater flood deposits. There is no evidence that the soils were waterlogged on the islands, prior to burial.

During the mid-Neolithic, the site was occupied by people of a culture similar to that at Shippea Hill, where the mid-Neolithic occupation phase was stratified between Mesolithic and Bronze Age material (Clark and Godwin, 1962). There is evidence of prehistoric clearance in the pollen record at Shippea Hill, but not at Fengate except in the buried soils. The pottery at Fengate is characteristic of the middle Neolithic, and occupation is interpreted as a small scale non-nucleated settlement, with seasonal exploitation of the peatlands. Wetter conditions in the 4th and 3rd millennium BC would have rendered fire clearance of forest unlikely (Pryor et al, 1986). There is a break in continuity of occupation which is contemporary with the Fen Clay deposition.

The Fengate site was reoccupied in the mid-3rd to late 2nd millennia BC. Large scale management of the surrounding land is demonstrated by extensive linear ditches and enclosures and evidence of cultivation of wheat and barley, and maintenance of the ditches. Occupation evidence is similar to that of the nearby Iron Age enclosures at Maxey, and also in southern Lincolnshire. The Northey 'island' also has evidence of linear ditches. During the 1st millennium, the settlement became more nucleated, possibly due to the increasing wetness of marginal lands. Settlement was concentrated above the 4.5m contour. Re-use of this settlement in 1-2C AD may be related to the proximity to the Roman Fen Causeway across the Fens, which followed an Iron Age ditch alignment. During the Upper Silt transgression, the site was abandoned due to flooding.

Regionally, the Fens represent an area of abundant Neolithic occupation, extending into the Upper Valleys of the Ouse and Nene during the Bronze Age. These areas were cleared of woodland by the beginning of the Bronze Age (Godwin and Vishnu-Mittre, 1975). Sites at Maxey and Barnack in the Welland Valley were also cleared (Crowther et al, 1985) The Nene Valley was occupied in the Iron Age, with an extensive, dispersed pattern of settlement. Increasing competition for resources, and environmental change encouraged nucleation of settlement and the construction of defensive hillforts (Pryor et al, 1986).

2.1.3 Flag Fen

The site at Flag Fen comprises a substantial timber platform constructed in an ancient channel between the fen-edge east of Peterborough and the sandy Northey island. It is of Bronze Age date, and was constructed and occupied during the phase of abandonment at the Fengate site. The wetlands and Flag Fen site are characterised by abundant metalwork finds. The area is one of sparse pre-Roman defensive occupation, and Pryor et al (1986) suggests that Flag Fen represents a late Bronze Age defensive site.

The site was discovered during a dyke survey in 1982. Timbers protruded over a distance of 80 m from the dyke sides, and underneath the Roman Fen Causeway, and separated from it by some 60cm of alluvium. A radiocarbon date on one of the protruding timbers gave an age of 1100-853 BC (1). The lattice of timbers rests on organic muds related to the Neolithic and earlier land surfaces. The site area is estimated to be 110 m by 50 m, based on auger surveys. The Fen Causeway follows the alignment of an earlier wooden trackway linking the platform with higher land to the east. The platform itself was constructed within the channel between the fen-edge and the Thorney sand island.

The platform consists of a lattice of timbers with upright stakes forming the remains of a palisade. There is the foundation of a long rectangular building incorporated into the platform, and

associated Bronze Age pottery sherds. Environmental evidence from the site indicates that the rise in freshwater table levels around 1000 BC drowned the Neolithic and Early Bronze Age occupation sites, possibly based at Fengate. The timbers are of local wetland species, and so local in origin (willow, alder, ash), but the oak timbers were all around 50 years at felling, suggesting some form of woodland management to provide standard timbers. The environment comprised open water and freshwater fen. Woody and detrital peat accumulated before construction, but after abandonment, the peat is more humic and mixed with clay and silt, reflecting rising water levels.

Dendrochronological investigations of the timbers have produced a master curve extending over 206 years and two others of 108 and 148 years from the Flag Fen site, and 200 years from a nearby site at the power station. These have been matched to produce a 397 year curve for the site and felling of the trees is estimated to have occurred between c.1250 and 967 BC, with most clustered around the last 150-200 years of occupation (Neve, 1992). The sequence was matched at Belfast, but there is an unresolved disparity between the radiocarbon dates and the age based on dendrochronology. This indicates the problems in accurate absolute dating and correlation between techniques.

The pollen evidence indicates open fen with alder carr and grass and reed communities. Diatoms from deposits at the dyke side and to the south of the site indicate shallow water fen carr and swampy carr. They are more poorly preserved in the lower layers, indicating some drying, possibly due to seasonal exposure of the surface. Above the platform, conditions have remained wet and diatoms are much better preserved (Pryor, 1986). The silty clay peat deposits demonstrate a return to open water conditions after abandonment. The site appears to have been built and occupied in damp but stable conditions. It must have been deliberately constructed in rising damp conditions in a marginal location for a purpose, and it has been suggested for these reasons that it represents a defensive site.

2.1.4 Chronological Control

The core site sampled for this project lies at the edge of the Flag Fen platform, between it and Catswater dyke. The stratigraphic sequence is discussed in Chapter 4, but a brief summary of the chronological control available for the site is given below. The basal part of the sequence is correlated with dated sea-level contexts, while the ages of the upper sediments are further controlled by the archaeological evidence.

At the base of the sequence is the Anglian boulder clay and late-glacial fluvioglacial deposits, including weathered and reworked till. These date from the end of the Devensian during a period

of fluvio-glacial meltwater activity, and before the first peat or transgression deposits. This is succeeded by a silty sand and represents a local variation of the Fen Clay deposit, being sandier in the channel. The Fen Clay was deposited between maximum time limits of 3450 and 1350 BC, depending on location and local differences in altitude and distance from the coast (see 2.1.1 above). The position of the sample in the channel between the fen-edge and island would have maximised the time limits for the transgression phases operating in the area.

The Fen Clay deposit is covered by the peat deposits in which the platform is embedded. The peat comprises a lower woody peat and an upper silty detrital peat. The platform lies at the contact between these deposits and its radiocarbon date in the dyke section is given above. Above the peat are the silts of the Romano-British transgression laid down during the Wash VII phase, between 400 and 800 AD. The Fen Causeway was constructed on the surface of the alluvium and is covered by further sandy silts of local fluvial origin, with the sandy material probably derived from the sandy islands nearby. These upper deposits are of recent origin, with the present soil surface developed into the upper part.

2.1.5 Summary

The Flag Fen sequence, sampled some 10m north-west of the timber platform comprises a series of deposits correlated with phases of sea-level changes within the Fenland (Shennan, 1985a, b). The archaeological importance of the site, in terms of major a Bronze Age occupation site in the Fens is significant, and provides a dating control for the sedimentary sequence.

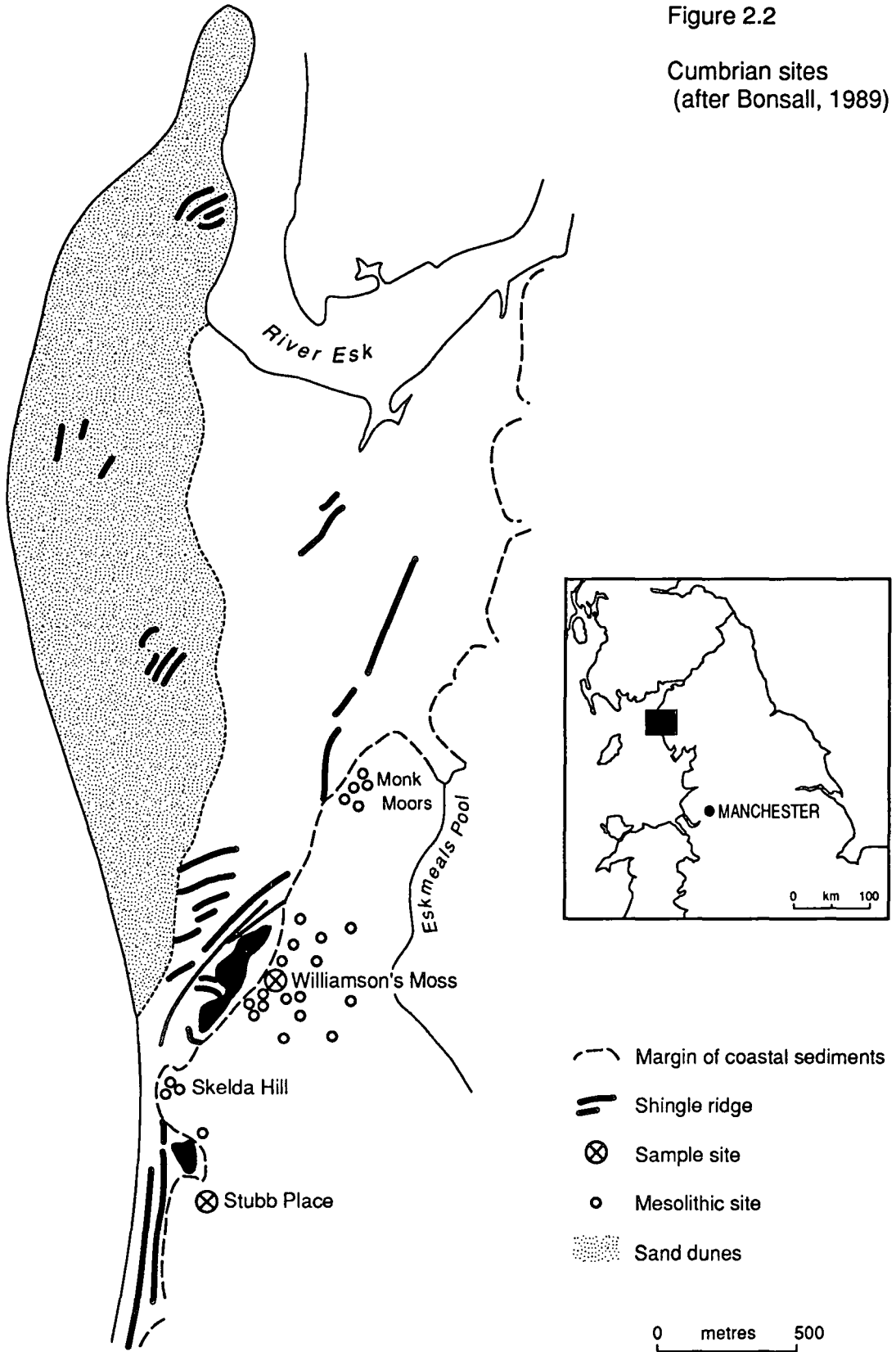
The sequence consists of a basal Anglian till overlain by late-glacial fluvial sands. This is covered by the Fen Clay deposits laid down between c. 3450-1350 BC. These are overlain by peats in which the Bronze Age timber structures are stratified. The platform has been dated by radiocarbon to 1100-852 BC (1) and by dendrochronology to between 1250 and 967 BC. The peats are overlain by silts of the Romano-British transgression deposited between 400-800 AD. The Roman Fen Causeway was built on top of the silts, and this is covered by local alluvial deposits into which the modern soils have formed.

2.2 ESKMEALS, CUMBRIA

The Cumbrian lowlands have been extensively altered during the Holocene by the interplay of coastal, aeolian and anthropogenic activity. The distribution of prehistoric sites of different ages is directly related to the changes in sea-levels during the Holocene. The north west of England has been subject to extensive research on sea-level change, particularly in Lancashire (eg.

Figure 2.2

Cumbrian sites
(after Bonsall, 1989)



Tooley, 1978a) and the Cumbrian coast has been comprehensively surveyed for its archaeological remains (Cherry and Cherry, 1983 to 1987), and excavated as at Eskmeals (Bonsall et al, 1986, 1989). The vegetational history of the coastal lowlands and the uplands has been investigated by Walker (1966) and Pennington (1975). There is therefore, a relatively detailed picture of changing environments during prehistoric times.

Two sites were sampled from the Cumbrian coast (figure 2.2); one at Williamson's Moss in a small channel adjacent to a Mesolithic occupation site; the second at Stubb Place, a depression to the south where concentrations of Mesolithic flint debris has been found. A close chronological control exists for the former, but only a maximum age for the beginning of deposition in the second site, as the radiocarbon dates from an adjacent borehole are difficult to correlate with the sequence in the sample borehole (see below).

2.2.1 Quaternary History

The Cumbrian coastal zone is topographically diverse, comprising a flat coastal plain, dunes and the glaciated upland massif which extends inland to the Lake District. The lowland area was covered by the Lake District ice during the last glaciation (Huddart et al, 1977). Deglaciation is thought to have been complete in the area by 14,000 years ago (Andrews et al, 1973; Coope and Pennington, 1977) with meltwater deposits of sand and gravel being deposited in channels and as sheets at Morecambe Bay (Gale, 1985). The cliffs at St Bees, Eskmeals and Drigg contain archaeological material stratified within peat and clastic sediments.

The oldest marine transgression in Cumbria occurred at Black Dub, north of Allonby (Eastwood et al, 1968) where a peat within clay was dated to 8480 ± 205 C-14 BP (2). (NB. this date could not be calibrated as it extends beyond the timescale of the calibration curve.) These have been interpreted as fossil dune slacks occurring at high sea-levels (Kidson and Tooley, 1977). A further transgression is recorded at Bowness Common between 5749-5640 BC (3) and 5051-4500 BC (4) (Walker, 1966) and also at Wedholme Flow between 5820-5640 BC (5) and 4510-3827 BC (6) (Huddart et al, 1977).

These transgression phases, of which the second and third are the most significant at Eskmeals, are important in relation to the sedimentary sequences sampled. The deposits of the second and third transgressions overlie the Mesolithic occupation evidence in the peat deposits, and predate the Neolithic activity on the foreland. The detailed chronology and formation of the individual sites are considered in relation to the individual sites below.

At Drigg, shingle representing a phase of high sea-level is covered by fluvioglacial sediments and peat containing fragments of wood which were dated to 5315-4945 BC (7) and 5694-5500 BC (8) and which is overlapped by shingle to seaward, representing another period of higher sea-level (Andrews et al, 1973). These deposits are overlain by aeolian sands in which hearths of late Neolithic-Early Bronze Age are stratified; these are dated to 2310-2138 BC (9) and 2878-2611 BC (10) (Cherry, 1982). Hearths of Mesolithic age have also been found at Haverigg where a palaeosol within dune sands containing Neolithic artefacts was dated to 362-40 BC (11) and 2273-1772 BC (12) (Tooley, 1990).

In south-west Cumbria, several phases of dune building are represented in the stratigraphic sequence, and these are dated to the end of Flandrian II (Tooley, 1990) with a period of stability represented by the Drigg hearths. These are correlated with the Older Dunes of the Western Netherlands (Tooley, 1978a). In Lancashire, a second period of stability has been dated to 50 BC - AD 530 (13) and AD 606-688 (14) and finally around AD 1150 at Starr Hills (Tooley, 1990) which correlates with dune building in Cumbria dated on shells at the base of the dunes to AD 680-953 (15) and AD 420-622 (16) (Andrews et al, 1973). The younger dunes of the Netherlands were constructed from AD 1200 onwards (Jelgersma et al, 1970).

2.2.2 Archaeology

The vegetation history and archaeology of the area indicate a long period of human activity, at different locations according to the prevailing contemporary climate and sea-level. Disturbance in the tree cover in Mesolithic times, before the elm decline is recorded in the Pennines up to ^{an} altitude of 450m (Switsur and Jacobi, 1975) in the Lake District and Cumbria (Walker, 1966; Pennington, 1975) and it has been suggested that early Mesolithic occupation and disturbance of the lowlands must also have been significant, but possibly drowned by later sea-level rises (Huddart et al, 1977). Mesolithic occupation is believed to be widespread due to the number of hearths and scatters of flint artefacts that have been located and dated to this period. Occupation on a similar scale is absent from the uplands, and these areas may have been used on a seasonal basis (Bonsall, 1981) as occurred elsewhere in Britain (Clarke, 1972).

The environmental record is one of complex, fluctuating conditions during the amelioration of climate during the Post-Glacial (Gale, 1985). Differences between the faunal and floral evidence indicates rapid rates of change, and anthropogenic activity has been shown to have been significant in terms of forest clearance and soil erosion around the tarns of the uplands, and in the lowlands (Birks, 1982).

A detailed survey of the occupation sites of the Cumbrian coast conducted by Cherry and Cherry (1983, 1984, 1985, 1986, 1987) has revealed the distribution of material of Mesolithic, Neolithic and Bronze Age dates. Particular concentrations of material occur in the Eskmeals area around Williamsons Moss, discussed further below. Stone circles and mounds of Bronze Age date have been located at Seascale, Annaside and Gutterby. At Drigg a timber structure embedded in grey sand and covered by peat and associated with Bronze Age material was found stratified above the previously mentioned Mesolithic hearths.

In summary, the results of Cherry and Cherry's survey shows some differentiation in the distribution of artefacts of different ages. Mesolithic material is clustered in the northern part of the coastal area. Neolithic material, which is of a similar form, age and degree of patination throughout the area, is concentrated in the southern part of the coast. The Bronze Age material occurs primarily to the south of the Neolithic concentrations on Eskmeals. There are scatters of material occurring beyond these observed divisions, which are based on the main concentrations of material. On the sandhills of Eskmeals, much of the material is of Bronze Age date, and includes a higher proportion of 'imported' artefacts, as distinct from the dominance in earlier cultures of local material derived from the beach.

Modification of the local Mesolithic woodland is indicated in the pollen spectra from Barfield Tarn (Pennington, 1970) and at Ehenside Tarn (Walker, 1966). Clearance, cultivation and soil erosion are related to phases of activity in between periods of partial recovery of the forest cover. Mesolithic occupation is concentrated in areas where there is easy access to the beach where abundant supplies of flint for tools was available, as well as the resources afforded by the sea itself.

The pollen and archaeological evidence typical of prehistoric occupation of Eskmeals is considered in more detail below with respect to the sites sampled, in particular, Williamson's Moss.

2.2.3 Williamson's Moss

The Moss lies in an enclosure formed by shingle ridges pushed up against the rising till surface, at an altitude of between +5 m and +7 m OD. The Moss is bounded by shingle ridges to the west, on which the dunes have formed; by the estuary of the River Esk to the north, and by a till ridge incorporating Skelda Hill to east and south where the coastal plain narrows. Marine clay is deposited in the base of the depression which is thought to be a former route of the River Esk before it was diverted to the north by the formation of the shingle ridges and dunes (Huddart and Tooley, 1972). The basal deposit is a blue-grey clay of estuarine origin, containing brackish water diatoms, and covered by a gyttja dated to 5345-5227 BC (17) (Huddart et al, 1977). This dates the regressive overlap prior to the isolation of the Moss. Isolation from the sea is estimated to have

occurred before the elm decline around 5000 BP (Tooley, 1972). A stream, Eskmeals Pool, flows northwards through the Moss to the present Esk estuary.

A series of shingle ridges have protected the coast from erosion, and controlled the development of the foreland. The innermost ridges, which instigated the formation of Williamson's Moss, were formed during the regression which deposited the estuarine clays. Later ridges formed north of Skelda Hill, pivoting round the till ridge. There are three groups identified on the basis of altitude, relating to three successively lower sea-level stands (Bonsall et al, 1986, 1989). These occur at heights of +7.5, +6.4 and +5.5m OD.

The beginning of lagoonal sedimentation in the Moss is marked by the formation of the inner shingle ridge, dated by an underlying organic layer to 4530-4407 BC (18). The second series of ridges were formed between 3260-2919 BC (19) and 2126-1889 BC (20) and the third by 1121-898 BC (21) (Bonsall et al. 1989).

Peat development on the estuarine clay began around 2123-1777 BC (22) and ended at 1685-1518 BC (23) after which a phase of aeolian dune building began on the ridges. A thin peat within the sand was dated to AD 118-322 (24) to AD 543-652 (25). Within the estuarine sedimentation area, Bonsall et al. (1986, 1989) has identified two land surfaces, at 5.8-6 m and 4.64 m OD, formed when sea-levels were 2-2.2 and 0.8 m lower than present. The dunes were later built up on the tops of the ridges, covering the earlier occupation levels, and were themselves occupied during the Bronze Age.

2.2.3.1 Archaeology

A number of flint concentrations were discovered on the edges of the bog, at a level corresponding to the shoreline when the Moss was connected to the sea and of much greater eastern extent (Cherry, 1969). Much Neolithic material, including imported Borrowdale Volcanic artefacts, was exposed by ploughing of the former bog edges. The seaward edge of the shingle bank has mainly Bronze Age material; the north and east edges mainly Mesolithic. The Monk Moors site located to the north of Williamson's Moss is dominated by Mesolithic material concentrated in shallow soils developed on the boulder clay. Four hearths were dated from this soil to 6570-5844 BC (26) and 5740-5490 BC (27) (Bonsall, et al. 1986). The dunes cover flint scatters and hearths on the raised beach, also of Mesolithic age, which closely follow the 8 m contour around the former edges of the bog. Later Neolithic and Bronze Age material occurs at lower levels and on top of the dunes, reflecting changes in the coastal configuration and topography.

The Williamson's Moss site lies on the crest of a till ridge within the Moss, and was excavated between 1981 and 1985 (Bonsall et al, 1986) along with an adjacent site at Monk Moors. A narrow channel is cut into the till to the south of the site, from which the core taken for luminescence dating was taken. Alluvial deposits in the base of the channel were initiated by the silting up following the ridge formation. A buried land surface lies below this alluvium, and represents a sealed archaeological context. This land surface occurs as a thin layer of sand on top of the till. The sand layer is much thicker in the channel, possibly resulting from erosion. The sand is interpreted as the remnant of a minerogenic soil and can be traced over much of the site (Bonsall et al, 1989).

Stratigraphic and radiocarbon dates indicate that there was around two millennia of occupation, throughout which the style and technology of the flint work remains noticeably uniform. Three main areas of occupation were identified: the till ridge, the lower lying ground, and the channel infill. The till ridge had high concentrations of worked stone, but no indications of settlement structures. Artefacts were mainly Mesolithic, but some later material was incorporated. The lower areas contained three hearths at different levels in the alluvium, and dated to 2134-1982^{BC} (28) for the shallowest hearth, 2320-1987 BC (29) and 3950-3526 BC (30) for the deepest hearth (Bonsall et al. 1986). The earliest occurred just above the Mesolithic land surface and represents the first phase of Neolithic occupation of the Moss.

The channel fill contained the most substantial remains on the site. The channel is less than 30m wide at its widest point and 3m deep. Several timber structures were recovered from the channel fill, comprising lattices of timber with bark and brushwood flooring. There was also evidence of made ground comprising dumps of sand, clay and stones held in by revetments of timber. These may have been constructed to stabilise the land surface when it was much wetter. The timbers were dated to between 5049 and 4355 BC (31, 32, 33) and the bark to 4462-4435 BC (34, 35). There were no associated diagnostic artefacts.

Pollen analysis at the site reveals substantial landuse changes in the Moss and small scale deforestation around 3650 BC, before the elm decline (c.3490 BC). Partial regeneration occurred c.3200 BC and the vegetation remained as alder-birch woodland until arboreal pollen frequencies fall from 2900 BC onwards, primarily associated with human exploitation.

2.2.3.2 Chronological Control

The dating control for this site is relatively good for the archaeological strata, providing an excellent test site for the application of luminescence techniques.

The basal deposit is the Devensian till, overlain by aeolian sands which correspond to the Mesolithic land surface. The till is a fine-grained deposit, indicating that it cannot have been the sole source for the soil material. The sand is the remnant of the Mesolithic soil, and probably is derived from fluvial sands deposited during deglaciation possibly with a wind-blown component, on top of the till. The Mesolithic activity is dated to a mean of 6570-5490 BC (26, 27) on hearths stratified within the soil at Monk Moors, and from the timber structures and associated artefacts sealed below the alluvium at Williamson's Moss.

In the deeper parts of the Moss, a grey clay above the sand is covered by an organic gyttja, dated to 5345-5227 BC (17) (Kidson and Tooley, 1977). The upper alluvial deposit at the excavation site comprises clay with some organic matter. The incorporation of the woody and organic material into the clay is interpreted as the effects of trampling during occupation (Bonsall et al, 1986). Three hearths stratified within the alluvial deposits at the site date the alluvial sediment to between 3950-1982 BC (28, 29, 30). Above this are recent peat and alluvial deposits incorporating wind-blown sand which may be contemporary with the later phase of dune building, dated to between 1350 BC and AD 150.

2.2.3.3 Summary

Williamson's Moss in Eskmeals, Cumbria, formed in an enclosure cut off from the sea by shingle ridges. The Eskmeals area has abundant remains of prehistoric occupation from the Mesolithic to Bronze Age. In the Moss itself, Mesolithic timber structures were found sealed below alluvium. Elsewhere on the Moss, periods of occupation can be correlated with contemporary sea-levels; for example, Mesolithic activity is concentrated along the 8 m contour around the Moss.

The stratigraphic sequence at the Moss site is located in a channel adjacent to the timber structures excavated. The sequence comprises a basal Devensian till covered by a sandy deposit, interpreted as the remains of the Mesolithic land surface, eroded into the channel. This land surface is contemporary with the timber structures at the Moss, dated to between 4355 and 5049 BC (31, 32, 33). Elsewhere in the Moss a basal clay deposit has been dated by an overlying gyttja to 5227-5345 BC (17). This deposit represents the period before isolation of the Moss by the shingle ridges.

The sand is overlain by a blue-grey clay. Hearths stratified within the alluvium have been dated to between 1982-3950 BC (28, 29, 30), giving a relatively close dating control for this alluvial unit. The upper part of the alluvium contains organic material incorporated by trampling during occupation phases. The upper part of the sequence contains sediments consisting of alluvium and blown sand, and represent more recent historical and modern soil horizons. The close dating

control for the sedimentary sequence, particularly for the alluvium, makes Williamson's Moss a valuable site for testing the viability of luminescence dating in an archaeological context.

2.2.4 Stubb Place

The site is a depression located to the south of the Skelda Hill till outcrop. It is protected by shingle ridges formed at the same time as the inner ridges at Williamsons Moss; the later ridges only formed to the north of Skelda Hill. The ridges to seaward of Stubb Place are not complete; ie. there is a small outlet which may have allowed later inundation by the sea to occur. This was not the case for Williamson's Moss. Sedimentation within the depression may have begun at the same time as at the Moss, ie. after c.4345 BC, but this is not certain.

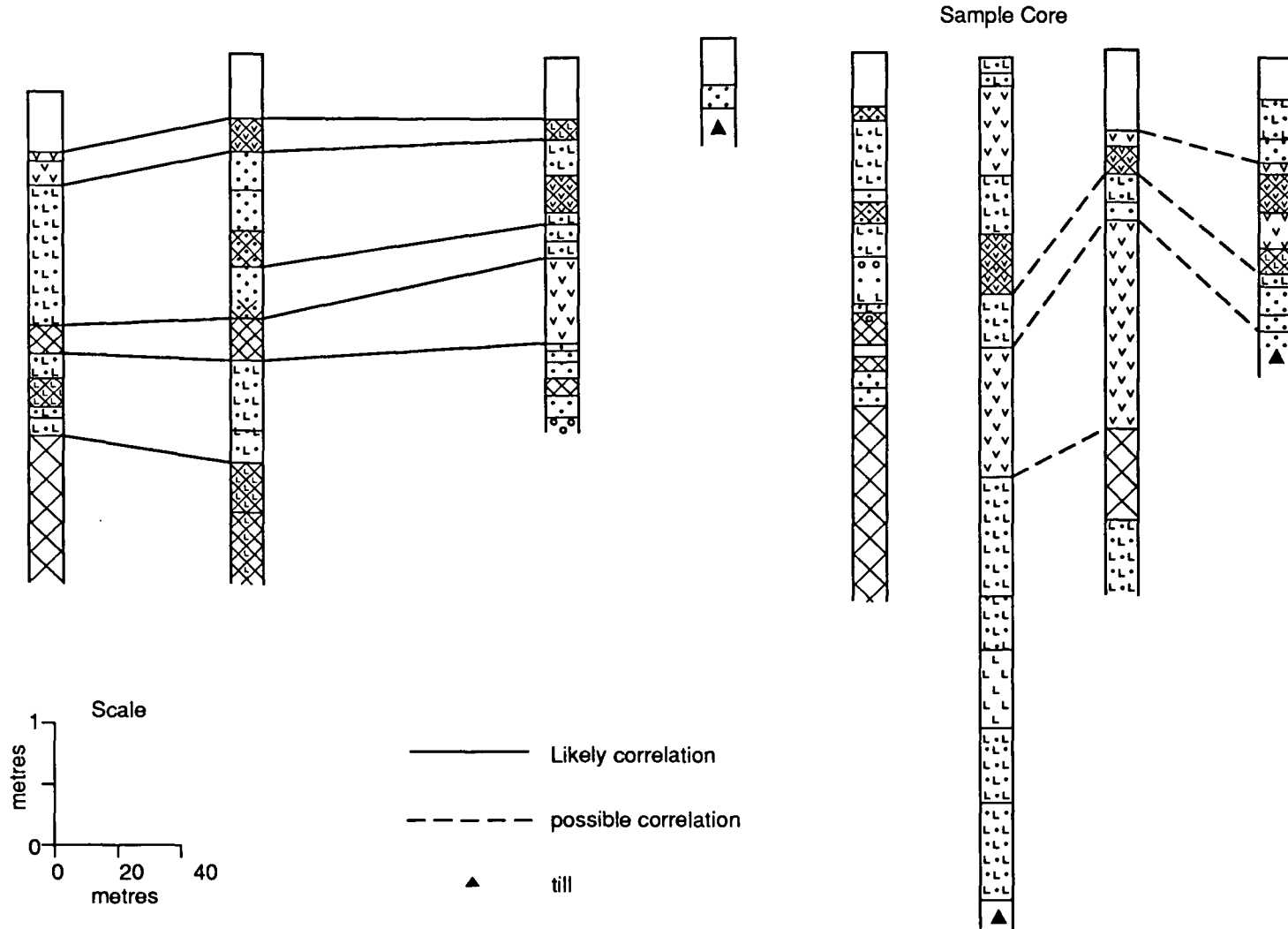
A transect of borings was made previously across the depression (Tipping, pers.comm.) which demonstrated considerable variability in the profile of the sediments infilling the basin (figure 2.3). The sample core was taken in the deepest part of the basin, where a channel appears to have cut into the till. Radiocarbon dates for the upper part of an adjacent core are difficult to correlate due to the great variation in type of deposit at equivalent depths in the sample core. The dates relate to an upper peat deposit 45-50 cm below the surface and to a lower humic sand at 120 cm below the surface. The dates have not been published and are not used in this study because of the difficulties in correlation of the strata between the dated core and the remainder of the transect. Pollen analysis of the upper of these peat samples indicates a grass and herb dominated vegetation, with a fall in arboreal pollen in the upper part of the layer, associated with increases in abundance of *Calluna*, *Plantago lanceolata* and *Cyperaceae*.

The depression is filled with alternating clastic and biogenic deposits up to a depth of 6.5 m at the point of sampling for this study. The basal deposit lies on till which corresponds to that at the base of the Moss. The dating of the clastic layers would enable correlation of the sequence of deposits with those at the Moss and with those relating to younger (post 4050 BC) sea-level changes. The transect indicates that the depression is divided by a till ridge between two depressions. Peat has formed in the deepest parts, overlain by silty clays and clay-sands with intercalated peats on the edges of the infilling depressions. It is possible that marine flooding could have occurred in the seaward depression, but not in the landward one, as more minerogenic sedimentation occurs in the former, but peat forms in the latter, at equivalent altitudes.

2.2.4.1 Chronological Control

The C-14 dates available for these sites lack sufficient reference to the samples taken. The correlation of deposits between the dated core and the core taken for luminescence dating is too

Figure 2.3 Stubb Place stratigraphic correlation
(after Tipping, pers. comm.)



poor to allow the radiocarbon dates to be applied as a chronological control. The sediment sequence in the core taken for luminescence dating is more complete, and represents a deeper sample than that dated by radiocarbon, and includes a greater number of inorganic strata suitable for luminescence dating. For this reason, the core was included in this study, rather than that dated. The core is important as a test site for the application of luminescence without a chronological comparison.

2.2.4.2 Summary

The site is located to the south of Williamson's Moss, and although Mesolithic flint material has been found scattered over the surface, there is no archaeological material represented within the sequence. Sedimentation within the basin in the till may have begun at a similar time to that at Williamson's Moss, as both areas were cut off from the sea by the same phase of shingle ridge formation; ie. around 4345 BC.

The sequence consists of alternating organic and inorganic strata. Radiocarbon dates available from a core within the basin have not been used as a chronological control due to difficulties in correlation of the deposits across the basin. However, the site has been included as a test site for dating sediments where no other dating method has been applied in order to assess the contribution of the luminescence techniques as a primary dating method.

2.3 HARTLEPOOL BAY, CLEVELAND.

Hartlepool Bay lies on the NE coast of England (figure 2.4) and is significant in terms of sea-level change studies, because it represents one of a relatively few locations on the north-east coast of England where marine transgression deposits have been recorded. Its archaeological significance is demonstrated by the discovery of a skeleton buried in the intertidal peats, in addition to a variety of prehistoric artefacts recorded from the area.

The site is important for this study because as the sediments come from an intertidal context, the relevance of mixing of sediments during the tidal cycle is important, although this is relevant only to the upper part of the sequence, and in that the sampling strategy was different; samples were taken in monolith tins, rather than from boreholes. The intertidal location of these samples is also important because the sediments are saturated with saline water, and are likely to have been for much of their burial history.

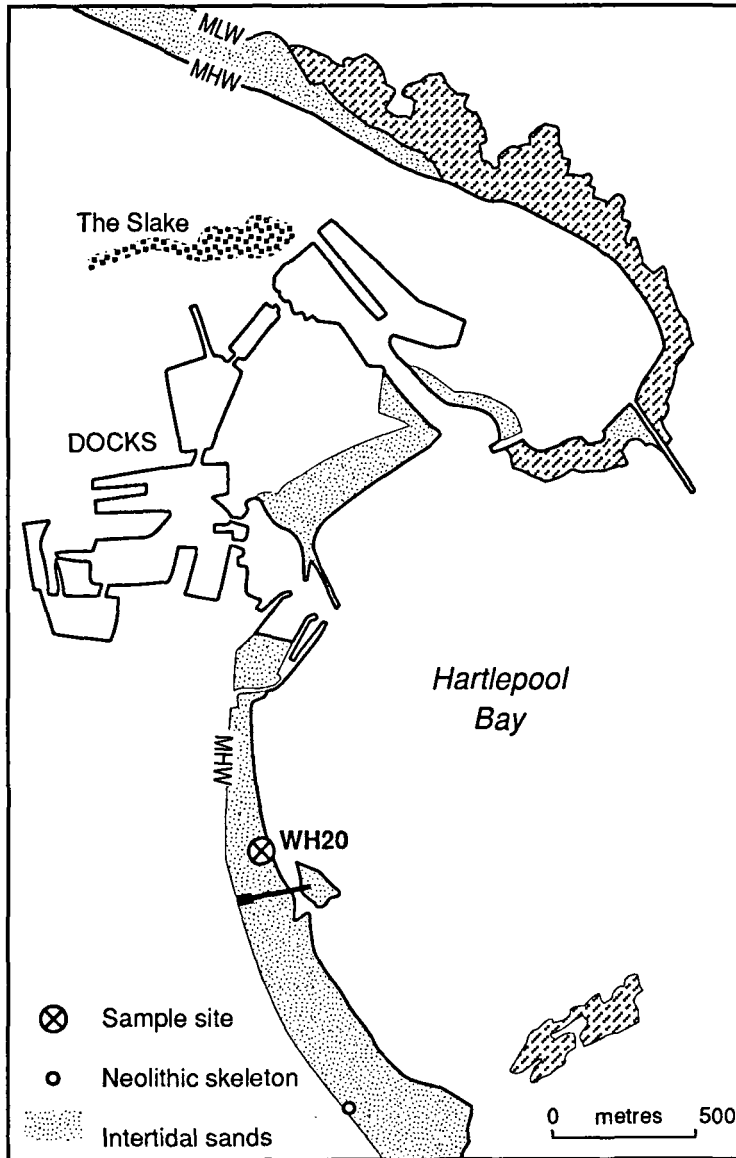


Figure 2.4

Hartlepool Bay
(after Tooley, 1978b)



2.3.1 Quaternary History

The Tees Valley and adjacent lowlands are covered by a Devensian till, which is a brown-grey deposit extending from Northumberland to Holderness. During deglaciation, laminated silts and clays were deposited in lakes and depressions. The solid geology of the Bay comprises Permo-Triassic rocks to the north, separated from the Bunter Sandstone to the south by the West Hartlepool fault. The till lies on these rocks and has been modified by the later cold interstadial, and covered by post-glacial marine deposits.

The Slake, which lies to the north of the Bay, is a buried valley infilled with uninterrupted biogenic sedimentation which has been analysed for its pollen content, giving a picture of the regional vegetation change of the Bay area. The Bay itself contains intercalated biogenic and clastic marine sediments reflecting changing sea-levels during the Holocene. To the north are saltmarshes which represent the remnant of a tombolo feature behind which the Slake formed (Tooley, 1984).

Transgressions in the north-east of England have generally occurred to a lesser extent than in the north-west (Tooley, 1978a) mainly due to the local topography. The main transgression deposit in the Bay, which is the oldest marine deposit in the region, has been dated at its upper and lower contacts with biogenic material to between 4328-3990 BC (36) and 4331-3820 BC (37) (Tooley, 1978b). The Tees estuary at this time was inundated and a grey silty-clay was deposited, containing molluscs characteristic of estuarine conditions and indicating a phase of quiet water sedimentation. The radiocarbon dates for the marine deposit represent a very short timespan for the deposition of some 1.7 m of material.

The transgression deposits at Hartlepool Bay are difficult to correlate with similar deposits in the Humber estuary. Here two transgressions are dated; one beginning at a mean of 6785 BP (Gaunt and Tooley, 1974), and a second, associated with the prehistoric boats at Brigg, at c. 2543 BP (McGrail and Switsur, 1975). There is no evidence of the transgression directly contemporaneous to that dated at Hartlepool Bay. In north-west England, however, a marine transgression is contemporaneous with that at Hartlepool Bay, but occurs at a higher altitude due to the subsidence of eastern England (Tooley, 1978a,b)

The deposits at Hartlepool were described by Trechmann (1936, 1947) who gave details of the mollusca, vertebrate fauna and flint artefacts. A red deer antler was found, dated to 7064 BC (38) to 8700±180 BP (39) (Barker and Mackey, 1961). The first of these dates was at the limits of the calibration programme so no calibrated range could be given; the second date could not be calibrated because it extended beyond the age range of the calibration programme.

The biogenic deposits lying on the till surface were by their pollen estimated to be of Atlantic age - ie. younger than 5050 BC (Trechmann, 1947). The intertidal deposits are variable laterally and in composition. Recent transects of borings have demonstrated that the units comprise a woody detrital peat changing into a rooty gyttja (*Phragmites* roots), and to a silty clay at the low tide mark (Tooley, 1984). These are overlain by 1.7 m silty clay, thickening landwards, and containing the mollusc *Scrobicularia plana* da Costa, *in situ*. This clay deposit is that constrained by the radiocarbon dates given above. Above this clay are a series of sandy, silty limnic deposits comprising eroded peat and marine material.

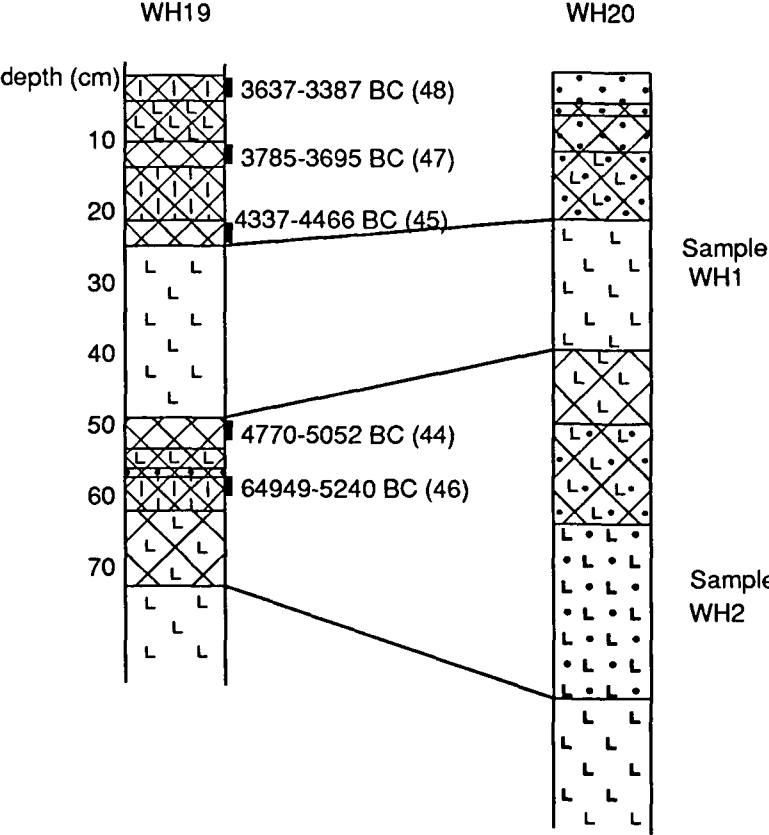
The stratigraphy of the core sample taken for dating (labelled WH20 on figure 2.4), has been correlated to the nearby core of WH19, with its radiocarbon dates. These are illustrated in figure 2.5. There are some lateral differences in the deposits; sample WH1 in the core WH20, comprises an upper grey clay as in WH19, but also a lower grey clay with a limus component, which may be derived from local incorporation of eroded peat during the initial phases of inundation. The lower sample, WH2 in core WH20 comprises a silty-clay with sand, with much less organic material than appears in WH19. This deposit either represents a fluvial or marine deposit laid onto the boulder clay, or more likely represents the weathered till and remnant of the Mesolithic soil identified by Trechmann (1936,1947).

2.3.2 Archaeology

Pollen analysis of the intertidal peats at the Slake has indicated significant disturbance of the natural vegetation by human activity. Archaeological evidence supports this, in the form of scatters of Mesolithic flints, flakes and wood fragments in the intertidal zone. The flakes include Langdale tuff material and an axe made from Borrowdale volcanic rock. Flint flakes, microliths and blades of Mesolithic affinity were found in levels containing pollen evidence indicating clearance. The Mesolithic land surface at Hartlepool is represented by the weathered surface of the till below the earliest biogenic deposits, formed in depressions in the till surface. Trechmann (1947) suggests the weathered till is the remnant of a mineral soil of Mesolithic age.

In 1972, a partial skeleton was uncovered in the intertidal peat further up the shore, together with a number of artefacts. The bones were dated to 3631-3380 BC (40) and described as a male of 25-38 years old, who had suffered two blows to the head during life (Tooley et al, in press)). The peat deposit in which it was found is the remains of a submerged forest in which many Neolithic artefacts were found which are primarily of Neolithic age. In the peat surface, stake holes and stratified charcoal indicate occupation of some sort at the site (Tooley, 1978b).

Figure 2.5 Hartlepool Bay stratigraphic correlation between sample core WH20 and adjacent core WH19 with radiocarbon dates (WH19 from Tooley, 1984)



The pollen evidence from the Slake indicates four phases of human disturbance and clearance. Initially low values of arboreal pollen and open water taxa are succeeded by reedswamp. Forest recession before the elm decline is recorded, and attributed to rising sea-levels or human activity. Rising water tables would promote the growth of reedswamp, but charcoal, and ruderal herb species indicate human interference. There is evidence of clearance preceding the elm decline at Williamson's Moss (see section 2.2.3.1 above) and in other parts of Britain (Pennington, 1975).

This phase is followed by much more extensive clearance, with increased frequencies of hazel, grasses and charcoal. This phase ends with the elm decline, and the vegetation becomes dominated by open herb taxa and some coastal species. The Slake sequence is correlated with the short sequence from the peats in the Bay. The intertidal peat has a darker upper layer rich in birch, and a lower more silty layer containing charcoal. This lower zone has been dated to 4315-4006 BC (40), which coincides with the elm decline, which is dated in the north east of England to between 4364-4241 BC (42) and 4222-3990 BC (43) (Bartley et al, 1976), but appears earlier in the uplands of the Pennines.

2.3.3 Chronological Control

The stratigraphy of the sample site (WH20) is correlated to the sequence dated nearby (WH19) by Tooley (1988) and is shown in figure 2.5. The upper sample, WH1 is closely dated to between 5052-4770 BC (44) and 4466-4337 BC (45). The lower sample, (WH2) lies between the biogenic deposits dated to 5240-4949 BC (46) and the weathered boulder clay surface which represents the Mesolithic land surface of c.7064 BC (39), based on the artefacts found on the beach by Trechmann. The close control on the samples provides an excellent site for luminescence dating of the sediments. The sediments comprise a marine/estuarine clay deposited under quiet water conditions (WH1) and a silty clay sandy deposit (WH2), interpreted as weathered till, or the remains of the mineral soil of the Mesolithic land surface.

2.3.4 Summary

This site is at present in an intertidal location and was the only site sampled using monolith tins instead of by coring (see chapter 3). Its present location has implications regarding the water content of the samples in the past, and the possibility of mixing of sediments during erosion and deposition during the tidal cycle. The site experienced intertidal and lagoonal conditions in the past, during the deposition of some sedimentary units. This is discussed further in Chapters 3 and 4.

The site sampled is located on the seaward end of a transect of borings (see figure 2.4). The depositional sequence comprises a Devensian till overlain by a sandy weathered boulder clay containing charcoal fragments. This is interpreted as the remnants of a mesolithic land surface. The top of this deposit is dated to 5240-4949 BC (46). This is overlain by a peaty sandy clay which is variable in composition. This is covered by a silty clay which thickens landwards, dated to between 5052-4770 BC (45) and 4466-4337 BC (45).

The relatively short timespan during which the upper deposit was laid down is important in this context as it serves to test the accuracy of luminescence dating compared to radiocarbon in this context. The top of the sequence consists of recent sandy deposits which were not sampled, due to uncertainties regarding their age and the effects of reworking under recent intertidal conditions.

2.4 THE RIVER DUNE AREA OF THE WESTERN NETHERLANDS.

The Quaternary history of the Western Netherlands has been one in which sea-levels have played a dominant role by directly affecting sedimentation and environment in the coastal and tidal flat areas, and indirectly, through the control of the level of groundwater tables, the sedimentation and environment of the river dune area inland. The river dune area is investigated in this study, because of the opportunities for occupation afforded by the river dunes (donken) and stream ridges acting as drier islands above the wetter peat areas (figure 2.6).

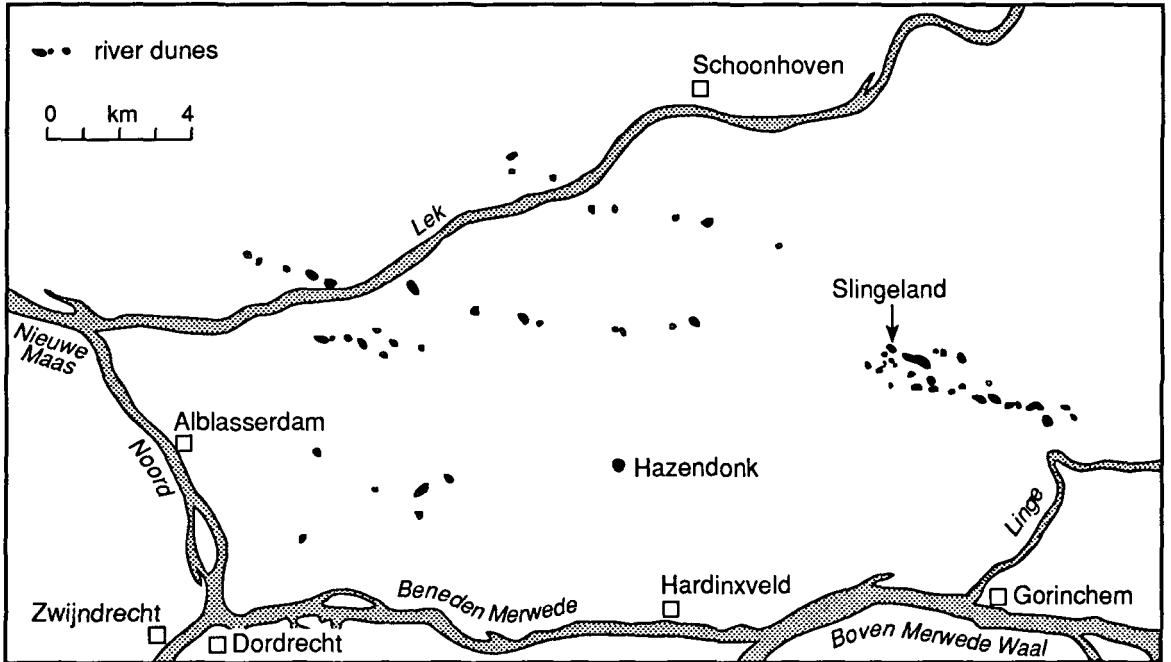
The investigation of the archaeology of the river dune area is based on the occupation of the dunes, and on the investigation of the sequences of sea-level changes which controlled the potential for occupation of the dunes during the Holocene. Investigation of sea-level changes has been a dominant research interest due to its important role in the Holocene. Three zones of deposition are recognised; coastal barriers, lagoonal and tidal flats, and river dune areas. These will be considered below in relation to the sea-level changes and the distribution of prehistoric settlement, before concentrating on the formation and archaeology of the donken. The river dune region lies within that defined as the 'perimarine' zone by Hageman (1969) which is defined as an area in which sedimentation is controlled by sea-level changes, but one in which no marine or brackish water deposits are found.

2.4.1 Quaternary History

The Netherlands lie in a subsiding basin with a relatively flat coast, so small changes in sea-level can have significant effects far inland (Pons et al, 1963). Sea-levels are estimated to have risen by 60cm/century during the Boreal/Atlantic periods, with the rate of rise slowing down during the mid

Figure 2.6

Location of Dutch sites
(after Verbraeck 1974)



and late Atlantic. The limits of the most extensive transgression are marked by the 15 m contour. The sea-level curve for the Netherlands was established by Jelgersma (1966) based on the radiocarbon dating of compaction-free peat samples. The transgression sequence consists of Calais and Dunkirk sequences of deposits, laid down during the time limits established by Hageman (1969) and given below in table 2.1.

TABLE 2.1 Transgression sequence of the Western Netherlands (after Hageman, 1969) and associated archaeological occupation (after Louwe Kooijmans, 1974, 1976).

Transgression	Dates (BP)	Archaeological period*
Dunkirk III	AD1100 -	Medieval
Dunkirk II		Early Iron Age - Roman
Dunkirk I	1949-2111 BC (49)	Late Bronze Age
<u>Dunkirk 0</u>		<u>Early Bronze Age</u>
Calais IV	3044-3332 BC (50)	Later Neolithic (Vlaardingen)
Calais III	3695-3782 BC (51)	Mid-Neolithic (Hazendonk)
Calais II	4043-4237 BC (52)	Early Neolithic (Swifterbant)
Calais I		

* Archaeological occupation during Dunkirk phases occurred during the regression phase following the transgression indicated. Occupation during the Calais phases occurred during the transgression phase itself.

Dates are based on those obtained from the Hazendonk.

The main Holocene stratigraphic units in the Netherlands together with the stream ridges and donken discussed below are embedded in the Holland Peat, formed during the Boreal period over much of the Netherlands and North Sea basin. During the Boreal, the coast of the Netherlands was protected by barriers with tidal inlets (Hageman, 1969). In the lagoonal and tidal-flat area behind the barriers, the Holland peat is succeeded by a series of freshwater lagoonal deposits intercalated with peat, as the area was largely protected from marine inundation by the coastal barriers until the Dunkirk 0 transgression.

In the beach and dune area, successive stages of coastal barrier systems reflect sea-level changes. These systems moved eastwards during the Atlantic when sea-level rise was rapid. Erosion and breaching of the barriers during the Dunkirk 0 transgression allowed marine inundation to occur, but from c.3000 BC, accumulation of the barrier systems associated with slower rates of sea-level rise allowed the systems to become fossilised as the Older Dunes. These

have been largely eroded in the south-west, but the Younger Dunes, forming from AD 1200 onwards have developed in the north-west coastal zone (Jelgersma, 1966; Hageman, 1969).

The coastal barriers themselves were occupied during certain periods, as well as the levees of the estuarine and tidal flat creek systems, during regression periods. The Calais and Dunkirk deposits have their direct counterparts in the Gorkum and Tiel deposits respectively, of the perimarine area.

2.4.2 The Perimarine area and the Donken

The perimarine area comprises the river dune and wood peat districts of the Netherlands. Sea-levels did not significantly influence fluvial sedimentation and peat formation until the later Atlantic phase of rapid sea-level rise (Hageman, 1969). During this time locally high water tables resulted in the deposition of heavy blue-grey clays. In the mid and late Atlantic, however, the lower courses of the rivers were inundated and silted up with fine sand and clay. An unstable braided river system developed with local peat growth and channel and gully infilling until the river system became more stabilised during the period of slower sea-level rise.

The Gorkum deposits of the perimarine area are directly correlated with the Calais transgression sequences, and the Tiel with the Dunkirk. The Gorkum deposits comprise sandy channel fills, with clay deposition on and behind levees. The Tiel deposits can be laterally differentiated into heavy basin clay deposits and sandy stream deposits. The latter are the forerunners of the later upstanding stream ridges on which later prehistoric occupation was concentrated.

The donken are aeolian dunes consisting of sand of mainly 200-300 μ (Pons et al, 1963) formed during the Allerød phase on the final stages of a braided river system. The dunes were blown up from the dry river beds in the Younger Dryas, and formed dunes on the right hand banks of the late glacial braided river system (Verbraek et al, 1974). Near to Nijmegen (figure 2.6), these dunes are buried by 1.5m river clay (referred to in the Netherlands as *loam*), but in the Alblasserward district, they stand above the Holocene deposits as isolated islands. They are elongated SW-NE and generally little eroded. The NW faces dip steeply at c.20°, and the SE slope tails off gently. The dunes lie on top of the 10-100cm thick late-glacial clays.

Occupation of the donken began in the early Neolithic and continued intermittently throughout the Bronze Age. Occupation of the nearby stream ridges occurred simultaneously, but began later, after the formation of the stream ridges. The latter are narrow sinuous ridges of sand which are the infill of stream beds, which became upstanding features during the Neolithic due to the compaction of the surrounding peat and clay. Their formation is closely related to the transgression sequence on the coast. They all predate the present Lek, Linge and Hagenstein

ivers (Verbraek et al, 1974). The stream ridges in Molenaarsgraaf, the area of study, date to the Calais III and II transgressions.

The period of occupation of the dunes and stream ridges coincides with the period of swamp forest that existed in the river-dune area. This was controlled by the level of the groundwater tables, and alternated between phases of fluvio-lagoonal and fluvio-lacustrine environments (Van der Woude, 1983, 1984). During the Neolithic, the fluvio-lagoonal environment consisted of open water bodies, with extensive alder carr and reedswamp. On the natural levees of the rivers, and on the higher dunes, a deciduous forest with oak, elm and birch was maintained.

Peat formation continued with the slow rise of water tables from 4050 BC to c.3650 BC when a sudden expansion of the lagoons took place, and extensive drowning of the swamp forest, creating a fluvio-lacustrine environment. The water bodies joined up, and the area of forest reduced. This was facilitated both by rising water tables above a critical point, and by compaction of the sediments in the lagoon. Fluvial clay was deposited on the levees and basin floors. Around 3650 BC swamp forest expanded, but was drowned again c.3950 BC. Occupation of the dunes, such as at Hazendonk coincided with the fluvio-lacustrine phases of relatively high water levels, when the donken would have been separated by contiguous water bodies with rich resources of fish, exploited by the Neolithic people.

2.4.3 Archaeology

Prehistoric occupation of the Western Netherlands is concentrated on the donken and stream ridges and coincided with periods of relatively lower sea-levels. Very few finds of Mesolithic and older date have survived, being drowned in the North Sea basin or buried under significant depths of deposits. The Neolithic period is that best represented on the donken and stream ridges. Occupation evidence from the donken comprises primarily of stratified layers of a black deposit, a few centimetres thick. These layers contain abundant remains of settlement, including sherds, flints, worked stone, charcoal, small animal and fish bones.

The Hazendonk is located near to the Schoonrewoerd stream ridge in Molenaarsgraaf polder. It has seven layers of occupation extending from the Neolithic into the Bronze Age covering an area of 100 m by 40-50 m (Louwe Kooijmans, 1974). Pollen evidence from the Hazendonk indicates human influence on vegetation from c.3400 BC. The oldest period of occupation is represented by the Swifterbant culture, named after an extensive early Neolithic site in East Flevoland. The coastal barriers by this time had to a large extent been reworked or broken down into dunes with no evidence of occupation except in the river-dune region. There are a number of Neolithic cultures represented on the Hazendonk, including the 'Hazendonk' culture first recognised there, stratified

between the previously known Swifterbant and later Vlaardingen cultures (Louwe Kooijmans, 1974).

The late Neolithic Vlaardingen culture is the best represented of the prehistoric cultures in the Netherlands, and occupation has been found on the coastal barriers between the rivers Rhine and Meuse, as well as on the donken. The coastal barriers were inhabited from the Vlaardingen culture onwards, but in the estuarine and river dune areas, marked periodicity is evident (Louwe Kooijmans, 1974, 1976). In the estuarine region, settlement is concentrated on the natural levees of the creeks relating to the Calais IV transgression. They also concentrated on the Older Dunes where abundant resources from forest, sea and river were readily available.

The dunes were not attractive for permanent agriculture and occupation due to their small size. No sites have been found north of the Rhine (Louwe Kooijmans, 1974, 1976) but indications of activity are given by scattered finds of the Vlaardingen culture on the dunes of the oldest coastal barriers. Settlement comprised small rectangular houses which were permanently occupied. The coastal barriers were used for grazing or limited cultivation. Relationships with the early Bell beaker cultures resulted in changes of landuse, with clearances occurring after trade contacts were established with the Protruding Foot Beaker culture (PFB).

Occupation by the Bell Beaker culture was curtailed by the onset of the Calais IV transgression which covered the levees and caused flooding. The following Bronze Age beaker cultures, those of the Veluwe and Barbed Wire beakers (the former from 1900-1700 BC and the latter from 1700 to 1500 BC) are found on the coastal barriers and on the dunes of the river clay district. Communication was by the then active streams, from which the stream ridges later formed. The Middle Bronze Age and later is marked by fewer settlements on the coastal barriers, which were eroded or buried by the Younger Dunes. Middle Bronze Age occupation is abundant in the river dune area, although no evidence from the estuaries of the Meuse and Rhine have been found. Flooding and clay deposition resulting from the Calais 0 ("Cardium") and Dunkerque 0 transgressions buried some sites, and caused depopulation of the coastal and estuarine regions.

There are several parallel trends in settlements in the Western Netherlands and in the Fenlands, which have been discussed by Louwe Kooijmans (1988). Both are to some extent concentrated on islands and controlled by sea-level changes as at Shippea Hill and Peacocks Farm (Clarke and Godwin, 1962).

2.4.4 Hazendonk and Slingeland

Two donken were sampled for dating in this study. The Hazendonk in Molenaarsgraaf polder is important because of its significance to the Neolithic sequence of occupation in the Netherlands. The Slingeland donk is one of a group of donken in the Nodeloos region, and supports up to five layers of occupation, rather than the seven demonstrated at Hazendonk. The correlations between cultural layers and dating at these sites is given below in figures 2.7 and 2.8.

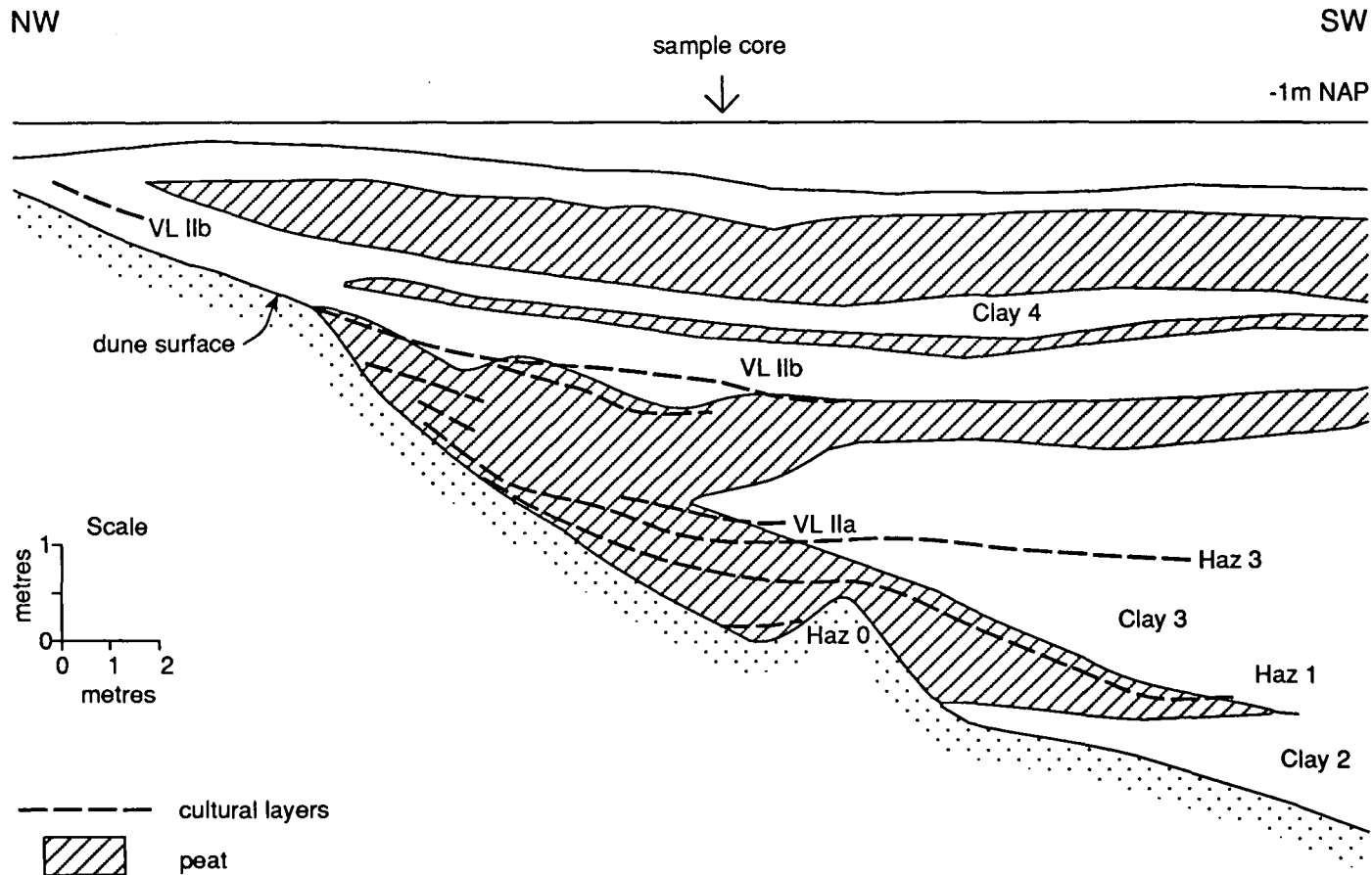
Detailed investigations of the Hazendonk by Louwe Kooijmans (1974) identified four main sedimentary units in the area (figure 2.7); the sandy clays of the flooding from the creek system; the sandy fill of the creek bed; thick clay with sandy lenses which is a flood deposit and occurs as a clay wedge associated with the stream ridges; the 'Alblasserwaard Cover', which is the cover clay deposited by the 16C transgression. The clay deposits are thicker away from the donk reflecting the depth of water at the time of deposition. Radiocarbon ages for the periods of clay deposition are given by van der Woude (1983) for a standard boring in the Molenaarsgraaf study area. These are given in table 2.2 below.

Table 2.2 Chronology of clay deposition in the Molenaarsgraaf area after van der Woude (1983).

Clay 4	-2.5 to -4.0 m NAP	3302-1523 BC (61, 62)
Clay 3	-6.0 to -7.3 m NAP	4506-3108 BC (59, 60)
Clay 2b	-8.2 to -9.5 m NAP	5490-4863 BC (57, 58)
Clay 2a	-9.5 to -9.7 m NAP	5540-5245 BC (55, 56)
Clay 1	-9.9 to -10.4 m NAP	5646-5539 BC (53, 54)

Estimates of compaction have been made for the four clay deposits (Louwe Kooijmans, 1974, which are of particular relevance when the past water content of the sediments is being estimated for the purpose of luminescence dating. The surface clay (clay 4) has been compacted by 80-100 cm, based on the difference in height on the donk slope and the river basin. Clay 3 is estimated to have been compacted by 60-120 cm during deposition, and only 30-60 cm after; clay 2 has undergone a total of 200 cm reduction, again primarily during deposition, rather than by the weight of later overburden. Clay 1 at the base is estimated to have compacted by about 3 m, of which 1.7 m are attributed to clay loading. South of the donk, compaction is much less, due to the tailing off of the donk slope, giving a well-founded base for the deposits.

Figure 2.7 Hazendonk stratigraphic section showing major depositional units and cultural layers (after Louwe Kooijmans, 1976)



Pollen analysis of the donk demonstrates varying degrees of clearance and cultivation coinciding with the dated culture layers. In general, cereal cultivation increases towards the later Neolithic and Bronze Age. Cultivation must have been severely restricted due to the lack of available land and wetness of the lower lying areas. The dune tops do not appear to have been extensively cleared in the earlier stages of occupation, suggesting that fishing was an important part of the economy initially. Grazing must have been limited by the small amount of available land, and communities may have had different specialisms depending where they lived (Louwe Kooijmans, 1976).

The Slingeland donk is similar to the Hazendonk, but larger in size, supporting bigger populations and greater variation in economy (Verbruggen, pers.comm.).

2.4.5 Chronological Control

The dates obtained by radiocarbon from the cultural layers and the peat deposits are directly related to the dates obtained for the sea-level curves on peat deposits near the coast. The chronologies of the Hazendonk and Slingeland dunes are based on a series of radiocarbon dates on the material of the cultural layers. The Hazendonk 1 level has been dated to 4149-4181 BC (63) (Louwe-Kooijmans, 1974), and the equivalent layer on the Slingeland dune to 4146-4179 BC (64) (Verbruggen, pers.comm.)

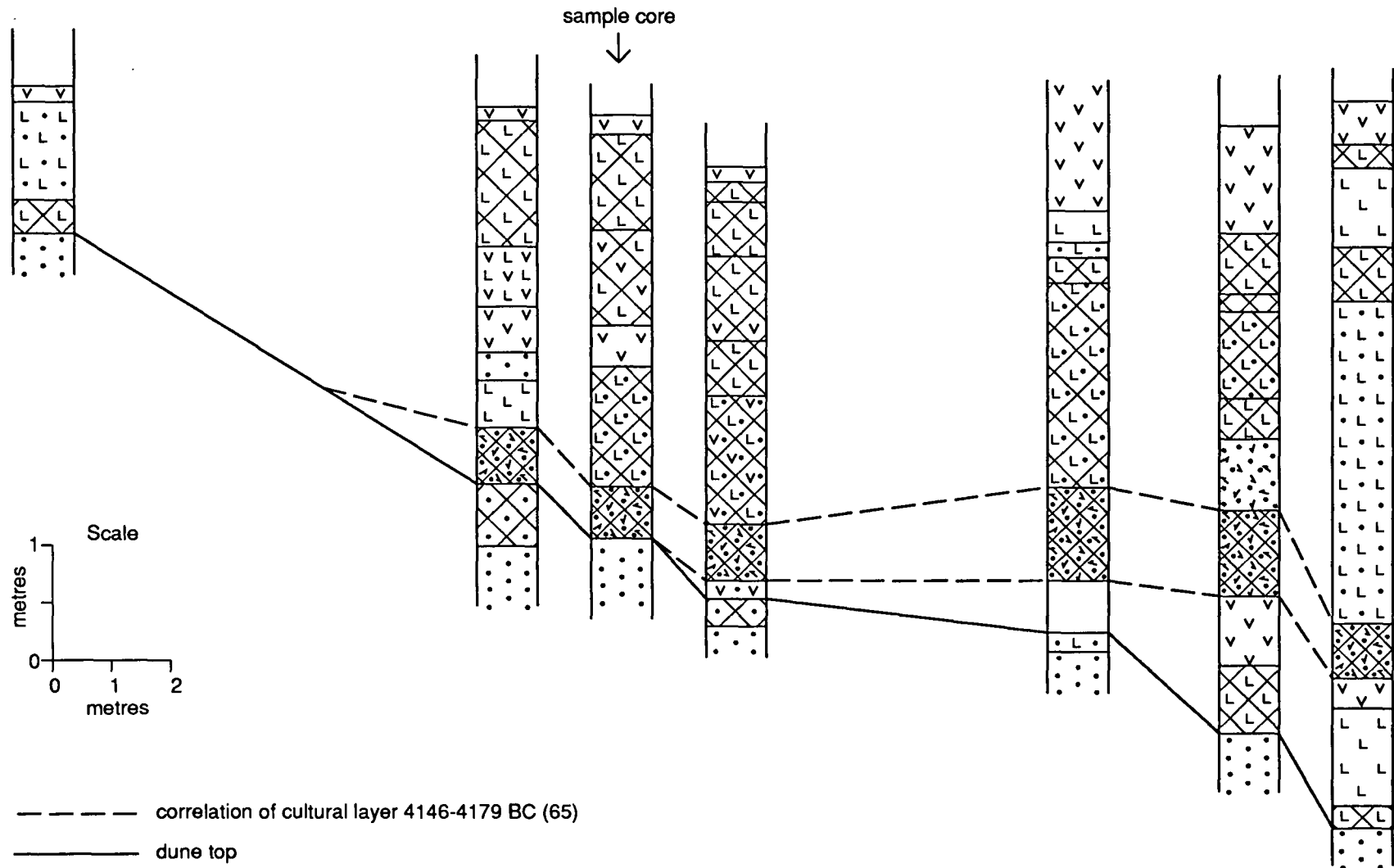
However, another date on the same material from the Hazendonk site gave a date of 3962-4000 BC (65), but was thought too young and not published. Verbruggen (pers.comm.) has suggested that this may be a more accurate date for the Hazendonk 1 layer, as it fits more accurately with the material from Slingeland and other dunes, and with Jelgersma's (1966) sea-level curve. However, the difference between the calibrated age ranges for Hazendonk 1 level consists of a minimum of 148 and maximum of 219 years. The application of luminescence in this case may contribute to the resolution of this disparity.

The clay deposits occurring in the Hazendonk core are the later Clay 3 and Clay 4 deposits. The former was laid down in the Molenaarsgraaf area between 3108 and 4506 BC (59, 60). The latter Clay deposit was laid down between 1523 and 3302 BC (61, 62). In the Slingeland core also, Clays 3 and 4 are identified.

2.4.6 Hazendonk and Slingeland; summary

Hazendonk in the Western Netherlands is an example of a 'donk', or sandy dune formed during the Younger Dryas from aeolian sand blown up from the dry river beds. Slingeland is one of a

Figure 2.8 Slingsland; transect through the sediments covering the dune (after Verbruggen, pers. comm.)



number of river dunes, formed when the sandy channel infill became upstanding from the surrounding landscape due to the shrinkage of the surrounding peat. The river dunes form series of sinuous disjointed ridges, and along with the donken, were foci for prehistoric occupation. They represented areas of relatively dry land within the lagoonal swampy environment of the region.

A number of periods of Neolithic and Bronze Age occupation are represented on the dunes. The sedimentary sequences consist of alternating peat and minerogenic horizons, although peat is more abundant in the sequences. The Hazendonk stratigraphic sequence includes three clay deposits which occur widely throughout the river dune region. Each of these were sampled. The ages of the clay deposits are determined by the intervening archaeological material, and can be correlated with a number of donken in the Western Netherlands.

The Slingeland sequence includes five layers of occupation compared to the maximum of seven on Hazendonk. The inorganic material, which represents periods of flooding, all post-date the Vlaardingen 1b culture phase, dated to 3044-3332 BC (46). The clays were laid down during the Dunkirk 0 and 1 periods of high sea-level stand, corresponding to Tiel 0 and 1 of the river-dune area. The clay deposits identified are the Clay 3 and Clay 4 units laid down between 3108-4506 BC and 1523-3302 BC respectively.

2.5 SUMMARY

All the sites selected for study, with the exception of Stubb Place, have an independent chronological control based on radiocarbon dates, calibrated to a standard curve. Stubb Place is included as a test site for luminescence dating of sediments without a chronological control. The sites have an additional dating control provided by an archaeological context, based on artefact and environmental (pollen) evidence as well as C-14. Additional environmental information is provided by sea-level data as in the Fenland (Shennan, 1985a, b), palaeosols and diatoms.

The archaeological context of the sites is important, not only as a dating control, but also as a demonstration of the application of luminescence to sediments from archaeological sites, in order to assess its value as an alternative dating technique to radiocarbon, for the time span of c.0-10 000 years. Most of the sites fall into the Neolithic and Bronze Age archaeological periods, and in many cases, the sedimentary deposits are close in age. The earliest occupation represented by the sites is of Mesolithic age, demonstrated at Eskmeals in Cumbria and at Hartlepool Bay. Neolithic occupation occurs at Hartlepool Bay, Cumbria and on the Dutch donken and river dunes. Bronze Age occupation is represented primarily by the major timber structure at Flag Fen. No archaeological horizons occur at Stubb Place.

CHAPTER 3 THE FORMATION OF SEDIMENTARY DEPOSITS, AND IMPLICATIONS FOR THE APPLICATION OF LUMINESCENCE DATING.

This chapter is in two parts; the first discusses the formation of sedimentary deposits, with particular reference to those processes which are directly relevant to later discussion of luminescence dating (chapter 5). These include exposure to sunlight during transport and deposition, and post-depositional effects such as those resulting from diagenesis and weathering. These processes affect the dose-rate to sediments and the physical state of minerals of importance for dating. The second part of the chapter presents the sedimentary analyses used in this study in order to examine selected aspects of the samples, such as mineralogy, particle size distribution and physical appearance.

The analysis of stratigraphic sequences is of great importance in the reconstruction of past environments of deposition and in wider environmental interpretations of climatic change. A sequence of deposits represents fluctuations in the depositional environment through time. For example, a change from marine to freshwater sedimentation may be represented by change in sediment type, rates of deposition and floral and faunal assemblages. This information can be used in support of luminescence dating in order to reconstruct the conditions under which sediments are likely to have been deposited, eg. to give an indication of water depth, sediment source and mode of transport. In this study, selected analyses of sediment samples are used in conjunction with luminescence dating, in order to assess the potential for dating waterlain material of Holocene age.

A graded boundary between two layers indicates a gradual change in depositional conditions, whereas a sharp contact generally results from a period of erosion followed by rapid burial (see section 3.1.2.2 for examples). The hiatus represented by the sharp contact may be of unknown duration, with an unknown depth of deposits removed. An example of this is at Chapel Point, Lincolnshire, where radiocarbon dating was applied to sediments relating to sea-level changes (Tooley, 1978a; p.155). Here erosional contacts were identified as the cause of discontinuities in the ages of the peats, and altitudinal differences in the contemporary overlying deposits. This stresses the importance of careful selection of dating samples, and, where possible, relying on the stratigraphic context of samples, and on additional independent dating techniques.

The type of sedimentary deposit is often indicative of the contemporary sedimentary environment. A sandy deposit indicates a higher energy flow than clays which settle in deeper, still water conditions. Peat formation indicates a period of saturation, or regular waterlogging, while pedogenesis indicates dryer conditions and surface exposure, allowing vegetation to develop, and soils to form. A deposit with graded or rhythmic layers within it may result from seasonal or

other cyclic control over sediment supply and deposition. Source and supply of sediment is itself a major controlling factor in the formation of deposits. A quantitative assessment of water depth and energy of flow cannot be made accurately, because so much depends on the source and abundance of the sediment supply, as well as local climatic conditions and the relationship to contemporary base-level.

Environmental reconstruction of sequences is problematic because of the 'pinhole' view afforded by cores. Lateral sections will reveal local variations in a layer while an individual core will not be able to do this, unless transects are made across a topographic feature. Correlation with nearby samples, can, therefore be difficult and erroneous, as in the case of Stubb Place. It is therefore important to have additional information relating to the stratigraphy of a site to enable correlation of sedimentary units to be made.

The identification of the depositional environment is important in terms of luminescence dating as transport and depositional processes affect the degree of exposure to light that the sedimentary particles receive before burial. Post depositional processes and activity associated with archaeological occupation may affect the stability of the luminescence signals over the timespan involved. Sedimentary processes are considered below in terms of the potential relevance to luminescence dating studies.

3.1 FORMATION OF SEDIMENTARY DEPOSITS

Sediments comprise minerogenic and organic material which may be derived from different sources and incorporated at different stages of transport, deposition or post-depositional alteration of a deposit. The formation of sedimentary deposits follows a cycle of erosion, transport, deposition and diagenesis. This simplified cycle of processes may be interrupted at any point and sediments may be reworked and redeposited several times before undergoing diagenesis. Each stage in this cycle will be considered in terms of its role in the luminescence dating potential of the deposits, and in identifying potential sources of error caused by these processes.

Stokes (1992) differentiates between multiple and single cycle deposits for the purposes of luminescence dating. Multiple cycle deposits include aeolian, beach and low energy fluvial sediments, and in this analysis are represented by sediments from the fluvial systems of the Dutch donken and the intertidal deposits at Hartlepool Bay. These sediments received repeated and more thorough exposure to sunlight before burial.

Single cycle deposits include fluvial flood, glacial and glacio-marine and colluvial deposits, which are exemplified by the tills at the base of the sequences in Cumbria and at Flag Fen. Such sediments tend to be 'dumped' in one event and are unlikely to be well-bleached during deposition. However, it should be noted that not all sediments in the 'multiple cycle' category may be sufficiently bleached. In some instances, the depth of water in a fluvial channel and the concentration of suspended sediment load is such that poor bleaching conditions prevail.

Forman and Ennis (1992) conclude that the depositional environment is a primary factor in the age determination of glacial sediments, and that present analogous contemporary environments are not necessarily good indicators of past environments, particularly where sea-level and climate changes are rapid. This applies to environments other than glacial, and emphasises the importance of the identification of the depositional environment by sediment analysis as an integral part of luminescence dating.

The comparison between testing the effectiveness of bleaching in known environments and using this as a key to past bleaching environments is difficult. The balance between sediment and water conditions is complex and so accurate reconstruction is not possible in many cases.

3.1.1 Transport and deposition

Sediments in this study were primarily transported by water, either fluvial, estuarine or marine. At some sites, such as Williamson's Moss, the sequences of waterlain material contain aeolian material derived from local dunes. As the dating of minerals by luminescence is based on exposure of the minerals to sunlight, the identification of different components which may differ in their bleaching histories (eg. by wind or water transport) is important in terms of the degree of zeroing before burial and the effect this may have on the age determination of the sample.

The mode of transport of minerals is reflected in the dominance of a narrow grain-size range, characteristic depositional structures, and in the surface appearance of grains (Reineck and Singh, 1980). Waterlain material is more rounded than aeolian grains, although the size and degree of sphericity will depend on the resistance of the mineral and the distance and conditions of the transporting water body. The marks of impact between airborne particles often forms crescentic hollows and the surface develops a matt finish, being abraded and slightly opaque. Grains are generally more angular than those transported by water.

Aeolian deposits fall into two main grain-size categories; loess, ^(silt) and sand sheets or dunes. Both are carried in the atmosphere. In the case of silt-sized loess this may be at considerable altitudes and therefore conditions for the solar resetting of the luminescence signal (bleaching) are ideal.

Loess has been deposited over extensive areas of Europe and Asia to depths of hundreds of metres. It was derived from devegetated landscapes under periglacial conditions during the last ice-age. Loess is not found at the sites selected, but sand dunes and sheets are locally extensive in Cumbria. The significance of the recognition of the aeolian component in these sediments has already been mentioned.

Several types of waterlain depositional environments are found at the sites investigated and each will be considered. These include fluvial (eg. Hazendonk, Slingeland), intertidal and lagoonal or lacustrine (eg. Williamson's Moss and Eskmeals) and estuarine and marine deposition (eg. Flag Fen and Hartlepool). A summary table of the potential effectiveness of bleaching in the different environments is given in Table 3.1. The application of luminescence dating may aid the identification of past depositional environments and the of the grain-size fraction of greatest potential for accurate age determination in different environments.

TABLE 3.1 Comparison of effectiveness of bleaching of different sedimentary environments

Sediment	Likely Degree of Exposure	Other Controlling Factors	References.
aeolian	full sunlight; good exposure	re-exposure and reworking of dunes.	Wintle & Huntley, 1980
fluvial lacustrine	Reduction in UV and short nm with depth	Depth at which sediment is in suspension, turbidity, amount of suspended load incorporated bed/bank material	Berger, 1990 Kronberg, (1983) Gemmell, 1988
intertidal	full exposure at each low tide	rate of deposition per tidal cycle, mixing and reworking	Rendell, et al, 1989 Berger, 1990
Soils	Variable; generally poor	bioturbation, incorporation of other material eg. aeolian weathering	Forman et al, 1988 Wintle & Catt, 1985 Rendell & Townsend, 1988
Tills/glacial	Negligible by sunlight:	grinding thought to be main zeroing mechanism.	Lamothe, 1988 Hütt & Yungner, 1992 Forman, 1988

3.1.1.1 Fluvial Environments

Sediment is transported by rivers either as bed-load, suspended load or as solutes. Here we are primarily concerned with the suspended and bed-loads of the river. The differentiation is based on grain size and the carrying capacity of the water body. The suspended sediment load generally consists of the silt and clay fractions. The sediment may be derived from a wide range of terrestrial, aeolian and marine sources, depending on location and environment. Different fractions of the sediment load are likely to have undergone different degrees of exposure, depending on previous modes of transport, grain-size, etc. Within the river, different fractions may be bleached to different degrees depending on distance or the depth at which they are carried in the water body (eg. Gemmell, 1988).

The grain size of the sediment may give an indication of the fluvial conditions but will also depend on the supply of sediment. Coarser material is deposited more rapidly in the event of a reduction in river velocity, whereas finer material may remain in suspension for considerable periods of time. Finer sediments tend to reflect slower velocities and deeper water. It is not possible to reconstruct the flow velocity and depth of water from the grain-size of sediment alone, as the source of supply, climate, channel configuration etc. are important controlling factors (Reineck and Singh, 1980).

The main concern with fluvially transported material to be dated by luminescence is the effectiveness of bleaching during transport and deposition. Some work has been done on the variation in intensity and wavelength of bleaching light with depth, turbidity and sediment load. Kronberg (1983) studied the attenuation of bleaching light with depth, and found that up to 0.7 m depth, there was no significant reduction in the efficiency of TL bleaching. However, an estimation of 50% reduction in efficiency under 7 m of lake water was observed. This indicates that relatively short bleaching times (c.17 hrs.) are needed for complete bleaching in relatively clear water of <1m depth.

Gemmell (1988) investigated the effect of distance on the degree of bleaching of sediment in a fluvio-glacial stream. This was found to increase non-linearly with distance from source, and this was attributed to the incorporation of 'older' unbleached material from the bed and banks. This created a significant discrepancy in age estimations of fine-grained material. Berger (1990) distinguishes between the bleaching of different waterlain deposits from different environments; the 2-11 μm fraction from sandy river bars was more effectively bleached than an associated silt bar deposit, and Berger suggests that Holocene fluvial sediments are only suitable for dating where the sand fraction is selected.

Poor bleaching of rapidly-deposited glaciofluvial sediments was also a problem encountered by Hütt and Jungner (1992). High levels of suspended material reduce the effective bleaching of sediments (Ervanne et al, 1992) and are a factor of greater importance than turbulence where suspended levels are high (>0.05 g/l), whereas low suspended sediment loads (<0.02 g/l) had little effect on the bleaching of the sediment (Ditlefsen, 1992). Comparisons between bleaching of the TL and IRSL components of the signal show that the IRSL bleaches by 95%, but the TL by only 25-50% for given levels of turbulence (Ditlefsen, 1992). Sediments carried in fluvial environments may also undergo some chemical alteration and changes in composition. There is generally an increase in the proportion of resistant quartz minerals, and a reduction in feldspars with time and distance. Clays become increasingly dominated by kaolinite and vermiculite types (Johnson and Meade, 1990).

The deposition of fluvial material results from a reduction in the velocity and therefore carrying capacity of the water. This may be due to entering a lake or the sea, or changes in the gradient of the river bed, or recession of flood waters from an alluvial plain. In the last case, exposure to sunlight is likely to be enhanced. In the former cases, the finer material is generally carried further out into the lake and will settle out more slowly and thus may receive additional bleaching light. Coarser material will often form a delta or fan deposit near the entrance of the lake, so only the surface may be completely bleached. This will depend on the depth of water, rate of deposition and amount of reflection from fine material in suspension.

The advantage of using IRSL in these conditions is that the sunlight sensitive luminescence signal within the crystals is measured using this technique rather than the sunlight insensitive signals which are not measured using optical techniques, but are measured using TL. This is important where samples may have been exposed to attenuated light for shorter periods of time. The size of the unbleachable residual is less important in measurements of the IRSL than in the case of TL (see Chapter 5). Examples of sites where the material is predominantly fluvial in origin are the Dutch river dune sites at Hazendonk and Slingeland. IRSL measures the signal predominantly from the feldspar fraction, which is known to be more sensitive to bleaching under sunlight; Ervanne et al (1992) demonstrated the effective bleaching of the TL of the feldspar fraction in alluvial sediments, but not of the quartz fraction. Feldspars in these cases are therefore the preferred mineral for dating.

3.1.1.2 Intertidal Environments

The sites sampled at Hartlepool Bay and in Cumbria experienced intertidal or perimarine conditions in the past. The Neolithic age peat at Hartlepool now exposed at the surface at low water is presently being eroded. The surface deposit comprises a mixture of eroded limnic material and

sand. The intertidal zone here includes a fossil tidal slack, mudflat or lagoonal deposit formed behind a ridge of till to seaward (Tooley, 1978b). These are the intertidal environments of greatest concern here. The formation of tidal mudflats occurs when the velocity of the wave is zero at high and low tides, and greatest at mid-tide (Pethick, 1984). Under these conditions, material is moved onshore and deposited faster than it is moved offshore. The material is exposed at each low tide and therefore well bleached before subsequent layers are deposited by succeeding high tides. The upper limit of mudflats lies at just below mean high tide, ensuring their exposure during each tidal cycle. Sand deposition occurs in a similar manner and the rolling of grains by currents increases the chance that they are adequately bleached. For this reason, intertidal deposits are likely to be well suited to luminescence dating. This argument is supported by Berger (1990) who suggests that such sediments are the most suitable coastal facies for dating.

However, if intertidal sediments are shown by luminescence to be poorly bleached, it may be inferred that they were deposited under different conditions, such as in a lagoon of relatively deep water, recharged with sediment at each high tide, or deposited as a deeper water marine facies under conditions of higher sea-level. In these cases, the use of diatoms and other micro-organisms can be valuable environmental indicators. TL could be used as a diagnostic tool in the identification of past depositional environments in such cases, together with biogenic, stratigraphic and other evidence.

3.1.1.3 Lagoonal and Lacustrine Environments

Sediments may be deposited in lagoons formed behind tidal barriers. These barriers may be sufficient to prevent all but the highest tides from entering, or they may be landlocked only at low tide. If they do not drain completely at low water, the sediment may remain in suspension, and so become bleached while in suspension. Alternatively, bleaching may be reduced for material which settles out faster. If the lagoon drains at low tide, the surface sediment is likely to be well bleached during each low tide period, and a layered effect may result from alternating bleached and unbleached sediment. This would require high rates of deposition at each tidal cycle, and minimal mixing of layers. In most tidal environments, these conditions are less likely than conditions where sediment deposited at each tide is mixed with material from the previous tide, and the amount deposited is such that it is all exposed to sunlight before burial.

The archaeological site at Flag Fen is constructed on a marshy area which was thought to have been open water at the time of occupation (Pryor et al, 1986). Deposition into a lake such as this would be differentiated according to grain-size, with coarser material forming a fan at the point of entry into the lake, and finer material settling in the open water area. Bleaching would depend on the depth of water, and degree of reflection from suspended sediment. In the Dutch river dune

area, where deposition results from alternating lagoonal and lacustrine environments, bleaching may not be complete during periods of flood deposition or greater water depth. This is difficult to estimate from the sediments alone. In addition, the incorporation of an aeolian component eg. at Williamson's Moss, where sand is derived from nearby coastal dunes, may increase the complexity of the sediment with respect to its bleaching history.

An influx of coarser material may be due to flood events from higher run-off from rivers, or tidal washover. The use of diatoms can aid the identification of the source of sediment (ie. predominantly fresh or marine water conditions). Berger (1985) studied the deposition of material in a glacio-lacustrine environment and observed no significant resetting of the silt fraction of a rapidly deposited silt of known age. He suggests that such material is not suitable for dating. The quartz fraction was also found to be insensitive to wavelengths above 400 nm, but the feldspar fraction was sensitive to all visible wavelengths. This supports the proposal of this study to date the feldspar fractions by IRSL in order to select ~~the most potentially~~ suitable fraction from deposits.

3.1.1.4 Estuarine and Marine Environments

Estuaries function as sediment sinks. Material is trapped by the estuarine circulation and tidal current patterns; by a reduction in current competence (ie. ability to carry sediment) and by flocculation of clays and organic complexes. During river flood periods, material leaves the estuary, but during high tides, material is trapped within the estuary, which represents a highly dynamic environment. There are no truly estuarine deposits identified in this study. Those demonstrating brackish water conditions from their fauna tend to occur in tidal slack lagoons, eg. Eskmeals and Williamson's Moss. Marine deposition occurred over the Fenlands and on the Cumbrian Lowlands as a result of Post-Glacial sea-level rise, when large spreads of clays and silts were deposited over the Fens and other areas of low-lying land around the British Isles. Such material may not have been sufficiently bleached due to the depth of water, rate of deposition and amount of suspended material. These deposits can be differentiated from lacustrine deposits due to their fauna, extent and associated changes in vegetation. The application of the IRSL may enable age determinations where TL is less successful.

The source of the marine-deposited material is important as it may affect its bleaching history. Deposits derived from terrestrial sources and transported by rivers may be more thoroughly bleached than that derived from marine sources. The identification of the source of material may be difficult, but the Fen Clay and marine silts on the Fenland are generally thought to derive from marine sources. If these were laid down under deep water conditions, bleaching may not be complete. The Fen Clay depositional environment is interpreted as one of quiet water sedimentation (Shennan, 1985a) but the depth of water is difficult to assess.

3.1.2 Post-depositional change

Following deposition of material, there are several processes which alter the nature and composition of the sediment. In terms of the application of luminescence dating these may affect the dose-rate and the ability of minerals to accumulate and store this radiation charge in a stable manner. The processes of greatest importance here are compaction and diagenesis, pedogenesis (soil-formation) and weathering of minerals *in situ*. The effects of human occupation on sediments is also relevant, in terms of trampling, incorporation of material from other sources, and disturbance of soils.

Properties of freshly-deposited material are controlled in part by the conditions of the depositional environment (Krumbein, 1942) and change is controlled by the diagenetic environment, such as pH, Eh, chemical activity and availability of ions for exchange. In addition, compaction affects the water content of the sediment, and the resultant reduction in porosity reduces the movement of water and ions, such as weathering products or radioactive isotopes. Water content has significant implications for the dose-rate to minerals. Pedogenesis involves the incorporation of organic material from vegetation and microfauna and allogenic minerals (eg. aeolian of alluvial deposits) into the profile, mixing older and younger material, and affecting the dose-rate by the presence of organic material. Weathering of minerals, such as during soil-formation, alters the crystal structure and may therefore affect the stability of a mineral with respect to storing trapped charge.

The identification of these processes in a sedimentary sequence is therefore of significance with respect to luminescence dating, as these processes may lead to greater errors or incorrect age determinations. Such potentially problematic samples could be avoided if identified before extensive laboratory measurements have been conducted.

3.1.2.1 Compaction and Diagenesis

As the depth of burial of a sediment increases with further deposition on the surface, the sediment will undergo some compaction or consolidation. These two processes are not synonymous; compaction is defined as "a decrease in bulk volume or thickness of, or porespace within, a body of fine-grained sediments in response to increasing weight of overlying material from continued deposition, or to pressures resulting from earth movements within the crust. It is expressed as a decrease in porosity due to tighter packing of sediment particles" (Bates and Jackson, 1980). Consolidation is defined as a "gradual compression of cohesive soil due to a mass acting on it, which occurs as water is driven out of soil voids" (Barker, 1981). Compaction is often seen as a

'natural' process while consolidation is caused by artificial pressures, such as construction works (Gillott, 1990).

The main result of compaction (ie. the 'natural' form of the process) is a reduction in porespace and consequently the water held within the sediment. Water is observed to have an attenuating effect on the dose-rate to sediments (Aitken, 1985; 22), but this is likely to have greatest effect where the water is stored in larger voids, which contribute to the attenuation of alpha rays in particular. Tooley (1978a) refers to primary compaction (up to 50% of the total volumetric reduction) which occurs very rapidly after deposition, and secondary compaction occurring much more slowly, at rates which may be linear with log-time (Barden, 1968). Compaction can also affect the environmental interpretation of sequences. Van de Plassche (1980) illustrates this in the Netherlands where peat overlying sand has become compressed, forming a more graded boundary between sand and peat than was originally laid down. Consolidation of sand is very slight, but peat may be reduced 90% by volume (Jelgersma, 1961).

The state of overcompaction, in which the sediments have been compressed beyond their capacity to recover their previous open structure when the overburden has been removed, is of great importance in the estimation of past water contents. Overcompaction will significantly reduce the pore space available for water, and this change will be permanent. However, it may also be thought to 'stabilise' older sediments, by reducing variations in water content through time. The packing of sands and the infilling of voids by silts and clays may significantly reduce the amount of water, and the freedom of flow through even relatively large-grained material. To some extent this will serve to reduce the amount of short term fluctuation in water content.

Estimates of the degree of compaction which the clays at the Hazendonk have undergone provides valuable information in terms of the estimation of past water contents. In this case, the compaction has been evaluated from differences in height of contemporary deposits (both upper and lower contacts) between the donk slope, where the sediments are 'well-founded' (ie. they have a firm, non-compactable base) and sediments lying in the centre of the basins between the donken. Louwe Kooijmans (1974) attributed much of this compaction to deposition under quiet water conditions. These sediments have been waterlogged since deposition, and therefore the measurement of the present porosity, and assumptions regarding minimal deviation from saturated conditions are more applicable here than in cases of sediments compacted after deposition. Such sediments may include those containing a mixture of grain sizes, and lying in the upper layers of a sequence, and have thus been affected by pedogenesis and possible water-table fluctuations, eg. the upper layers of the Cumbrian cores.

3.1.2.2 Water Content

Water content in sediments lying below the groundwater table or below base level, will vary primarily as a result of the grain size distribution and packing, which controls the amount of interparticle space, and on the degree of compaction, discussed above. Skempton (1970) observed that fine silts and clays laid down under transgressive conditions which settled slowly without disturbance may be laid down with 95% compaction (eg. at Hazendonk). There is a direct relationship between the amount of clay and the porosity of a sediment, but this cannot be used to predict the amount of compaction a sediment has undergone. Coarse grained sediments are less affected by compaction and resultant water content changes are less than for finer clays and silts. However, variations in compacted silts and clays will be less than for compacted sands.

Modern delta deposits investigated by Skempton (1970) were deposited at rates of several metres per year, and had higher porosities, although this was in part related to the higher organic content. Estuarine sediments from the early part of the Holocene were deposited at rates of around 0.002 metres per year (2 m/kyr). The depositional water content of these consolidated clays could be estimated from the Atterberg limits of the deposits, in relation to the water content of the top 25 cm of the unconsolidated material. This would not apply to the sediments which are consolidated at the top of a stratum, or which have been truncated by erosion or exposed at the surface for sufficient time to allow desiccation to occur.

Over-consolidation of deposits is permanent and so the water content of the material will be effectively stabilised with respect to significant variation, and the value of the water content will be the same for the period since overconsolidation was complete. The length of time since this occurred may be difficult to evaluate and so this value cannot be taken as the assumed water content for the whole burial time.

3.1.2.3 Pedogenesis

Sediments exposed at the surface may be subject to pedogenic (soil-forming) processes. Palaeosols can be difficult to identify within stratigraphic sequences, especially where younger soils have developed into older ones, or profiles have been truncated by erosion. Different processes can lead to the same soil characteristics. Particular formations can result from different processes or combinations of processes. Changes in climate, landuse, drainage and particularly vegetation, whether natural or anthropogenically induced, can reverse processes, and breakdown formations already developed. This reflects the dynamic nature of soil as a cause and effect of vegetational change and other local factors.

Micromorphological analysis is generally required for the identification of soil horizons. However, this requires that the samples have not been significantly affected by compaction either during burial or sampling, and the latter case was a problem affecting the application of such analysis in all core samples in this study. The sequences at Flag Fen, Stubb Place and Williamson's Moss contain layers which are remnants of old soils or land surfaces, but the firm identification of these as such rests on their archaeological associations, described in the previous chapter, and in the structures identified in the profiles of corresponding strata from different sites or samples. The descriptions of the Fenland buried soils (French, 1988a, b) are an important environmental indicator, although the soils themselves are not represented in the Flag Fen profile.

Soil development can only begin when sediments are no longer affected by regular seasonal waterlogging or conditions of continuous saturation. This is effected by a lowering in the local water table by artificial drainage or by changes in climate and sea-levels. This enables a flow of water through the sediment along moisture gradients, and associated movement of elements in, through and out of strata, leading to the development of soil horizons. Where significant peat accumulation has occurred, soils will often only develop once most of the overlying peat has wasted away (Catt, 1979).

The process of soil formation is of greatest importance in terms of luminescence dating for several reasons. Soils can form important stratigraphic markers in Quaternary sequences, eg. the Valley Farm and Barham Soils in southern East Anglia (Kemp, 1985; Rose et al, 1985). Their accurate dating is therefore of great value to regional Quaternary chronologies. The processes of primary concern are those related to bleaching of the minerals (translocation and bioturbation), dose-rate to minerals (incorporation of organic matter) and alteration of minerals (weathering). This last case is discussed in the following section.

Bleaching of minerals in soils has been recognised as a problem in the application of luminescence dating generally. Soils comprise material derived from weathered bedrock or from colluvial, alluvial or aeolian material. Much of this material may not be exposed to sunlight during soil development. The incorporation of well-bleached aeolian material results in a deposit containing material of very different 'ages'. Mixing occurs by bioturbation and by translocation of fine particles by percolating groundwater. Pedogenesis may be very slow, and exposure of individual components limited to the surface only. For this reason, many soils have been dated successfully, despite lack of close chronological control, producing an age estimate for the time of burial of a soil, by dating the upper 'A' horizon.

Dating of the A horizon has been successful in loess sequences (eg. Wintle and Catt, 1985), although Berger and Huntley (1986) indicate that A horizons developed in alluvium or colluvium

are not suitable. Wintle and Catt (1985) found stratigraphic reversals in their dated sequence. This was attributed to the reworking of B horizon material, but they also refer to 'some process associated with soil development' which had partially reset the TL of feldspars in loess. Forman et al. (1988) demonstrate some difficulties in dating soils developed into colluvial and alluvial sediments due to incomplete zeroing.

Translocation of material in profiles increases the complexity of the bleaching history of a soil. The material may be redeposited at depth and if derived from near the surface, will be more completely bleached than the surrounding material. This mobility will affect the choice of grain-size to be dated. The movement of clay minerals within profiles often results in the coating of mineral grains by clay particles. If the clay coating is sufficiently thick, it may reduce the potential bleaching of the mineral grains before burial. Coatings of clay minerals are proposed as a cause of incomplete bleaching of quartz (Prescott and Fox, unpublished data) and for low intensities of luminescence emissions (Questiaux, 1991).

Translocation includes the movement of ions and water, which has repercussions in terms of the variation in water content and in the movement of radio-isotopes. The incorporation of organic material, which preferentially absorbs isotopes such as uranium, can also affect the dose-rate if present in large quantities. Grains extracted from peat may be affected by dose-rate problems. This makes them difficult to date, as clays can absorb organic matter which is enriched in uranium and will be more affected than larger grains due to their greater surface-area to volume ratio.

3.1.2.4 Weathering

Weathering of minerals results in the physical or chemical alteration of minerals. Physical weathering processes are based first on changes in temperature, which exploit the differential heat capacity of minerals, particularly in arid regions with a high diurnal range of temperature; secondly on the crystallization of salts causing local pressures, and thirdly of water as in freeze-thaw action which also relies on temperature change. Chemical weathering processes are of greater importance, particularly in temperate and tropical climates where temperatures and water supply are likely to be sufficient to activate the processes throughout much of the year. Chemical weathering affects the structure of minerals, especially quartz and feldspar, causing compositional change which may alter their ability to accumulate trapped electric charge.

Hydrolysis is a chemical process involving the H^+ and OH^- ions from water and is very important in the breakdown of feldspars. The reaction of orthoclase (potassium feldspar, $KAlSi_3O_8$) and water for example, produce potassium hydroxide and alumino-silicic acid, which, together with carbon dioxide from the atmosphere, produce potassium carbonate and water. The alumino-silicic acid is

unstable and breaks down to form clay minerals and colloidal silica which is removed in solution, following the formulae given in the following section. This process is accelerated by the presence of carbon dioxide.

The presence of humic acids produced from the breakdown of organic matter is important in the mobilisation of metals from otherwise insoluble solids, by the process of chelation. Chemical complexes form between organic molecules and metal ions, particularly iron and aluminium, which are then removed by leaching. Humic acids are generally stronger than carbonic acids and so have a greater effect. Organic acids also attack minerals in wetter conditions, producing soluble ions and clay minerals. Proximity of samples to acidic influence therefore, needs to be considered in stratigraphic sequences.

The stability of minerals varies with their structure and presence of impurities. Quartz is highly resistant to both chemical and physical weathering and clay minerals tend to be inert except through lattice impurities. However, it has been demonstrated (Bennett, 1991) that the presence of organic electrolytes increases the solubility and mobility of silica at near neutral pH and low temperature conditions. Simple dissolution is the dominant process in quartz weathering, and causes an increase in the porosity of the material (Nahon, 1991), especially in soils where water flow is unimpeded and compaction is minimal. The presence of organic acids in natural water greatly enhances the rate of feldspar dissolution compared to dissolution in water of a similar pH, but with no organic acids (Lundström and Ohman (1990).

The potassium feldspars are the most resistant of the feldspar group and the calcium varieties are the least, due to the high susceptibility and mobility of the calcium component. Where suitable ions are present, kaolinite formation is favoured in acid conditions, and montmorillonite in more alkaline and wet conditions. Clay minerals are formed during weathering, and may be deposited as grain coatings, thus impeding further degradation of the coated mineral. The expanding layer clays (2:1) are highly susceptible to further breakdown, mainly by ion exchange, but the 1:1 layer clays, such as kaolinite, are more resistant to alteration, having a more stable structure.

The effects of the weathering of feldspars is considered in more detail in Chapter 7. This is important in this study because feldspars are the main mineral from which luminescence measurements are made. This is because feldspars are abundant in most sediments, they possess a strong luminescence signal and can be measured using both IRSL and TL dating.

3.1.3 Summary

A variety of sedimentary environments are demonstrated by the selected sites. These include fluvial, intertidal, lagoonal-lacustrine and marine environments. The analysis of the sedimentary environment is important with respect to luminescence dating for two main reasons. First, the potential bleaching of the sediments before burial will depend on the conditions under which they were deposited. The spectrum and intensity of sunlight is reduced by depth and turbidity of water, and the concentration of suspended sediment load. The environment of deposition can to some extent be inferred from the sediments of a stratigraphic unit, although this will also be determined by other factors such as source of sediment.

Secondly, post-depositional changes may also extensively affect the chemical and physical properties of a sediment, and therefore its luminescence signals. Such changes include compaction, which reduces the pore-space, and hence water-content, and the effects of pedogenesis and weathering *in situ*. Uncertainties in the evaluation of past water-contents contribute a significant proportion of the total error of luminescence dates which may be reduced for sediments shown to have been compacted at deposition, rather than later in their burial history as a result of loading. This is the case for the Dutch river-dune sediments.

Pedogenesis may be difficult to recognise in sedimentary sequences. Exposure of minerals in soils is facilitated by bioturbation and the incorporation of material at the surface, eg. aeolian material. In the latter case whereas aeolian material may be of younger luminescence age, related to exposure before incorporation, but material in the soil profile may not have been exposed and may therefore reflect the age of the parent material rather than the period of soil formation. The recognition of such events in the soil profile is important as it may determine the most suitable fraction for luminescence dating. The sequences at Williamson's Moss and Stubb Place both indicate that material has been incorporated from an aeolian source.

Finally, the weathering of minerals, particularly feldspars in the sediment profile after burial is a process which has not been studied before with reference to luminescence dating of sediments. Examination of the sediments and the evidence of weathering is an important aspect included in this study, and is investigated in detail in Chapter 7.

3.2 TECHNIQUES OF SEDIMENT ANALYSIS

There are a wide variety of techniques available for the analysis of sedimentary deposits. The techniques selected for this study are those which give the best indications of the origin, transport, environment of deposition and post-depositional processes affecting deposits sampled.

For the purposes of this investigation, the emphasis is first on the reconstruction of the "bleaching history" of a sediment, and the potential effectiveness of bleaching under the indicated conditions of transport and deposition. Secondly, post-depositional processes may have affected the dose-rate or crystal structures of quartz and feldspar which will cause errors in measurements of trapped charge as a function of dose-rate and time since deposition. Thirdly, changes in water content are due to compaction and to variations in groundwater tables; these may be recognised in a stratigraphic sequences by recurrence surfaces and soil formation. Finally, the stratigraphic sequence as a whole is an important source of information regarding changes in environmental conditions relevant to the dose-rate. This is considered in more detail in Chapter 5. Interfaces between minerogenic and highly organic sediments may be centres of enhanced weathering activity and variable dose-rate to sediments. Sampling near to such interfaces needs to be treated with caution.

The characteristics selected for study were the particle size distribution, mineralogy and elemental composition, physical state of the grains, and organic carbon and water contents. In order to evaluate the variability within the deposit and to identify evidence of post-depositional change, associated particularly with diagenesis, the particle size distribution, water content and the level of organic carbon were also measured at 10 cm intervals throughout the minerogenic parts of the cores. The sediment sequences were described using Troels-Smith's (1955) method of classification, and interpretations of the depositional environment with respect to luminescence dating were made based on the descriptions and results of the analyses. These are presented in the following chapter.

3.2.1 Sampling

Samples were taken using a piston corer, which enables samples of the sediment to be taken without exposure to daylight. The corer extracts a 1 m long sample, 6 cm diameter, in steel tubes. These were then extruded under controlled red light conditions in the laboratory. There is a significant amount of compaction of the sediments during sampling and in order to correct for this, a narrow bore Dutch auger sample was made first, and the stratigraphy and depths recorded in the field, using the system devised by Troels-Smith (1955). The piston core holes were then made immediately adjacent to this control, and the stratigraphy matched up with the Dutch auger record.

After extrusion, the cores were split horizontally. One half was then wrapped in black plastic for dating, while the matching half was used for sedimentary analysis.

In the case of Hartlepool Bay, a machine trench was dug, and the sample face cleaned and recorded. The samples were taken in 0.5 m long monolith tins, wrapped in black plastic and returned to the laboratory. Samples were extracted from the centre of the units in the tins, to ensure that the part sampled for dating had not been exposed to light.

3.2.2 Dosimetry

The dose-rate to samples is measured by the placement of sealed copper capsules containing annealed natural calcium fluoride into the ground for one year, after which they are retrieved and measured. For the sections sampled at Hartlepool Bay, the dose rate was measured using a portable gamma ray spectrometer. Where possible it is advantageous to use both methods and then make a comparison. However, for most deep core samples, it was not possible to take gamma-ray spectrometry measurements, and at Hartlepool Bay, dosimeters could not be left *in situ*.

The dosimeters were suspended level with the minerogenic and organic strata in the boreholes, at depths determined from the Dutch auger core. This enabled dose-rate measurements to be made for the different sample layers and intercalating peats throughout the depth of the cores.

Dose-rate measurements can also be made from the sample, using alpha counting, beta TL dosimetry and XRF analysis of the potassium content. These are discussed in Chapter 5. This was performed on all samples, both as a comparison with the dosimeters, and as primary dose-rate data for one site (Stubb Place) where the dosimeters could not be retrieved.

3.2.3 Water Content

Changes in water content of sediments is known to have significant effects on the dose-rate and is a major component of the error in calculated ages which increases with greater water contents of samples (Aitken, 1985; 250). The present water content of samples is easily measured, but it is not always appropriate to extrapolate this back through several thousand years, eg. Rendell (1983) identified collapse structures in loess resulting from loading which significantly reduced the saturation water content of the material, as compared to uncollapsed material from the upper part of the section. The effects of compaction of waterlain sediments is important and has been discussed above with respect to sediments, and in Chapter 5 with respect to luminescence dating techniques.

The recognition of such evidence is important in terms of the evaluation of the past water content. The water-content at the time of sampling and saturation water-content values are measured and a correction factor applied for the attenuation of the dose-rate due to the presence of water in the pores. Aitken (1985) used a figure of 80% of the saturation value with an error margin of 20%. The validity of this is assessed in terms of the measured water contents of the samples in Chapter 5.

The variation in water content between layers is also important; fine-grained silts can hold more water than freely draining sands, because of the great abundance of small interstitial pores. However, water flow through fine material is restricted by the small size of pores, so weathering products may not be carried away as quickly as in coarser sediments. Sands are dominated by quartz which is highly resistant to weathering. The advantages of free leaching will not always therefore result in faster rates of degradation, except where the coarser deposits contain relatively susceptible minerals such as some feldspars. Changes in water content of coastal areas will in part reflect changes in sea-level. During periods of higher sea-levels, the local groundwater table will rise.

Water content is normally calculated as a percentage of dry weight or wet weight of soil which has been oven dried at 105°C for about 24 hours. Reconstructions of the water holding capacity (consisting of void space and pore space) can be achieved by soaking sediments and calculating the volume of water absorbed. This gives a maximum saturation value for the sediment, relevant to the error used for age evaluations. However, this requires that the sample has been structurally undisturbed. This will not be the case in samples extracted using some coring devices including the piston corer used here.

3.2.4 Particle Size Distribution

The analysis of the particle size distribution of a sediment is a fundamental sedimentological technique and is important in the reconstruction of the environment of deposition. For example, compared to material deposited by coastal or fluvial processes, aeolian sediments tend to have a very narrow range of sizes, predominantly silt in the case of loess, or sand in the case of dunes (Reineck and Singh, 1980). The size distribution of waterlain material will reflect the supply of sediment and the velocity of the water body and the energy of the depositional environment. This does depend on the source and supply of the sediment. Floodplain material is often characterised by a fine 'tail' in its particle size distribution; the fines are left on the surface as the floodwaters drain away. Fine-grain river channel deposits do not have this tail, as the very fine fraction is maintained in suspension, even at very low velocities.

Particle size analysis (PSA) is important in the context of this study as it is an indicator of the depositional environment. It does not, for example, distinguish between aeolian and fluvial material. PSA however should not be used alone as the physical appearance (shape, roundness and surface texture) of the grains will also reveal features characteristic of transporting agents. The use of core samples requires a correlation with the sediment sequences identified in the surrounding area; eg. the Rhine-Meuse delta area has been extensively researched and a regional environmental reconstruction through time can be proposed, into which the sample core is fitted. Thus the regional interpretation, which may include the wider contemporary processes and sediment sources is of great importance in the identification of past environments. PSA can serve as a tool for the correlation of sediment types within such a region.

The grain-size of a sediment is to some extent an indication of the mode of water transport; coarser material is more likely to travel as bed-load and therefore may not be so completely bleached as the suspended silt fraction. PSA will also determine the modal grain-size, which may determine the most representative size fraction to be selected for dating a particular sediment.

The measurement procedure followed that described by the BSI 1377(1975) procedure. The subsample was sieved. The fraction above 63 μm was sieved further using 2 mm, 600 μm and 210 μm sieves. The percentage proportions of the sand fractions were calculated using the formula $100W_f/W_b$, where W_f represents the weight of a given sieve fraction, and W_b the weight of the original air-dried sample.

The material finer than 63 μm was subdivided by sedimentation in 500 ml water containing 20 ml sodium hexametaphosphate as a deflocculating agent. The sedimentation extraction times were based on a mean sample specific gravity of 2.65, so an extract was taken after 4m 5s, 46m and 6h 54m. These were dried and cooled in a desiccator and weighed. A control extraction of the sodium hexametaphosphate in water was also taken, weighed (P) and this was subtracted from the weight of the original dry sedimentation sample.

The calculations for the percentage proportions of the original sample were made using the pretreated weight (W_b). The proportions were evaluated by $M = (W/V_p)500g$ where M is one of the extraction weights, M_1 (4m 5s), M_2 (46m), M_3 (6h 54m) or M_4 (weight of deflocculant), W is the weight of solid material in the 500 ml suspension for the different extraction times (ie. corresponding W_1 , W_2 , W_3 , and W_4), and V_p is the calibrated volume of the pipette (here 9.9238 ml).

The percentage proportions of the sample size fractions of the original sample are calculated by :

medium silt (0.02-0.006mm) = $(M1-M1/Wb)100$

fine silt (0.006-0.002mm) = $(M2-M3/Wb)100$

clay (<0.002mm) = $(M2-M3/Wb)100$

and the coarse silt fraction by interpolation.

In addition to this, selected samples were measured using a Fritsch laser particle sizer, to obtain more accurate data for samples consisting almost entirely of silt-sized material. This was done at the Hydraulics Research Laboratory, Wallingford.

3.2.5 Mineralogy

The main purpose of analysing the mineralogy was to assess the amounts of quartz and feldspars in samples and to determine where possible the type of feldspar, which was the main mineral used for dating (especially in IRSL). The identification of the presence of minerals such as metal oxides and carbonates which cause spurious luminescence (ie. additional signals which are not part of the signal used for dating measurements) is also important. It is also useful to analyse the total amount of clay minerals present in the samples. Clays are relatively inert with respect to luminescence (Questiaux, 1991) and an abundance may 'dilute' the signals emitted for other minerals. They are also an indicator of feldspar weathering, particularly an abundance of mixed-layer types.

X-ray diffraction (XRD) is a widely used technique for the study of minerals and sediments, especially for the study of weathering processes. It is primarily used for clays but will identify most minerals. Samples are settled on glass slides and subjected to X-rays which are diffracted at angles determined by the interplanar (d-) spacing of the crystal structure. This produces a pattern of diffraction peaks on a chart. By comparing the pattern with that produced from known standards, the mineralogy of the sample is identified. The samples were analysed using a CoK α source of x-rays (Hardy and Tucker, 1988).

Clay minerals are phyllosilicates, and have a layered structure. When allowed to settle undisturbed, they will orientate preferentially parallel to their basal plane (001). If randomly orientated, definition only between subgroups rather than individual species can be made as the diffraction angle will not be restricted to the basal plane alone. Various chemical treatments can be applied such as heating and impregnation with ethylene glycol to refine the identification of clays, but these were not applied here. The clays were settled slowly from evaporation of water rather than acetone. This proved sufficient to identify the abundance of the main groups of clays, such as kaolinite, montmorillonite and illite, and the abundance of amorphous and mixed-layer clays.

Mineralogically similar clays will be produced under different weathering conditions, depending on the availability of ions, but they will differ in chemical composition and structure, which is reflected in the diffraction pattern (Carroll, 1970). Kaolinite forms where there is a deficit of cations which are removed in free draining conditions; halloysite tends to form directly from the alteration of plagioclase; montmorillonite forms in drier environments and requires the presence of some cations (Degens, 1975). Amorphous iron and aluminium oxides and quartz and feldspars of clay size are identified, but highly amorphous material, including clays, will tend to produce a high background luminescence signal (see Chapter 5), compared to samples without these minerals.

Quantitative estimation of minerals is difficult to obtain, requiring the additions of known quantities of a pure mineral to compare its diffraction response. Careful selection of an appropriate type and size of control is necessary. However, a semiquantitative estimate of the relative abundance of the major identifiable minerals can be made by calculating the areas under diagnostic diffraction peaks (Hardy and Tucker, 1988) which was sufficient for samples in this study. This was supported by SEM analysis which is particularly useful for clay mineral identification.

Each of the fractions obtained from the sedimentation particle size analysis was examined by XRD to assess variations in mineralogy between consecutive size fractions, including the medium and fine silt fractions used for fine grain dating. The objective of this was to assess the variability in the abundance of minerals relevant to dating (quartz and feldspar) with grain-size fractions. Thus the difference in mineralogy between the fraction selected for dating and the modal grain-size could be evaluated, where the latter was of an unsuitable size for dating.

3.2.6 Elemental Composition

Elemental analysis by XRF (X-ray fluorescence) of luminescence dating samples is performed in order to evaluate the K_2O content of the bulk sample. This is used to determine the amount of $K-40$. This can be used to evaluate the gamma radiation contribution to the total dose-rate. This is used in conjunction with alpha counting and beta TLD to evaluate the dose-rate from the sample in the laboratory. This is discussed further in Chapter 5.

Elemental composition is also useful in the analysis of the degree of weathering in a profile. The relative proportion of soluble to insoluble ions is used to give a weathering or chemical alteration index for a sediment (Fairchild et al. 1988). These have been used to differentiate between degrees of weathering in strata within a stratigraphic sequence (eg. Pye and Johnson, 1988). Weathering indices have been applied selectively in this study to sediments which have been affected by weathering, either in the past or at present. The ratios and applications are discussed in the following chapter.

XRF is a process by which a sample is bombarded with x-rays causing emission of secondary radiation which is dependent in its wavelength and intensity on the type and abundance of elements present. Comparisons are made with calibrated standard samples. The Energy Dispersive (ED) technique was used rather than the Wave Dispersive (WD) XRF, as it identifies a wider range of minerals (Jenkins and de Vries, 1970; Fairchild et al, 1988). Samples are prepared using a compressed powder of the sample impregnated with resin. This gives a sample which is of similar packing density to all others, and is homogenised with respect to its composition. The elements identified include the more common elements Si, Al, Mg, K, Ca, Fe, Na, Ti, S and P, as well as trace metals such as Pb, Zn, Cd, Cr and Mn.

3.2.7 Weathering Indices

The degree of weathering that minerals have undergone can be measured by the application of weathering indices to the samples (Parker, 1970). These generally comprise an evaluation of the ratio between mobile and less mobile cations as measured by XRF analysis; eg. Ca, Na, K : Al, Si, Fe. The comparison of the weathering index of the parent rock and of the soil/sediment derived from it indicates the degree of alteration that has been effected, and the potential for further alteration at different depths in the profile.

Weathering indices were applied to loess sequences with some success (Pye and Johnson, 1988) based on the assumption that the original composition of the loess did not vary greatly and that through time, progressive leaching and soil formation has altered the elemental composition. The ratio used in this case was $\text{Al}_2\text{O}_3 + \text{Fe}_2\text{O}_3 / \text{Na}_2\text{O} + \text{K}_2\text{O}$. Other elements were also measured, and it should be noted that the U concentrations did not vary significantly with depth, but that Th concentrations were higher in the weathered loess, than the unleached loess. They have also been applied to brickearths in South-East England for the purpose of determining provenance and uniformity of loess (Parks and Rendell, 1992).

However, in the above case concerning loess, comparisons are based on a common original composition, and in the case of rock weathering studies, the composition of the parent material is known. In the case of the present study, such comparisons are not available as the sediment has been transported for some distance away from its source, and is derived from more than one such source. The homogeneous nature of many of the strata sampled suggests that there has not been significant weathering within the strata. Differences between weathered and unweathered parts of the stratum are difficult to identify in many cases, and may reflect differences in depositional environment rather than weathering or leaching. The application of weathering indices in these

cases would only reflect the mineralogy of the sample, rather than its past or potential alteration by weathering, and therefore represents an inappropriate technique for the purposes of this study.

3.2.8 Physical Appearance of Grains

High resolution microscopic examination of individual grains is a valuable source of data relating to the mode of transport and the effects of processes such as weathering. Comparisons between size-fractions and samples are facilitated by the use of photography. Both optical and scanning electron microscopy were employed in this study. This was in order to evaluate the effects of weathering on selected samples, and to aid the identification of the types and forms of the clay minerals where these were particularly abundant.

Characteristic features such as etch pits and delineated cleavage planes develop in feldspars as a result of weathering. Additional features resulting from redeposition of elements, and clay formation and alteration were investigated and observed. These are discussed in the following chapter.

Selected samples were prepared by using the discs prepared for luminescence dating measurements (see Chapter 5). The sediment is settled onto aluminium discs. These were either discs which had been measured, or additional discs prepared for the SEM, as the exposure to white light subsequently invalidates their use for dating. The discs were gold coated and examined under a variety of magnifications (x50 to x2000) at working distances of between 6 and 38 mm. Photographs of some of the samples are given in the following chapter. In addition, the sphericity of grains and features diagnostic of different modes of transport could also be identified; eg. the opaque surface and crescentic impact marks of windblown grains is diagnostic of aeolian transport (Culver et al, 1983). The clarity of these features would suggest that additional transport modes had not affected the sediment thereby 'blurring' the features.

3.2.9 Feldspar Identification

In a few cases, samples were subjected to Cathodoluminescence. The application of CL is primarily in the study of limestones and dolomites, but has also been applied to feldspars and quartz of a sedimentary origin (Marshall, 1989). Samples are bombarded with electrons, stimulating luminescence of characteristic wavelength to be released. Ruppert (1987) used the technique to distinguish between allogenic quartz and feldspar derived from igneous or metamorphic parent rocks which produce luminescence, and authigenic minerals formed *in situ* which do not. This gave an indication of the weathering environment to which the sediment had been subjected.

Different types of feldspar, have different major cationic components. This will produce different emission spectra which can be used to identify the feldspar (Marshall, 1989). For example, albite (sodium-plagioclase) produces a weak emission in the blue waveband, and a more strongly detected signal in the orange-red band. Orthoclase (potassium feldspar) has a much stronger blue signal, and weaker orange-red. This has important implications in the detection of the signal stimulated by infra-red light during optical dating as it is primarily the blue signal which is detected and measured and if this is weak due to the predominance of albite, it may give the appearance of a very young sample.

Although the CL emission from feldspar is not directly related to the TL or IRSL emission, each technique stimulates different combinations of traps, so it may be used as a method of feldspar identification. Albite, for example, is known to have a low IRSL emission. The identification of proportions of feldspars which are highly sensitive to IRSL, or which are less responsive, can aid the resolution of problems of low signal counts, which arose in a number of samples. These are discussed in Chapter 5.

3.2.10 Organic Carbon Content

There is no direct method of measuring the amount of organic matter in a sediment, as this may exist in a variety of chemical complexes. The most common method is to measure the amount of organic carbon in the sample by the loss on ignition method. A dry sample is heated for 2 hr at 1050°C. The percentage weight loss can be multiplied by a factor of 1.7 (Brady, 1990) to give an approximate measure of organic matter.

The organic component is important with respect to the dose-rate to minerals; peat is known to preferentially absorb uranium. The amount of organic matter may therefore relate to the dose-rate. The evaluation of the organic carbon content also allows a more accurate evaluation of the relative elemental components as measured by XRF.

3.2.11 Summary

The sediments sampled for dating were subjected to a selection of analytical techniques, in order to determine their environment of deposition and changes due to post-depositional processes. The Particle size distribution of the samples identifies the size fractions present, and the relationship between the modal grain size and that isolated for dating. The mineralogy, examined by X-ray diffraction and X-ray fluorescence, and the physical appearance of the grains is important with respect to the minerals present (which may affect the signal intensity or stability observed in

luminescence measurements) and in the recognition of alteration of minerals such as feldspars due to weathering.

The PSD, water and carbon contents were measured at 10 cm intervals throughout some cores. This enables an assessment to be made of the homogeneity of individual strata, which is indicative of turbation during pedogenesis or reworking during deposition. This may affect the bleaching of the bulk sediment and identify cases where later incorporation of material with a potentially different bleaching history has occurred, or the dose-rate where significant quantities of organic matter may have accumulated within the profile. The techniques selected, together with standard stratigraphic description, can therefore be valuable tools in the identification of processes affecting sediments which may affect their suitability for luminescence dating.

CHAPTER 4 RESULTS OF SEDIMENTOLOGICAL ANALYSES

4.1 Preliminary Considerations

The results of the various sedimentological investigations are discussed below by site, concentrating primarily on the considerations listed below. These best characterise the samples with regard to the mode of transport, depositional environment and post-depositional alteration that the samples have undergone.

- Stratigraphic position; giving estimated age and relationship between strata
- Estimated age; aided by chronological control, eg. radiocarbon
- Thickness of strata; for dose-rate calculation, and possible post-depositional alteration
- Over- and underlying strata; for dose-rate calculation and interstratal relationships
- Particle size distribution; environment of deposition, weathering
- Mineralogy: feldspar type, clay minerals; burial alteration, depositional environment
- Mixed layer clays; weathering during burial
- Microscopy; abundance, distributions and state of mineral grains; mode of transport, weathering
- Variation within strata; pedogenesis.

XRF data are presented in Table 4.1. The particle size, water and loss on ignition profiles are given on compound stratigraphic diagrams within the text, together with the particle size distribution and silt mineralogy of samples taken for dating. The key to the stratigraphic figures is located in Appendix B.

4.2 Sediment analysis by site

4.2.1 FLAG FEN, PETERBOROUGH TL 2270-9890 Ground Altitude +1.33 m OD.

4.2.1.1 Stratigraphy (figure 4.2.1)

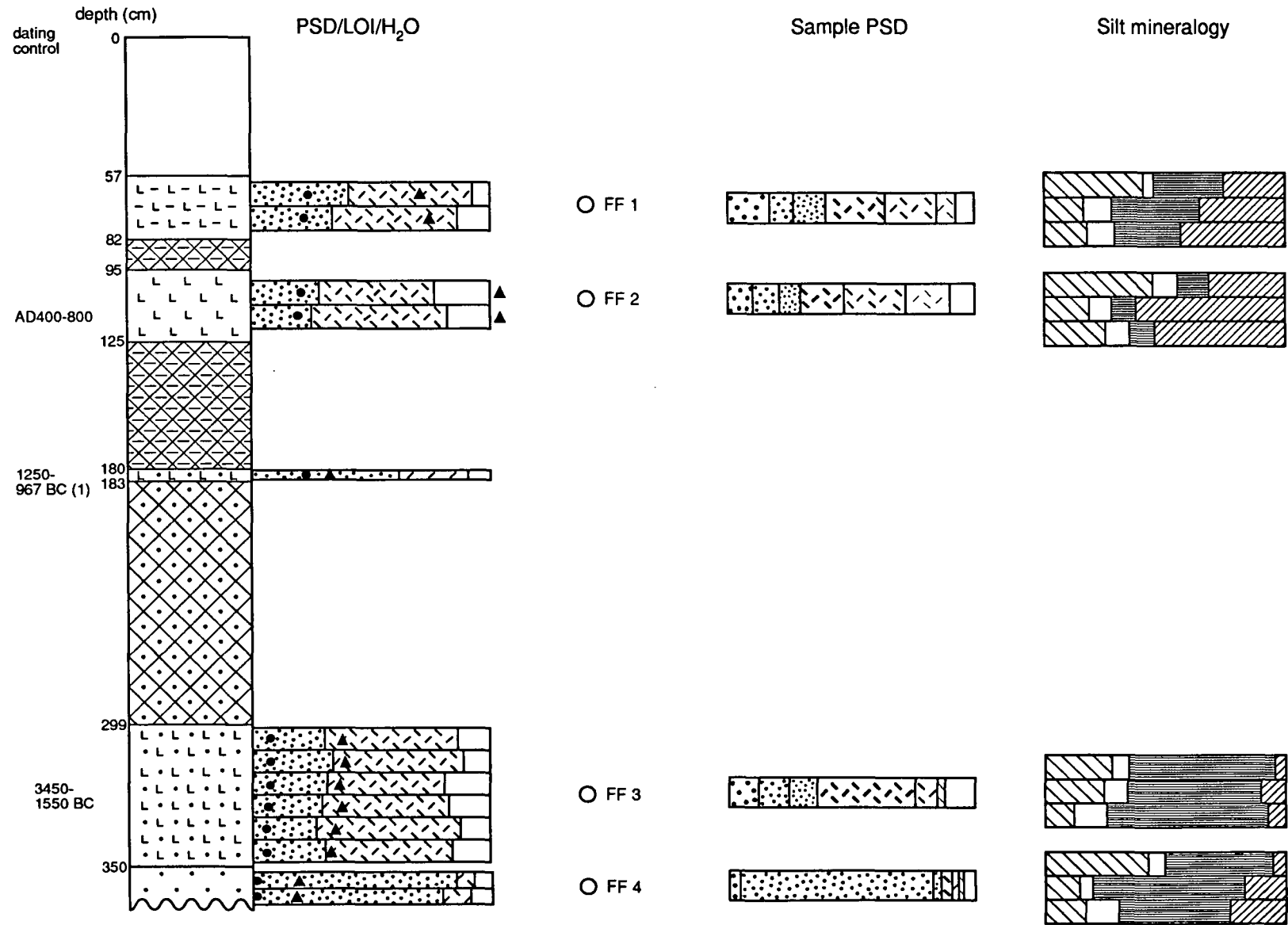
0-57cm	Stratum confusum - dump material from excavations.
57-82cm	Sh ₂ , Ag ₂ , Ga ⁺ , Th ¹⁺ Nig ₃ , str ₁ , elas ₃ , sicc ₂ , lim.sup ₃ Well-humified dark humic silt with some plant fragments and sandy, oxidised inclusions. <u>Sample FF1</u>

Table 4.1 Results of XRF analyses for all samples

Sample	SiO ₂	Al ₂ O ₃	Fe ₂ O ₃	MgO	CaO	Na ₂ O	K ₂ O	TiO ₂	MnO	P ₂ O ₅	S
FF1	57.46	16.79	11.89	1.27	8.54	0.31	2.16	0.8	0.1	0.36	0.32
FF2	51.76	16.32	17.2	1.37	9.26	0.22	1.89	0.77	0.12	0.38	0.71
FF3	46.05	6.92	18.0	0.93	24.74	0.31	1.43	0.62	0.23	0.25	0.23
FF4	80.67	2.34	3.91	0.13	11.35	0.22	0.7	0.1	0.02	0.22	0.33
WM1	72.72	17.21	2.58	1.91	0.09	0.86	3.39	0.85	0.02	0.34	0.12
WM2	72.71	17.09	2.46	1.99	0.08	0.93	3.38	0.89	0.02	0.35	0.09
WM3	75.58	14.75	2.49	1.95	0	0.93	3.08	0.78	0.02	0.23	0.19
WM4	85.07	8.13	1.83	1.08	0.09	0.79	1.99	0.46	0.01	0.26	0.37
WM5	91.98	3.58	1.43	0.56	0.18	0.67	1.03	0.31	0.02	0.13	0.21
SP1	65.3	21.61	4.23	1.97	0.27	1.02	3.83	1.23	0.02	0.37	0.15
SP2	78.16	11.98	2.67	1.57	0.08	1.05	3.06	0.8	0.23	0.15	0.46
SP3	65.13	15.99	7.14	2.76	0.39	0.92	3.47	0.92	0.06	0.22	3.25
SP4	66.32	14.28	6.63	2.16	1.6	1.54	3.02	0.9	0.08	0.47	2.83
SP5	61.13	19.02	7.28	3.52	0.22	1.07	4.18	1.05	0.08	0.2	2.26
SP6	67.25	15.9	6.26	3.08	0.06	1.08	3.61	0.95	0.08	0.18	1.57
SP7	59.5	18.38	7.9	3.39	0.34	0.86	4.13	1.03	0.08	0.15	4.22
SP8	77.22	11.72	3.58	2.02	0.34	0.98	3.0	0.65	0.03	0.13	0.32
SP9	77.26	10.46	5.22	1.86	0.16	1.46	2.81	0.57	0.04	0.11	0.05
WH1	68.73	12.7	2.0	1.22	0.41	3.83	2.21	0.75	0.01	0.06	0.4
WH2	65.99	13.83	2.0	1.24	0.34	1.44	2.36	0.83	0.01	0.07	0.2
HAZ1	88.78	4.76	1.47	0.31	0.81	0.89	1.74	0.16	0.01	0.13	0.95
HAZ2	58.21	18.16	12.67	2.36	3.36	0.39	2.7	0.85	0.14	0.56	0.59
HAZ3	67.87	17.26	5.89	2.71	1.35	0.61	3.1	0.82	0.03	0.17	0.18
SLG1	59.91	15.16	6.53	3.25	10.59	0.62	2.68	0.76	0.09	0.28	0.12
SLG2	66.89	17.13	6.56	2.74	1.39	0.68	3.16	0.8	0.04	0.21	0.41
SLG3	83.28	8.57	2.74	1.38	0.71	0.58	1.98	0.37	0.02	0.32	0.05

All figures are in %. Error is +/- 0.05%.

Figure 4.2.1 Flag Fen stratigraphy



82-95cm	Sh2, As1, DI1. Nig4, str0, elas2, sicc2, lim.sup0 Humic silty peat with abundant woody detritus.
95-125cm	Ag2, As1, Gg(min)1, Gg(maj)+, Dh+. Nig1, str0, elas0, sicc3, lim.sup1. Brown silty soil with some fresh plant remains and gravel. <u>Sample FF2</u>
125-180cm	Sh3, Th ³ 1, Ga+, Dh+. Nig4, str2, elas0, sicc3, lim.sup0. Dark humified detrital <i>Phragmites</i> peat with some fine sand.
180-183cm	Ag2, As1, Gg(min)1, Gg(maj)+, DI+. Nig1, str0, elas0, sicc3, lim.sup1. Brown sandy silt with gravel and plant fragments.
183-299cm	Sh3, Ga1, Ag+. Nig4, str0, elas0, sicc3, lim.sup1. Dark, well humified peat with some fine sand.
299-350cm	Ag2, As1, Ga1, Sh+. Nig1, str0, elas1, sicc4, lim.sup0. Pale brown sandy silt with fine sand and humus towards the top. <u>Sample FF3</u>
350cm –	Ga2, Gg(maj)1, Gg(min)1. Nig2, str0, sicc1, elas0, lim.sup0. Red-brown wet gravelly sand. <u>Sample FF4</u>

4.2.1.2 Sample Descriptions

FF1

This stratum lies above FF2 and is separated from it by 13cm silty peat. FF1 lies below the present soil surface, and incorporates the lower B horizon of the modern soil. It consists of a brown humic silt with plant fragments of stems and roots. There were also some oxidised inclusions, indicating that the stratum had experienced aerated conditions, and therefore the assumption of a saturated level of past water content for much of the burial history are invalid.

The particle size distribution was dominated by silts (66%) and sand (25%), both of which were extracted for dating on coarse and fine-grain fractions. The mineralogy of the silt fraction comprised mainly clay minerals (kaolinite and chlorite), including abundant mixed-layer clays. Potassium feldspars were more abundant than plagioclases, but both were heavily weathered with adherent clay minerals on their etched surfaces. This stratum is the lower part of the modern soil, which would account for the degraded state of the feldspars and abundance of mixed-layer clay minerals (figure 4.2.2).

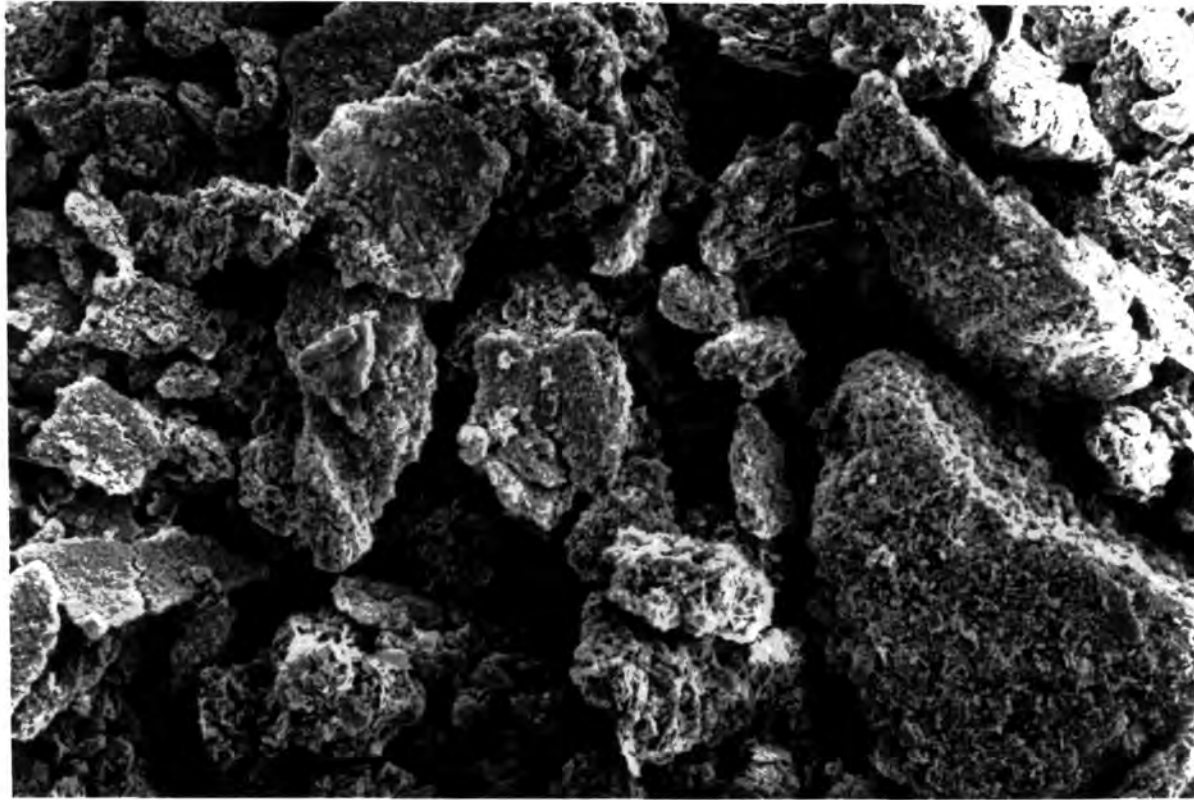


Figure 4.2.2 Sample FF1 showing the overall degraded nature of the sediment grains, which are heavily etched and partially clay-covered. The appearance of the grains in this sample is typical of samples from strata affected by pedogenesis. WD 7 mm; x500; 1 cm= 15 μ m.

The organic carbon content of the stratum (25%) is similar to that of the FF2 sample, although FF1 is darker in colour. The water content is high (70%) but less than for FF2 which is exceptional. The proximity of the stratum to the surface would enhance desiccation of the layer during dry periods, and annual variation in water content is therefore likely to be significant. The stratum is a soil developed into the transgressive and flood deposits of the channel, and is of relatively recent date.

FF2

This stratum was a silty soil, 30cm thick, overlying the fine detritus peat which buried the Bronze Age platform. It is equivalent to the Romano-British transgression deposits. The matrix contains some decomposed fragments of unidentified plant stems and roots, and a small amount of gravel. The deposit was well-mixed, with a sharper upper contact and a lower contact graded over 2-3cm.

The particle size distribution was dominated by silt and clay (77.5%) with some sand (14%). The coarse and fine-grain fractions were both extracted for dating. The mineralogy of the sand fraction is dominated by quartz with some feldspar (mainly potassium types), although this has been severely weathered. The silt fraction was also dominated by quartz and clays; the latter being more abundant in the medium and fine-grain silt fractions where they account for 64% of the identified minerals.

The samples contained a significant quantity of organic carbon (23%), which together with the observed indications of severe weathering of the feldspar and abundance of clays, suggests that pedogenic processes have operated in the stratum. The water content of the sample was extremely high (217%) which suggests that accuracy of the luminescence dates may be severely reduced, due to the greater uncertainty and correction of the dose-rate necessary for such a high water content.

The water content and loss on ignition do not vary significantly with depth, but the abundance of clay minerals increases lower down the profile. There were no mixed-layer clay minerals observed, suggesting that weathering of the feldspars and formation of the clay mineral products has been in equilibrium with the available ions in solution. This would be enhanced by a high water content surrounding the individual grains, which would facilitate both the dissolution of ions and their mobility within the soil matrix.

The sample appears to have been affected by active pedogenic processes which have degraded the feldspar grains to a significant extent. The high water content of the sample will affect the accuracy of the luminescence dates. The stratum represents an ancient soil of Iron Age or later

date, and may in part have developed into the silts deposited from the Romano-British transgression over the Fenland.

FF3

This stratum was 51 cm thick, and directly overlies the red sand of the FF4 sample. It was overlain by a dark, well-humified peat. FF3 comprised a pale brown sandy silt with some fine sand and humic material incorporated into the upper part of the matrix where the stratum grades into the overlying peat over an interface of 2-3 cm.

The particle size distribution was dominated by the silt fractions (54%) forming a homogenous matrix, with some fine sand and clay. The fine-grain fraction was isolated for TL and IRSL dating. The silt mineralogy varies between size fractions: quartz was more abundant in the coarse fraction while feldspars and clay minerals were more abundant in the fine fractions. This reflects the differential breakdown of the more susceptible feldspars relative to the more resistant quartz minerals. The feldspar grains comprised similar proportions of plagioclase and potassium types and the grains were in a partially degraded condition.

The loss on ignition value was higher (9.4%) than for FF4, reflecting a higher humic content, even though the sample was taken from the middle of the stratum, away from the greater concentration of humic matter observed near the top of the layer. A significant amount of mixed-layer clays were observed in the XRD trace, likely to originate from breakdown of the feldspars. In some cases the clays were observed to be adherent to the surfaces of the feldspar grains although they did not cover the total grain surface and formed discrete clusters (figure 4.2.3). This, together with the humic content, mixed grain size and the weathered nature of the feldspar grains suggests that some pedogenic processes have operated within the stratum.

The abundance of mixed layer clays may be due either to incomplete alteration or the paucity of necessary cations required for the formation of pure clays. The XRF results (table 4.1) show a relative abundance of Ca, which is due to the chalky nature of the underlying stratum, and relative rarity of Na, K and Mn, which are required for the formation of some clays. The water content of the stratum is higher than for FF4 (40%) due to the uncompacted nature and mixed matrix of the sample.

This sample represents the Fen Clay deposit. Here it is sand-rich due to its position in the deeper channel. The pedogenesis of the FF3 sample is not strongly developed as the site lies at a lower level than the other sites where the soils were found and would have been an open water environment. However, the slightly weathered nature of the feldspars may be a relict characteristic of the material deposited during the Fen Clay transgression. The sand grains are



Figure 4.2.3 Sample FF3 showing in the centre a 'clean' quartz grain with negligible clay covering and clearly defined fracture faces. On the top right is a grain consisting of loosely bound clay minerals which form discrete particles in this sample. WD 7 mm; x10 000; 1 cm= 0.8 μ m.

sub-rounded to sub-angular, and may in part be derived from erosion of the nearby sandy islands and fen-edge. The peat overlying this stratum is the Upper Peat in which the Bronze Age structures were recovered. The Lower Peat between the glacial deposits and the Fen Clay is absent from the sequence examined. The depth of the channel may have locally prevented peat formation during this time.

FF4

This sample was a fluvial sand (90% sand) and likely to be an outwash deposit related to the terraces in the Nene and Ouse valleys. It was on these terraces that the Fengate site was constructed. The stratum comprised a red-brown sand with gravel. The dominant size fraction is the medium sand size. There was a fine silt and clay component of the sand matrix (9% of the size distribution) which was isolated for dating. The sand fraction was predominantly quartz in composition, thus making it unsuitable for IRSL dating, although it was measured by TL. Feldspars were more abundant in the fine-grain fraction (14% of identified minerals) and were dominated by plagioclases. The fine-grain fraction also contained significant quantities of calcite, probably derived from incorporation of material eroded from the underlying chalky boulder clay of the Fenland, during transport and deposition. The calcite was removed from dating samples.

The sand grains were predominantly sub-rounded in shape and of even size (0.2-0.6 mm) and in an undegraded condition. Clay minerals were relatively rare, and were not adherent to the grain surfaces as is the case where the clays were derived from weathering of the larger grains. The size and shape of the grains, and the narrow sand size range indicates a fluvial mode of transport for the sediment. The water content of the stratum was quite low (25% dry weight) due to the compact nature of the sand and silt matrix. Organic carbon content was very low (3.4%).

This sediment is related to outwash deposition following the last glacial. The sand is mixed with a fine silt and clay component which may be derived from erosion of exposed till surfaces. It would be expected that under fluvial conditions, the sand and fine-grain fractions would be adequately bleached in terms of the IRSL signal of the feldspars, but the TL of the quartz fraction, which comprises the greatest source of luminescence signal for this fraction, may be only partially bleached. The mineral grains were in a clean, unweathered condition, indicating that no weathering had taken place before or after burial.

4.2.1.3 Summary

The samples selected for dating from the Flag Fen sequence are the basal fluvioglacial sands. This sample is FF4. The sand was dominated by quartz, but feldspars formed 14% of the finer fractions. FF3 is the local Fen Clay unit. The sediment is a sandy silt. The silt fractions (54%)

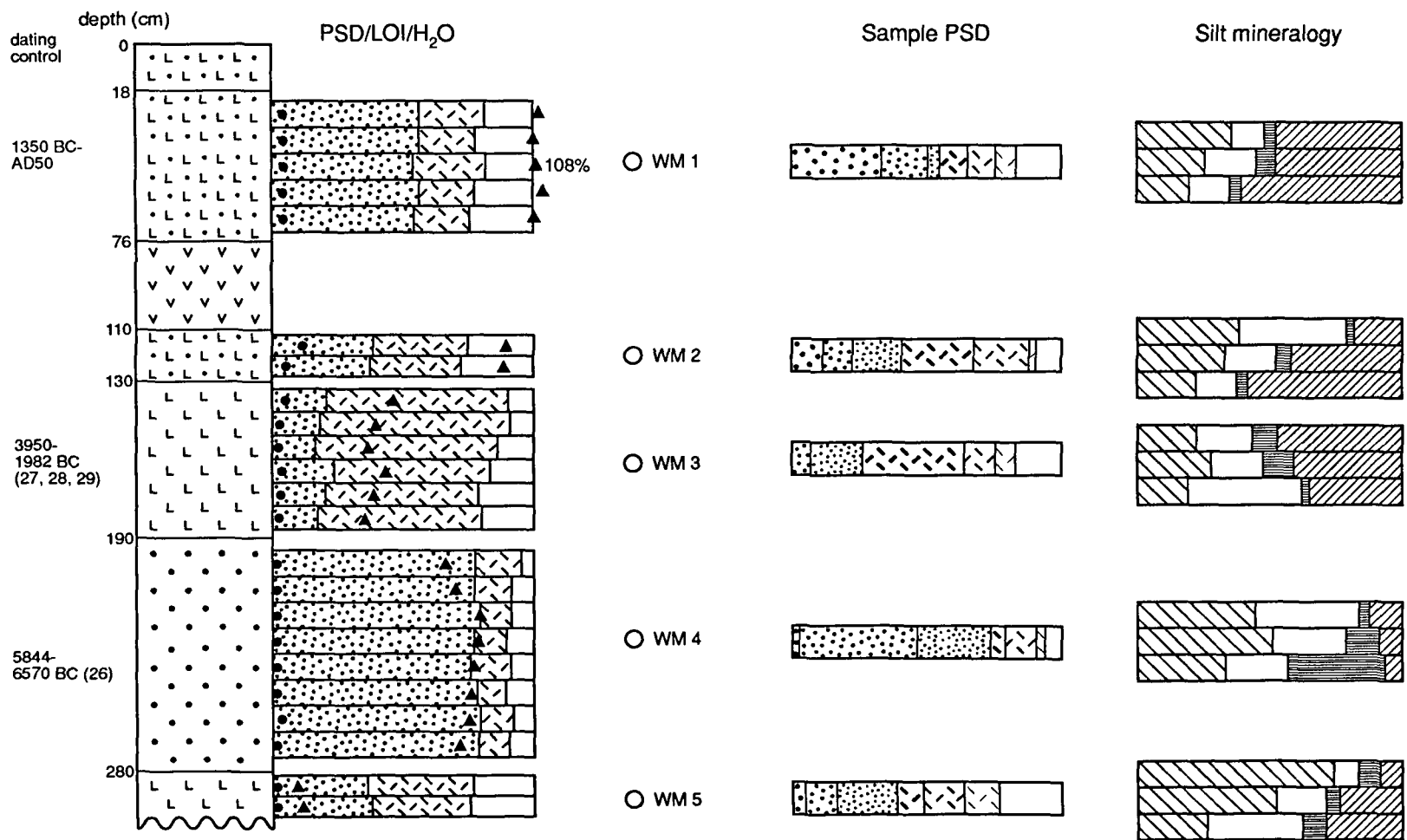
contained 45% feldspars. Quartz was more abundant in the coarser grain size fractions. The sample contained an abundance of clay material, which may be a result of weathering of the feldspars. FF2 is a silty sediment representing the deposits of the Romano-^{British} transgression. The mineralogy is dominated by quartz. The feldspars show abundant evidence of weathering. FF1 lies below the present soil and is a humic silt. Feldspar are heavily weathered, and potassium feldspars are more abundant than plagioclases, which may reflect differential susceptibility to weathering.

4.2.2 WILLIAMSONS MOSS; TL3085 4917 Altitude +7.5 mOD

4.2.2.1 Stratigraphy (figure 4.2.4)

0-18cm	Ag2, As2, Sh+, Th ⁴ . Nig3, str0, elas0, sicc3, lim.sup.0. Dark brown crumbly topsoil; base marked by large rounded to sub angular pebbles.
18-76cm	Ag2, Ga1, As1, Th ² (Phra)+ Nig1, str0, elas0, sicc3, lim.sup.0. Mid brown sandy-silt, with occasional humic fragments. <u>Sample WM1</u>
76-110cm	As2, Sh2, Dh+, Gs+. Nig3, str1, elas2, sicc2, lim.sup.1. Dark brown well humified clayey peat with small rootlets; some sharp flint inclusions (<2mm).
110-130cm	As2, Ag1, Gs1, Dl, Sh. Nig1, str1, elas0, sicc3, lim.sup.1. Grey sandy silt with occasional horizontally lying woody inclusions (<20mm) <u>Sample WM2</u>
130-190cm	As2, Ag1, Ga1, Dl. Nig2, str.0, elas0, sicc3, lim.sup.0. Grey to blue-grey silty clay; compact and homogeneous; some humus flecks, fine sand grains and occasional fresh woody fragments. <u>Sample WM3</u>
190--280cm	Ga3, As1, Ag+, Sh+. Nig2, str0, elas0, sicc3, lim.sup.0. Wet, grey sandy deposit with silt-clay matrix, with organic fragments. <u>Sample WM4</u>
280cm ----	As2, Ag1, Ga1. Nig2, str0, elas0, sicc2, lim.sup.0. Red boulder clay; homogeneous and fine-grained. <u>Sample WM5</u>

Figure 4.2.4 Williamson's Moss stratigraphy



4.2.2.2 Sample Descriptions

WM1

This stratum lies below the present topsoil and represents the subsoil horizon. It is a sandy-silt, 58cm thick and mid-brown in colour. There are occasional humic fragments but the loss on ignition value of the matrix is only 2%. This is however higher than for the other samples from the Moss.

The particle size distribution was dominated by the silt and clay fractions (50%) and coarse and medium sand (50%). The abundance of the clay fraction may be due to illuviation from the upper horizons. Much of the clay was of mixed-layer types, which partially coated the mineral grains (figures 4.2.5, 4.2.6 and 4.2.7). This is characteristic of clay illuvial horizons. The sand is similar in character to that from WM2 below, but larger in size (0.6-2 mm), indicating either that the source is different or climatic conditions (ie. wind strength) were different and dunes were closer to the site. The quartz-rich coarse-grain fraction of the sand was isolated for TL dating and the fine-grain fraction for IRSL and TL dating.

SEM analysis revealed significant weathering of the feldspars and abundant fresh mica, both indicating active pedogenic processes. Fragments of *Phragmites* were identified in the matrix of WM1, but were not present in the top soil. This suggests that the WM1 sample may contain material derived from the underlying peat horizon, although no *Phragmites* could be identified from this peat, and the organic content of WM1 is only 2%.

This sample is part of the lower horizons of the modern soil. It is likely to be subject to significant variations in water content.

WM2

This stratum overlies WM3 and was a grey silty-sandy, 20cm thick. It is separated from WM1 by a peat. WM2 is a sandy (40%) silt (50%) with some clay, containing some woody fragments. It represents the upper part of the alluvium in which the Neolithic hearths were found and is the younger of the two land surfaces identified by Bonsall et al (1986, 1989) on the Moss. The clay content increased with depth, indicating that the soil developed into the alluvium with the incorporation of components from different sources.

The silt fractions were dominated by feldspars, with potassium types being more abundant than plagioclases (by a ratio of approximately 2:1). There were no mixed-layer clay minerals identified. Kaolinite and chlorite were abundant particularly in the fine silt fraction. The organic carbon

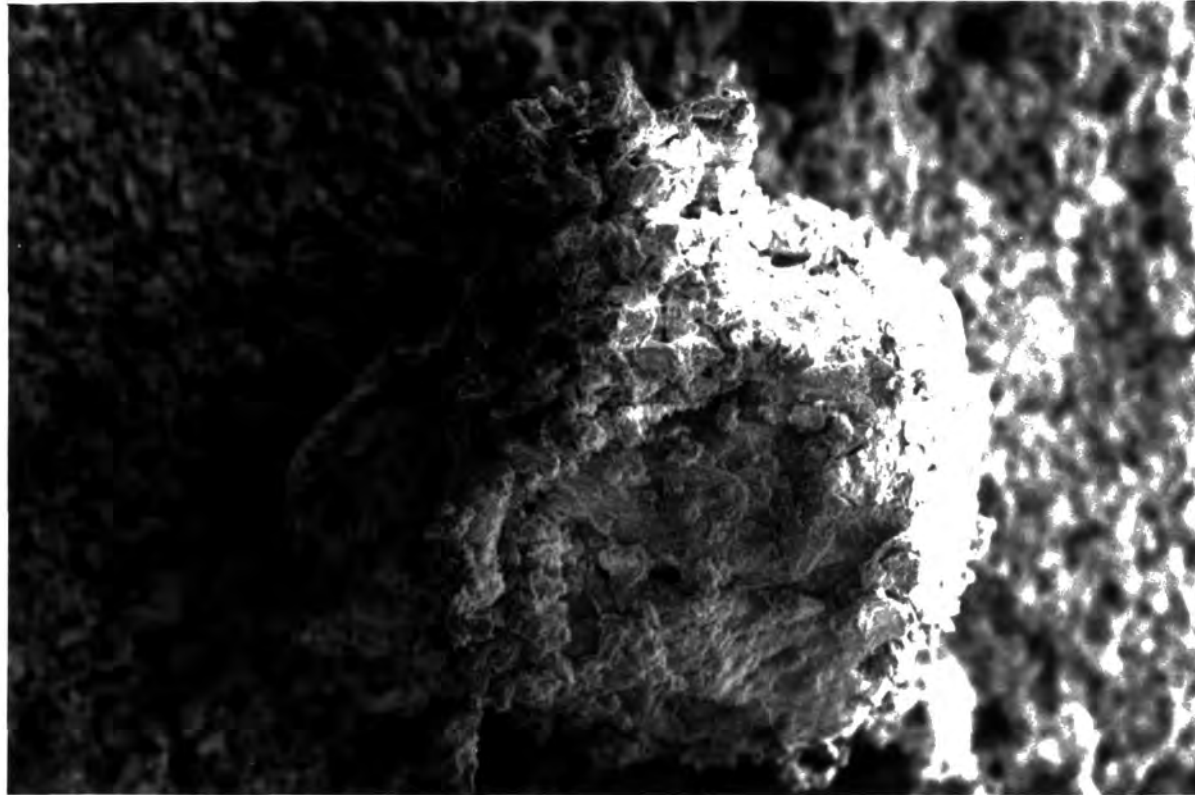


Figure 4.2.5 SEM of sample WM1 showing a large mineral grain coated with clay minerals. The formation of such coatings may prevent optical bleaching at deposition.
WD 6 mm; x500; 1cm=15 μ m

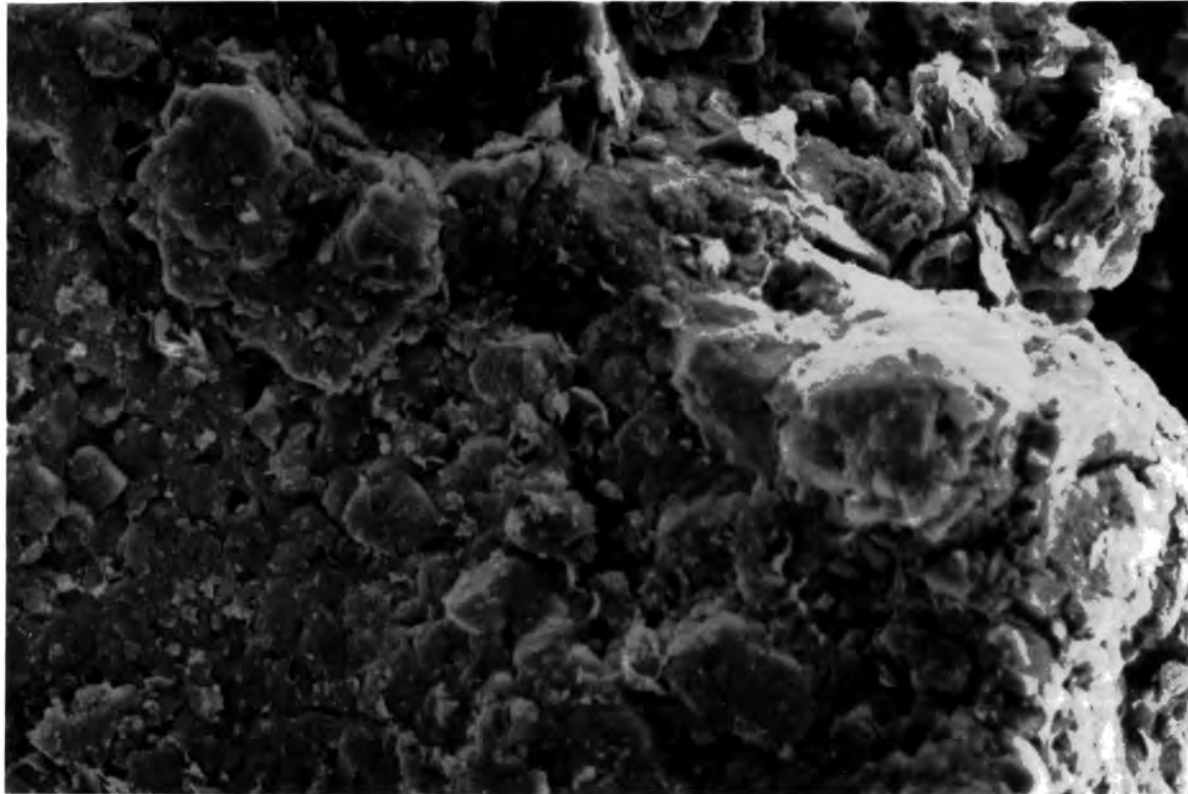


Figure 4.2.6 Higher magnification of grain in 4.2.5, showing the continuous nature of the clay mineral coating over the mineral surface. These clay minerals may be derived from weathering of the feldspars or from translocation of clays within the profile. WD 6 mm; x2000; 1cm=3 μ m.

content of the sample is negligible. This is consistent with a minerogenic B soil horizon rather than with an organic A horizon of a soil.

The water content decreased with depth; the value was 80% in the middle of the stratum. The sample was dominated by coarse and medium silt fractions together with fine sand. The sand was mainly quartz and the grains tended to be sub-angular in shape with some opaque facets indicative of an aeolian origin, in this case most probably from the dunes nearby. This has been incorporated into the alluvial matrix during pedogenesis or possibly during trampling associated with occupation nearby.

The stratum is likely to represent the minerogenic remnant of a soil which has developed into the surface of the underlying alluvium. An aeolian sand component was incorporated when the soil was exposed at the surface. It has been affected by trampling, creating an upper compacted layer and lower uncompacted layer with a correspondingly higher water content. If the incorporation of the aeolian component is contemporary with soil formation, the age of the sand fraction should reflect the age of the soil. The fine-grained fraction may not have been exposed to sunlight during soil formation and may reflect the age of the alluvial deposit (WM3) from which it is derived, rather than the soil and associated with occupation.

WM3

This stratum comprises the main alluvial unit deposited over the Moss after the formation of the shingle ridges, when water was ponded up behind the ridge. This is assumed to be fresh water although there were no diatoms in the deposit to verify this. WM3 is a 70cm thick blue-grey clayey silt which is compact. Some humic flecks and fine sand were observed in the matrix and occasional woody fragments, but the loss on ignition value of the matrix was negligible. This deposit is equivalent to the alluvium on the Moss surface in which the Neolithic hearths were stratified.

The particle size distribution was dominated by the coarse silt fraction (30%). The silt and clay fractions combined to comprise 67% of the particle size distribution. The fine-grain fraction was taken for TL and IRSL dating. The silt mineralogy was primarily feldspars, with the potassium types being more abundant than plagioclases. Clay minerals were also very abundant, including some mixed layer clays (figure 4.2.7). The water content was relatively low (49%) and it is likely that this predominantly fine-grained deposit was laid down in a compacted manner as was the case for the clays in the Dutch river dune area. The error on the water content estimations would therefore be subject to less uncertainty than, for example, in the cases of FF1 and FF2.

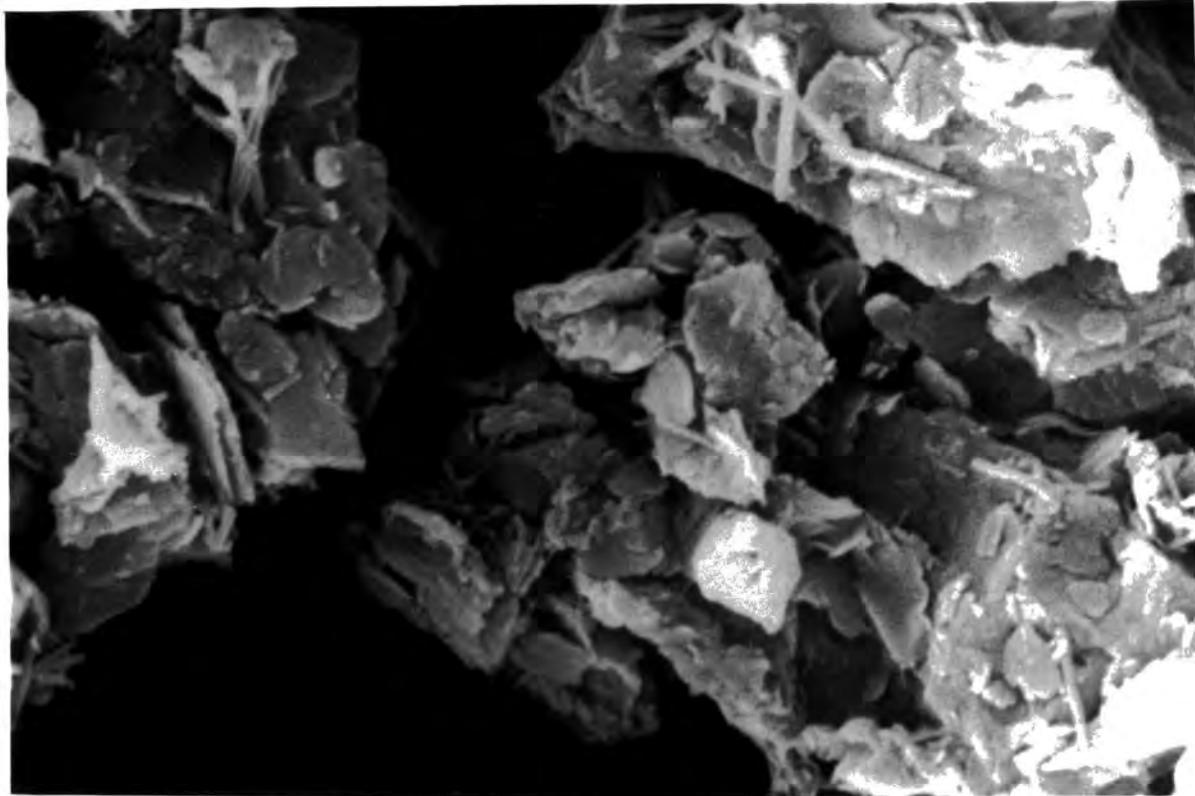


Figure 4.2.8 SEM of clay mineral forms observed in sample WM3. The thin cylinders are curled up flaked of montmorillonite, although some needles may be filaments of illite. To the left, mid way down are the pseudo-hexagonal flakes of kaolinite which when undisturbed form stacks. Here the flakes are end-on. WD 7 mm; x10 000; 1 cm=0.8 μ m.

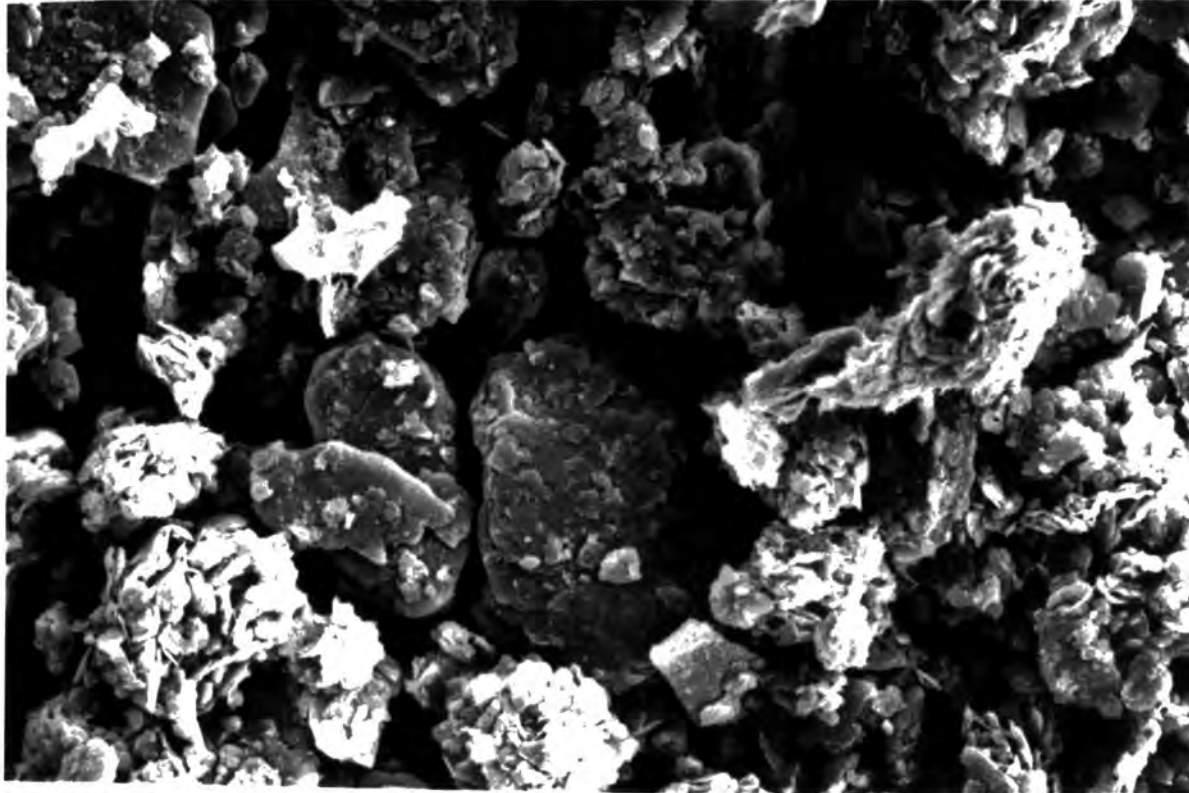


Figure 4.2.9 SEM of sample WM3. In the centre of the picture are larger grains partially coated with clay minerals, surrounded by clusters of clays. WD 7 mm; x2000; 1 cm=3 μ m.

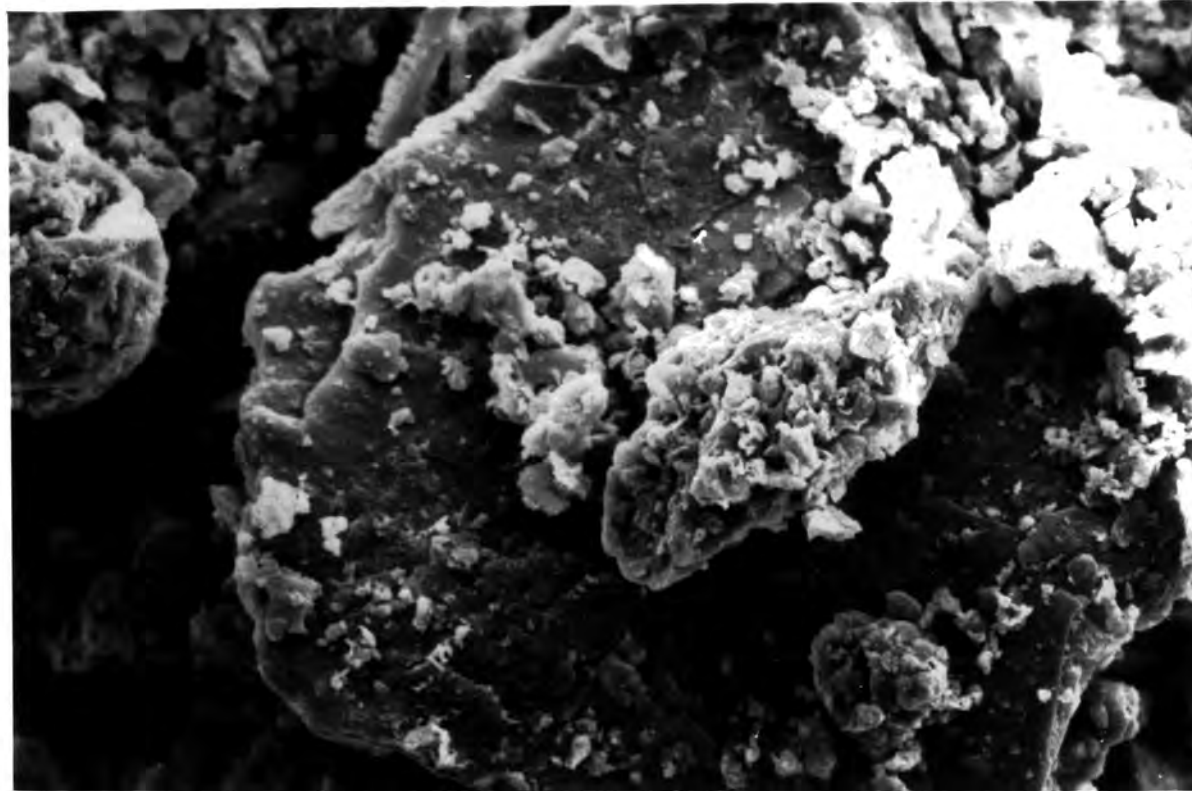


Figure 4.2.7 SEM of large mineral grain from sample WM1 partially covered by clay minerals forming layers on the surface. The grain may be mica, due to the layering exhibited at the edges. To the left is a heavily eroded spherical grain, possibly quartz. WD 7 mm; x2000; 1 cm=3 μ m.

During SEM analysis, a number of amorphous silica nodules were observed, deposited within the matrix (figure 4.2.10 and 4.2.11). This occurs when the surrounding solutions are saturated with respect to silica and the amorphous material is deposited. Because these nodules are amorphous, they are not suitable for dating as there is no crystal structure. The appearance of these is inconsistent with the lack of diatoms, as an abundance of silica in the solutions tends to preserve diatoms. However, there may have been an absence or paucity of diatoms in the original deposit.

This deposit is likely to be highly suitable for luminescence dating due to the predominance of feldspars, and the likelihood that the sediment was exposed to sufficient sunlight during deposition in quiet water conditions, particularly in the case of the more sensitive IRSL signal, to be fully bleached at deposition. Berger (1990) however, indicates that silt-rich alluvial deposits should be avoided in the case of TL dating, due to a variable relict TL signal remaining after burial, which was not the case for the clay fractions. The application of both techniques to this sediment serves to test this.

WM4

This is a wet grey sandy sediment, with a silty clay matrix containing some organic fragments. It overlies the boulder clay and is covered by alluvium. WM4 is 90cm thick and of a fairly homogeneous appearance throughout its depth. The fine matrix has a negligible organic carbon content.

The particle size distribution was dominated by medium sands (45%), fine sands (26%) and medium silts (14%). The fine-grain fraction was isolated for dating by IRSL and the coarse-grain for TL. The mineralogy of the sand fractions was primarily quartz, with small amounts of plagioclase feldspars. The silt fractions were dominated by plagioclase feldspars and quartz, but clay minerals were relatively rare compared to other samples such as FF1 and FF2. This may reflect the nature of the depositional environment.

This deposit represents the channel equivalent of the Mesolithic land surface of Williamson's Moss, which occurs as a thin sandy layer above the till in which Mesolithic artefacts were stratified. The thickness of the channel deposit is attributed to erosion of the land surface and drainage of the surrounding area into the channel, where the sands and coarser silts were deposited and the fine silts and clays were carried away.

The organic carbon content is low indicating that little topsoil material has been deposited in the channel. The WM4 deposit is likely to represent the eroded mineral soil component. Some mixed-layer clays were observed which may be derived from material affected by weathering

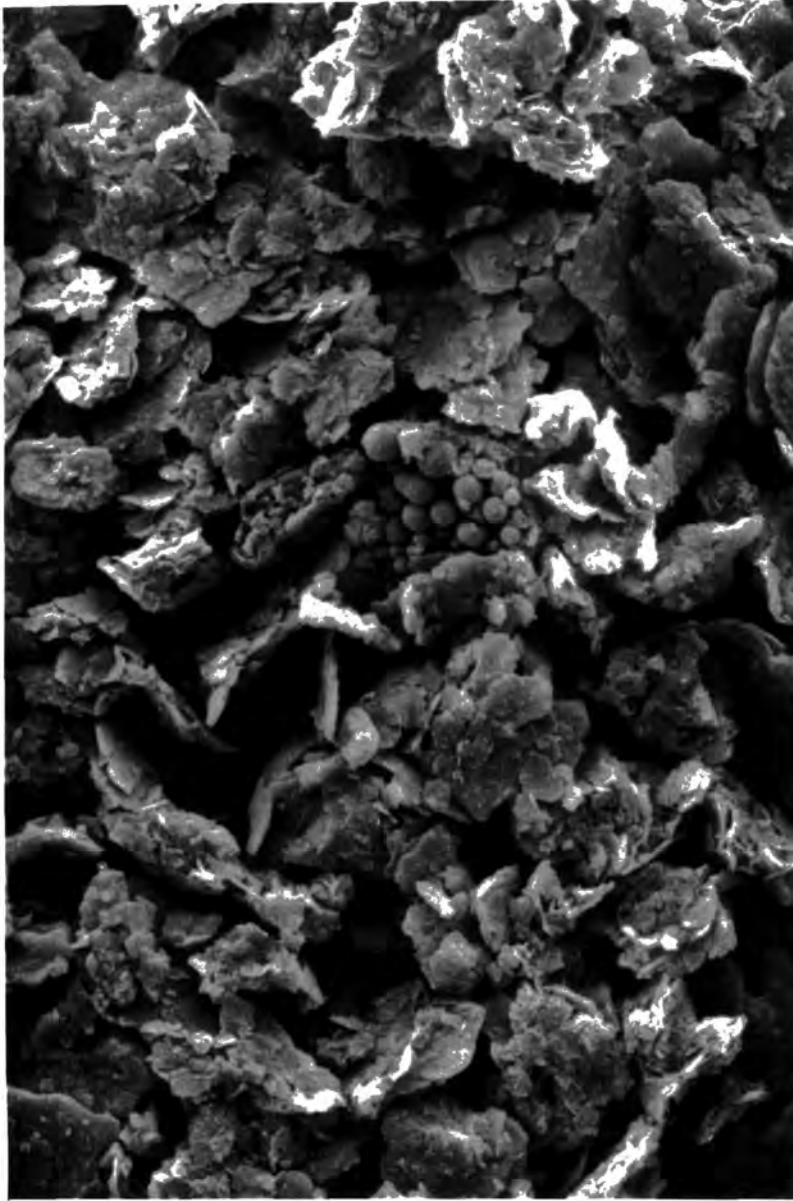


Figure 4.2.10 Sample WM3 showing amorphous silica nodules deposited from a saturated solution. WD 6 mm; x2000; 1 cm= 3 μ m.

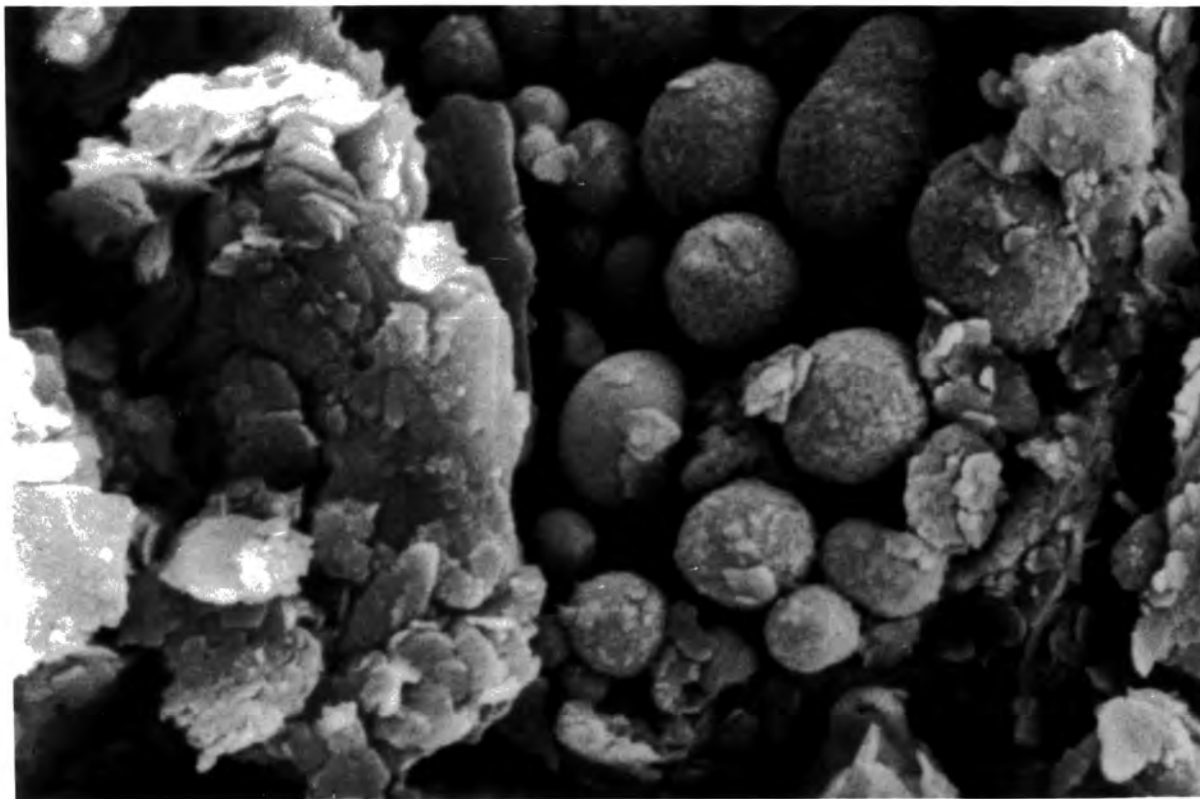


Figure 4.2.11 Higher magnification of nodules in figure 4.2.10. The furry appearance of the surfaces of the nodules may be due to authigenic christobolite.
WD 6 mm; x10 000; 1 cm= 0.8 μ m.

during pedogenesis. The water content was high (93%) due both to the uncompacted nature of the sediment and to its present location below the water table.

WM5

The basal stratum from the Williamson's Moss channel is a red boulder clay (WM5) which is homogenous in texture, and fine-grained. The dominant size-fractions were the fine sand (20%), coarse and medium silts (22%) and clay (20%). The fine-grain fraction was extracted for TL and IRSL dating. The coarse fraction was also isolated for IRSL.

The mineralogy of the silt fraction was dominated by quartz in the coarser fraction but by plagioclase feldspars in the medium and fine fractions. No mixed-layer clays were observed, as would be expected from a relatively unaltered and compact fine-grained till. Clay minerals were abundant, but these were not adherent to the grain surfaces and formed discrete aggregates of similar grain size to the silt fractions (figure 4.2.12).

The sample had a very low water content (16%) due to its compact nature, and a negligible organic carbon content. The mineral grains were relatively unaffected by weathering, with only very slight etching and delineation of cleavage plane.

The zeroing of glacial tills is thought to occur by grinding during transport rather than by exposure to light (Lamothe, 1988), and it is recognised that the zeroing of basal till deposits is likely to be partial and may cause problems in the evaluation of the ED. By comparing the dates obtained from the various fractions, some internal consistency may determine the apparent age of the material. However, only a minimum age can be determined for this deposit.

4.2.2.3 Summary

Five samples were taken for dating. The upper two samples, WM1 and WM2 are both pedogenic horizons, being part of the modern B horizon and a remnant of an ancient soil respectively. These sediments contained weathered feldspars. They had low organic carbon contents. WM3 is an alluvial deposit containing silts and clays which are dominated by potassium feldspars. The water content is relatively low reflecting the compact nature of the deposit. WM4 is a sandy deposit with a silty matrix. The deposit is an eroded remnant of the Mesolithic land surface and contained some partially eroded feldspars but few mixed layer clays. The water content was high, as this sediment is below the water table and uncompacted. WM5 is the basal Devensian boulder clay. Quartz is dominant in the sand fractions, and feldspars in the finer fractions. The sediment is highly compact and has a very low water content.

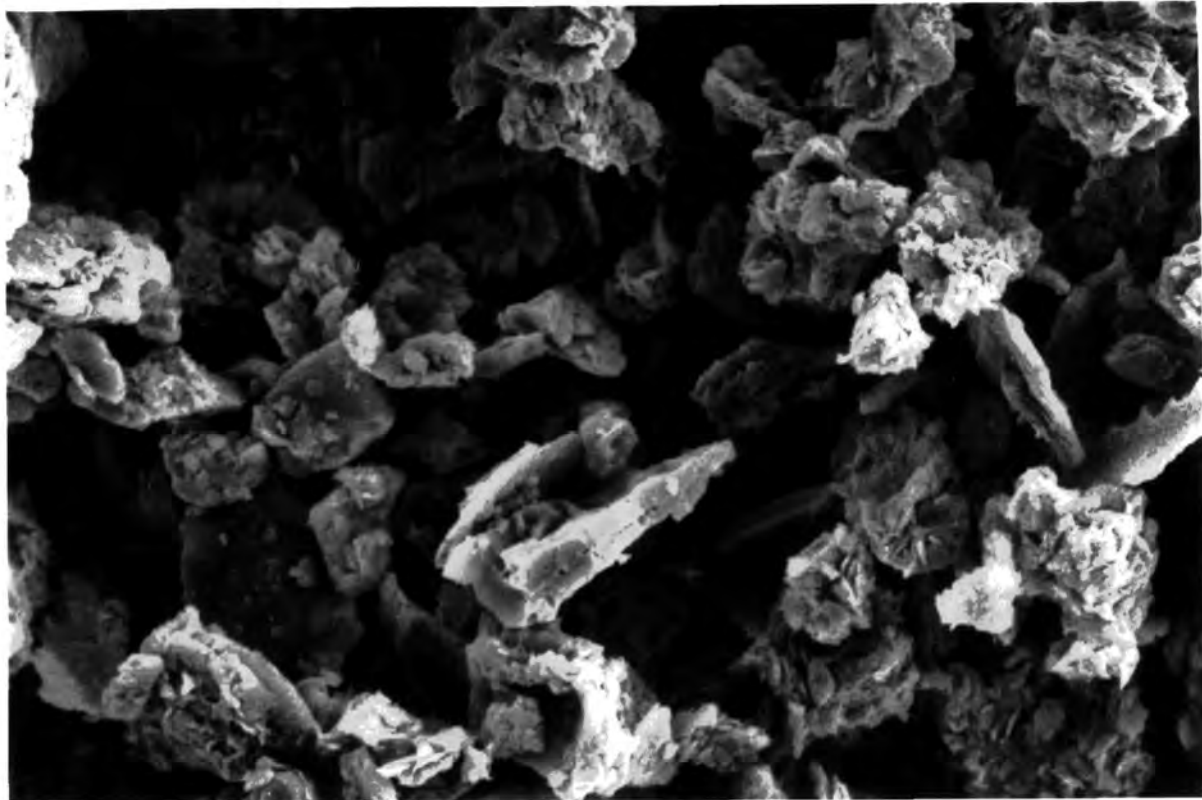


Figure 4.2.12 Sample WM5; in the centre of the picture are grains which are partially coated with clay minerals. Surrounding these grains are concentrated clusters of clay mineral fragments forming discrete particles.
WD 7 mm; x2000; 1cm=3 μ m

4.2.3 STUBB PLACE, ESKMEALS TL3080 4906 Altitude 5.5 m OD.

4.2.3.1 Stratigraphy (figure 4.2.13)

0-10cm	As2, Ag2, Lf+. Nig2, str0, elas0, sicc3, lim.sup0. Brown silty clay with some orange ferric mottles.
10-47cm	As3, Gg(min)1, Ag+, Sh+. Nig2, str0, elas1, sicc3, lim.sup.0. Brown silty clay with some sand and humic matter near base. <u>Sample SP1</u>
47-97cm	Sh2, Th ¹ 2, Ga+, As+. Nig3, str1, elas2, sicc2, lim.sup.1. Dark moss peat with some partly broken down stem and root near top.
97-135cm	Ag2, Ga2, As+, Sh+. Nig2, str0, elas3, sicc1, lim.sup.0 Grey-brown silty sand with some humic matter near top. <u>Sample SP2</u>
135-198cm	Sh2, Th ¹ Phra1, As1, Ga+. Nig3, str0, elas0, sicc1, lim.sup.1. Dark <u>Phragmites</u> peat with large plant remains, clay and some fine quartz.
198-236cm	Ag2, Ga2, As+, Sh+. Nig2, str0, elas3, sicc0, lim.sup.0. Dark grey sandy silt with reddish colour at peat contacts. <u>Sample SP3</u>
236-341cm	Sh2, TI2, As+, Ga+. Nig3, str0, elas2, sicc1, lim.sup.0. Dark mossy peat.
341-435cm	As2, Gg(min)2, Ag+, Sh1. Nig3, str0, elas2, sicc1, lim.sup.0. Dark grey-brown silty-clay, finely laminated; some organic matter at top. <u>Sample SP4</u>
435-472cm	Ag3, As1, Sh+. Nig2, str1, elas1, sicc.2, lim.sup.0. Grey, slightly laminated clay-silt, with a large piece of softwood. <u>Sample SP5</u>
472-540cm	As2, Ag2, Sh+. Nig2, str0, elas1, sicc2, lim.sup.0. Blue-grey clay, with some small scattered humic inclusions. <u>Sample SP6</u>
540-627cm	As2, Ag2, Ga+, DI+. Nig2, str1, elas0, sicc3, lim.sup.0. Brown-grey silty-clay; fine sand content; woody fragments at 4100mm. <u>Sample SP7</u>

627-680cm	Ag2, As1, Ga1, Sh+. Nig2, str1, elas1, sicc3, lim.sup.0. Brown-grey silt; becomes mixed with underlying layer. Increased sand with depth. <u>Sample SP8</u>
680cm --	Ag2, Ga2, As+, Gg(maj)+. Nig2, str0, elas0, sicc2, lim.sup.0. Wet, red sand with clay and gravel. <u>Sample SP9</u>

4.2.3.2 Sample Descriptions

SP1

This stratum is a brown silty clay with some humic matter near the base where it grades into a dark mossy peat. It is dominated by coarse to medium silts. Clay minerals are the most abundant (40%) in all fractions. Quartz is the next most abundant mineral especially in the sand fractions, and then feldspars (18%), which consist mainly of potassium types. Variation in mineralogy between silt fractions is minor. The water content of the sample is 70.8% which is relatively high, and loss on ignition is 10.3%, which reflects the humic content mentioned above. This stratum is the B horizon of the modern soil. A dark mossy peat separates SP1 and 2, which contains some fine sand. The grains showed some signs of chemical weathering.

SP2

This sample is a grey-brown silty sand. The sand grains are rounded to sub-angular, which appear slightly opaque under microscopic examination. This suggests that they have been transported by wind, probably from the nearby beach. This is likely to account for the origin of the sand in the peats in the upper part of the core, as well as the minerogenic layers. The sample has a significant silt content (up to 79%), which decreases slightly with depth.

The water content (116%) increases slightly with depth, probably reflecting the unconsolidated nature of the material, and proximity to the water table. The silt sized fraction comprised mainly quartz, which is the most abundant mineral in all fractions. Feldspars, predominantly potassic, are of variable abundance in the different silt fractions, with a mean of 28.8% of identified minerals. No mixed layer clays were identified. Chlorite and kaolinite are the most abundant clay minerals. The coarse grain fraction was extracted for TL and IRSL dating.

SP3

This stratum lies below a second peat, which is dark and contains fragments of *Phragmites* within its matrix, together with more aeolian sand. This layer is a dark grey sandy silt with clay and sand. Quartz strongly dominates the mineralogy of the coarse silt fraction and clays increase with a

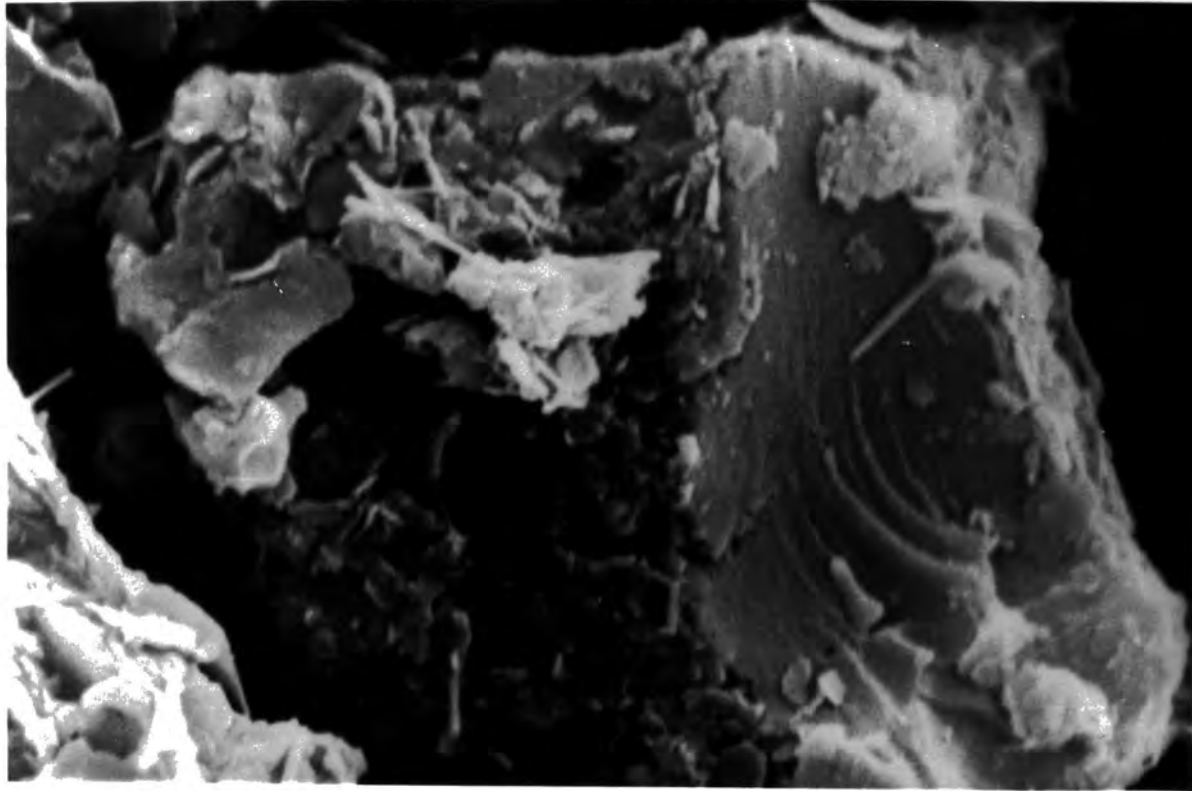


Figure 4.2.14 Quartz grain from SP3 showing relatively clean fracture face on the right, which has the conchoidal form and stepped features characteristic of quartz. WD 7 mm; x10 000; 1 cm= 0.8 μ m.



Figure 4.2.15 Sample SP3 showing an unidentified (possibly salt) crystal within the sample. The recognition of such inclusions in a sediment demonstrates the importance of isolating feldspar emissions from minerals whose emissions may be unstable in terms of dating (see Chapter 5).
WD 7 mm; x10 0000; 1 cm= 0.8 μ m.

decrease in grain size. Feldspars are less abundant than in SP2, but potassium types are more abundant. This layer has a high water content (128%) and the amount of organic carbon increases slightly with depth (mean 17.7%). This represents a greater variation than in the other samples. The fine-grain fraction was extracted for TL and IRSL dating.

A significant quantity of mixed layer clays was identified. Together with the abundance of clay minerals, this suggests that some alteration of the finer grained minerals, especially feldspars has occurred. Mineral grains under SEM showed some features of weathering, and relatively fresh fracture faces did not demonstrate totally clean faces (figures 4.2.14). There were also some unidentified sharply defined crystals in the samples, which are of unknown type and origin (figure 4.2.15). The reddish upper and lower contact of this layer indicates oxidation or exposure before and after deposition. There may be greater aeration on the interface between the peat and the minerogenic deposit. A third peat separates SP3 and 4. This is dark, well humified and mossy, similar to that between SP1 and 2.

SP4

This stratum is a grey brown silty sand, which is semi-stratified, with the highest organic carbon content in the core, and increases slightly with depth, except in the basal sample where the value is much less. Water content is 92%, and fluctuates within the layer, but is less at the base, where clays are more abundant. Clay minerals dominate all silt fractions, and mixed-layer clays are quite common.

This sample appears to be highly heterogeneous, although its semi-stratified structure indicates a fluvial mode of deposition, with variations in the energy of flow or supply of sediment. Although care was taken to take representative samples of the layer for analysis, some of this variation may be attributed to changes associated with the stratified nature of the deposit. However, overall, the homogeneity of the deposit is poor, in terms of the problems related to dose rates and equivalent dose evaluation. The fine-grained fraction was isolated for dating.

SP5

This layer has graded upper and lower contacts, into SP4 above, and SP6 below, and has the appearance of a transitional deposit between different depositional conditions. The sediment is a compact grey clayey silt and contains much less sand than the overlying layers. It also contains mixed-layer clays. The feldspars are dominated by plagioclases which are almost equal to quartz in abundance, except in the coarse silt fraction where the quartz dominates. Loss on ignition values were negligible. SEM examination revealed the remains of diatoms, although these could not be isolated in samples taken for diatom analysis. In addition, a number of 'fresh' mineral grains were seen, which carried impact marks on the surfaces characteristic of quartz (figures 4.2.16 and

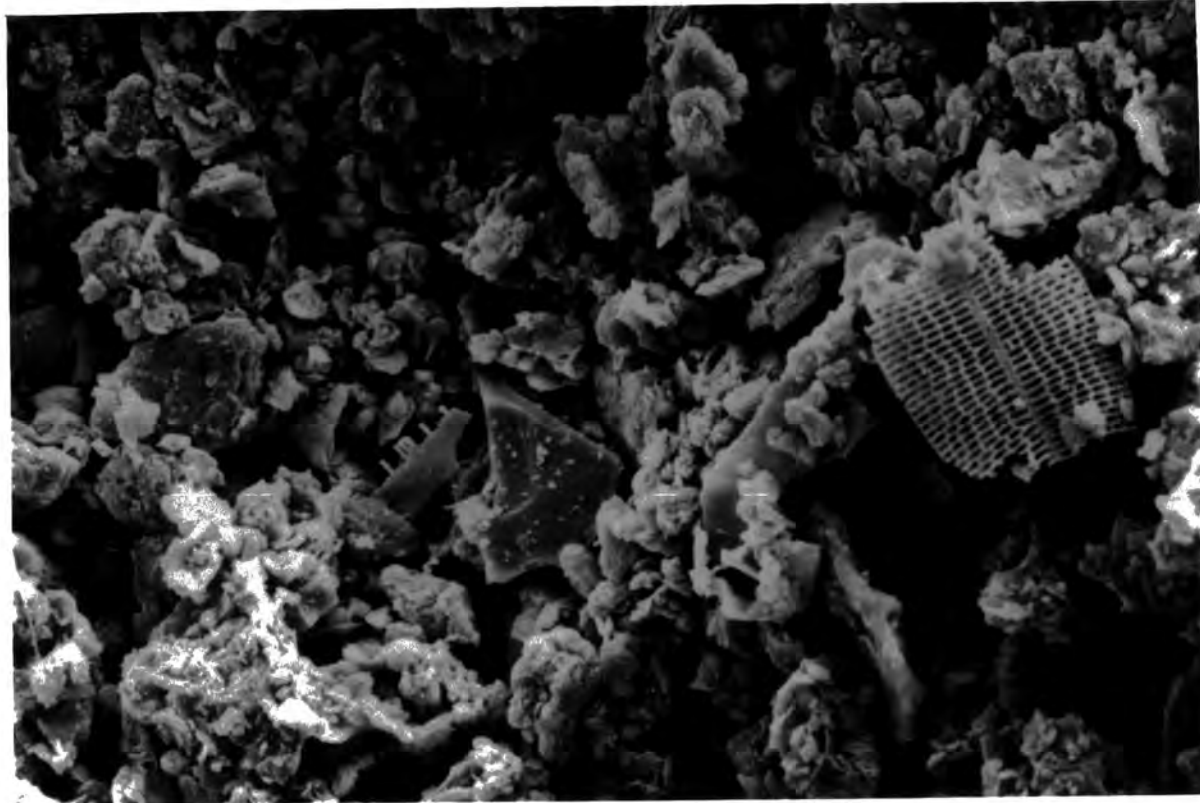


Figure 4.2,16 Sample SP5 showing the presence of fragments of diatoms in centre and to right. Quartz and feldspar grains in this sample are not affected by clay mineral coatings. Diatoms are not suitable for luminescence dating as the silica is in an amorphous form and so cannot absorb or emit luminescence.
WD 7 mm; x2000; 1 cm= 3 μ m.

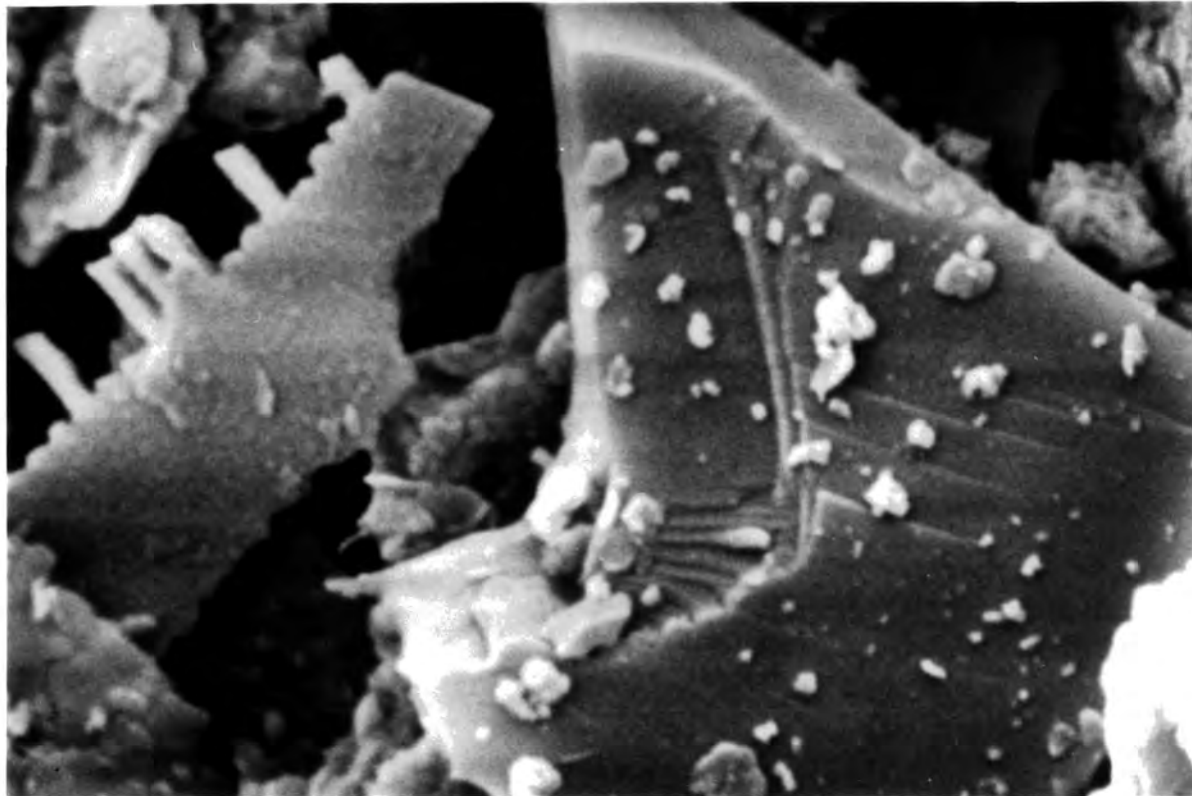


Figure 4.2.17 Higher magnification of SP5 showing quartz grain on right with characteristic stepped fracture resulting from impact during transport. The edges of the grains have not been eroded by transport. To the left is a fragment of diatom skeleton. WD 7 mm; x10 0000; 1 cm= 0.8 μ m.

4.2.17). These grains appeared unweathered suggesting little alteration during transport or burial.

The particle size distribution contains an even mix of different grain sizes. The organic carbon content is significantly lower than SP4, as is the water content (42%), which also reflects the more compact, less sandy structure of this layer. The deposit indicates a shallowing of water conditions, and increased turbulence, resulting in the mixing of suspended silts and clays with the bed load of sandy material. Both the coarse and fine-grain fractions were extracted for dating.

SP6

This is a blue-grey clayey silt with a negligible sand content compared to the upper layers of the core. The water content decreases with depth, and organic carbon is very low. The compact nature of the lower layers of this deposit probably accounts for the decreasing water content, and the low organic component (2%) may reflect a marine rather than a terrestrial source of the sediment, although there were no diatoms present to aid identification of the depositional environment.

Feldspars (particularly potassium feldspars) are the most abundant minerals, except in the medium silt fraction where quartz is more abundant. The water content has a mean value of 30%, and decreases with depth. This may be due to compaction of the deposit. This stratum grades into the underlying SP7, without any indication of a break in sedimentation.

SP7

This stratum contains slightly more sand, which increases with depth. It is a brown silty clay, and the colour suggests a significant iron content. The water content increases as the proportion of sand rises up to a value of 50%, when the water content value remains constant. The sand in this layer appears to be of a fluvial origin, having none of the cloudy appearance of the aeolian sand in the upper strata. Loss on ignition (mean 10%) rises near the upper boundary, and remains constant throughout the deposit.

Plagioclase feldspars are the most abundant mineral in the coarse silt and quartz dominates the medium and fine silt fractions. Clays however, are less abundant, and no mixed-layer clays were identified. The occurrence of large feldspar grains (mainly potassium types), and relative paucity of clays suggests a minimum amount of alteration by post depositional weathering. This is supported by the homogeneity of the sample, and the graded boundaries reflecting changing depositional environments rather than soil horizonation.

SP8

This stratum underlies SP7. The sample is a silty sand, with very little clay. It has a much lower water (33%) and organic carbon (1.4%) contents than the layer above. In the case of the water content, this reflects the relative amount of compaction that the overlying layer has undergone, reducing the amount of available pore space, but also the abundant silt matrix which would serve to fill any remaining voids, reducing porosity. Quartz is the most abundant mineral in all size fractions. The sand content is variable throughout the stratum, indicating variations in the depositional environment.

Clay minerals are relatively rare, comprising only 14% of identified minerals. No mixed-layer clays were identified. Feldspars were dominated by plagioclases, which were not severely degraded. There were with few adherent clay particles which indicated minimal post-depositional alteration of the feldspar in this stratum. This is consistent with a sediment that is relatively compact and has not been exposed before burial, as indicated by the apparent continuity of deposition throughout the lower part of the core.

SP9

The basal sample is a red sand with a silty matrix. It is a fluvial deposit associated with the Devensian boulder clay. SP9 has the lowest water (28%) and organic contents in the core due to its compact structure. The silt mineralogy is dominated by quartz, although feldspar becomes increasingly abundant in the finer grain size fractions. Clay minerals are rare, and feldspars comprised 24% of identified minerals.

The sample was very compact and SEM analysis of the grains showed an abundance of evenly sized, angular grains, with rare adhering flakes. A few pitted and partly rotted grains of feldspar (primarily plagioclases) were visible, but these, and the clay aggregates, which formed discrete clusters, were sparse. The appearance of the grains suggests a mode of transport which was of short distance, or which did not result in excessive abrasion of the grains. Quartz grains from glacial environments tend to be angular with blocky and conchoidal fractures, such as these sand grains. These do not appear to have been significantly altered in their present burial position.

4.2.3.3 Summary

The sediments in the lower part of the core do not appear to have been significantly altered since deposition. The upper strata may have undergone pedogenesis and weathering of mineral grains *in situ*. This may have been accelerated by the abundance of decomposing organic material and organic acids provided by the peat layers.

The close packing of the lower sediments may make irrelevant the impacts of the high water table levels near to the coast in all but the upper, uncompacted layers. Estimations of past water contents in compacted sediments will be more accurate, unless the compaction is recent and reduction in pore volume significant. In some fine-grain material, this may not be the case.

An overall fall in the amount of sand with depth may indicate a deeper water depositional environment at the beginning of the deposition of this stratum, and consequently a lower input of aeolian sand. Samples SP2, 3 and 4 are similar in the heterogeneous nature of the material. In the first two cases, this may be attributed to pedogenic processes in operation during burial. This is reflected by high clay contents, abundance of amorphous clays and, as each is adjacent to peat, there is a ready supply of organic acids for chelation and mineral dissolution processes. The fluvial environment of deposition should allow sufficient bleaching before burial, particularly of the IRSL signals.

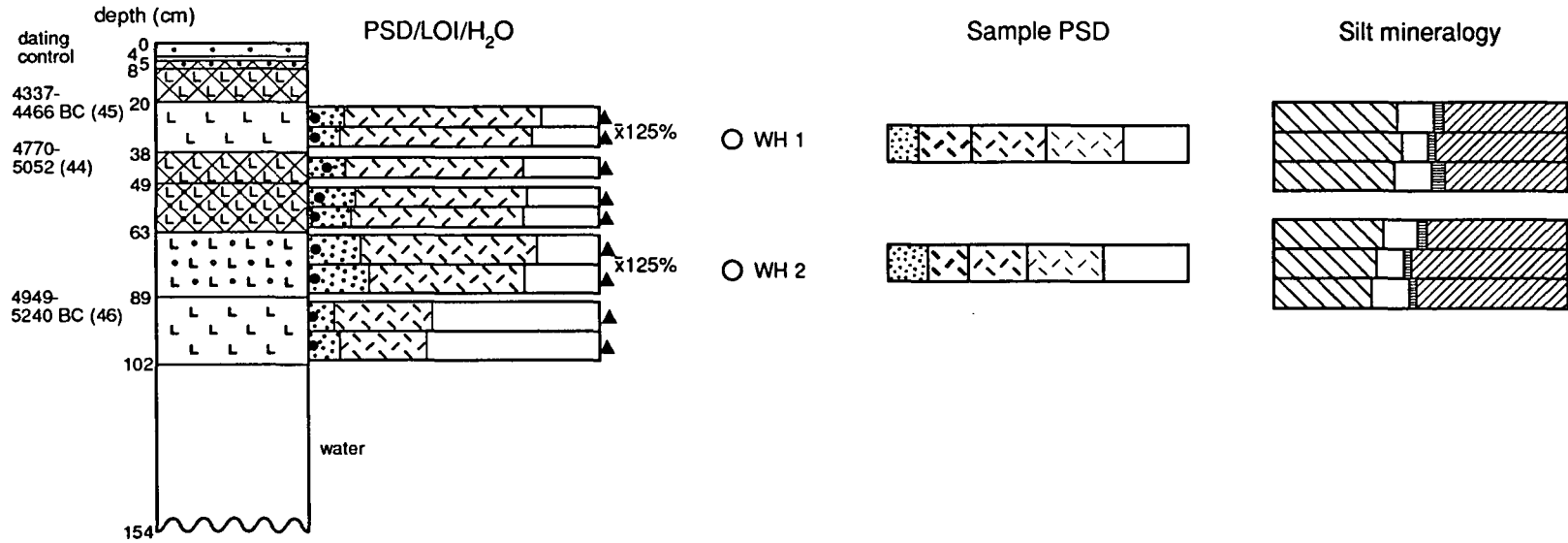
It is possible, from the degree of similarity between SP9 and 8, that the latter is derived from the basal boulder clay, and may contain a mixture of glacially derived and fluvial material. It grades into the minerogenic sequence of SP7, 6, and 5, and then into 4. This last contains sand of a probable aeolian origin, which appears in all the overlying peat and mineral layers. The lower minerogenic part of the core seems to represent deposition resulting from a deepening of a basin, with calmer water conditions, and then shallowing with a mixed sand and silt deposit, some of this sand being aeolian in character. The upper layers were deposited during alternating periods of waterlogging with peat formation, and submergence when sandy silts were deposited. The abundance of aeolian sand in the mineral layers strongly suggests periods of surface exposure or soil development, allowing input of wind blown sands. This sand fraction is more likely to have been well bleached than the waterlain sands, but the silt matrix, which is either aeolian or pedogenic, may not have been bleached in the latter case.

4.2.4 HARTLEPOOL BAY, CLEVELAND. NZ 5140 3210 Altitude -0.37 mOD

4.2.4.1 Stratigraphy (figure 4.2.18)

0-4mm	surface sand and algae
4-5cm	Ld3, Ag1, Ga ⁺ . Nig3, str1, elas+, sicc2, struc. laminated. Black limus with sand and some silt.
5-8cm	Ld ³ 3, Ag1, Ga+, Th Phra ⁺ Nig2, str2, elas2, sicc2, struc. laminated. Laminated buff sandy silty limus with <i>Phragmites</i> .

Figure 4.2.18 Hartlepool Bay stratigraphy



8-20cm	Ld ² 3, Th ^{Phra} 1, Dl+. Ag+. Ga+. Nig2+, str3, elas3, sicc2, struc. laminated. Brown well laminated limus with <i>Phragmites</i> in laminations.
20-38cm	Ag3, As+, Ga1, Th ^{Phra} + Nig2, str0, elas2, sicc2, struc. buttery. Battleship grey clayey, fine sandy silt with <i>Phragmites</i> . Gamma-spectrometer probe at 28-35cm <u>Sample WH1.</u>
38-49cm	Ag3, As+, Ga1, Ld+, Dh+. Nig2, str0, elas0, sicc2, struc. malleable. lim.sup. 5cm variation. Battleship grey clayey sandy silt with flecks of eroded limus; some mica.
49-63cm	Ld4, Dh+, Ag+, Ga+. Nig3, str1, elas+, sicc2, struc. slightly laminated. Slightly laminated sandy limus with rare herbaceous woody detritus.
63-89cm	As2, Ag1, Ga1, Anth+, Gg(maj)+, Gg(min)+. Nig2, str0, elas0, sicc2, struc. malleable. Battleship grey sandy silty clay with coarse sand partings, and rotten pebbles/gravel. Rare charcoal and limnic and peaty partings. <u>Sample WH2</u>
89-102cm	As3, Ag1, Gg(maj)+. Gg(min)+. Tenacious red boulder clay. Water depth 52cm.

4.2.4.2 Sample Descriptions

WH1

This stratum is a silt (70%), with some sand (10%) and clay (20%). It is of very homogenous composition with a consistently high water content (125%). This relates to the uncompacted nature of the material, and to its present intertidal position. It has a low organic carbon content, which suggests a marine rather than a terrestrial source for the silt. The silt mineralogy is dominated by quartz. Little feldspar or clay was identified. There is a small amount of calcite in the sample and a high sodium content. This may be related to the abundance of relatively soluble salts from the sea water. This is also reflected in particularly high content of sodium in the XRF analysis, compared with the underlying sample.

WH1 lies between two sandy silty limus deposits and is thought to have been derived from contemporary land surfaces. The notable homogeneity of the silt indicates a consistent depositional environment, and a constant source of material. No post-burial change has been observed, and its present intertidal position would prevent pedogenesis from occurring. The absence of mixed layer clays and the clarity of the grains under SEM, also reflect the nature of the deposit (figures 4.2.19 and 4.2.20). Mica was abundant in these micrographs, but this may be expected where there is an abundance of elements in solution. In the centre of figure 4.2.20, is a larger grain which appears to have a very open 'skeletal' structure. This cannot be firmly

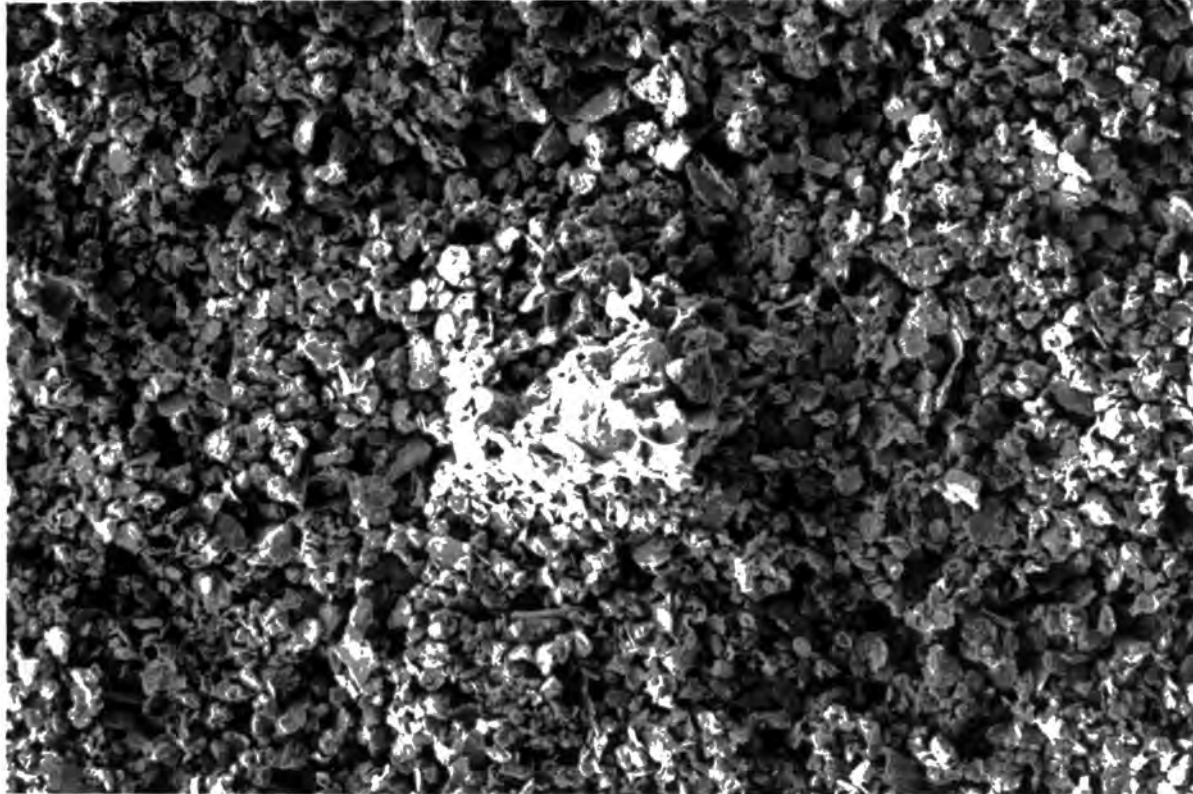


Figure 4.2.19 Sample WH1 showing clearly defined grains forming the matrix of the deposit. These grains show little signs of weathering. The inclusion in the centre of the photograph is shown at greater magnification in figure 4.2.20.
WD 6 mm; x500; 1 cm= 15 μ m.

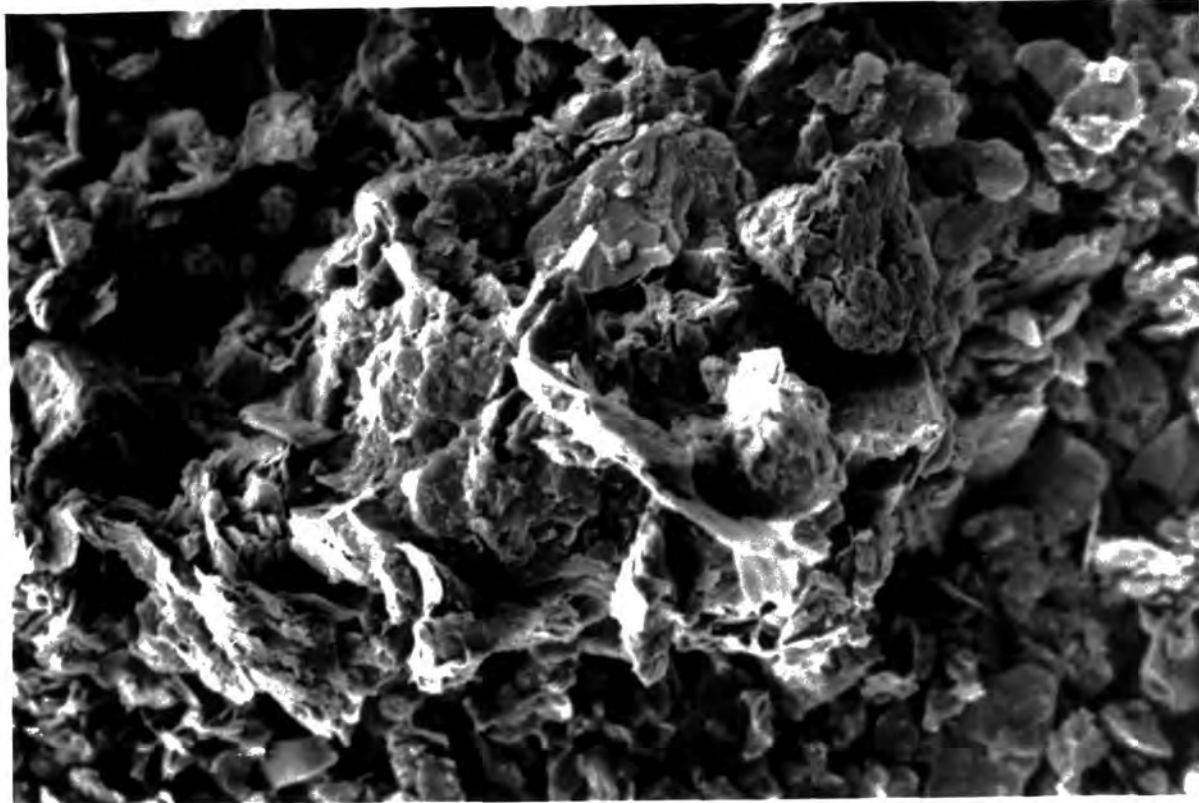


Figure 4.2.20 Sample WH1. This inclusion has a very open 'honeycomb' structure. It appears to consist of mica and clay minerals loosely joined together. Such inclusions are unlikely to affect the luminescence as these minerals are relatively inert with respect to luminescence.

WD 6 mm; x2000; 1 cm= 3 μ m.

identified, but it may represent a cluster of clay and mica grains. The quartz tended to be blocky, with rare platy aggregates adherent to the surfaces. The water content of the sample is high (125%) due to its uncompact nature and its intertidal position.

The depositional environment of this sediment is likely to be marine with the fine material settling out in lagoonal or lacustrine conditions, ponded up behind the low till 'ridge'. There are no laminations or shells which are common in many intertidal mud deposits.

WH2

This stratum lies below the lower sandy silty limus deposit. It is a silty clay containing 15% coarse sand with charcoal and rotten pebbles. The charcoal is rare, so a low organic carbon content (2%) is consistent. However, there is some increase with depth of the clay sized fraction. The silts are predominantly quartz and clay minerals are more abundant than in WH1. Feldspars are also rare and both calcite and the high sodium contents of WH1 are absent from this layer. This reflects the more compacted nature and greater depth of this sediment. No mixed layer clays were seen, and clay minerals were mainly stable kaolinites, illites and chlorites. This sample does not appear to have been weathered as there are no intermittent phases of clay formation or amorphous material.

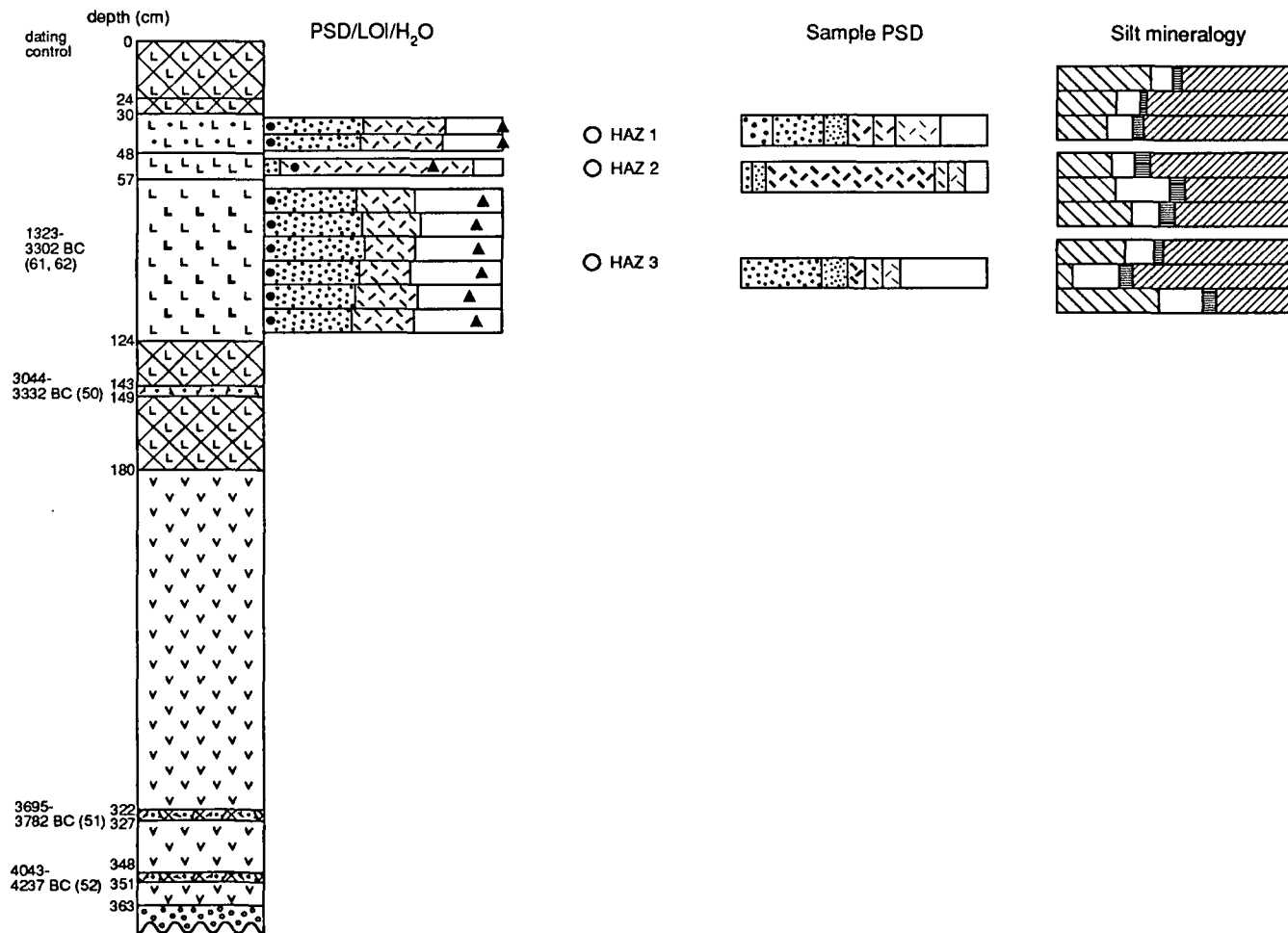
WH2 is underlain by weathered boulder clay. It may in part be derived from this, and mixed with runoff deposits from the contemporary land surface. There was also evidence of pedogenic mixing before submergence. This would account for the charcoal and other material, as well as the mixed grain size content. The boulder clay has significantly more clay and less sand than WH2, but if mixed with other material, it could be derived in part from the boulder clay. The water content of this sample is similar to WH1 (c.125%) which increases the uncertainties associated with dose-rate corrections for water content, and thus reduces the accuracy of the date. The fine-grain fraction was dated by TL and IRSL.

4.2.5 HAZENDONK, MOLENAARSGRAAF 1165 4313. Altitude 0.6 m NAP

4.2.5.1 Stratigraphy (figure 4.2.21)

0-24cm	As2, Sh1, Th ⁰ 1. Nig4, str0, elas0, sicc2, lim.sup.0. Soft humic clay, with some rootlets and humus.
24-30cm	As3, Ag1, Sh+. Nig3, str0, elas0, sicc3, lim.sup.1. Dark humic clay-silt.

Figure 4.2.21 Hazendonk stratigraphy



30-48cm	Ag2, Ga2, As+, Th+. Nig1, str0, elas0, sicc1, lim.sup.0. Reddish sandy-silt; crumbly, with many rootlets. <u>Sample HAZ1</u>
48-57cm	Ag3, As+, Ga+, Th ³⁺ , Ld+. Nig1, str0, elas1, sicc2, lim.sup.0. Reddish silt with white shelly fragments and angular sand grains (>= 1mm). <u>Sample HAZ2</u>
57-124cm	As2, Ag1, Ga1, Tb+. Nig2, str1, elas0, sicc2, lim.sup.0. Grey sandy silty clay with intermittent, thin peaty layers. <u>Sample HAZ3</u>
124-143cm	Ld ⁰ 2, As1, Ag1. Nig3, str1, elas3, sicc3, lim.sup.0. Silty-clay peat, semi-stratified, dark brown.
143-149cm	Sh2, Ag1, Ld ⁰ 1, Th+, part test moll+, anth+. Nig3, str1, elas1, sicc3, lim.sup.1. Cultural layer; shelly fragments, charcoal in dark silty peat.
149-180cm	Sh2, Ag1, As1. Nig3, str1, elas0, sicc2, lim.sup.0. Silty-clay peat, semi-stratified.
180-322cm	Ld ⁰ 3, Tl ² 1, Ag+. Nig2, str0, elas2, sicc2, lim.sup.0. Woody peat as lumps within silty peat.
322-327cm	Sh2, Ag1, Ld1, Th ³⁺ , part test moll+, anth+. Nig3, str1, elas0, sicc3, lim.sup.1. Cultural layer with shelly fragments and charcoal.
327-348cm	Sh3, As1. Nig3, str0, elas1, sicc2, lim.sup.0. Soft dark homogeneous peat.
348-351cm	Sh2, Ag1, Ld1, Th ³⁺ , part test moll+, anth+. Nig3, str0, elas0, sicc2, lim.sup.1. Cultural layer, with shell fragments and charcoal.
351-363cm	Sh4, Th ³⁺ . Nig4, str0, elas2, sicc2, lim.sup.0. Humic peat.
363cm –	Gg(min).2, Gs.2, Dl. ² Nig1, str0, elas0, sicc2, lim.sup.1. Dune sand; quartzite, poor matrix, with large piece of wood.

4.2.5.2 Sample Descriptions

HAZ1

HAZ1 lies beneath the topsoil, which was not sampled. It was a reddish sandy-silt, comprising a mixture of grain sizes. The organic carbon content was low (1.2%) but the water content was high (102%). The silt mineralogy was dominated by clays (including some mixed-layer clays) and quartz which decreases in the finer fractions. Feldspars were predominantly plagioclases and were relatively rare. The particle size distribution was dominated by the sand fractions. The high water content is attributed to the open structure of the deposit which lies at or below the ground water table.

This near surface sample may be undergoing subsoil processes at present, as the B horizon, although it has a low organic content. It contains some mixed layer clays, which may represent intermediate phases of feldspar dissolution. Under SEM examination, the clays were shown to have a very open structure (figure 4.2.22) and occasional large mineral grains were coated with adherent clay minerals (figures 4.2.23 and 4.2.24). The fine-grain fraction was extracted for TL and IRSL dating, and the quartz-rich sand for TL. This however was not suitable for IRSL.

HAZ2

This stratum comprises a red silt which lies directly below the HAZ1 layer. It contains predominantly silts with very little clay or sand. HAZ2 has a relatively high organic carbon content (12%), which may be incorporated with clay minerals into silt-sized complexes. The lower water content (74%) is related to the more compact nature of the deposit relative to the overlying layer. HAZ2 contains some shelly fragments, which may account for some of the carbon content. The presence of shelly fragments is indicative of a cultural horizon. The sediment may be primarily a fluvio-lagoonal deposit incorporating eroded terrestrial debris from occupation on the donk surface. This deposit may therefore represent a denuded cultural horizon. The cultural horizons on the donken consist of thin layers of charcoal, shells, small animal bones, flint and pottery sherds.

SEM analysis of this layer indicates an abundance of clayey aggregates, including mixed-layer forms. However these tend to form discrete particles, rather than adhering to grains. Quartz grains are slightly weathered on some older surfaces, but the fresh fractured surfaces are clean and show clear conchoidal fractures. Some feldspar grains are weathered, and have adhering clay flakes, indicative of feldspar weathering. Potassium feldspar types are more abundant than plagioclases. The fine-grain fraction was extracted for dating.

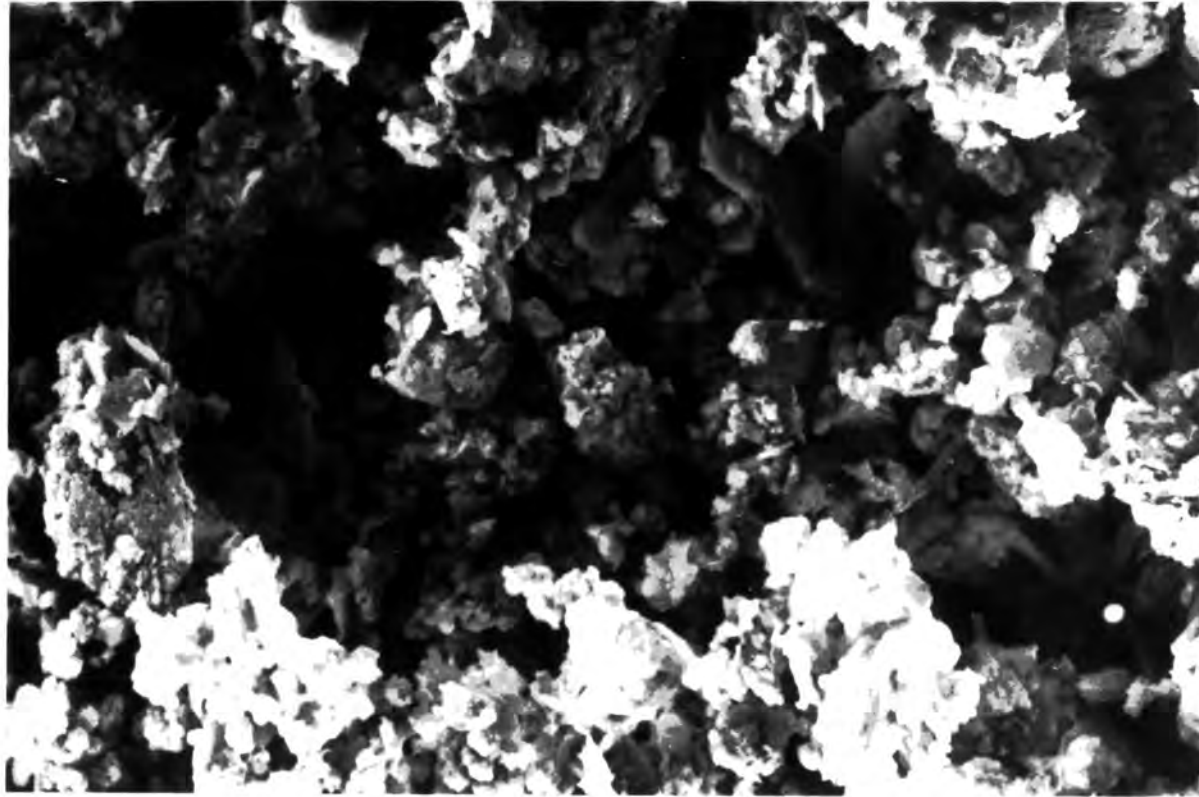


Figure 4.2.22 Sample HAZ1 showing the abundance of highly amorphous particles comprising largely of clays, of which many were identified by XRD to be mixed layer types. Few quartz and feldspar grains were observed in this sample. WD 7 mm; x2000; 1 cm= 3 μ m.



Figure 4.2.23 Sample HAZ1 - occasional larger mineral grains observed in this sample tended to be clay-coated and weathered, as in the case of this feldspar grain.
WD 6 mm; x500; 1 cm= 15 μ m.

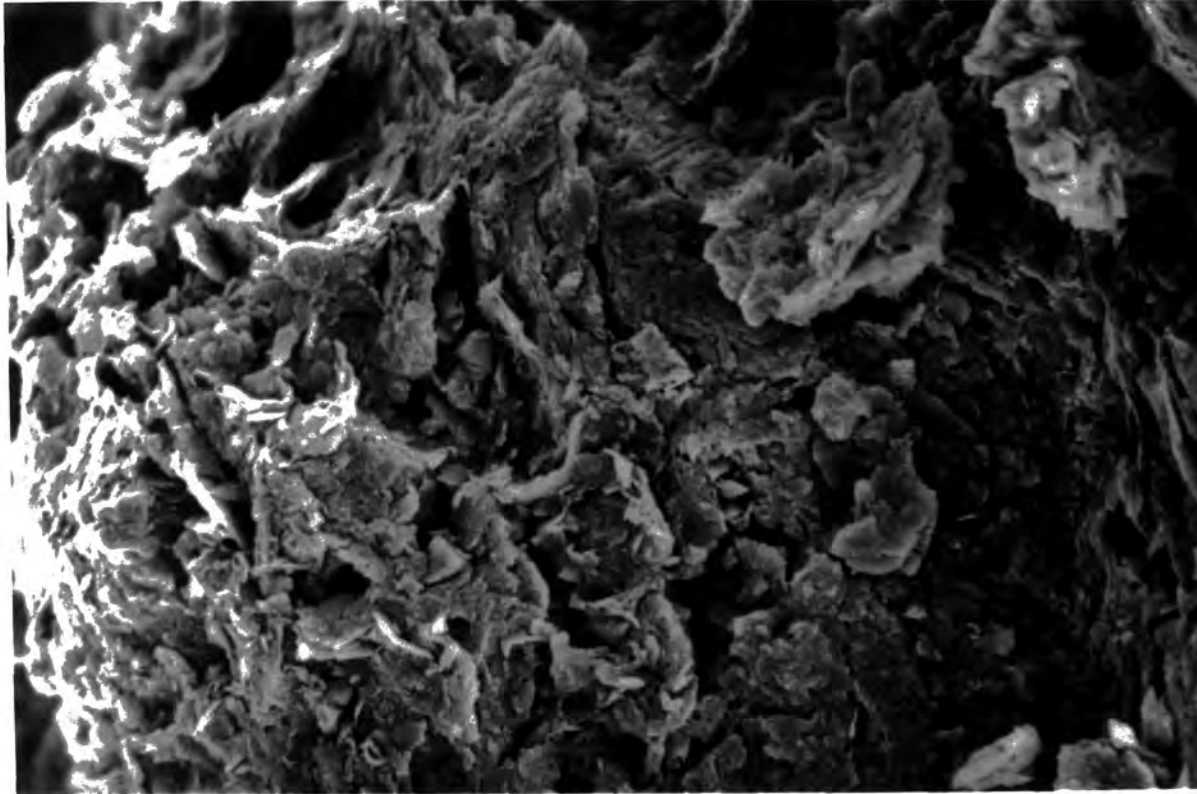


Figure 4.2.24 Higher magnification of clay coating of feldspar grain in figure 4.2.23. The coating consists of overlapping clay flakes resulting from deposition from percolating water.
WD 6 mm; x2000; 1 cm= 3 μ m.

HAZ3

HAZ3 is a grey sandy silty clay. It is relatively homogeneous in its particle size distribution, dominated by the silt and clay fractions. The silt mineralogy of HAZ3 is dominated by clay minerals, including some mixed-layer types, except in the fine silt fraction where quartz is more abundant. Feldspars are dominated by plagioclases. The water content is 93%, suggesting that the sediment has not been highly compacted. This also reflects its present position below the local water table.

Under SEM, the grains appeared to contain clean, fresh edged grains, with visible conchoidal fractures characteristic of quartz. Older surfaces, similar to those in HAZ2, tends to be more rough and with some adhering flakes. Water content and the organic carbon content of this sample tends to increase with depth, particularly at the interface with the overlying peat, indicating some mixing and possibly active weathering at this point.

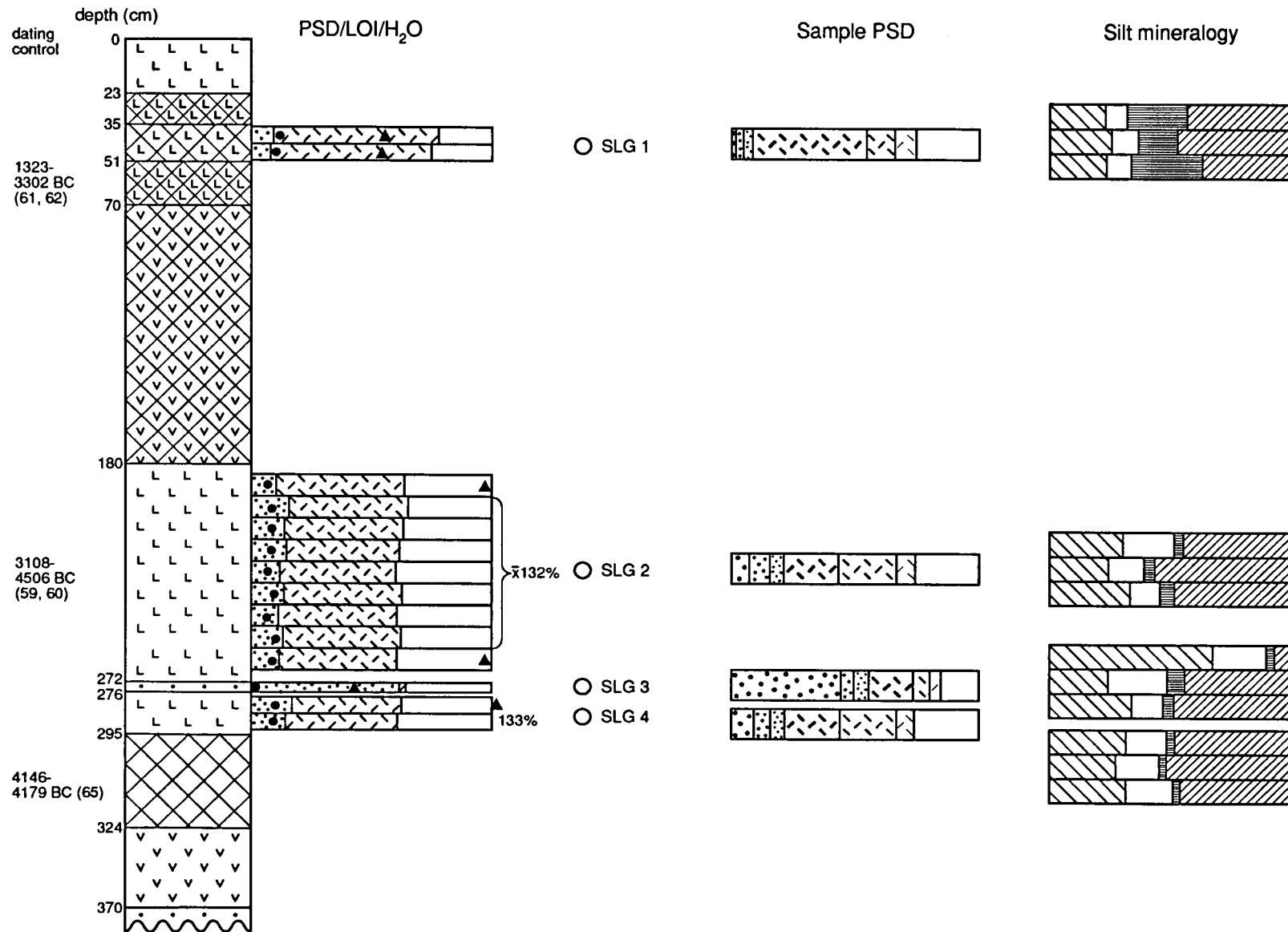
This deposit is a fluvio-lagoonal sediment and appears to have been little altered since burial. However, the high proportion of clay minerals and mixed layer clays may indicate either some alteration, or that the material deposited was already in a degraded state when deposited. Bleaching of the sediment is potentially good under quiet water conditions and in shallow water. The former conditions are likely to have applied, but it is not possible to estimate the depth of water at deposition. The IRSL signal is likely to be better bleached than the TL in these conditions.

4.2.6 SLINGELAND, NORDELOOS 1230 4333. Altitude -0.8 m NAP.

4.2.6.1 Stratigraphy (figure 4.2.25)

0-23cm	As2, Ag2, Ga+. Nig1, str0, elas0, sicc3, lim.sup.1. Reddish clay.
23-35cm	As3, Dh1. Nig3, str0, elas2, sicc2, lim.sup.1. Peaty clay, eroded upper boundary.
35-51cm	Ag3, As1. Sh+. Nig2, str0, elas0, sicc3, lim.sup.0. Grey clay silt, some humic flecks. <u>Sample SLG1</u>
51-70cm	As3, Sh1, DI ² . Nig3, str0, elas0, sicc2, lim.sup.0. Humic clay with woody fragments.

Figure 4.2.25 Slingeland stratigraphy



70-180cm	As2, Sh2, TI ² . Nig2, str.0, elas1, sicc2, lim.sup.1. Peaty clay, with woody fragments.
180-295cm	Ag2, As1, Ga1, Sh+. Nig2, str0, elas0, sicc3, lim.sup.0. Grey clay silt with peaty inclusions and layer of fine sand at 272-276cm. <u>Sample SLG2 (220-230cm)</u> <u>Sample SLG3 (272-276cm)</u> <u>Sample SLG4 (282-184cm)</u>
295-324cm	Ag1, Sh1, Ld1, Ga1, part test moll+, anth+, os+. Nig3, str0, elas0, sicc3, lim.sup.0. Cultural layer with shell, sand, bone and charcoal in an organic silt matrix.
324-370cm	Sh4, As+. Nig3, str0, elas2, sicc2, lim.sup.1. Organic peat.
370cm ->	Gs2, Ga1, Gg(min)1. Nig1, str0, elas0, sicc2, lim.sup.0. Dune sand.

4.2.6.2 Sample Descriptions

SLG1

SLG1 lies below the modern topsoil. It is a grey clayey silt with humic flecks, overlain by a silty peat. This has an eroded upper contact, suggesting exposure prior to peat formation. The silt content falls abruptly in the lower parts of the SLG1 layer. Water content is 58%, which may be reduced due to a degree of compaction during deposition. Most of the clays are illites and chlorites (together 42% of identified minerals), but no mixed layer clays were found. Clay minerals dominated the silt sized fractions, and the particle size distribution is skewed towards the coarse silt fraction. Feldspars are dominated by plagioclases which were significantly degraded by chemical weathering.

The higher organic matter content is caused by the distribution of humic flecks throughout the deposit, and some mixing of the layers may have occurred during or after formation of the overlying peaty clay. The high clay content of this sample suggests deeper, still water lagoonal conditions. The abundance of aggregates suggests that pedogenesis and chelate-related translocation may have occurred, although average quantities of aluminium and iron remain in the profile. The rarity of feldspars, and their degraded state also suggests alteration on a significant scale. Free draining conditions would have been necessary to maintain a state of disequilibrium between solution and solid, and this will have been restricted in such a fine-grained deposit.

SLG2 and SLG4

This stratum is another grey clayey silt, separated from SLG1 by a peaty clay. This layer contains more sand (20%) than SLG1. The particle size distribution is dominated by fine silt and clay fractions. Clay minerals are the most abundant mineral in the silts, although to a lesser degree than in SLG1. Quartz and feldspars are more abundant in this sample, even in the fine silt fraction. Feldspars are mixed potassium and plagioclase types.

This layer is 115cm thick, and contains a thin sandy band at 275cm (sample SLG3). The clay above and below the sand layer were both sampled for TL and IRSL dating. SEM analysis of SLG2 revealed a high proportion of micas and clay aggregates (including mixed-layer clays), which in some cases form characteristic open honeycomb structures. Visible quartz grains appear clean and sub-rounded, without clay adherence. The layer exhibits considerable variation in water content which shows an overall reduction with depth, particularly just above the sandy layer (75%). Below the sand layer, water contents are lower (73%) than in the upper clay. This reflects a greater degree of compaction. Organic carbon decreases with depth but not very significantly.

SLG2 and 4 are both very similar deposits, indicating that they essentially relate to a similar depositional environment, interrupted by a period of higher energy flow, depositing the sand layer. The clay was deposited in a lagoonal/lacustrine environment. The organic carbon component (9.4%) is derived from eroded humic flecks and possibly chemical complexes between silt and organic particles.

SLG3

This thin stratum is a sandy layer within the grey clay described above. It probably represents a high energy flood event, and a different source of material. The silty matrix may be derived from the grey clay, and there may have been some erosion of the clay. The sand contains no organic matter, and water content is higher than for the sand (95%) than for the clay due to its more open structure. The mineralogy of the matrix is variable, with clays more important in the finer fractions. The particle size distribution is dominated by medium sized sand. The silt-sized material comprises a small proportion of this layer, and the application of luminescence dating to this fraction would not be representative of the bulk material. The sand fraction was isolated for TL and IRSL dating, although the abundance of feldspars was low (23%). The feldspars were, however, dominated by potassium types.

SEM analysis shows the grains to be blocky with some possible secondary overgrowths of amorphous silica. Some adhering flakes occur, and abundant aggregates, especially kaolinite which occurs as disturbed pseudo-hexagonal stacks. Some of this disturbance may be caused

during sample preparation. Overall, the grains do not have the 'woolly' appearance of weathered material.

4.3 DISCUSSION

The samples can be roughly divided into two groups; the relatively unaltered 'depositional' types and the more obviously degraded 'pedogenic' types. This classification is based on the characteristics of a layer, particularly its degree of homogeneity, variability of silt mineralogy, abundance and form of clay minerals and evidence of weathering of the grains.

The 'pedogenic' type of sediment is characterised by a variation in the profile of particle size distribution, and water and organic carbon contents. This variation is due in part to mixing of the sediment by bioturbation, and by translocation of clays and organic-metal complexes by percolating groundwaters. The silt mineralogy of these sediments tends to be dominated by clays with smaller proportions of feldspars and quartz in the finer silt fractions. Mixed layer clays are common and often abundant. The grains are generally weathered, with significant amounts of adherent material on their surfaces. These included samples FF1, 2, 3; WM1, 2, 3; SP1, 3, 4; HAZ1, 2; SLG1.

The 'depositional' type of sediment is characterised by a much greater degree of homogeneity within the profile, including more constant values of organic carbon and water content. The silt mineralogy is less dominated by clay minerals, and there is a greater abundance of feldspars and quartz in the finer grain fractions. There tends to be no mixed layer clay material in these samples. Some do have high clay contents, but these are likely to have been deposited at the same time as the remaining fractions. These clays tend to be the more stable end products of weathering - kaolinite, chlorite and illite. Under SEM, the grains are clean, and in some cases, the edges and fractured faces are still sharp and clear, although older surfaces are rougher, but with very few adherent flakes. Mica grains, which are structurally relatively weak, are also well preserved in these samples.

The samples appear to have undergone some alteration, but not a significant amount, and not all the grains are affected. The abundance of the clays may be due in part to allogenic material rather than authigenic. Without micromorphological analysis, this is however difficult to determine. The restricted through-flow of ground water may have prevented significant alteration since deposition, and the low water contents, even when below ground water levels tends to support this. The grains themselves, for the most part, do not appear to be significantly altered. These include samples FF4; WM4, 5; SP2, 5, 6, 7, 8, 9; WH1, 2; HAZ3; SLG 2, 3, 4.

The degree of alteration in the pedogenic sediments may be significant, and affect the potential of the sample for luminescence dating. Provided they have been sufficiently bleached at deposition, sediments should be suitable for dating, with respect to the form and preservation of the mineral grains.

The low porosity and permeability of fine grained silts and clays, results in a closed system with respect to the mobility of ions within the sediment body. This is to be compared with open soil systems, where exposure at the surface, and an active mixing of the components, enhances the movement of elements and particles within and without the profile. The reduced mobility of ions will prevent excessive dissolution within a closed system, indicating that alteration observed in grains from a sediment characterised as 'depositional' is more likely to have occurred prior to burial, or prior to deposition in the present state. This will be most applicable to those sediments which were laid down in a compacted state before burial, as in the case of the Dutch clay deposits.

Work by Manheim (1970) shows that the ionic diffusion rates in sediments are 1/2 to 1/20 that of free solutions when the sediments have porosities between 100-20% (ie. sandy-silts and silty-sands). Where swelling clays are present, they will expand to fill the porespace of sands thus reducing their permeability significantly. In the case of sands, porosity may be as low as 9.6% where the grains are very densely packed. For this reason, the water content of sandy deposits may be very low, even below the water table level. Water contents of well sorted sands are generally lower than for poorly sorted sands (Meade, 1966). Water content increases with the type of clay mineral present, ascending in the order Kaolinite-illite-montmorillonite.

For most of the sediments considered here, it is likely that soil forming processes occurred when the deposit was a part of an active soil profile. If this was a subsoil B horizon the bleaching of the deposits at the time of burial may be difficult to assess. In terms of bleaching, the 'depositional' type of sediments are most likely to be controlled by the mode, rate and distance of transport. The finer grain sizes are more likely to be carried within the suspension load, and so exposed to sufficient sunlight to bleach the signal. The heavier sandy deposits may not have been bleached if carried in shallow water.

The samples examined in this study exhibit evidence of weathering. Some samples contained concentrations of badly degraded grains (eg. FF2, WM1, 2), with clear etch pits and cracks on the surfaces. Many of these samples also had high proportions of clay material, some of which still adhered to grain surfaces after treatments including washing and sieving.

Quartz grains were often heavily coated with flakes. They also had flakes lifting off the older surfaces, indicating either that material had been deposited by percolation or weathering of grains had occurred with the precipitation of amorphous silica on the surfaces. These tended to be samples which displayed other indications of pedogenic processes, implying that deviation from saturated water content conditions prevailed for sufficient periods of time to allow at least partial development of soils. Other strata were thinner and were stratified between peaty deposits where an abundance of organic acids would have been available to facilitate the mobilisation of aluminium, which is a major element in the crystal lattice of feldspars.

Many samples did not display evidence such as etching which could be regarded as indicative of weathering. These samples included deeper clay and silt deposits and those not juxtaposed with peat. It is not possible to distinguish between the clays formed from the weathering or alteration of minerals in the deposit from those laid down initially, particularly in relatively disturbed samples such as those obtained from coring. However, some of these samples were high in clay minerals (eg. SLG2, HAZ2), which are more likely to be allogenic, because the feldspar grains were not highly degraded. Some grains showed some cracks and others were coated with flaky platelets which may have formed during suspension before deposition, with grains forming a nucleus to which clay plates may have been electrostatically attracted. If these bonds were strong, it would not be surprising for the platelets to survive sonication during preparation, and desiccation of the sample may be the cause of them lifting away.

Many of the clays identified in the less eroded samples were kaolinite and illite-type minerals, which represent the more stable, end products of a weathering sequence. This may suggest that no further alteration of the primary minerals in these samples occurred during burial. Kaolinites and illites were also abundant in highly degraded samples. These often occurred as aggregates and may originate in two ways. First, they may be depositional minerals, originating from the unaltered material. Secondly, they may be the end products of mineral alteration *in situ*. The latter case may suggest that either weathering conditions occurred very rapidly, or without the formation of intermediate phase minerals, or that they operated over significant periods of time. In many calculations, the formation of clay minerals in soils is very slow, although very difficult to measure and highly dependent on variable factors such as the chemistry of percolating waters, local climate, vegetation and drainage. In the case of feldspars, variation in rates will depend on the amount of defects or crystal dislocation and twinning. These are often higher in plagioclases and igneous rocks of shallower, rapidly cooling origin which makes them relatively more susceptible to dissolution.

Experiments investigating the effects of pH and grain size on the dissolution of alkali feldspar (Speyer, 1986) have shown that mildly acid conditions do not influence the release of silica, but

aluminium is preferentially released. This is likely to be the result of chelating processes, where the acidity is induced by organic acids and mobility by chelation bonds and leaching. The effect of grain size was shown to be less than might be expected from available surface areas. This however reflects the localised nature of weathering related to the defect sites, rather than surface area. Larger grains, which break down into smaller fragments, may be expected to have a greater proportion of defect sites, but this depends on the structure of individual grains.

The effect of weathering on feldspar grains in particular, in terms of its relationship to the potential for luminescence dating, is considered in Chapter 7.

CHAPTER 5. LUMINESCENCE TECHNIQUES

This chapter is divided into five sections. The first presents the principles of luminescence as a dating technique; 5.2 describes the different luminescence techniques and 5.3 the methods adopted in this study. A review of previous work done on the TL and IRSL dating of waterlain sediments is incorporated into sections 5.3 and 5.4; the latter section discusses the investigations into selected aspects including optical bleaching (referred to hereafter as bleaching), water content and sensitivity changes affecting the samples. The final section comprises a summary of the method adopted for dating in this study. Figure 5.1 is a summary of the techniques in luminescence dating, and the sections in which they are discussed in this chapter.

5.1 INTRODUCTION

Luminescence dating is based on the measurement of trapped electric charge. The charge is derived from the radioactive decay of naturally occurring isotopes of uranium (^{238}U , ^{235}U), thorium (^{232}Th) and potassium (^{40}K). These isotopes emit ionizing radiation which is absorbed by matter, such as mineral crystals, and stored in defects in the crystal structure, known as traps. The trapped charge is evicted by a thermally assisted process, stimulated by heating or exposure to light such as natural sunlight, or artificial sources, eg. green lasers (Huntley et al, 1985) or infra-red diodes (Poolton and Bailiff, 1989). Following eviction, electrons may be re-trapped or recombine with a 'hole' (an ion from which an electron is missing) (figure 5.2.1). Recombination of electrons and holes may be radiative (ie. with emission of light) or non-radiative (Aitken, 1985); in the former case, the recombination occurs at luminescence centres, and the light emitted is the luminescence measured for the sample.

The minerals most commonly used for sediment dating are quartz and feldspar. This is because they are ubiquitous in most sediments and their luminescence characteristics are better understood than for many other minerals. Both of these minerals emit relatively bright luminescence signals and are able to retain their absorbed charge in traps which are stable for long periods of time, exceeding the present age range of the technique (c. 200 ka.). Quartz and feldspar are also sensitive to sunlight bleaching: ie. on exposure to sunlight, their stored charge is evicted, thus 'resetting' the luminescence 'clocks' to zero.

The exposure of sediments to sunlight is the key to sediment dating. The event that is dated is the last exposure of a crystal to light before burial. Problems associated with incomplete, or partial bleaching due to insufficient exposure, or to attenuated intensity and spectrum of the sunlight, as

Figure 5.1 Flow Chart showing luminescence techniques and locations in chapter 5.

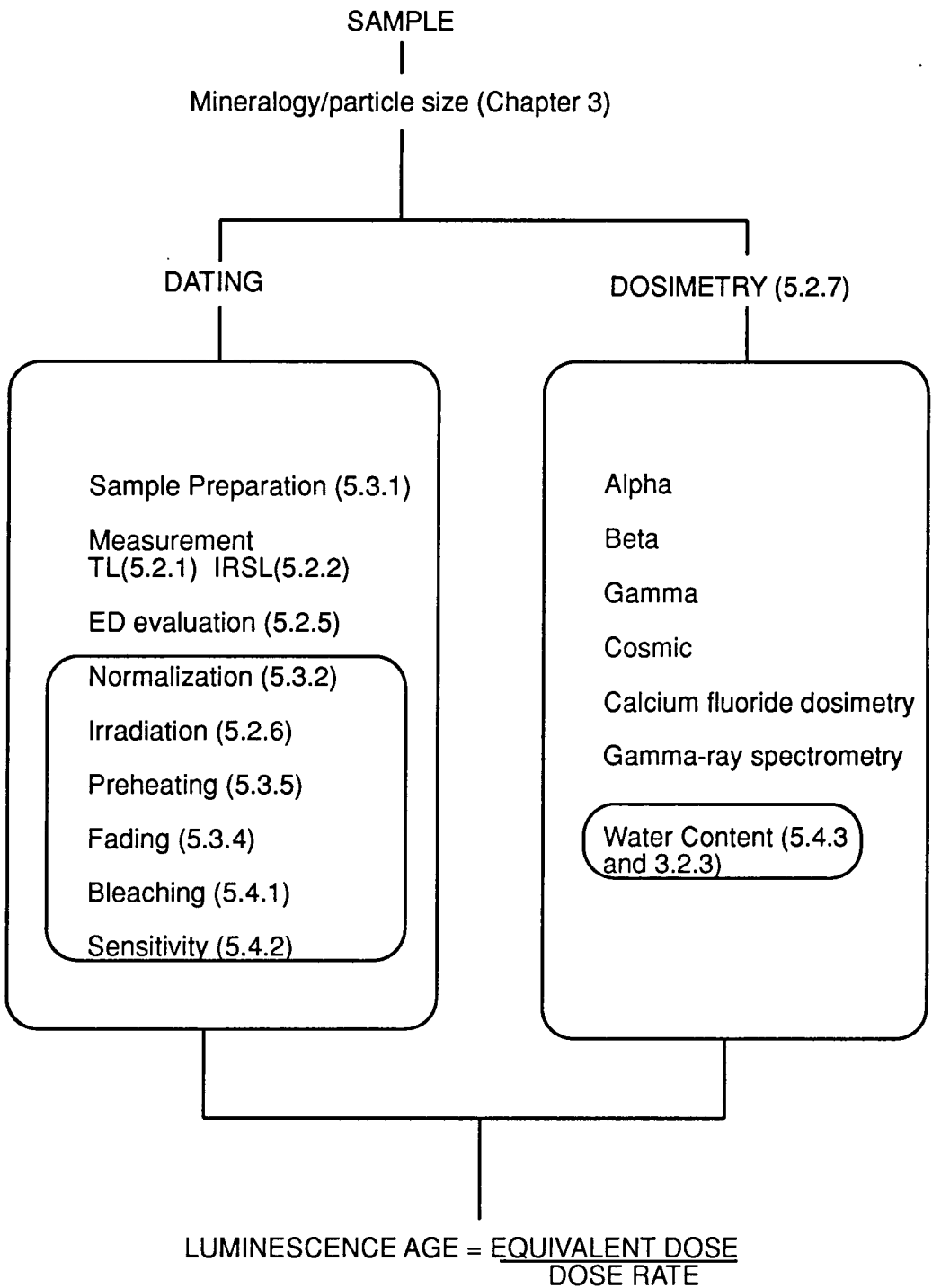
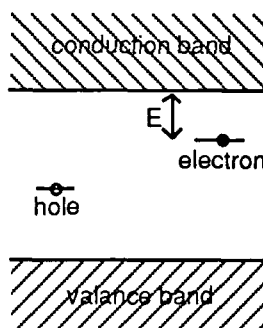
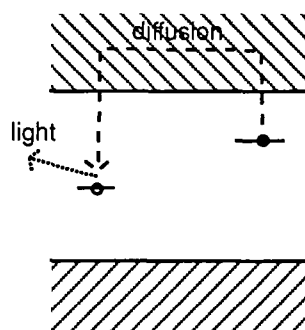


Figure 5.2.1 Diagrammatic representation of the luminescence process

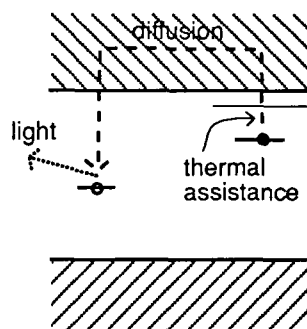
a. During ionization, electrons and holes (ions from which an electron is missing) are trapped and stored at defects in the crystal structure. The lifetime of these traps is determined by their depth, E .



b. Heating causes vibrations in the crystal lattice which evict the electrons. These diffuse through the conduction band and recombine with holes, or are retrapped in deeper traps. Recombination at luminescence centres is radiative, and light is emitted. Recombination at killer centres is non-radiative and no light is emitted.



c. In the case of IRSL, eviction is a two-stage process. First thermal assistance causes eviction through lattice vibrations. Optical stimulation then 'lifts' electrons in the conduction band where they diffuse and later recombine as for TL.



in the case of waterlain sediments, are discussed with reference to laboratory measurements in section 5.4. Chapter 3 discusses bleaching with reference to sedimentological processes.

Following bleaching and burial, the crystals absorb radiation charge from isotopes in the sedimentary environment. The amount of trapped charge measured in the laboratory is related to time, and to the annual dose-rate to the crystals. The dose-rate is related to the natural radioactivity of the sedimentary environment. The age of a sediment since deposition is therefore described by the equation:

$$\text{AGE} = \frac{\text{EQUIVALENT DOSE}}{\text{ANNUAL DOSE} = \chi_{\alpha} D_{\alpha} + \chi_1 (D_{\beta} + D_{\gamma} + D_c)}$$

where the Equivalent Dose (ED) represents the amount of trapped charge in the sample at deposition and χ_{α} and χ_1 represent the sample sensitivity to alpha radiation and light ionizing radiation respectively; D represents the respective dose-rate components derived from α , β , γ and cosmic respectively.

5.2 LUMINESCENCE TECHNIQUES

There are a number of methods by which the trapped charge can be evicted, and the emitted light signal (the luminescence) measured. The charge can be thermally evicted by heating up to c. 500 °C, which is the case for thermoluminescence (TL), or by optical stimulation from a light source. Optically stimulated luminescence (OSL) refers mainly to stimulation by light from a green argon-ion laser (c. 514.5 nm.), as distinct from infra-red stimulation by LED's (IRSL). There are other optical methods involving phototransfer of trapped charge, using UV light as a stimulation source, but this is applied more commonly to pottery rather than unburnt sediment, and not directly relevant to this study.

5.2.1 TL Measurement

TL was first applied to loess in the USSR (Morozov, 1968) using a method based on the techniques established for dating pottery. Huntley and Johnson (1976) took the next step by applying TL to siliceous shells from ocean sediments. They recognised an increasing intensity of TL signal with depth, which was derived from the sediment adhering to the grains, rather than the siliceous tests. Since then, the development of TL dating of a wide variety of sediments has been rapid, including volcanic materials, ocean sediments, varves, glacial tills and with greatest success

to dune sands and loess. The dating of aeolian materials is facilitated by the intense bleaching that occurs by direct exposure to sunlight during transport of the material.

The TL apparatus used was a semi-automated system, used at Durham for the Dating Service (Bailliff and Younger, 1988). The oven is controlled by a Servo unit, and the glow curves recorded on an X-Y recorder. The photomultiplier (EMI 9635 QB) was equipped with a Chance Pilkington HA-3 heat filter, and either Corning 5-60 or 7-51 light filters through which the emissions passed (see below). The irradiation sources are described in section 5.2.6. During all measurements, the oven was flushed with oxygen-free nitrogen, to reduce spurious TL, and using a standard heating rate of 10 °C/sec.

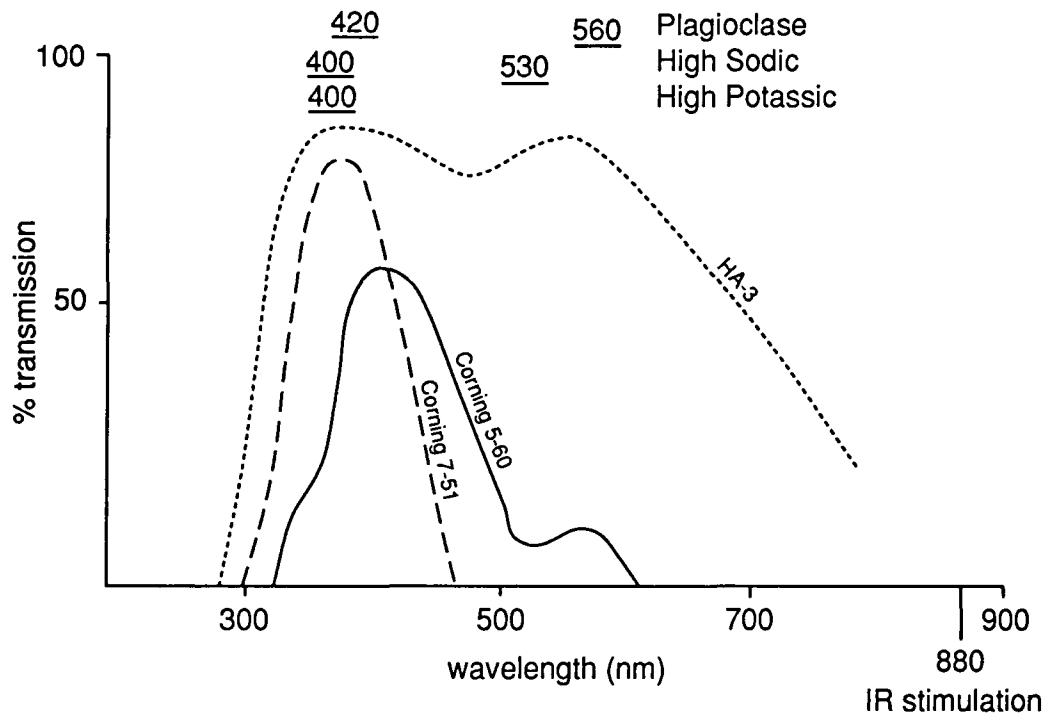
Samples are prepared in the laboratory (see 5.3.1) and selected grain size fractions (coarse = 90-120 µm; fine = 4-11 µm) are deposited on a number of aluminium or stainless steel discs. Measurements are made of the natural signal emitted from the sample discs, and of signals resulting from irradiation and laboratory bleaching of the discs in order to construct a growth curve. The growth curves are used to evaluate the ED of the sample (see 5.2.5).

A pause of a few hours was allowed between irradiation of samples and preheating as described in 5.3.4. Normalization was by weight, except where significant scatter ($> \pm 5\%$) in the natural samples required otherwise. In these cases the post-measurement procedure was used (see 5.3.2). After each disc had been measured, a black-body (background) measurement was made and subtracted from the measurement signal. The black-body measurement checks for any regenerated signals after measurement, on the sensitivity of the detection apparatus, and for contamination in the heating chamber.

The selection of optical filters is of great importance in the dating of polymineralic samples, as the emissions from different grains can be selected or blocked. This allows growth curves to be constructed from the signals from, for example, feldspars rather than quartz. This is important where the bleaching of the former may be significantly more complete than the latter, and the regeneration ED will reflect this disparity. The Chance Pilkington HA-3 filter is a heat absorbing filter, and used (or its equivalent) in all combinations, in order to remove spurious emissions arising during the heating process.

The wavebands detected in the emissions of feldspars were studied in detail by Huntley et al (1988). They show that the main wavebands relevant to TL dating lie at 390, 450 and 570 nm. The 570 nm band only occurs in plagioclases and is thought to arise from the substitution of Ca by Mn. The blue emission, which is of greatest importance for dating, comprises both the 390 and 450 nm bands. Strong emission from quartz and feldspar in wavebands other than blue was

Figure 5.2.2 TL filter transmissions and feldspar emissions (after Spooner and Questiaux 1989)



demonstrated by Akber and Prescott (1985) and Bailiff et al, (1977). It was also shown that emissions from polymineralic samples was dominated by green, red and infra red wavebands.

A wide range of filters is used for TL measurements to select the detected wavelengths from samples. A blue filter such as the BG-39 was commonly used for TL dating. However, other filters have been used to overcome certain problems observed during dating. Debenham and Walton (1983) used a Schott UG-11 (see figure 5.2.2) with a near UV pass to separate out the non-quartz emissions from detected signals. These emissions had been shown to be sensitive to optical bleaching but caused underestimations in the ED. A similar effect was recognised using a Corning 5-58 (Proszynska-Bordas, 1985, Proszynska-Bordas et al, 1988) which gave lower EDs than with a Schott BG-12. These problems are most significant for samples which are much older (c. 120 ka.) than those in this study.

The Corning 7-51 /HA-3 filter combination used here has been shown to enhance feldspar emission peaks and produced good results for old and young TL samples (Grün et al, 1989; Li and Aitken, 1989; Strickertsson, 1989). Balescu and Lamothe (1992) compared the efficiency of UG-11 and Schott 7-51 on the EDs of old samples. The error was reduced using the 7-51 filter, although there was still an underestimation in the EDs of very old samples. This is unlikely to be a significant problem in the samples studied here, as they are all less than approximately 12 ka in age.

The application of TL to waterlain sediments is hampered by the problem of incomplete zeroing of the sediments at deposition due to the attenuation of the sunlight spectrum by water. During dating measurements, samples are bleached in the laboratory in order to assess their response to applied radiation doses. In the case of TL, an unbleachable residual remains even after prolonged exposure, representing charge which is held in traps (eg. defects) which are not sensitive to sunlight stimulation. There is no adequate physical justification for this yet. An insufficient exposure, or exposure under attenuated light conditions, as in the case of waterlain sediments (see Chapter 3), may result in a larger residual, leading to uncertainties in the complete zeroing of sediments (Kronberg, 1983; Mejdahl et al, 1984). It is the violation of the assumption of total bleaching which has stimulated a number of workers both to investigate the zeroing mechanisms of minerals, and to develop methods of evaluating the equivalent dose (ED) which account for partial bleaching. These are discussed in section 5.2.5.

5.2.2 IRSL Measurement

The Photoluminescence technique was first proposed by Hütt et al (1988) as a development of the earlier optical dating work by Huntley et al (1985) on the stimulation of quartz by a green laser

source. Hütt and Jaek (1989) used a xenon lamp with a monochromator, to measure the stimulation spectrum of feldspars using an infra red laser (860 nm), and later 930 nm wavelengths.

The IRSL signal of feldspars is zeroed completely in daylight and more rapidly than for the TL signal (Godfrey-Smith et al, 1988). The potential of this method was taken up by Poolton and Bailiff (1989) who built an array of IR emitting LEDs (950 nm) as a stimulation source for feldspars. Both this system, and the 880 nm LED array recently developed at the Risø laboratory as an addition to their automated TL system (Bøtter-Jensen and Mejdahl, 1984; Bøtter-Jensen, 1988), are used in this project.

Two infra-red systems were used in this study; first the original semi-automated system built at Durham using 950 nm diodes (Poolton and Bailiff, 1989), and secondly the Risø semi-automated system (Bøtter-Jensen, 1988) using 880 nm diodes. The first was applied to all samples in a survey exercise in order to select the most promising samples for further dating, and to characterise the signals emitted from the samples with respect to the sedimentological and mineralogical characteristics. The dating measurements were all performed on the Risø set.

The Durham set is described fully in Poolton and Bailiff (1989), but its features are outlined below. The diode array comprises sixteen 15mW, 950 nm (1.3eV) LEDs (Telefunken TSUS 5402) which are connected in parallel, and mounted at 30° to the horizontal, pointing inwards onto the sample. The array fits over a standard TL oven, with the sample resting on the heater plate, which allows temperature regulation during measurement. The same photomultiplier tube was used as for TL, but the filters comprised Scott BG-38 or BG -39, which reduced detection of the red-light emission, which may in part derive from the stimulation source.

The characteristics of the 950 nm LEDs were shown to be uniform across the sample disc, and output was proportional to power up to a maximum level which stabilised after 10 secs. This power level was used to ensure a rapid settle down of the diodes during measurement. A shutter system was incorporated to ensure uniform output of the LEDs onto the sample, which fell substantially after switch-on (Poolton and Bailiff, 1989); Spooner and Franks, (1990). Stabilisation was within $\pm 0.5\%$ of the mean level of emission of the diodes, giving a power of $<60 \text{ mW/cm}^2$ on the sample. The comparative bleaching time to zero of the samples using both sources are given in table 5.2.1. The samples were bleached faster by the 880 nm wavelength, and it was noted that the initial signal values were lower for the same sample using 950 nm than for 880 nm diodes. Each sample was exposed for up to 10 mins., but the background level was often attained within 5 mins.

TABLE 5.2.1 Comparison of initial IRSL intensity stimulated by different wavelengths.

Sample	*I ₀ 950 nm	*I ₀ 880 nm
FF3	1008	1254
FF4	207	606
WM3	396	1603
WM4	10177	16613
WM5fg	1889	2527
HAZ2	2405	3950
SLG3	5250	7031
WH1	18340	19063
WH2	12242	22091
SP2	526	734
SP3	937	128
SP4	407	739
SP6	1224	1606
SP8	5630	6555
SP9	973	1234

*I₀ refers to the initial intensity in photon counts during the first second.

The Risø set comprised a TL automated unit (Bøtter-Jensen, 1988), with the addition of a diode array similar to the Durham design, but with 31 diodes (880Δ80 nm) wired together and arranged in two circles. Up to 24 samples could be placed in a rotating holder at any one time. The software programme allowed irradiation, measurements of samples and background, but did not allow for the irradiation or measurement of IRSL samples at higher temperatures. However, the signal intensities of most of the dated samples were high enough not to require this treatment (see below).

The physical processes involved in the emission of luminescence stimulated by IR light were studied by Hütt and Jaek (1988, 1989a, b). They suggested that the emission resulted from a two-step process of thermo-optical eviction of trapped charge. This process involves the excitation of charge by IR stimulation, and the transfer of the excited charge into the conduction band by the acquisition of additional thermal energy (see figure 5.2.1). Only small amounts of

thermal energy are needed for the eviction of charge, and thus there is a substantial luminescence signal at room temperature.

Work by Bailiff and Poolton (1991) has shown that this is substantially reduced at liquid nitrogen temperatures, and that stimulation at elevated temperatures increases the rate of emission, as there is a direct transition into the conduction band at higher temperatures (Hütt and Jaek, 1989a, b). This supports the theory of the two-step process, in which the thermal assistance accounts for the temperature dependence of the emission.

The sunlight bleaching of the IRSL signal from feldspars is relatively rapid when compared with the bleaching of the TL signal. The IRSL signal also has the advantage of there being a negligible residual level, thus eliminating the problems associated with evaluation of the correct TL residual level. The form of the IRSL decay curve has been shown to decay under constant stimulation in a manner described by non-first order kinetics, as predicted by a thermally assisted process (Bailiff and Poolton, 1989, 1991).

Quartz and feldspar have different sensitivities to optical bleaching. Quartz is measured using a green laser source and its sensitivity both to sunlight and green laser stimulation has been studied by Spooner (1992). Feldspar has been shown to bleach rapidly and 50% of the feldspar signal may be removed during 5 minutes of sunlight exposure (Hütt and Jaek, 1989a). This indicates that for waterlain material the feldspars are likely to have been bleached despite potential attenuated sunlight conditions. The optical bleaching of feldspars still results in an unbleachable residual signal remaining after exposure. This residual level is reached faster for feldspars than for quartz (Spooner and Questiaux, 1989). The bleaching of feldspars is dependent on wavelength, and the effects of charge transfer induced by sunlight bleaching are discussed in 5.4.1.

The ED values are calculated using the additive and regeneration techniques as for TL, and constructing the growth curves using either the integral of the photon counts, or the initial signal value. These should result in similar EDs if the sample is following the predicted kinetic behaviour proposed by Hütt and Jaek (1989a, b).

Problems experienced with low signal intensities were significant for a number of samples. The behaviour predicted by Hütt et al (1989a, b) predicts that an increase in temperature at which the IRSL measurement is made will result in an increase in the intensity of emission. This is because of an increased thermal eviction of traps. An increase in the power of the stimulation source should also increase the intensity of emissions.

This was tested on sample FF3 in order to assess the potential for increasing the intensity of low-emitting samples (table 5.2.2). This was determined by first measuring the IRSL signal emitted from a disc to which 15 Gy have been given. Immediately after this measurement, a second measurement of the same disc was made to determine the background level. This was repeated for different voltages. An increased voltage resulted in an increase in emission intensity, but also affected the signal to noise ratio such that the background signal detected comprised an increased proportion of the total signal detected, at higher voltages. Therefore, measurements made at lower voltages are less intense, but more accurately defined from the background level.

TABLE 5.2.2 Effect of voltage on the initial intensity and signal:noise ratio of the IRSL of FF3.

Power (kV)	Io(cps)	S:N ratio
1250	154	17.1
1350	179	6.2
1450	228	3.04
1550	359	5.5

The switch-on characteristics of the 880 nm diodes were measured, as there is no shutter system incorporated into the Risø system. These were measured for different power settings, but the greatest deviation was 0.005% of the mean stabilised value, which settled within 3 seconds. This represents a minor source of error, which would be the same for all individual discs, so should not affect the ED. The background and LED emission levels were measured at the beginning and end of long programmed runs (2-4 hours). Each measurement of a disc was for the maximum of 160 secs., but a second, and if needed, a third run was used to obtain the background count after all IR-sensitive signal had been removed.

5.2.3 Relationship between TL and IRSL

The relative novelty of IRSL compared with TL has resulted in some confusion in published work over the relationship between the traps associated with the two signals, and the assumptions that can be applied to IRSL based on the knowledge of the TL process. Hütt et al (1988) showed that exposure to IRSL reduced the 310 °C TL peak, but later work by Li and Aitken (1989) showed reduction in both 280 and 330 °C peaks; the disparity was attributed by the latter authors to the differences in preheating treatments of the samples. It may also, however, be due to different heating rates or sample types. For samples in this study, some reduction was noted in the 325°C

TL peak after exposure to IR stimulation, which may also be due to phototransfer. In a few samples, which were not suitable for dating (see discussions below), there was a notable rise in lower temperature TL peaks after IR exposure, suggesting charge transfer effects, possibly associated with unstable traps in these samples.

However, the fact that the stable traps (in terms of fading; see section 5.3.4) associated with the glow curve peaks used for TL dating are those which also give rise to all, or part of the IRSL signal, has given rise to the assumption that these traps are sufficiently stable for dating by IRSL. This has been extended to cover the assumptions that the procedures used with respect to fading and bleaching for TL are equally applicable to IRSL.

The emissions from feldspar have been shown to correlate with their elemental composition; the feldspars were shown to have peak emissions at c. 390, 450 and 570 nm which are used for TL dating (Huntley et al, 1988) with the 570 nm band only occurring in plagioclases, associated with Mn ions. The blue emissions which are the main detection wavebands for IRSL comprise a combination of the 390 and 450 nm bands. Bailiff and Poolton (1991) demonstrate similarities between the emission spectra of IRSL and specific TL glow curve regions of feldspars. They also demonstrated a UV emission peak at <340 nm. Potassium feldspars (microcline and orthoclase) correspond primarily with the 200-400 °C region, albite with the 350-400 °C region, and sanidine with the 300-400 °C region. Jungner and Huntley (1991) demonstrated a strong emission from K-feldspars under 633 nm stimulation in the 400 nm waveband, weaker emission at 340 nm and little at 300 and 500 nm which were very similar to the TL emissions from the same samples.

Bailiff and Poolton (1991) demonstrated the relationship and similarity in the emission spectra of feldspars under IRSL stimulation with specific regions of the TL glow curves. Under 950 nm stimulation, the spectrum of emission was similar to that for the 200-400 °C TL glow curve for microcline and orthoclase, 350-400 °C for Albite and 300-400 °C for sanidine. Godfrey-Smith et al (1988) and Bøtter-Jensen et al (1991) found that erasure of the IRSL signal of feldspars left the TL signal of the same samples unchanged, suggesting that the trap spectrum for IRSL is different to that for TL, although the emission spectra may be similar. The similarity between the emissions of the TL glow curve regions and the IRSL indicates that the major source of the IR signal comes from stable regions of the glow curve, and is therefore suitable for dating within the Quaternary timespan. However, some uncertainty remains over the stability of the traps giving rise to artificially stimulated IRSL.

5.2.4 Other OSL techniques

IRSL of feldspar was developed after work established on the green-stimulated OSL of quartz using a green laser was first published by Huntley et al (1985). This was shown to be successful for aeolian quartz. IRSL does not stimulate pure white quartz, but does stimulate some emission from pink quartz. IRSL has thus been used as a method for testing the purity of such quartz extracts (eg. Rhodes, 1990). Feldspar inclusions in quartz will, however, be sensitive to IR stimulation, but this is likely to be of greater value in dating single grains due to the high variability of the inclusions, and the size of the grains involved.

OSL using green lasers has become a widespread technique for dating aeolian quartz, and can be used as a complementary technique for optical dating of polymineralic sediment extracts. Some comparative work has been done using both techniques (Spooner and Questiaux, 1989). OSL dating of quartz formed the basis of the IRSL technique, in terms of the analysis of the signal data. This technique was not used in this study due to the dominance of the sample luminescence emissions by feldspars, and the availability of equipment.

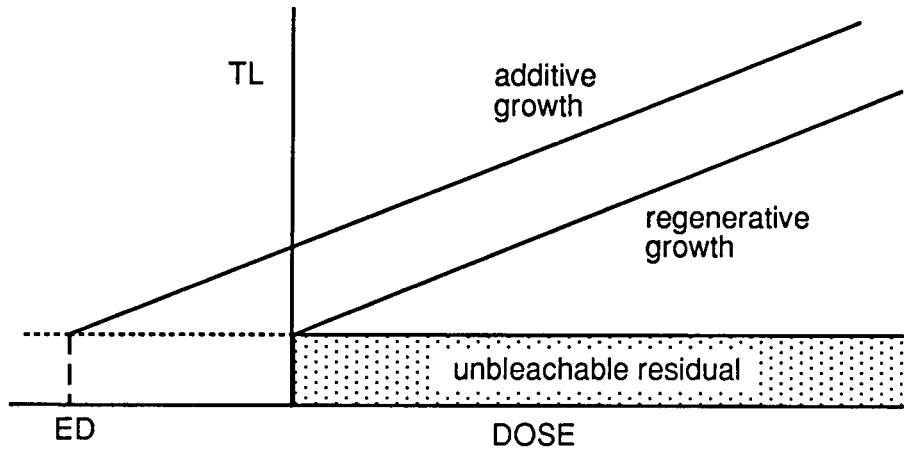
Other optically based techniques include phototransferred TL (PTTL) which uses the easily transferred component of the TL signal of quartz from 320 °C peak to the 110 °C by exposure to UV light (Bailiff et al 1977). This does not affect the stable 370 °C peak in many samples, but the process does not have significant advantages over standard techniques for pottery (Aitken, 1985, 168). Wheeler (1988) describes possible methods of using phosphorescence stimulated by exposure of quartz and feldspar samples to 514 nm laser sources. The phosphorescence lasts only a few seconds, and is too weak to be accurately measured for dating.

5.2.5 ED evaluation and the age equation

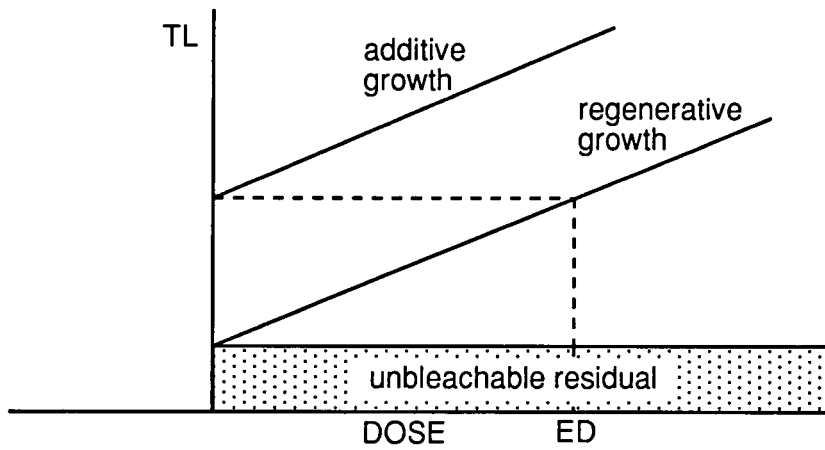
The TL ED can be evaluated in three main ways. First the additive technique (developed for pottery dating) where the growth characteristic of the sample is measured by giving artificial radiation doses. These are measured, and the growth curve constructed (see figure 5.2.3a) of the luminescence (ie. peak height for a given temperature) against added radiation dose. The growth curve is extrapolated to a point on the abscissa, giving the ED value in grays; the point on the abscissa is not equal to zero due to the subtraction of a residual value, which is the amount of luminescence remaining in the sample after a long bleach, as for the total bleach method given below. This residual represents the unbleachable part of the signal, and is therefore not a part of the sunlight-sensitive signal used for sediment dating. The growth curve is generally linear for Holocene age sediments, but for older samples, a sublinear curve may result, indicating the onset

Figure 5.2.3 Methods of ED evaluation

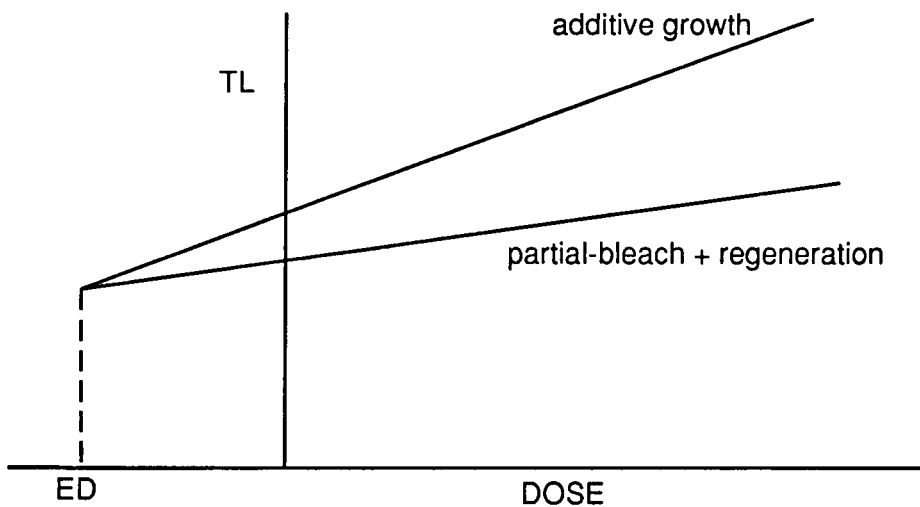
a. Additive Dose



b. Regeneration



c. Partial-bleach



of saturation of the sample. Samples in this study were generally characterised by linear growth curves.

The second method of evaluating TL ED is by the regeneration technique (figure 5.2.3b). Here, the natural signal is measured, and all other samples are bleached to a laboratory determined residual level. A growth curve is constructed by adding different radiation doses to sample discs, and plotting the curve as before. The ED is given on the dose axis, where the second glow curve crosses the point equivalent to the natural signal level.

For most TL samples, both growth curves are constructed in order to check that the response of the sample to artificial irradiation approximates to that experienced under natural conditions with respect to the linearity and gradient of the growth curve. Changes in the linearity (slope) between the two growth curves (ie. they are not parallel), indicates changes in sensitivity of the dose-response of the sample, as a result of heating, bleaching or irradiation. Sensitivity changes arising from bleaching are discussed in section 5.4.2.

The third method of ED evaluation is the partial bleach technique proposed by Wintle and Huntley (1982), and advocated by a number of TL workers, notably Berger (1985a, 1990). This method is based on the assumption that exposure of sub-samples of a sediment, some of which have been given an additional artificial radiation dose, to optical bleaching will reduce the signal intensity of all sub-samples by the same proportion. Additive and partial bleach regeneration curves are constructed. The intersection of these two curves represents the ED value (figure 5.2.3c). The correct time of light exposure can be determined by plotting an 'ED plateau', which represents the ED determinations over the peak TL temperature range, for different bleaching times. The longest plateau is taken to represent the correct bleach time.

The total bleach technique, adopted by Singhvi et al (1982) is where the additive curve and a regeneration curves following a long, total, bleach of the subsamples are constructed, and the ED is given where these intersect. Again, as for the regeneration method, the problem of sensitivity changes in the sample can result in erroneous ED evaluations due to changes in slope of the growth curve.

For IRSL dating, both the additive and regeneration techniques can be used. The growth curves are plotted using the initial signal intensity (photon counts) or the integrated signal count over the total exposure time, against dose. The ED is determined in the same way, on the dose axis.

In this study the additive and regeneration techniques were used for ED evaluation. In the calculations for age determination the additive intercept was used in each case. This is justified for

these samples as they are relatively young, and problems of non-linearity of the growth curve, eg. due to saturation of the sample, were not anticipated. The regeneration growth curve was used in order to determine the level of the unbleachable residual, and to check for sensitivity changes after laboratory bleaching.

In order to demonstrate good reproducibility between discs and consistency in the points on the additive and regeneration glow curves, up to 6 measurements were made at each point on the growth curves, and up to fifteen points were constructed on the growth curve, giving a total of up to 90 measurements on each growth curve. This enables greater confidence to be placed in measurements from samples showing poor reproducibility by weight normalisation.

The errors on a luminescence date are divided into 'systematic' errors which comprise errors in the calibration of radiation sources, uncertainties in dose-rates due to water content attenuation, uncertainties in the evaluation of past water content and sampling errors. The 'random' error component comprises the error in ED and dose-rate evaluations. These are calculated by the system developed by Aitken and Alldred (1972). There is no other published method of error evaluation.

5.2.6 Irradiation

In order to evaluate the palaeodose, or the ED, as described in 5.1.3, a number of discs are irradiated for different times to construct the growth curve of a sample. For this study a beta and an alpha source were used to measure the growth response to alpha and beta radiation respectively. For TL and IRSL using 950 nm diodes the irradiation facility described by Bailiff (1980) was used, and for IRSL using 880 nm diodes a source incorporated into the Risø automated system was used. The dose rate is different for fine and coarse grains, and details are given below in Table 5.2.3. The alpha source used for all measurement was an AM-241 delivering $0.45 \mu\text{m}^{-2}/\text{min}$ (units of track length of alpha particles).

TABLE 5.2.3 Beta radiation sources and dose-rates (after Bailiff, 1992)

Source	Laboratory designation	Dose to fine grains of quartz (Gy/min.)	Dose to coarse grains of quartz (Gy/min.)
$^{90}\text{Sr}/^{90}\text{Y}$	B(40)	1.08	1.22
$^{90}\text{Sr}/^{90}\text{Y}$	B(42)	0.55	0.70

5.2.7 Dosimetry

Sediment extracts, such as the fine grain fraction, are a part of the bulk material, and measurements of the radioactivity of the bulk material, as opposed to that of the separated fraction are necessary. These measurements give the environmental dose-rate. On-site dosimetry using gamma-ray spectrometry and laboratory measurements of the alpha activity and beta dosimetry are made to test for disequilibrium in the decay series. The greatest source of error is in the estimation of past water content in the sample, an aspect which has been investigated by Rendell (1983, 1985) with respect to loess.

Radioisotopes of U, Th and K decay with the emission of alpha, beta and gamma radiation, which, with a minor cosmic component, make up the components of the annual dose-rate to a sample. The dose-rate can be evaluated in a number of ways, including direct measurement by dosimetry and indirect measurement of the activity of a sample, and converting it into dose-rate.

The sources of radiation contributing to the dose-rate may be internal or external to the crystal. External dose is derived from the isotopes present in the sample matrix, and internal dose is derived from isotopes present within the crystal. The differences in energy of particles emitted during decay have different effects on the crystal, as the attenuating effects of the crystal lattice reduces the ionization by particles of lower energy. The effect of grain-size is therefore important.

Measurement of the dose-rate is done on-site by gamma-spectrometry and calcium-fluoride dosimetry, or in the laboratory by measurement of the concentrations of elements, or the activity of the samples. The values for the dose-rates for all samples are given in Appendix C, Table 1. For fine grain dating, the most important components of the dose-rate are the beta radiation from potassium and the alpha radiation from uranium and thorium.

5.2.7.1 Alpha radiation.

Alpha radiation arises during the decay of U and Th. It comprises heavily ionizing particles with relatively low penetration distances. The range of penetration of alpha particles is 10-50 μm . The particles follow straight paths through mineral grains. Alpha radiation is measured in track length which is a function of their energy. Typically, an alpha particle with an energy of 5 MeV will travel 20 μm (Bowman, 1976). Fine-grains are considered to have received a complete alpha dose as their diameter is less than the penetration distance of the alpha particles. However only the outer portion of coarse grains are affected by alpha radiation, due to the inability of the alpha rays to



penetrate further into the crystal. The outer part of coarse grains is therefore removed by etching leaving a core which is unaffected by external alpha radiation.

Alpha radiation is measured in track lengths, as the amount of luminescence arising from alpha radiation is proportional to the total length of tracks passing through the minerals. The effective TL/Gy of alpha rays is less than that for beta radiation by a factor of 0.05 to 0.5, depending on the substance (Aitken, 1985; Appendix K). The ratio of this difference is referred to as the a-value. However the a-values for the optical and TL dates for the same sample are consistently different, an effect not as yet understood. The a-values for samples in this study are given and discussed in Chapter 6.

The alpha component of the dose-rate is measured indirectly by thick-source alpha-counting, ie. a measurement of the alpha activity of the sample (Aitken, 1985; 86). A layer of powdered sample is laid onto a 42 mm diameter ZnS scintillation screen. The screen detects scintillations arising from the collision of alpha particles against the screen. The detector window is set to exclude the lower energy beta and gamma emissions. The term 'thick-source' of an 'infinite' matrix refers to the relative thickness of the sample with respect to the maximum 50 μm penetration of the alpha particles, so emissions from the lower two thirds of the sample are measured.

Typical alpha counting values for samples investigated are 800 -1200 counts per day. Values are usually based on the assumption of equal activity of U and Th but if the alphas are all emitted from one isotope the variation in this value is less than 5%. Samples are counted sealed and unsealed (ie. with or without a lid). This measures the escape of radon gas which is a source of disequilibrium in the decay chain. Ratios of sealed:unsealed above 1.2 indicate a problem of this nature and such samples were rejected. The alpha dose for fine grains is treated as entirely external to the grains as they are so small. For coarse grains, part of the alpha dose is derived from internal sources of isotopes contained within the grain. The external alpha dose must be corrected for water content attenuation (see 5.4.3)

5.2.7.2. Beta Radiation

Beta radiation is emitted by the decay of U, Th and K isotopes, and is measured by laboratory dosimetry. This measures the dose-rate directly, assuming an infinite medium of material and corrected for grain-size and water-content. Beta radiation has a higher penetration distance than alpha, but is less heavily ionizing.

Dosimetry measurements are made by placing c.1 g of powdered sample into a lead container. An annealed calcium fluoride dosimeter is placed above the sample. The container is sealed and left

for two weeks, after which the beta radiation absorbed by the Calcium Fluoride is measured by TL (heating rate 5 °C/sec; up to 300 °C). This measures the beta activity of the sample (Bailliff, 1982).

A correction for water-content is applied, as the dose-rate is measured in the dry state (see below) and a correction for grain-size is also applied. Aitken (1985; 259) gives values of 1.0 for fine-grains, and 0.9 for coarse grains due to attenuation by the crystal lattice. The measurement of beta dose is made assuming equal activity of U and Th, which is important due to the different energies, and therefore penetration distances of betas emitted by these isotopes. For ⁴⁰K the beta particle energies range from 0-1.32 MeV, with the most common particle energy being around 0.4 MeV. Beta radiation comprised between 24 and 56% of the total dose-rates of samples (table 2, Appendix C).

5.2.7.3. Gamma Radiation

Gammas are emitted by the decay of U, Th and K and is commonly measured by spectrometry in the field. Here, the gamma activity of a stratum is measured using a portable gamma spectrometer. The probe of the spectrometer containing a scintillator is placed within the stratum. The scintillator detected the passage of radiation through the probe. The measurements on a four-channel spectrometer are converted into U, Th, K and cosmic concentrations (based on the different energies of emitted particles). The spectrometer used for this study was a Nutmaq Harwell 95/0466-1/6 model with a sodium iodide crystal. Counts were collected over a period of 60-90 mins. and the response of the detector checked with a calibrated thorium source impregnated in resin.

Gamma radiation has a range of 0.3 m in a homogeneous soil matrix, depending on the energy of the particles. Typical energies range from 0.1 to 3 MeV. The gamma dose may be an important component of the dose-rate. The attenuation of the gamma dose is complex as there is a wide range of energies represented by the particles. In a low activity environment, the gamma dose attenuation is more significant. Assumptions of uniformity of a sedimentary deposit with 0.3 m of a sample are difficult to apply in many cases, and a sample may have a significant contribution from the over- or underlying strata. It is therefore useful to evaluate the contribution from adjacent strata, particularly where the sedimentary sequence is complex. The density and water-content of the soil can be used to assess the attenuation of gamma particles of specific energies (Aitken, 1985; 73).

In this project, the gamma dose contributions were calculated using computer software authorised to I K Bailliff based on data from Løvborg and Kirkegaard (1974) for samples where the thickness was less than 0.3 m, or for complex and long sequences, where the contribution from adjacent

strata can be evaluated. For most samples, the gamma dose came entirely from within the sample stratum, but in a few cases the adjacent strata contributed a small proportion of the total gamma dose.

The gamma dose comprised 17-36% of the total dose rate for samples. The gamma component is more significant for fine-grains where the external dose (ie. not from inside the mineral grains) is more important. Alkali feldspars contain potassium which is an important internal and external source of gamma radiation.

5.2.7.4 Cosmic radiation.

The cosmic component of the radiation dose is relatively small in most environments, except where the natural radioactivity is very low, and the sample is near the surface. Aitken (1985; 74) gives typical values of 150 $\mu\text{Gy/a}$ at 1 m depth, twice this at the surface and half this at a depth of 5m.

5.2.7.5 Calcium Fluoride dosimetry

The burial of dosimeters containing annealed calcium fluoride allows an average annual dose-rate of the gamma component to be measured. The alpha and beta rays are stopped by the capsule walls. The dose-rate varied throughout the year according to changes in water-content and temperature, so an average annual value is more accurate than the value measured at the time of sampling which represents current conditions in the stratum.

Natural Calcium Fluoride is a sensitive phosphor. It is annealed at 400°C for 20 mins. and sealed in 0.1-0.2 mg quantities in copper capsules. These are buried in the ground, suspended by wire in the borehole from which the sample was taken. The capsules lie within a narrow plastic drainpipe to aid retrieval. The levels at which the capsules are suspended can be carefully measured, and allows measurement to be made of a variety of strata in the core, including peat layers as well as minerogenic strata.

After at least one year, the capsules are retrieved, and the absorbed dose measured. A beta dose giving rise to a signal of equivalent signal intensity is administered, and a subtraction made for the self-dose of the phosphor (100 $\mu\text{Gy/a}$). A correction is made for the attenuation effect of the copper capsule walls; for 0.7 mm wall, the dose received by quartz is x1.10 that received by the phosphor (Aitken, 1985;98).

Significant problems were experienced with the retrieval of dosimeters in the field. For capsules which were recovered from Williamson's Moss and the Dutch sites, dose-rate evaluation was within 7% of the values determined by laboratory techniques. In calculations for age determination, the laboratory data was used for all samples.

5.3 ADDITIONAL ASPECTS RELEVANT TO DATING

5.3.1 Sample preparation

Sediments usually comprise a variety of different sized grains of contrasting mineralogies. For dating, the fine-grain fraction (4-11 μm) or the coarse-grain fraction (90-120 μm) are most commonly used for dosimetry reasons (Aitken, 1985). The advantage of fine grains is that in the waterlain sediments of this project, these are often the most dominant grain size fraction, and thus more representative of the sediment. Also, during transport they are more likely to have been carried in suspension and thus more effectively bleached than coarse grains.

Fine-grain samples were prepared based on the technique of Zimmerman (1971). The sample is dried and gently broken up into its constituent grains, taking care not to crush individual grains. Calcium carbonate is removed by standing the sample in 2% acetic acid for two hours, or until an HCl test indicates that no carbonate remains. The organic material is removed by treatment with 30% H_2O_2 . This was added until all frothing stopped, and gentle heating to temperatures no higher than 40°C was applied to ensure all reaction had ceased. The residue was removed by thorough washing with distilled water.

The sample is then carefully washed several times in distilled water, meths. and acetone to remove traces of reagents. The sample is centrifuged to precipitate the sediment after washing, and an ultra-sonic bath to agitate during washing. When cleaned, the sample is examined, and if substantial flocculation of the clay minerals has occurred, these are dispersed by using sodium oxalate in distilled water, before cleaning again with distilled water, meths. and acetone.

Once the sample is clean and flocs are dispersed, the fine-grain size fraction (4-11 μm) is separated by sedimentation in acetone for 2 and 20 mins (the Stokes' law settling times for suspension in 6 cm depth of acetone). The separated fraction is suspended in acetone. A 1 ml fraction is taken from this suspension, shaking the tube each time to ensure even mixing of the sediment. The fraction is deposited on abraded and cleaned aluminium discs placed in a flat bottomed tube. The acetone is evaporated overnight in a warm oven (50°C). Around 120 discs were prepared for each sample.

The fine-grain fraction is polymineralic, containing mainly quartz and feldspar, with smaller amounts of clay minerals. The quartz and feldspar could not be successfully separated by density separation techniques due to the overlap in specific gravities for the two minerals. Etching the sample can only isolate the quartz fraction, and is in any case less suitable for fine grains as the quartz is more susceptible to acid attack.

The coarse grains are sieved, to isolate the 90-120 μm fraction. These grains were cleaned as for fine grains, including the dispersal of flocs, which were often present in this size fraction after drying. After the carbonates had been removed, and the grains cleaned, they were etched in HCl for 40 mins. This was done in order to remove the external layer exposed to alpha radiation, and to remove coatings of clay minerals and oxides from the grain surfaces, which are often strongly adherent even after treatments.

The cleaned grains are settled onto abraded aluminium or stainless steel discs in the following way; a drop of silicone oil is deposited in the centre of the disc, keeping the outer surface millimetre clean. The discs were inverted into the grains, and tapped to remove loose grains. This ensured that a monolayer of grains was deposited on the discs, which is important with respect to the measurement of the dose-response of coarse grains to irradiation.

The prepared sets of fine or coarse grain discs were stored in disc libraries at room temperature and in the dark, unless undergoing treatments for fading, or prior to measurement.

5.3.2 Normalization

The normalization of the intensity of emissions from sample disc is necessary to reduce the effects of scatter in the data which results from the distribution of the grains contributing to the luminescence. In fine grain samples, the luminescence may be derived from many grains which are evenly distributed between discs, resulting in similar intensities of luminescence with respect to the natural signals and to discs which had received an artificial radiation dose. However, the signal may arise primarily from a few bright grains, which are not evenly distributed between discs, and so the relative intensities of different natural and additive discs will be highly variable. Normalization is a method of correcting for this variability.

There are three main ways of normalizing a set of sample discs; for TL fine grains weight normalization is often adopted, whereby the amount of luminescence emitted is assumed to be emitted from an equal weight of grains deposited on each disc. This is often appropriate for fine grain polymineralic samples. If the scatter in intensities between discs of one sample is

significant, the luminescence is likely to have been emitted from a few bright grains. Weight normalisation was used for most TL samples in this study.

Weight normalization, however, is not always sufficient, and some form of dose normalization is used, where the response to a standard small radiation dose is measured. If this is done before measurement, it is known as the equal pre-dose technique.

The most widely used technique for TL, and the one adopted here, is normalization by second glow, where the response to a standard test dose is given directly after measurement of the natural signals. This can be complicated because of the sensitivity changes induced by heating, bleaching and irradiation, but it can be standardised if they all show the same behaviour.

In this study, weight normalization was acceptable for most samples, having a disc-to-disc reproducibility of $< \pm 5\%$. Some samples showed very poor reproducibility, and in three cases this was associated with fading of the signal without reaching a stable level, and these were rejected as not suitable for dating (see section 5.3.5). In two further cases of TL dated samples, the post-measurement normalization was carried out, because the assumed weight normalization before measurement was not sufficient. In all other cases, a parallel check on the suitability of weight normalization was done by applying the second glow method to discs selected at random.

For IRSL measurements, a short exposure of one second was given before measurement and other treatment of the discs (eg. bleaching), and the number of photon counts recorded. The few discs which exceeded the $\pm 5\%$ level of variation within the sample were discarded. The short exposure did not significantly reduce the initial signal level of the measurement exposure, and in most cases the initial count was similar for both the one second normalization and the measurement exposure. The integrated number of counts detected during the normalization is less than 5% of the total integrated counts, and so would not significantly affect the signal used for dating. The percentages of the total integrated count for the natural of each sample represented by the normalizer are given in table 5.3.1 below.

TABLE 5.3.1 IRSL Normalization as a % of total emission (signal + background).

Sample	N%
FF3	4.6
FF4	4.7
WM3	3.2

WM4	3.1
WM5fg	2.9
WM5cg	2.7
HAZ2	4.8
SLG2	3.6
SLG3	3.2
SLG4	2.4
WH1	1.3
WH2	1.2
SP2	3.2
SP3	2.4
SP4	4.8
SP6	2.7
SP8	3.6
SP9	3.3

The use of IRSL normalization for TL is not considered to be appropriate. The TL signal is derived from many other traps which are different to those which give rise to IRSL. Also they may not be stimulated by IR light and therefore not normalized.

5.3.3 Stability of the luminescence signal

TL and IRSL age range is determined by the level of saturation of minerals with absorbed radiation dose, and by the stability of the traps in which the charge is held. The saturation level is higher for quartz than feldspar and thus the potential age range (assuming equal dose-rates) will be greater for quartz. In the case of TL, the age range may be substantially reduced by the incomplete zeroing of the signal at deposition; and may only extend to 5-10 ka. However, it may be over 200 ka for quartz rich dunes with low dose rates (Aitken, 1985).

For TL and IRSL, there are two main considerations with respect to stability. The first is the emission stimulated from traps which are not stable over archaeological timescales, and therefore not suitable for dating. Secondly, there are traps which for kinetic reasons are considered stable over these timescales, and therefore suitable for dating, but which are in fact unstable (see discussion on anomalous fading in 5.3.4). The unstable and short-lived components of the signal therefore need to be removed from the stable signal in order to obtain an accurate ED.

The stability of the charge held in traps is determined by their lifetimes. The lifetimes of many traps decreases with increasing temperature of storage; Wintle and Huntley (1980) predicted lifetimes of 10-100 ka for ocean floor sediments stored at 4 °C, but this is reduced by a factor of five at 10 °C, by predictions based on measurements of known age samples. The lifetimes of K-feldspar TL traps as evaluated by Strickertsson (1985) are given in table 5.3.2, which indicates that the 280, 320 and 350 °C peaks (at heating rates of 10°C) are sufficiently stable for dating purposes, particularly in this study where sediments are estimated to be less than 12 ka.

Hütt et al (1988; Hütt and Jaek, 1989a, b) identified two traps which contribute to the IRSL signal at depths of 1.62 and 2 eV. The former corresponds to the 310 °C TL peak which has a similar lifetime as the 280 °C trap given in table 5.3.2. These traps correspond to maximum ages of 500-600 ka, but this is reduced by saturation effects, fading and incomplete bleaching at deposition.

At a meeting in Oxford (1989), the short and long range limits for OSL and TL were discussed, and most of the older-age limits average around 100 ka for both techniques. This limit was first established by Debenham (1985), and has not been substantially extended. However, for the purpose of this study, where the sediments are of Holocene age (ie. <12 ka), saturation effects are only a problem where little resetting of the signal at deposition has occurred. The older age limit may be up to 200 ka where the dose-rate of the environment is very low, as in the case of quartz dune sands.

TABLE 5.3.2 Trap depths and lifetimes for TL of K-feldspar at 15 °C assuming first order kinetics. (data from Strickertsson, 1985)

*Temp (°C)	Depth (eV)	Lifetime (yr)
90	0.76	0.16×10^{-3}
110	1.10	43×10^{-3}
210	1.40	3.6×10^3
280	1.62	3.9×10^6
320	1.60	1.0×10^9
350	1.68	9.2×10^9

* refers to the TL glow curve peak temperatures

5.3.4 Anomalous fading in feldspars

Anomalous fading is the loss of signal in a sample which has been stored following artificial irradiation, but it also affects the natural signal. In samples where the luminescence is dominated by a few bright grains, the signal loss may not be significant if these grains do not fade, but a great problem if they do. Significant fading of the luminescence signal was observed in three samples in this study. These samples were rejected for dating. Severe fading refers to samples which do not fade to stable levels and which experienced a loss of over 40% of the signal arising from artificial irradiation. The loss observed in the samples is shown in table 5.3.3.

TABLE 5.3.3 Loss by fading observed in three samples, FF1, FF2, HAZ1.

Sample	TL6wk50°C(RT)	TL6mth50°C	IR6wk50°C(RT)	IR6mth50°C
FF1	30 (28)	46	22 (15)	38
FF2	43 (40)	68	29 (26)	48
HAZ1	49 (48)	73	45 (44)	64

Figures are % of original signal intensity.

(RT) refers to storage at c.18°C.

Figures in () refer to losses observed after storage under RT conditions.

Because of the significant loss observed in these samples and the variation between the TL and IRSL signal losses, a detailed consideration of fading of feldspars is necessary. The causes of fading are not well understood, but they may be related to mineralogical or sedimentological characteristics. An account of the mechanisms of fading is given below, and the relationship between samples which faded and their sedimentological characteristics is discussed in Chapters 6 and 7.

Fading was first observed by Wintle (1973, 1974) in plagioclase feldspars. It is now known to be common in most minerals used for dating, particularly feldspars. Wintle observed losses of 17-40% after 17 hours storage. This was concentrated in the 350-400 °C TL peak, which is normally considered the stable region suitable for dating. The loss in some minerals is temperature-dependent, and increases with higher storage temperatures. Loss in Wintle's (1973) work was not affected by the type of radiation used, except that it was 10% faster for alpha due to the shorter effective range of alpha rays.

Non-volcanic and loessic feldspars are less prone to significant fading, but are still affected (Berger, 1984, Lamothe, 1984, Lamothe and Huntley, 1988 for waterlain sediments). Berger (1988) observes that in dating studies little attempt is generally made to identify the feldspar types which contribute to the signal. There are however some exceptions to this (eg. Rendell et al, 1983; Lundqvist and Mejdahl, 1987), in part because of the range of feldspar compositions and difficulties in their evaluation. More recently, attempts have been made to correlate the amount of fading with feldspar types. Spooner (1991) observed fading in plagioclases and one alkaline feldspar sample, which had been shown to fade in other TL work. Not all these samples faded to stable levels, even with thermal acceleration of the decay.

Akber and Prescott (1985) related observed fading to composition of plagioclase feldspars. These are classified by their relative sodium:calcium contents and were shown to suffer increased fading and decreased emission in the yellow waveband with increasing calcium. This implied more intense fading in calcium-rich types, and the authors suggested filtering the yellow emission with which the fading is associated. Hasan et al (1986) showed that high temperature forms (ie. having a disordered structure) showed little fading compared with low temperature forms (ordered structure). Hasan et al also imply that preheating will only successfully remove the unstable component of the signal if a favourable mixture of high and low structural forms is present.

Differences in laboratory techniques may also lead to differences in the observation of fading in the same material (eg Wintle (1974) and Berger (1984) for an Alaskan loess). Rendell et al (1983) attempted a correlation between bulk composition of feldspar using the Al:Si ratio as an indicator (see Chapter 3) and the amount of relatively bright feldspar, and TL sensitivity to dose. This proved difficult and the Al:Si ratio showed poor correspondence with sensitivity to dose for a polymineralic loess, containing quartz, feldspar, calcite, mica and clays. This may be due to the range of sensitivities represented by the polymineralic bulk sediment. Differences in the fading of 5% and 15% for similar silt deposits were attributed to compositional changes by Berger (1985a,b).

The traps associated with IRSL or green-OSL signals, are in part those which give rise to TL (see 5.1.3). Fading may relate to these or to other traps which are related to the form, composition and thermal history. Spooner (1991) shows that it occurs with IR and green stimulation, and that it correlated with composition but not to the luminescence sensitivity of the samples. The brightest samples were Na- and K-rich, and the dimmest were dominated by Ca, which has been shown to be more prone to fading (Akber and Prescott, 1985).

The greater losses observed in samples FF1 and FF2 for the TL signal probably reflect the stabilities of traps associated with TL rather than IRSL signals. There is some temperature-

dependence as losses are marginally higher for storage at 50 °C than at room temperature. However, this is not very significant.

Some samples in this study were affected by fading; they tended to be derived from weathered strata. This connection was observed during an experiment investigating the effect of artificial weathering on the IRSL signal, where fading was observed in a previously stable sample, as described in Chapter 7. The inducement of fading by chemical weathering could be related to the destabilisation of traps due to chemical exploitation of the defects.

5.3.4.1 Mechanisms of Fading

Two models have been adopted to illustrate the process of anomalous fading; the Quantum Mechanical Tunnelling model (QMT) and the Localised Transition Model (LTM). The former illustrates the process of activation of electrons in traps but only sufficient to reach the conduction band, without passing through it (Visocekas et al, 1976). Charge can leak away and become re-trapped elsewhere. The initial rapid rate of decay observed in samples is attributed to the number of empty traps (holes) nearby which can trap leaking charge. The rate of loss decreases with time as the holes only exist further away.

Tunnelling is likely where energy differences between electrons and holes are relatively small, or if the electrons are in an excited (higher energy) state. This thermally assisted process (where raised temperatures 'excite' the electrons) increases the rate of loss, and competes with athermal loss after irradiation at lower temperatures. The athermal component is thought to represent the continual fading in Spooner's (1991) samples, which did not become stable even after preheating. Thermal assistance accounts for the temperature dependence of the process, and may explain why shallower traps are less stable and more prone to fading than deeper traps (Bailliff, 1976 with references).

The LTM (Chen and Kirsh, 1981; Clark and Templer, 1988) explains the significant temperature dependence of fading in some minerals and polymineralic fine-grains. The electron-and-hole (pairs) transitions occur without electrons passing into the conduction band and are thus limited to moving to localised holes only; spatially remote transitions (greater than a few Å) require passage within or through the conduction band.

Wintle (1978) isolated stable and unstable components of the TL signal which were separated by storage at increased temperatures (preheating). This accelerates the rate of decay without eroding the natural, stable signal, because it is not activated by the temperatures at which the unstable component is removed. Rates of decay at ambient temperatures are very slow, but thought to be complete, or in equilibrium with the lower dose rates in the natural environment.

Clark and Templer (1988) identified two unstable components, one of which had a faster rate of decay and was eliminated with preheating, and another which was temperature independent and much slower. Treatment of fading samples is dealt with under preheating (5.2.5). Mejdahl (1988b) investigated fading in feldspars and their long-term stability, and calculated corrections which could be applied for older samples, based on estimates made from the measurements of infinite age samples. These were not necessary in the samples examined in this study, because they were all estimated to be of Holocene age. Thus the effect in ED evaluation of a long term component would be much less than for samples approaching 100 ka.

5.3.4.2 Tests for fading

The samples in this project were given a beta dose of 30 Gy, and then stored at 50 °C for up to six months before preheating and measurement. Three samples were rejected for dating because the signal had not decayed to a stable level even after prolonged storage (see table 5.3.3). The natural signals did not decay for these samples, indicating that the signal had reached stability *in situ*, which may be due to the lower natural dose rate when compared to artificial sources. However, the time when stability was reached *in situ* is not known, and large errors in the ED value would result from this uncertainty. Mejdahl (1988b) introduced a correction for long-term fading in TL, referred to above.

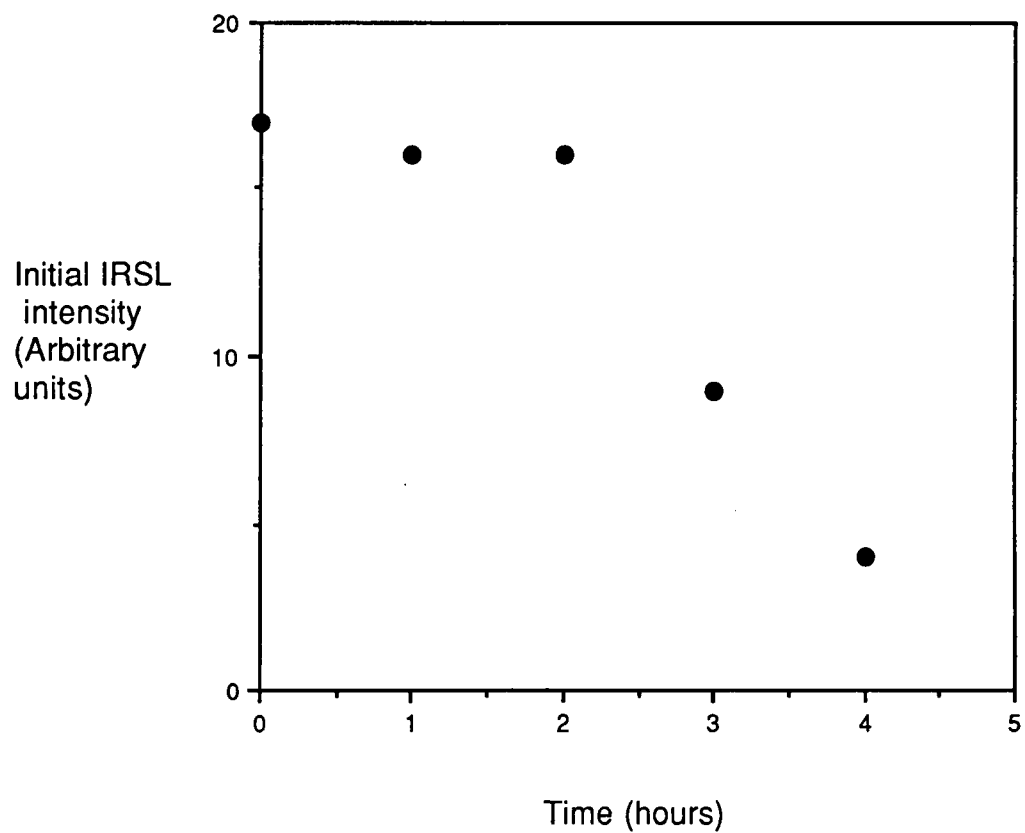
5.3.5 Preheating

Preheating is a treatment applied to dating samples involving storage at elevated temperatures for variable periods of time. It is applied in order to evict the unstable component of the trapped charge. It was first used by Wintle (1985) for TL, but has since been widely adopted for TL and IRSL. This is done in order to remove the unstable component of the signal induced by irradiation. Any fading components in the signal (see section 5.3.4) are removed by accelerating the process by thermal treatment. All samples dated in this study were preheated before measurement.

Clark and Templer (1988) suggest two methods; one is to preheat all samples so if erosion of the stable component of the signal occurs, it applies to the same degree in all samples. The alternative method is that a post measurement test is applied. The former procedure is better for bright samples and is the method adopted by most workers. The latter is more complicated but is best for weak samples.

Zöller and Wagner (1989) discussed the process of 'thermal washing' of samples before TL measurement of loess. Two treatments were explored; 'Strong thermal washing' (STW) designed so that the partially unstable 250 °C polymineral fine-grain peak was completely annealed. 'Partial

Figure 5.3.1 Effect of different preheat times at 160°C on sample WM4



thermal washing' (PTW) comprised 1 hour at 160 °C based on a suggestion by Aitken to the authors, supported by kinetic considerations (not described). Both procedures showed good agreement with ED values based on non-preheated samples, but the alignment of peaks to the natural glow curve was less easy for the PTW method, but after PTW none of the sensitivity changes was observed that occurred for STW.

Li and Aitken (1989) and Spooner and Questiaux (1989) studied the optimum storage conditions and preheats for feldspars. The former recommend 2 hrs at 160 °C and 3 days at 100 °C. The latter authors confirm this, and plotted a preheat plateau which showed that after 30 mins at the higher temperature, the natural and additive samples were behaving in a similar manner with respect to thermal stability. This was compatible with Zöller et al's PTW method. This was used here for TL and IRSL samples - ie. 2 hours 160 °C and 3 days at 100 °C.

Li (1991), however, in a study of three K-feldspar samples and two different preheating arrangements recommended a short, hot preheat of 220°C for 10mins or a longer preheat of 160°C for 5 hours. He found that the preheat of 10 mins. at 220°C removed the lower temperature TL peaks and isolated the stable TL signal. This was not the case for samples which had not been preheated. The preheat at 160°C demonstrated that after 30 mins at this temperature the same TL response was observed from samples, and the OSL was observed to arise from a similar temperature range. The longer preheats at 160°C ensured removal of the unstable component.

However, Spooner (1992) demonstrated that some feldspar samples are affected by athermal decay; ie. a fading signal where loss is not accelerated at higher temperatures. On this basis, it is not always certain whether the unstable signal has been removed by preheating, and he recommends long term monitoring of the fading signal. This was followed for samples in this study, where samples were stored for up to 6 months.

For the samples in this study, a preheat of 160°C for 2 hours and 100°C for 3 days was adopted. The efficiency of the preheat can be tested by comparing the TL glow curves for irradiated and natural discs, both having been preheated. The low temperature peak arising after irradiation is unstable and should have been removed, and the plateau test should be met both for TL and IRSL samples.

In figure 5.3.1, a plot of the initial IRSL signal is given for different preheat times at 160 °C, but all having 3 days at 100 °C. There is a sharp fall off in the intensity of the signal after 2 hours at the higher temperature. This corresponds with the findings of Spooner and Questiaux. However, three samples were stored for three months at 50 °C, and their initial signals correspond closely with the initial signals of the preheated samples (table 5.3.4), indicating that for these samples, a

long storage at lower temperatures was sufficient to remove any unstable component. However, it is not always convenient to store all samples for this length of time, and it may not remove the unstable components in all cases. Consequently, the higher temperature preheat was given as a standard treatment before measurement to all discs, including TL, IRSL and fade tests.

TABLE 5.3.4 Comparison of initial IRSL signal from preheated and stored samples.

Sample	Preheat1	Preheat2	Long Storage
FF3	1254	632	1176
WM4	16613	9876	16214
WH1	22091	16370	21763
SP8	6555	2784	6398

Preheat 12hr 160°C + 3 days 100°C; Preheat2 4hr 160°C + 3 days 100°C;
 Long storage 3mth. at 50°C. Figures are photon counts in first 5 secs.

5.4 CONTRIBUTIONS OF THIS STUDY

5.4.1 Bleaching studies

Samples are optically bleached in the laboratory in order to check for supralinearity at low doses (see 5.1.1), for the regeneration technique of ED determination, and to check for changes in sensitivity in the luminescence signal. The light source employed is usually natural sunlight or a solar simulator, but these do not resemble the attenuated spectrum which occurs under water. The reduction of the UV component of the bleaching source reduces the effects of phototransfer of charge. This is because the UV wavelength region which is primarily responsible for phototransfer and which forms the basis of the PTTL method referred to in 5.1.4.

Laboratory overbleaching by too long an exposure compared to that received at deposition, or the induction of transfer effects by using different bleaching wavelengths to those in antiquity, will result in an erroneous ED value. This is caused by the fact that overbleaching of the residual level determined by laboratory bleaching to lower levels than the residual level contained within the sample at deposition. This results in an overestimate of the ED and hence the age of the sample.

The partial bleach technique used for TL involves the administration of a short bleach. The ED plateau for different times indicated whether the correct (ie. similar to natural) bleaching conditions have been given. Overbleaching (ie, exceeding the natural bleaching level) causes a systematic rise in regenerated ED values with increasing TL glow curve temperature, while underbleaching (below the natural level) results in a fall in regenerated ED values with glow curve temperature. Thus a flat plateau is assumed to predict the correct bleaching conditions in the laboratory, and thus the correct ED value (Wintle and Huntley, 1982; Berger, 1985a,b; Proszynska-Bordas et al, 1988).

Robertson et al (1991) investigated the bleaching of TL of feldspars under sunlight. The high K and Na feldspars were the brightest samples but the least easily bleached. Those with an intermediate K and Na content bleached comparatively quickly. All samples, however, were sufficiently bleached after 16 hr exposure to be suitable for dating. Only one oligoclase sample has an identifiable TL peak which was selectively more bleachable (280 °C). All samples bleached rapidly initially, but rates slowed with time. This is consistent with the results of studies by Kronberg (1983), Dijkmans et al (1988) and others. Robertson et al also suggest a connection between highly bleachable signals and samples which faded, and suggest that a bleaching test could indicate a propensity to fade. In this study, however, it was the least bright samples which tended to fade.

A number of problems exist during laboratory bleaching of dating samples. These include phototransfer of charge, changes in sensitivity of the signal, failure of the TL plateau test and recuperation of the signal after bleaching. With the exception of the last, all of these effects were observed in samples in this study and were primarily associated with the source of light used for bleaching.

Charge transfer is a process whereby charge is evicted by optical bleaching and is retrapped. The charge may therefore be transferred from sunlight sensitive to traps which are not sensitive to sunlight or laboratory bleaching. The transferred charge therefore contributes to the unbleachable residual measured in the laboratory and therefore results in lower ED values and underestimation of the age.

For waterlain sediments charge transfer may be a substantial problem because of differences between the wavelengths contributing to the bleaching by sunlight (or attenuated sunlight) and the laboratory bleaching source. In this case the use of, for example, sunlight or white light for laboratory bleaching of sediments which were laid down under sunlight attenuated by water depth may result in significant problems relating to the residual levels of the TL and IRSL signals.

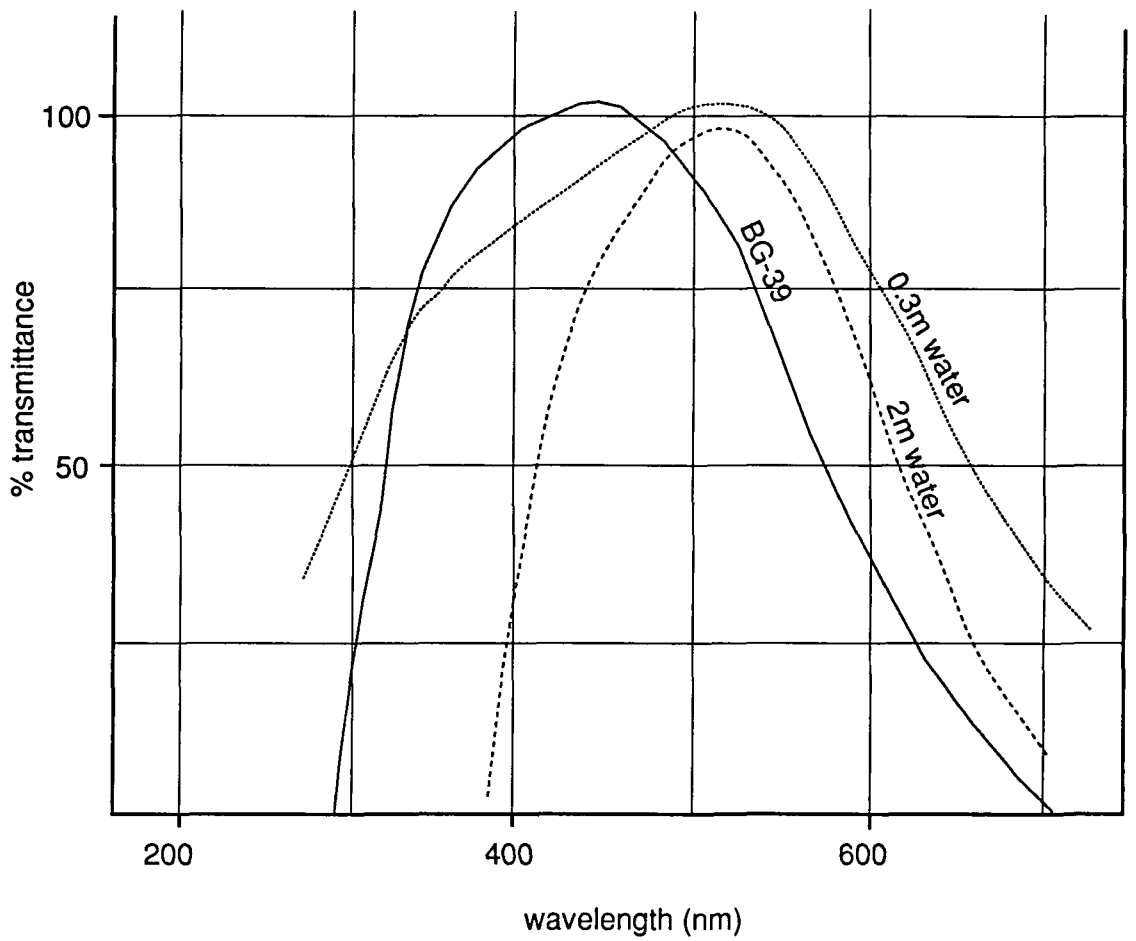
Work by Berger and others (Berger et al, 1984, Berger, 1984, 1990) illustrates the importance of bleaching wavelengths and stresses that the wavelengths shorter than 550 nm need to be cut out, as these would not be present in the subaqueous spectrum. He also suggests eliminating the red band of the spectrum (650-700 nm) and has produced accurate EDs by blocking all wavelengths below 660 nm. Red light does cause bleaching - this is the basis on which the IRSL technique rests. A comparison between the attenuated spectra of sunlight underwater and transmission of white light through a BG-39 filter (used in the studies below) is shown in figure 5.4.1.

Dijkmans and Wintle (1989) observed a failure of the TL plateau in the additive growth characteristic of K-feldspars bleached under direct sunlight. This could not be rectified by altering the exposure times of the samples. Poor plateaux may be due to non-linear growth of the TL, greater errors due to lower sensitivity at higher TL glow curve temperatures, second-order kinetics and inappropriate bleaching light sources used in experiments. In the last case, bleaching waterlain sediments under full sunlight may cause poor TL plateaux as the spectrum of light differs from that to which the sample was exposed at deposition, and therefore samples a different trap spectrum in the measured signal. Sensitivity changes due to optical bleaching of minerals was not significant for samples bleached under sunlight and mercury lamp (Bluszcz, 1988) but this may not apply for waterlain sediments bleached under sunlight.

Filtered bleaching sources (ie. where some wavelengths have been selectively blocked) have been used in a number of studies, particularly for dating waterlain material. Rendell et al (1989) used a 300 W sunlamp intercepted by a sheet of glass to cut out the wavelengths less than 320 nm for the zeroing of TL in dune and beach sands. Spooner et al (1989) refer to a 1000 W solar simulator 'adjusted to resemble sunlight' but no details are given. In a study of the sunlight an UV bleaching of quartz and feldspars Jungner (1988) used a UV lamp with a range of 320-400 nm. This effectively cuts out both the shorter and longer wavelengths similar to underwater conditions where the peak wavelengths are in the green region. He also observed that there was no difference in the ED plateau for sunlight and lamp bleaching in feldspars, but there was a significant change in quartz.

Bowall et al (1987) studied the effect of the temperature at which a sample is held while a bleach is administered. The rate of signal decay was much faster at +50 °C than at 0 °C or -35 °C, which is to be expected as the eviction of charge is thermally assisted. Whether this is affected by populations of traps evicted under the same light at different temperatures is not indicated. A filter cutting out <430 nm reduced the effect of a sunlamp bleach by 18%.

Figure 5.4.1 Transmission of light through water (after Berger, 1990) and through Schott BG-39 filter used for bleaching



An additional problem associated with bleaching is that of recuperation of the signal (Aitken et al, 1989), recognised at Oxford. Several types of recuperation were proposed and this was observed in quartz samples bleached by green laser, and stored for short periods of time, after which a regenerated, phototransferred signal could be measured (Aitken et al, 1989, Rhodes, 1990). Recuperation has not been recognised in the TL or IRSL of feldspar or polymineralic samples in this study, or in previous samples studied at Durham (Bailliff and Poolton, 1991). This was checked for by remeasuring after storage at 50 °C and at room temperature (c.18 °C) for a period of up to six weeks after IRSL measurement.

5.4.1.1 Laboratory bleaching

All the samples in this study were initially exposed to natural sunlight for bleaching. In the case of IRSL samples given the same treatment, an unexpected and significant residual was observed. However, bleaching of untreated discs of the same sample using a 240 W tungsten halogen lamp, intercepted by a BG-39 filter which transmits a spectrum closer to that of underwater conditions, eliminated the residual from the IRSL signal and substantially reduced that of many of the TL samples. The residual levels are given in table 5.4.1, and plots of the reduction in TL and IRSL signal against time for the first 3 hours for sample WM4 bleached under both conditions is given in figure 5.4.2. Sensitivity changes observed in the signal after bleaching are discussed in the following section. The observation of a residual in IRSL samples was useful in the identification of the problem, as a residual after bleaching of TL samples is expected, although the level is unknown.

TABLE 5.4.1 Bleaching residuals after exposure to sunlight and filtered artificial light.

Sample	TL(SL)	TL(F)	IRSL(SL)	IRSL(F)
FF3	26	24	3.9	0.03
FF4	39	23	1.04	0.04
WM3	15	6.5	11.6	0.08
WM4	66	38	7.40	0.01
WM5	24	18	9.30	0.01
HAZ2	27	16	11.4	0.01
SLG2	34	17	17.2	0.08
SLG3	29	23	11.7	0.03
SLG4	38	15	13.1	0.01
WH1	20	11	6.70	0.06
WH2	24	16	9.40	0.06

SP2	30	24	3.60	0.01
SP3	40	23	9.70	0.10
SP4	33	21	14.8	0.06
SP5	36	19	15.3	0.04
SP6	44	26	16.3	0.07
SP7	41	26	19.2	1.20
SP8	39	28	18.2	0.04
SP9	64	27	2.60	0.03

All figures represent % reduction of the unbleached natural signal.

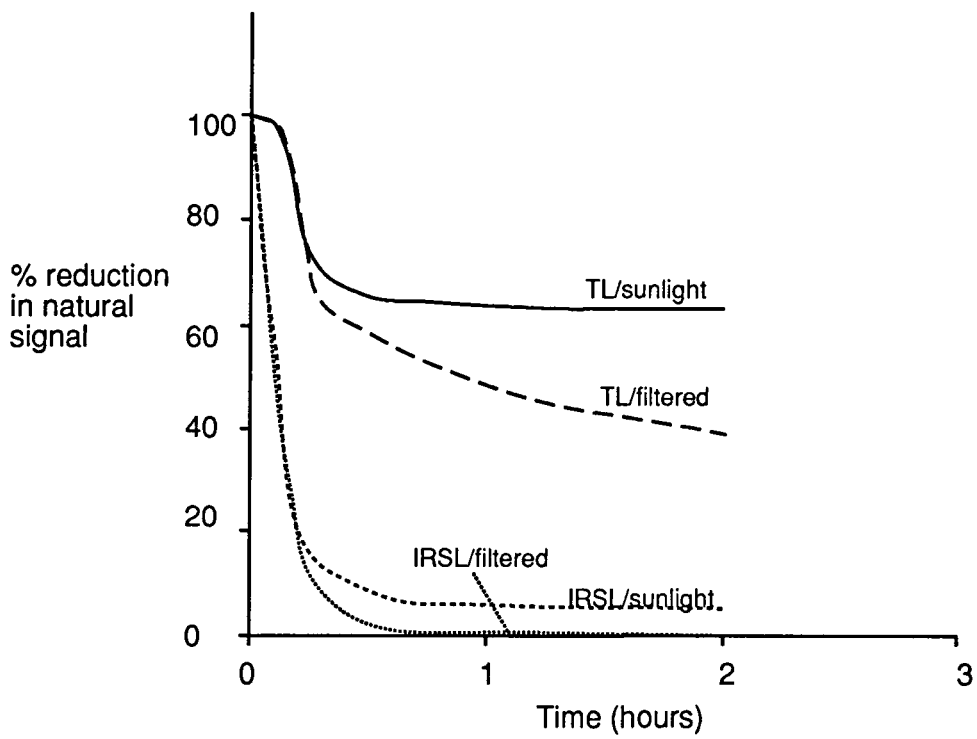
The significant differences between the residuals using the different bleaching sources is attributed to charge transfer effects. These have been investigated by Bailiff and Poolton, (1991) ^{Poolton & Bailiff} (1989). These authors show that the effects of transfer need to be understood as they can substantially affect the ED value of a sample. In order to solve the problem of charge transfer during bleaching under sunlight, samples were then exposed to a bleaching source which comprised light from a tungsten-halogen lamp which was passed through a BG-39 filter.

The BG-39 filter transmits wavelengths from 300-700 nm (figure 5.4.2), with a peak range of 320-560 nm (>50% of these wavelengths are passed). The comparison between Berger's (1990) underwater transmission data for 0.3m depth is closer to the BG-39 transmission than the 2m depth spectrum. However, Kronberg (1983) demonstrated that no significant changes were observed in sunlamp bleaching up to 0.7m. Thus, the bleaching spectrum used in the study is closer to sediment carried at water depths of around 1 m, depending on the turbidity and suspended sediment load. However, total bleaching of the samples in this study using this spectrum has produced dates consistent with expected ages in the majority of cases, suggesting that at some point in their bleaching history the majority of sediment samples were exposed to relatively shallow water spectra for sufficient time to bleach the signal.

Berger (1990) stresses the need for short bleach times, based on evidence of incomplete zeroing of suspended sediment samples. This work, however, has concentrated on the partial bleach method whereby a short bleach can be used for ED evaluation so long as it is less than the exposure the samples had undergone at deposition. It is difficult in these cases to check for charge transfer, which may only be observed in the residual after total bleaching.

However, in this study filtered bleaching has produced a correct ED (ie. one which agrees with known age or zero age samples) where the bleach was total rather than partial. The relatively short times needed under filtered light to remove all the IRSL signal and all the bleachable (under

Figure 5.4.2 Reduction in natural signal of TL and IRSL of WM4, after bleaching with different light sources.



filtered light) TL signal, given in table 5.4.1 and figure 5.4.2 indicate that in the majority of cases, even for waterlain material, the regeneration or related techniques are appropriate.

5.4.2 Sensitivity changes in the luminescence signal.

Changes in the sensitivity of the luminescence signal can be induced by laboratory treatments such as irradiation, bleaching and heating of unburnt materials during measurement of the TL signal, and are widely recognised in sediment dating (eg. Wintle and Huntley, 1980; Wintle, 1982; Rendell et al, 1983; Berger, 1984; Rendell and Townsend, 1988). Changes in sensitivity are caused by changes in the luminescence efficiency (amount of charge evicted), or in the number of traps available for retrapping or eviction of charge.

These may be identified in the TL signal by changes in the slope of the growth curve, peak shifts and disruption of the plateau. Sensitivity changes in the IRSL signal of feldspars has not been widely studied due to the novelty of the technique. The observations of the IRSL emissions in this study are considered below. Figure 5.4.3 illustrates changes in the form of the TL growth curve of WM4 under different bleaching conditions. Filtered bleaching induces no sensitivity changes as sunlight bleaching does.

Li and Wintle (1991) found that IRSL ED values were consistently smaller than predicted for colluvial samples. Sensitivity changes were observed after bleaching with a solar simulator and with IR. These were related to the degree of sunlight exposure the sample received prior to deposition. A reduced sensitivity in the IRSL signal was not found for loess samples which are well-bleached at deposition, only for the poorly bleached colluvial material.

In samples in this study, some sensitivity changes were observed in the IRSL signal. This was identified by plotting the ratio of the decay curves of $N + \text{bleach} + \beta_1$ to $N + \text{bleach} + \beta_2$, where N is the natural signal and β_1 and β_2 are two irradiation doses of different sizes given after bleaching and prior to measurement. Aliquots of sample WM4 were measured under the same conditions, except that for one ratio plot bleaching was under direct sunlight and the other was for bleaching under filtered light as discussed above. These are shown in figure 5.4.4.

The sloping ratio plot in the figure represents the sunlight bleached aliquots and the horizontal, flat ratio plot the aliquots given filtered bleaching. The changes in form and rate of the IRSL decay curve cause the ratio plot to deviate from the horizontal.

Changes in sensitivity were also observed in the TL signal. These were primarily recognised as failure of the plateau test. In two cases where peak shifts were observed after measurements,

Figure 5.4.3 Bleaching-induced TL sensitivity changes for WM4. The non-linearity of the sunlight bleached growth curve demonstrates the sensitivity change, which has not occurred under filtered bleaching.

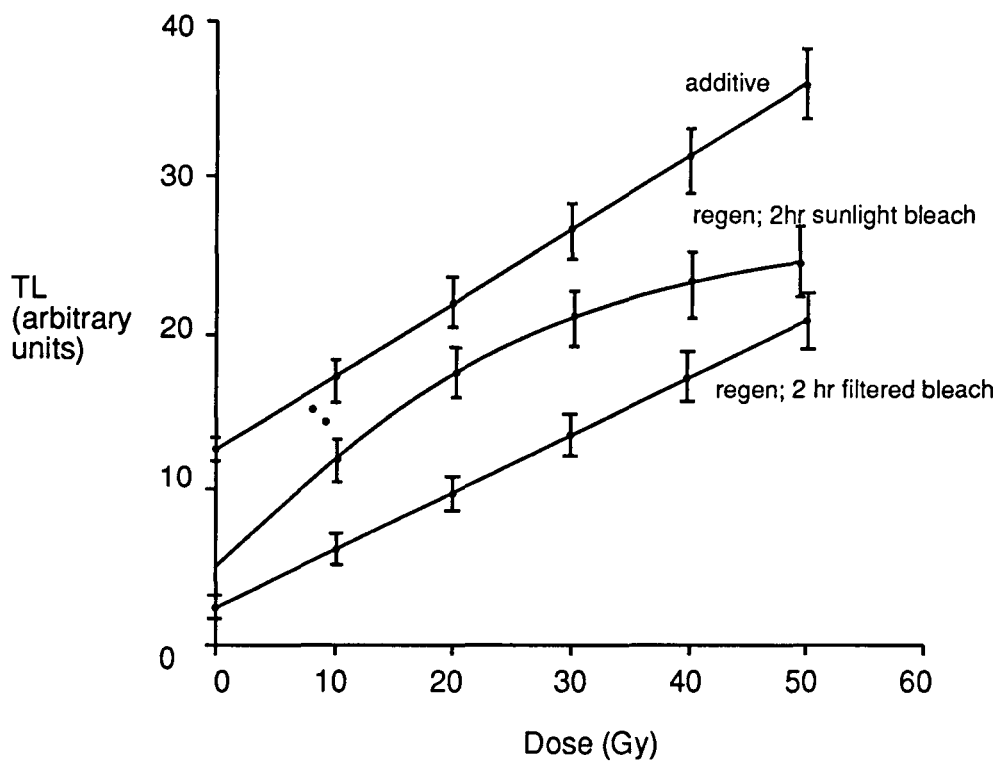
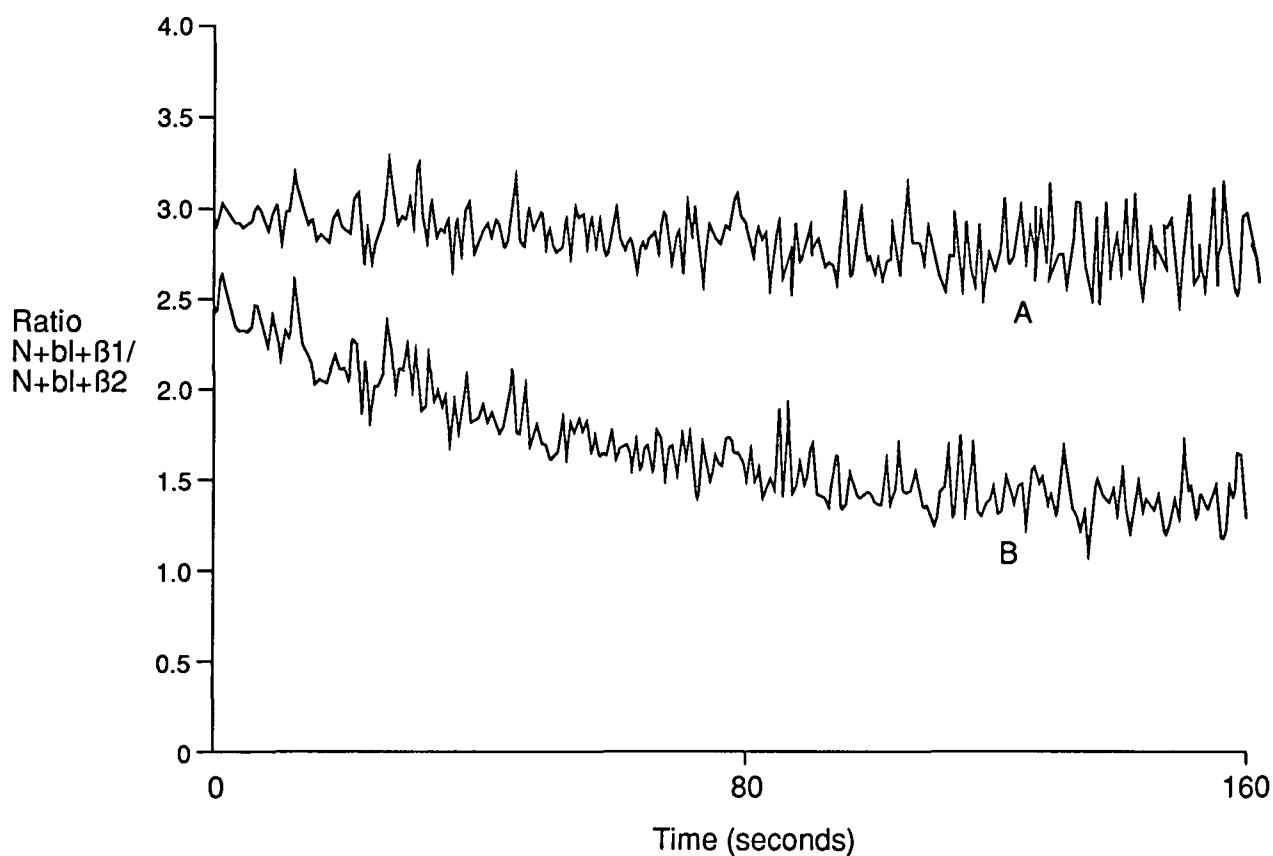


Figure 5.4.4 IRSL decay curve ratios for WM4 showing change in the form of decay. The ratio curves are calculated using decay curves of a bleached natural signal plus beta doses 1 and 2, where beta dose1 is larger and is divided by the curve of the signal from the smaller beta dose. The upper ratio plot (A) shown here represents sub samples bleached under filtered light conditions; the lower curve (B) shows sub samples bleached under direct sunlight. The sunlight bleached ratio plot is sloping and the represents a change in the form and rate of decay of the IRSL decay curve.



second order kinetics was thought to be the cause. Berger and Huntley (1982; Berger, 1985) observed such peak shifts in fine-grain sediment samples. This was overcome by matching the additive and regenerated TL peaks before applying the plateau test, using physical justifications given by Chen et al (1983).

Where this has been used, Berger has produced acceptable ages, and this practice was adopted in two cases where the peak shifts were relatively minor. In a number of samples in this study, however, the shifts were too great to justify using this approach, as the changes in sensitivity caused by heating were too large to be dismissed. These samples had other problems, which are discussed in Chapter 7.

Bowall et al (1987) observed non-linearity in the regenerated growth curves after bleaching for 1 hour. This was caused by the rapidly decaying component of the bleaching signal. This non-linearity did not occur after 8 and 16 hours bleaching after which the residual was reached (in the 280-320 °C TL region). These results suggest that shorter bleaches such as those given in the partial-bleach technique may result in sensitivity changes which would not occur using total-bleach and regeneration. Advocates of the partial-bleach technique would undoubtedly concur that the laboratory bleach administered would be too short to cause this effect to any extent.

Bowall et al's work^(op cit) also demonstrated an initial rise in sensitivity after 1.5 hours bleaching of +4 to +8%, but a decrease after 5 hours of -10 to -20%. Storage after bleaching, but before irradiation for 2 months, caused a 50% decrease in the signal. However storage after bleaching and irradiation induced no change in the signal. The delay between bleaching and irradiation also caused a shift from 260 to 290 °C peaks. This was attributed to the variety of minerals and luminescence behaviours contained within a polymineralic fine-grained sample. It held significant implications for the ability to separate the bleachable part of the natural TL and regenerated signals.

Sensitivity changes may also arise following irradiation treatments of samples. Wintle (1985) proposed a dose-dependent sensitivity change on exposure to light for loess TL, and Rendell and Townsend (1988) modelled this in terms of changes in the TL efficiency caused by laboratory treatment, although dose-dependence did not appear to be the cause of sensitivity changes. Natural bleaching at deposition may induce some transient changes, but the natural accumulation rate is so low that these changes do not affect long term sensitivity. In laboratory measurements, the dose rate is around $\times 10^8$ that of the natural, and may be more affected by such short term changes. This may well explain the findings by Bowall et al. Berger (1988) attributed dose dependent sensitivity changes to individual sample characteristics. Even the partial-bleach technique cannot infallibly separate the post-depositional (accumulated) signal from the relict TL.

Zhou and Wintle (1989) tested the model developed by Rendell and Townsend (1988) for sensitivity changes induced by delayed irradiation after bleaching. They applied a 16 hour 140 °C preheat between bleaching and irradiation which eliminated the sensitivity changes observed in the unpreheated sample. The preheated sample produced the same ED as for a sample given a preheat of 16 hours at 175 °C after irradiation. They concluded that sensitivity changes did not occur in younger samples, and that this supported the model of Rendell and Townsend. If the occurrence of sensitivity changes was due to time-dependent changes as suggested by Debenham (1985), the ED would be affected regardless of the method used.

Sensitivity changes may therefore arise in samples as a result of laboratory treatments such as bleaching, irradiation and heating. The IRSL plot of the ratios of decay curves can be used, as it has been here, as an indication that changes in the form and rate of the IRSL decay have occurred. In this study, such changes were observed as a result of the use of sunlight rather than the filtered bleaching source which did not cause such changes.

TL samples affected by sensitivity changes were recognised by failure of the plateau test. Minor peak shifts in two samples were attributed to second order kinetics. Samples were stored for a short time between treatments such as bleaching and irradiation, before measurement in order to overcome possible transient changes in sensitivity in the samples arising from these treatments.

5.4.3 Water Content

The estimation of past water contents is a potential source of error and a significant limitation to the accuracy of luminescence ages (Fleming, 1979 31-34; Aitken, 1985, 74-76; Aitken, 1988) and must be closely monitored. This is because water absorbs more radiation than air when present in pores. In effect this attenuates the dose rate to sediments. Measurements of the dose-rates are made on dry samples, so the presence of water in the natural state must be corrected for.

An underestimate of the saturation water content results in ages which are too low. The effects of groundwater movement on the leaching of isotopes (Fleming, 1979) and the effects of de-watering by compaction or artificial drainage (see Chapter 3), may result in significant changes in the saturation water content through time. The structural changes in sediments may be identifiable in stratigraphic sections. These may be important indicators of such changes (Rendell, 1983 with respect to loess). Seasonal and longer term fluctuations in groundwater levels, and the effects of compaction and de-watering on the dose rate to sediments also contribute to the errors in the evaluation of the annual dose.

The saturation level of the water uptake sample (porosity) gives an upper limit for the amount of water the sample can hold. In most burial conditions including those studied here, sediments are close to saturation. Important exceptions occur in very arid regions and in elevated, freely draining sand dunes. The corrections applied to dose rate calculations are given by Aitken (1985, Appendix B). Measurements are made of the saturation water content (W) and the fractional uptake (F) which is the amount of water in the sample at the time of sampling. Some 'typical' values of the percentage error in the age resulting from water content using samples from this study are 12.6% for a water content of 50%; 22.4% for 90% water content and 29.6% for 120% water content (the error percentages refer to a percentage of the total error in the age).

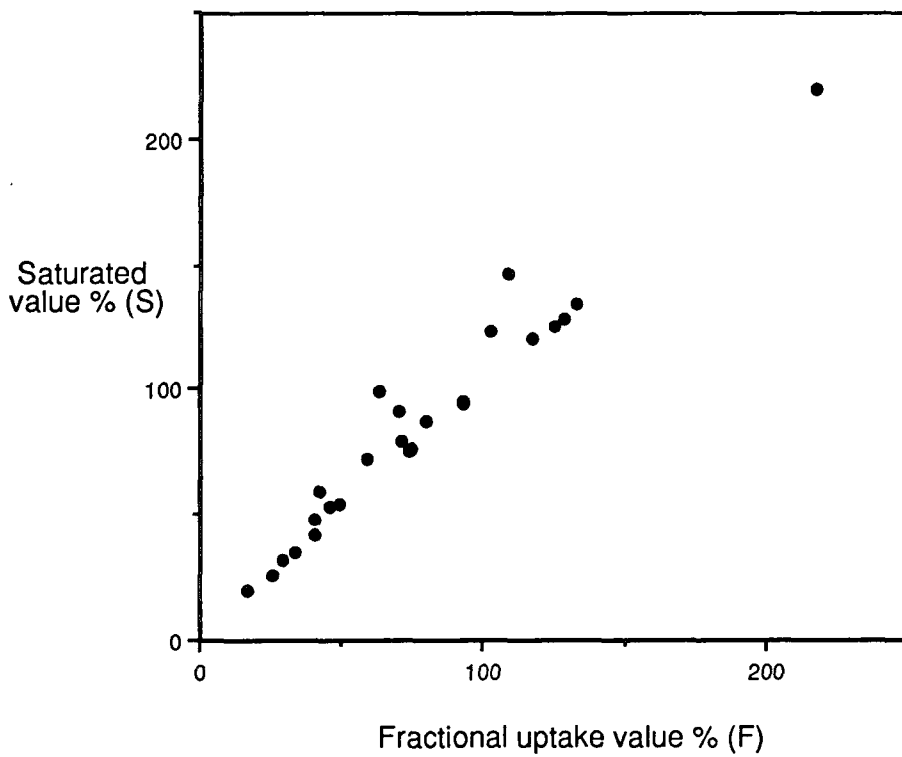
Aitken's error values are based on an 80% fractional uptake of water ($F = 0.8 \pm 0.2$) but it is the variation in the F value which is most important and contributes to the uncertainty on which the error values are based. In order to test whether this is an appropriate value for the sediments in this study, the saturated water content (see Chapter 3), and the water content of the sample at the time of sampling (F) are plotted in figure 5.4.5. The mean value of F is 81% ($F = 0.81$) which supports the use of Aitken's recommendations. The error should not be reduced, because of the unknown effects of drainage and sea-level change on the water content through time.

Zimmerman (1971) calculated that water absorbs 50% more alpha radiation, 25% more beta radiation and 14% more gamma radiation than air. The corrections are based on the specific stopping powers and absorption coefficients of water and soil. The reduction in the alpha dose-rate assumes that water is present in pores which are smaller than the alpha particle range. Correction factors are given for an estimated mean of the range of energies present in alpha, beta and gamma radiations.

The corrections calculated by Zimmerman (1971) and Bowman (1976) are 1.49 for alpha and 1.25 for beta. Zimmerman's value for gamma correction is 1.14, but Bowman (1976) suggests 1.0, based on a different spectrum of energies. Aitken and Xie (1990) recalculated Zimmerman's (1971) correction factors for gamma dose, but did not recommend modifications of them. Aitken and Xie (1990) did however point out that the ratio would be affected by compaction of sediments, as the ratio of water to mineral would be further reduced. This was not taken further in the paper, nor was any change made to Zimmerman's correction of 1.25 for the beta component. The work here adopted the Zimmerman values of 1.14 for gamma and 1.25 for beta and 1.49 for alpha.

For sediments used in this study, the uncertainty in the saturation value, is taken to be 20%, is an overestimate of the variation likely to have occurred in the sediments *in situ*. Figure 5.4.5 also shows that except in a very few cases, the sediments were to close to saturation with respect to

Figure 5.4.5 Saturated versus fractional uptake water content values for all samples. This graph shows that most samples were at or near to saturation at the time of sampling. It should be noted that it is the uncertainty in the water content variation that contributed to the error on luminescence dates, not the actual water content itself. The measurement uncertainty in these values is 1%.



their water content. Variation in this value may have arisen due to periods of drying associated with better drainage, lower sea-level stands, or wetting due to subsidence or submergence, or changes associated with partial compaction or consolidation of the sediments with time. For these reasons, the error value was not reduced, but it is unlikely to have been exceeded. This is supported by the sedimentological evidence, such as the lack of recurrence or compaction surfaces associated with exposure or desiccation. The effect of applying a 90% fractional uptake and 10% error for water-content of some compacted samples is discussed in Chapter 6.

5.5 SUMMARY OF DATING PROCEDURE

A summary of the conditions of TL and IRSL measurement are given in table 5.5.1 below. This includes the aspects concerning the apparatus, preheating and other conditions.

TABLE 5.5.1 Summary of procedures used.

1. PREPARATION (5.3.1)	Carbonate removal	2% Acetic Acid 2 hrs. or until rxn. ceases
	Organic removal	30% H ₂ O ₂ until reaction ceases
	Deflocculation	Calgon (sodium oxalate)
2. SEPARATION (5.3.1)	Fine-grains	Sedimentation 4-11 μm (2 & 20 min settling)
	Coarse-grains	Sieving 90-120 μm
	Disc preparation	120 discs per sample.
3. NORMALIZATION (5.3.2)	TL	Weight or post-measurement dose response
	IRSL	1 second exposure before measurement
4. IRRADIATION (5.2.6)	TL	β(40) ⁹⁰ Sr 1.08 and 1.22 Gy/min to fg and cg
	IRSL	β(42) ⁹⁰ Sr/ ⁹⁰ Y; 0.55 and 0.7 Gy/min to fg and cg
	Alpha source	(TL and IRSL) Am-241, 0.45 μm ⁻² /min.
5. BLEACHING (5.4.1)	240W Tungsten-Halogen lamp passed through BG-39 filter	
6. PREHEAT (5.3.5)	2 hrs 160°C and 3 days at 100°C	

Figure 5.5.1 TL plateaux for WM1 (failed) and WM5 (passed)

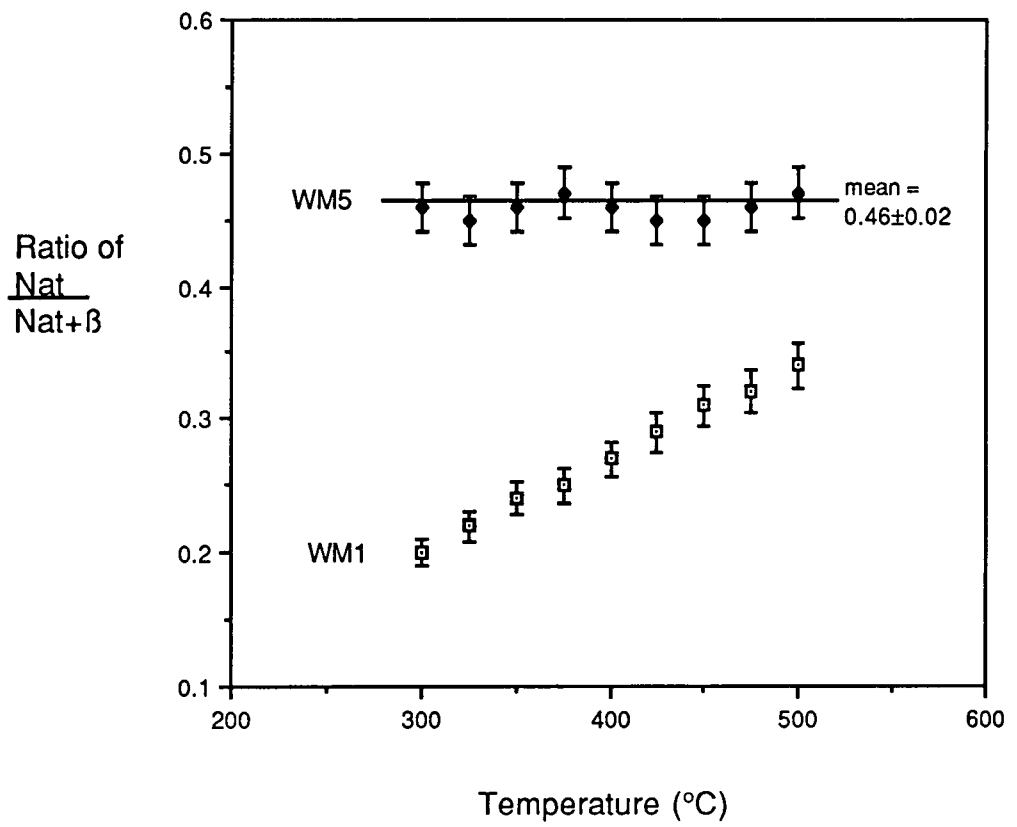


Figure 5.5.2 TL growth curves for WM5 (top), showing linear growth and no change in form of growth curve after filtered bleaching; and HAZ3 (bottom) showing non-linear growth and changes in form of growth curve after filtered bleaching.

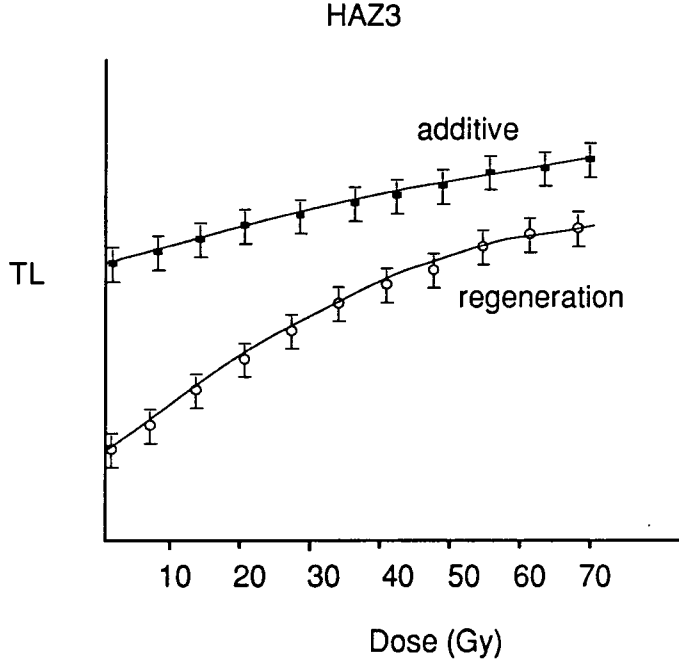
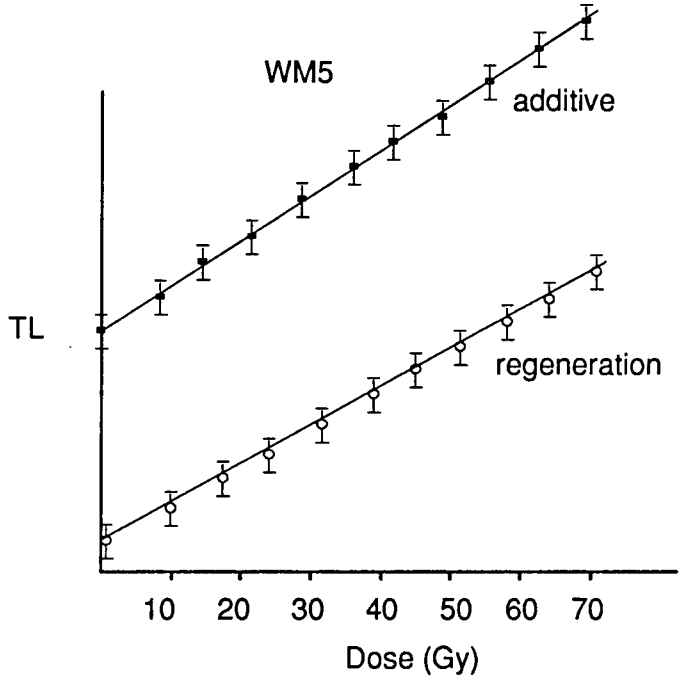
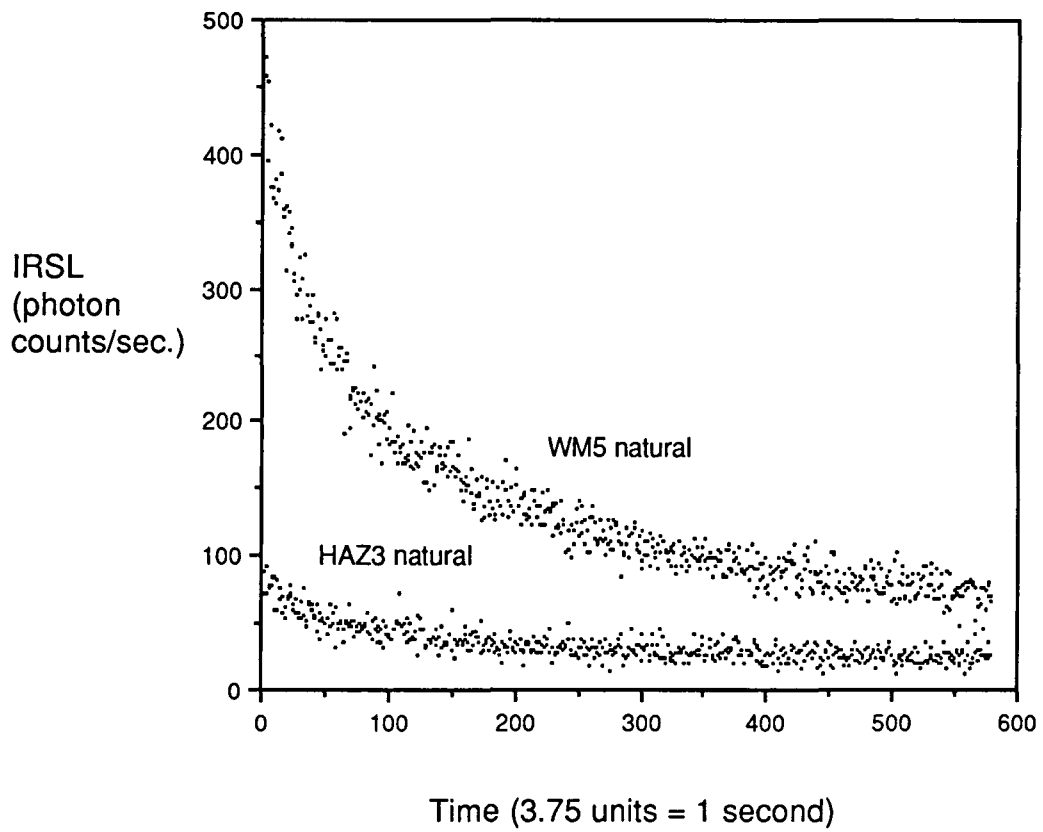


Figure 5.5.3 IRSL decay curves; high intensity WM5, and low intensity HAZ3. Decay curves measured with 880 nm LEDs at 18°C; background subtracted.



7. TL MEASUREMENT (5.2.1)	Manual set; heat-rate 10°C/sec. Corning 7-51 and Chance Pilkington HA-3 filters. Up to six repeat measurements per point on growth curves
8. IRSL MEASUREMENT (5.2.2)	Durham set, semi-automated: 950 nm leds; 600 sec exposure Risø set, automated: 880 nm leds; 160 sec exposure per run Up to six repeat measurements per point on growth curve
9. FADE TESTS (5.3.4)	N+30Gy (β); store at RT (c.18°C) 50°C for 6 weeks and 6 months
10. DOSIMETRY (5.2.7)	Thick source Alpha-counting Beta- TLD XRF for potassium content (Gamma) Calcium Fluoride dosimetry in field Portable Gamma spectrometry in field

The identification of such criteria is important, in order to select those samples most suitable for dating before lengthy experimental work has been done on them. The relationships between accepted and rejected samples, and their sedimentological characteristics which aid their recognition, are discussed in Chapter 7.

1. Samples of Holocene age (<10ka) are expected to show a linear growth characteristic with added radiation dose, and samples which exhibit signs of saturation are likely to have been insufficiently bleached at deposition (cf. figure 5.5.2).
2. The TL plateau is still accepted by many as an indication of stability in the region of the glow curve corresponding with traps of suitable lifetimes for luminescence dating. This criterion was used here, and failure of the plateau test was taken to represent instability or changes in sensitivity of the sample to radiation or bleaching (figure 5.5.1).
3. The form of the regenerated and additive growth curves should be similar (ie. parallel and producing similar EDs), and demonstrate measurable growth with added dose (figure 5.5.2).
4. The intensity of the measured signal should exceed the background levels by a factor of at least 4 (ie. a signal-to-noise ratio of 4.0 or above). This was introduced because of the problems

experienced in some samples under infra-red stimulation, which had signals too close to background to allow accurate measurement (figure 5.5.3).

5. The samples should show no signs of fading.
6. There should be no indication of radon loss during alpha counting.
7. The TL residual after bleaching should be less than 10% of the total signal; any more than this level indicates a significant amount of charge which is not sensitive to sunlight and may affect the accuracy of ED evaluation. A large residual level may also indicate a proportion of transferred charge following bleaching, which does not represent the true unbleachable residual.
8. There should be no indication of sensitivity changes after bleaching or irradiation or preheating treatments, which may affect the ED values.

CHAPTER 6 LUMINESCENCE DATING RESULTS

The results of luminescence dating are presented in table 6.1. Additional data relating to the dose-rate and to measurements of TL and IRSL signal characteristics are given in tables 1 and 2 in Appendix C. These include stability, intensity and correlation coefficients of the fit of the growth curve data to the weighted linear regression programme used for all ED evaluations. The additive ED was used for age determination in all cases and the residual levels were determined by laboratory bleaching under filtered light as described in section 5.4.1. As all samples were relatively young (less than 10 000 years) the growth characteristic of the sample was expected to be linear. The correlation coefficients of the fit of additive growth curve data to the weighted linear regression curve were all >0.84.

6.1.1 Flag Fen

Four samples were taken for dating, as described in section 4.2.1. Two samples, FF1 and FF2 from the upper part of the sequence were rejected due to problems with disequilibrium of the radioactive decay chain. This was manifested as radon escape and detected during alpha counting. The ratio of sealed:unsealed counts was 1.39 for FF1 and 1.26 for FF2 indicating radon escape amounting to c. 40% and 25% respectively.

Both these samples also demonstrated marked instability of the signal, detected during fading tests. Loss due to fading after 6 months storage at 18°C was 32% of the TL signal of FF1 and 28% of the IRSL signal. FF2 faded by 57% for TL and 49% for IRSL. The unstable component of the signal was not removed by preheating at 160°C for 2 hours plus 100°C for 3 days. The IRSL signal was also of low intensity for these samples. The initial intensity in the first second amounted to 334 counts for FF1 and 299 counts for FF2. This gave signal-to-noise ratios of 3.1 and 2.8 respectively, which were considered too low for accurate measurement.

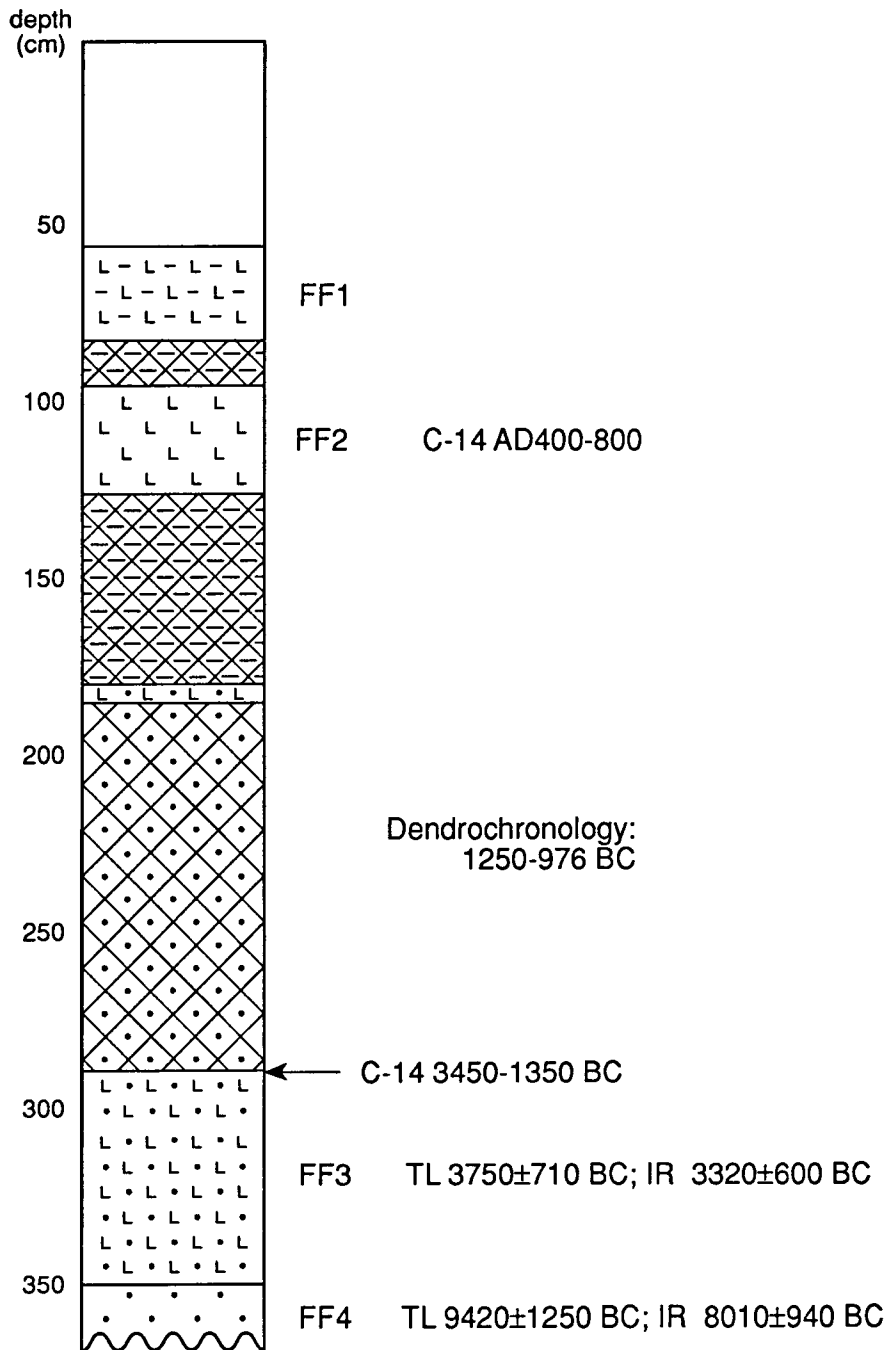
Samples FF3 and FF4 were both dated by TL and IRSL (figure 6.1.1) on the fine-grain fraction. FF3 was dated to 3750 ± 710 BC for TL and 3320 ± 600 BC for IRSL. These age ranges are therefore 4460-3040 BC for TL and 3920-2720 BC for IRSL. There is good agreement between the luminescence age ranges for FF3. The age ranges overlap for 880 years, representing 51% of the age range of both dates. The luminescence dates are also in close agreement with the C-14 based chronology. The calibrated C-14 age range for the deposit is 3450-1350 BC with 35% of this falling within the luminescence age range. The errors on the luminescence ages for FF3 are 18.9% for TL and 18.1% for IRSL. This falls within the 20% 'limit' of acceptability proposed by Aitken and discussed in Chapter 5.

Table 6.1 Luminescence age estimate data

Laboratory Code	AGE (YrBC)	Random error(Yr)♦	Overall error(Yr)♦	Dose-rate (Gy/a)‡	a-value	Water content %	Additive ED (Gy)‡	Regen. ED (Gy)‡
Dur90TL.FF3	3750	280	710	3.65±0.5	0.28	40.6	23.6±1.5	20.5±1.1
Dur90IR.FF3*	3320	190	600	3.75±0.5	0.15	40.6	16.66±0.3	15.4±0.9
Dur90TL.FF4*	9420	830	1250	3.33±0.2	0.2	25.14	38.09±0.4	31.1±1.2
Dur90IR.FF4	8010	520	940	3.13±0.2	0.15	25.14	29.07±0.9	27.6±1.2
Dur90IR.WM3	2100	300	600	4.18±0.2	0.13	49.02	16.92±0.4	15.3±1.3
Dur90TL.WM4	3090	710	1430	2.62±0.5	0.35	93.0	17.36±0.6	16.9±0.9
Dur90IR.WM4	3030	470	1200	2.62±0.5	0.07	93.0	10.42±0.4	11.03±0.7
Dur90TL.WM5	8580	760	960	2.62±0.3	0.11	16.5	30.43±0.9	28.5±1.1
Dur90IR.WM5	8470	550	800	2.62±0.3	0.08	16.5	28.44±0.7	27.6±1.1
Dur90IR.WM5*	10180	820	1040	2.82±0.3	0.05	16.5	28.74±0.3	22.1±0.7
Dur90TL.HAZ2	3050	590	1600	2.75±0.1	0.06	74.7	13.88±0.8	11.3±0.5
Dur90IR.HAZ2	2080	280	1290	2.75±0.1	0.04	74.7	10.8±0.9	18.3±0.9
Dur90TL.SLG2	2200	220	840	4.56±0.2	0.26	132.95	20.8±0.8	17.7±0.6
Dur90IR.SLG2	2320	330	890	4.56±0.2	0.2	132.95	18.61±2.7	15.7±0.5
Dur90IR.SLG3*	2940	220	1170	3.36±0.2	0.17	45.72	16.42±0.6	45.28±1.3
Dur90TL.SLG4	5060	1060	1790	4.45±0.9	0.5	133.95	47.18±1.7	39.73±1.4
Dur90IR.SLG4	3490	480	1100	4.45±0.9	0.12	133.95	28.99±1.8	27.5±0.9
Dur90TL.WH1	13960	1720	5500	4.49±0.4	0.41	125.13	80.2±1.1	78.19±1.3
Dur90IR.WH1	11470	950	4300	4.49±0.4	0.16	125.13	53.2±1.6	54.26±1.6
Dur90TL.WH2	17450	950	6200	3.72±0.5	0.18	125.79	70.1±2.9	68.32±2.1
Dur90IR.WH2	19050	890	7030	3.72±0.5	0.34	125.79	87.06±3.2	86.79±2.3
Dur90IR.SP2*	610	140	450	2.51±0.3	0.11	116.76	6.56±0.2	7.3±0.3
Dur90IR.SP3	2390	410	1400	2.38±0.2	0.11	128.12	10.31±0.7	9.8±0.4
Dur90IR.SP4	3420	1060	1600	2.12±0.3	0.08	92.61	11.39±0.4	10.3±0.6
Dur90TL.SP6	4390	660	970	4.82±0.5	0.29	40.35	34.54±0.8	31.7±1.3
Dur90IR.SP6	4410	490	1120	4.82±0.5	0.14	40.35	27.65±0.4	25.6±0.7
Dur90TL.SP8	6070	340	890	5.22±0.6	0.47	32.91	73.95±3.2	71.84±1.9
Dur90IR.SP8	4960	250	660	5.22±0.6	0.12	32.91	46.1±0.9	48.21±0.9
Dur90TL.SP9	8570	520	1090	4.86±0.7	0.34	29.26	89.31±1.1	88.36±1.7
Dur90IR.SP9	7760	770	1060	4.86±0.7	0.06	29.26	62.24±0.6	63.45±1.1

* denotes coarse grain sample; ‡ see tables in Appendix C for details; ♦ at 68% confidence level

Figure 6.1.1 Flag Fen age comparison



FF4 was also dated by TL and IRSL. The ages were 9420 ± 1250 BC for TL and 8010 ± 940 BC for IRSL. These ages are also in good agreement, with 25% of the age range overlapping between the two dates. There is no independent C-14 based chronology for this stratum, but the luminescence ages are in agreement with the identification of the stratum as a post-glacial outwash sand deposited after the Devensian cold stage between 10 000 and 8000 years ago. The errors on the FF4 dates are 13.3% for TL and 11.7% for IRSL. These are less than for FF3 due to the reduced uncertainty in past water content history.

6.1.2 Williamson's Moss

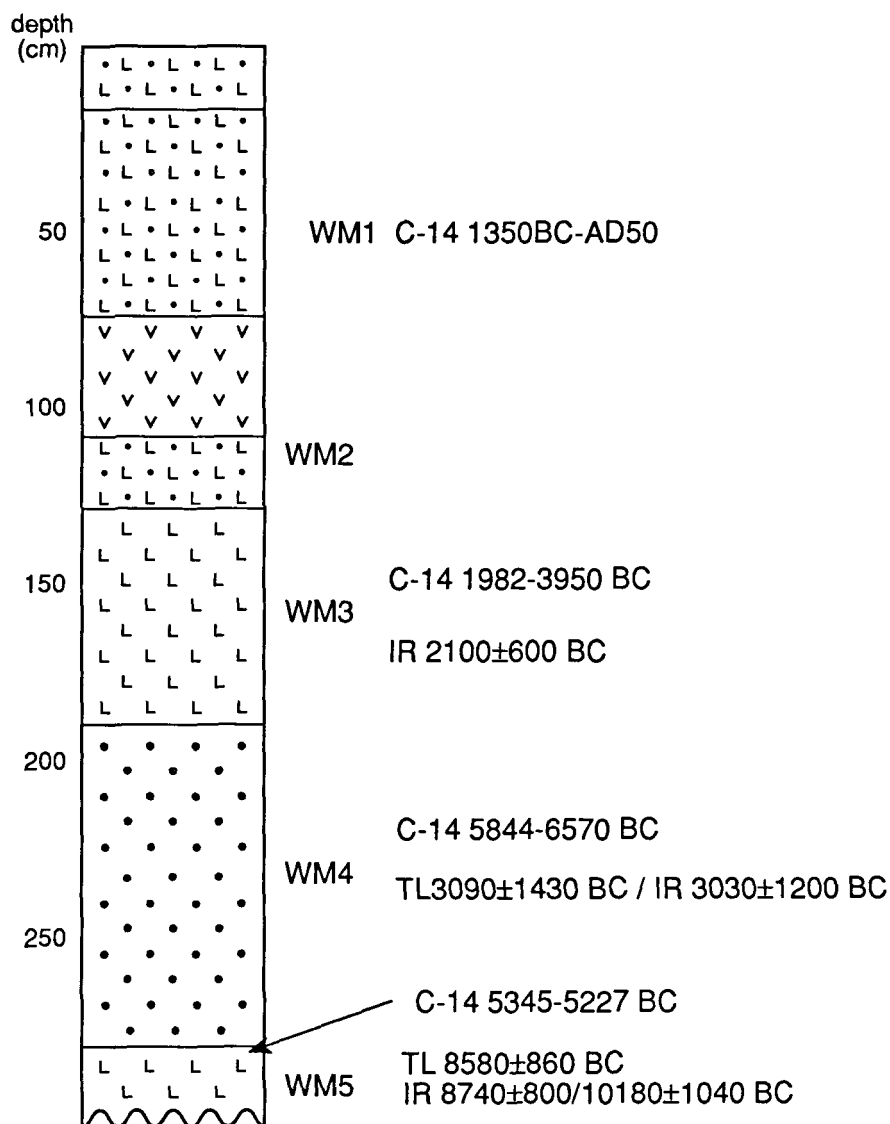
Five samples were taken from this sequence which is described in 4.2.2. Two samples, WM1 and 2 from the upper part of the sequences were rejected for dating. This was due to low intensities of IRSL signals. The initial natural signal of WM1 was 329 counts and for WM2 177 counts. This gave signal-to-noise ratios of 3.0 and 1.6 respectively (table 2, Appendix C) which were not considered sufficient for accurate measurement. Both WM1 and 2 failed the TL plateau test, indicating instability in the signals used for dating.

WM3 was dated by IRSL only to 2100 ± 600 BC (figure 6.1.2). The TL signal of this sample was not considered sufficiently stable as the plateau only extended over 25 °C. All other TL samples dated have plateaux extending over 50°C or more. The range demonstrated by WM3 was thought insufficient in terms of the relatively small number of traps represented within the 325-350 °C region of the plateau. The correlation coefficient of the additive growth curve is also very low (0.21) indicating a poor fit of the data to the linear regression. This would result in an unacceptable degree of uncertainty in the ED evaluation.

The IRSL age for WM3 however, agrees with the calibrated C-14 age range for the stratum. Forty percent of the IRSL age range falls within the C-14 age range for the deposit. The error in age determination is 28%. This is higher than the 20% 'limit' but when viewed in terms of the agreement between luminescence and independent chronology, the age is acceptable despite the error. The error is due mainly to uncertainty in the evaluation of past water content.

Samples WM4 and WM5 were both dated by TL and IRSL. In the case of WM5 both the coarse and fine grain fractions were dated by IRSL. WM4 was dated to 3090 ± 1430 BC (TL) and 3030 ± 1200 BC (IRSL). The age ranges are in close agreement as the IRSL age range falls entirely within the TL age range. However, both these ages are younger than the calibrated C-14 range of 6570-5844 BC for the deposit. The C-14 ages were based on material derived from hearths stratified within the sediment. The disparity represents a minimum of 1324 years between ages determined by the different techniques and is discussed in section 6.2.

Figure 6.1.2 Williamson's Moss age comparison



WM5 was dated to 8580 ± 860 BC (TL), 8740 ± 800 BC (IRSL fine grain) and 10180 ± 1040 BC (IRSL coarse grain). The TL age ranges falls within the fine grain IRSL age range demonstrating good agreement between the techniques. The IRSL age of the coarse grain fraction however is slightly older (1440 years) than the fine grain IRSL age. However, the younger age limits of the coarse grain age overlap the older limits of the fine grain age by 300 years (14% of the coarse grain age range). This demonstrated a wider disparity between ages than for the fine grain TL and IRSL ages. The possible reasons for this difference are considered in the discussion.

The error limits for the three luminescence ages are all around 10% of the age. This demonstrates a high degree of accuracy in the ages and reinforces the close agreement between the fine grain ages.

6.1.3 Stubb Place

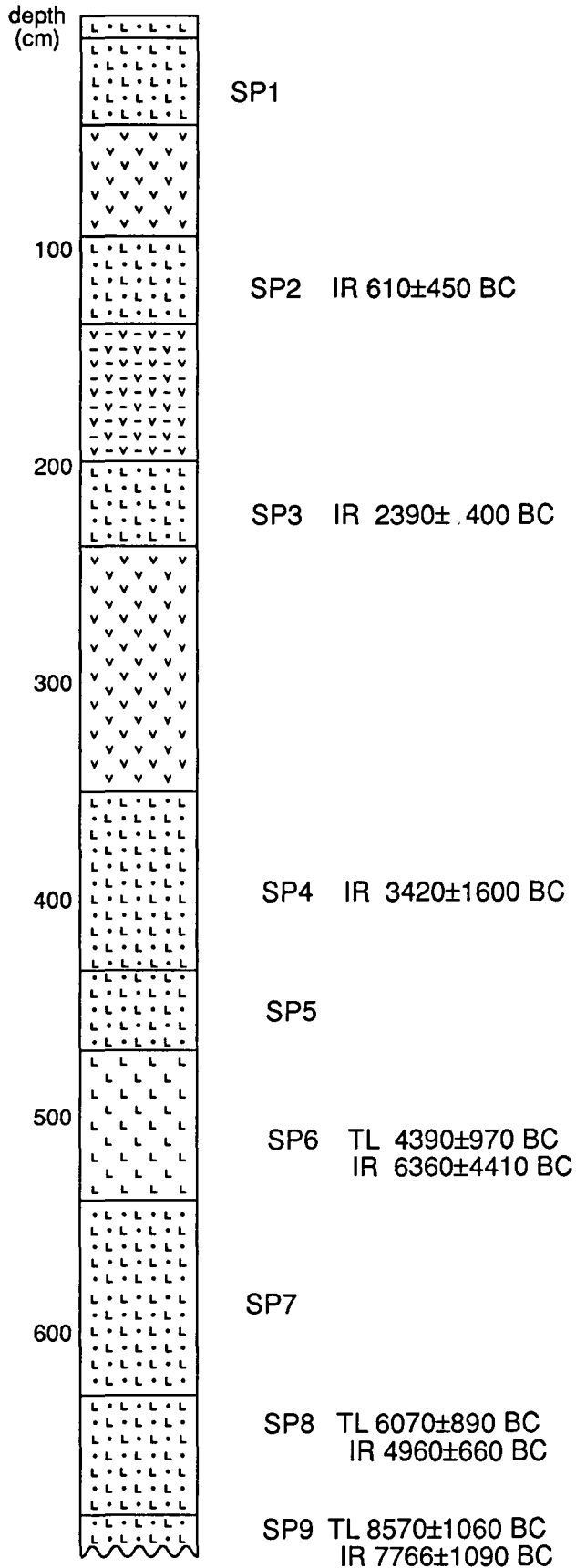
Nine samples were taken from this site as described in section 4.2.3. Six samples were dated by both luminescence techniques and three (SP1, 5 and 7) were rejected after initial measurements. There is no independent dating control for this sequence but the site is important as a test site for the application of luminescence to sediments of relatively 'unknown' age.

SP1 was rejected because of disequilibrium in the decay chain. Radon escape was detected during alpha counting, where the sealed-to-unsealed alpha count ratio was 1.12, indicating c.15% radon loss. There was also evidence of instability in the signal. The TL signal faded by 12% over 6 months, although the IRSL signal remained stable. The instability in TL emissions resulted in failure of the plateau test. The IRSL signal was of low intensity, giving 394 counts in the first second and a signal-to-noise ratio of 3.0. This is considered too low for accurate measurements.

SP2 was dated by IRSL only to 610 ± 450 BC (figure 6.1.3). The IRSL signal was stable over the test conditions and of sufficient intensity (signal-to-noise ratio of 5.6). The TL signal however failed the plateau test test indicating that instability or changes in sensitivity had occurred which did not affect the IRSL signal. The error in the IRSL age is 78%. This is primarily attributable to uncertainties in the evaluation of past water content. This is particularly important in samples from strata near the surface, such as SP2, which are exposed to seasonal variations in water tables.

SP3 was also only dated by IRSL, to 2390 ± 400 BC. This is stratigraphically consistent with the SP2 date. The error is less (58%) reflecting lower uncertainties in past water contents. The age range however, is still significant and overlaps the SP2 age range by 60 years, although the strata are separated by a peat. The TL signal of the stratum had a very short plateau, extending over a

Figure 6.1.3 Stubb Place age comparison



maximum of 25 °C. This is likely to represent too small a proportion of the total number of traps giving rise to the luminescence signal, as in the case of WM3. The short plateau indicates that only a small proportion of the traps giving rise to the signal are sufficiently stable for dating.

Sample SP4 was similar to SP3 in that it was dated by IRSL and the TL signal characteristics were similar. Here, the plateau was only 15 °C in extent. The IRSL age was 3420 ± 1600 BC. This date is stratigraphically consistent with the ages of the overlying strata. The error is less than for SP3, being 46% of the age. The age ranges of SP3 and 4 overlap by 1370 years, which is 42% of the age range of SP4, although these samples are separated by a peat stratum. However, the mean ages for the samples are stratigraphically consistent, and the age ranges are largely a function of the uncertainties in water content history.

Sample SP5 was rejected due to saturation of the TL and IRSL signals. This is demonstrated by lack of growth in signal intensity with added radiation dose. Saturated samples are usually either very old (ie. near to the limits of the luminescence age range) or they have not been bleached at deposition. Both TL and IRSL signals were saturated. This indicates that bleaching did not occur at deposition, as the IRSL signal which is very sensitive to optical bleaching was also saturated. Saturated samples cannot be dated because the time at which the onset of saturation occurred is not known. The onset of saturation is also accompanied by changes in the form of the growth curve, becoming sublinear.

SP6 was dated by TL and IRSL to 4390 ± 970 and 4410 ± 1120 BC respectively. These age ranges overlap and the TL age range falls entirely within the IRSL age range. The ages are also stratigraphically consistent with overlying strata. Both signals showed good stability and linear growth characteristics. The error on the dates are 22% for TL and 25% for IRSL, representing a higher degree of accuracy than that obtained for samples in the upper part of the sequence. Samples SP7 was rejected due to saturation of the signal, similar to SP5.

Samples SP8 and 9 were both dated by TL and IRSL. SP8 was dated to 6070 ± 890 BC (TL) and 4960 ± 660 BC (IRSL). The dates show some disparity between the different luminescence techniques. However, there is an overlap in the age ranges for each date of 33% of the IRSL age range and 24% of the TL age range. This is sufficient to demonstrate that within the levels of accuracy attained by the luminescence ages, there is agreement between TL and IRSL age ranges. In the absence of an independent dating control, these ages have given a timespan for the deposition of the stratum. The errors on these ages are 15% and 13% of the age for TL and IRSL respectively. This supports the agreement between the dates as the overlap between age ranges occurs within a relatively small range, compared to the age ranges evaluated for samples in the upper part of the sequence.

SP9 was dated to 8570 ± 1090 (TL) and 7760 ± 1060 (IRSL) BC. The IRSL age range falls within the TL age range, despite the difference of 810 years between the mean ages. These dates are stratigraphically consistent with overlying strata (see figure 6.1.3). The errors are low; 13% for TL and 14% for IRSL. It should be noted that there is a trend for decreasing error limits with depth for this sequence. This reflects the reduction in uncertainties associated with water content evaluation and can be seen in the falling proportion of the systematic (ie. non-random) error of the overall error with depth. The greater compaction and depth of the lower strata result in less seasonal variation in water contents.

6.1.4 Hartlepool Bay

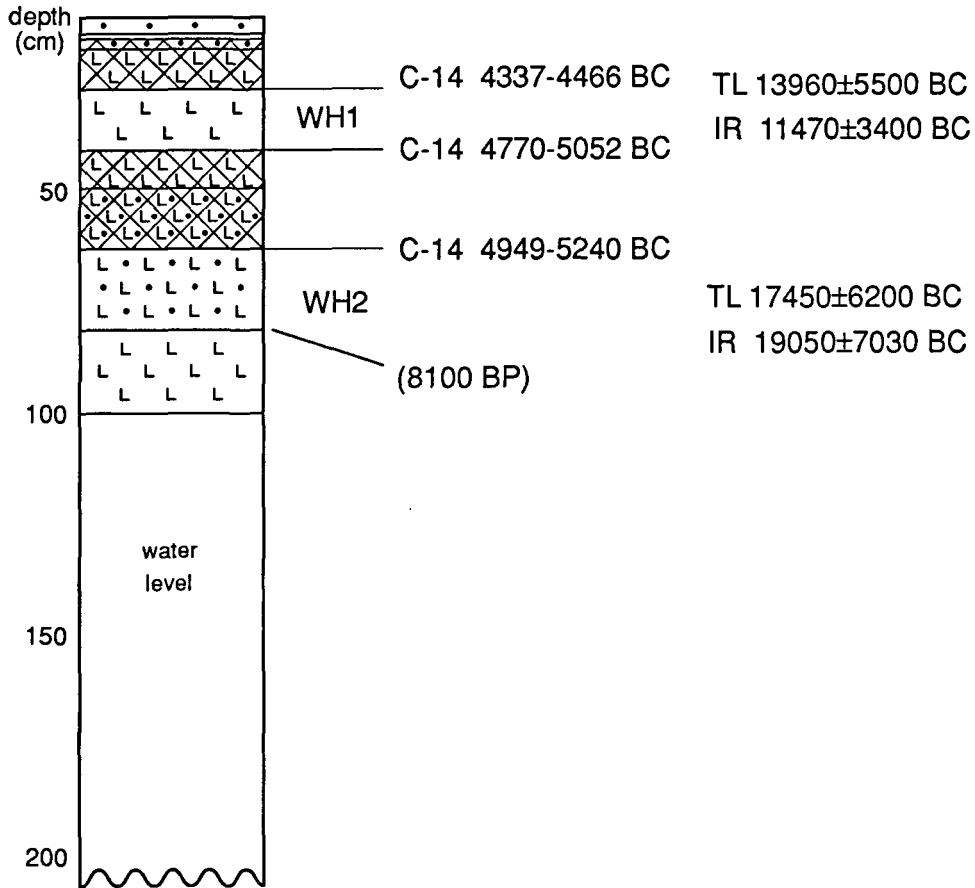
Two samples were dated from this sequence by TL and IRSL (see section 4.2.4). The dates for WH1 were 13960 ± 5500 (TL) and 11470 ± 3400 (IRSL) BC (figure 6.1.4). The dates for WH2 were 17450 ± 6200 (TL) and 19050 ± 7030 (IRSL) BC. These ages are stratigraphically consistent and for both samples the TL and IRSL ages agree. For WH1 94% of the IRSL age falls within the TL age ranges and for WH2 this overlap is 95%.

The significant degree of agreement between techniques indicates that these dates are acceptable as ages for the deposits. The errors however are 35% for TL and 37% for IRSL for both samples. The error is mainly derived from water content uncertainties.

The chronology based on calibrated C-14 dating however, demonstrates significant differences to that based on luminescence. WH1 is dated by C-14 to between 4770-4460 BC, which is 12835 years younger than the WH1 TL age and 14435 years younger than the IRSL age. WH2 is younger than 5240 BC based on calibrated C-14 dates and is thought to be the remnant of the Mesolithic soil surface from which artefacts were dated to around 8100 BP (uncalibrated; see Appendix A). Even bearing in mind the approximate age of the soil, the luminescence ages for WH2 are significantly older than the radiocarbon chronology implies.

This disparity is discussed in section 6.2. Suffice to say here, that the luminescence ages are as acceptable based on their error limits and the measurement criteria which were met, as the samples from other sequences in this study whose luminescence ages agree with the radiocarbon dates. This demonstrates the difficulties of using independent dating techniques as a comparative chronology where the methods are based on different materials and different events. Hartlepool Bay is an important example of this problem.

Figure 6.1.4 Hartlepool Bay age comparison



6.1.5 Hazendonk.

Three samples were taken for dating from the sequence described in section 4.2.5. Only one sample was dated. HAZ1 from the top of the sequence was rejected because of fading of the signals. The TL signal faded by 64% in 6 months at 18 °C while the IRSL signal faded by 60% under the same conditions. This fading component could not be removed by preheating. The IRSL signal intensity was also very low; the natural signal had a signal-to-noise ratio of only 1.4.

HAZ2 was dated to 3050 ± 1600 BC by TL and 2080 ± 1290 BC by IRSL. This is consistent with the C-14 ages for the underlying sediment (figure 6.1.4). However, no closer comparison is available for the luminescence ages. The agreement between the luminescence ages is good. The IRSL age range overlaps the TL age range by 75%, although the mean ages differ by 970 years. The errors are 52% for TL and 62% for IRSL. This high uncertainty is mainly due to water content variations. This is significant for near surface samples particularly those affected by drainage of the land surface as in the river dune area of the Netherlands.

Sample HAZ3 was rejected due to saturation of the signals, similar to samples SP5 and SP7 discussed in section 6.1.3 above.

6.1.6 Slingeland

Four samples were taken from the sequences described in 4.2.6. Only one sample was rejected for dating, SLG1. This was due to failure of the TL plateau indicating instability in the luminescence signal. The IRSL signal was also of low intensity, with only 206 counts detected in the initial natural signal. This gave a signal-to-noise ratio of 1.9 which is too low for accurate measurements.

SLG2 was dated by TL to 2200 ± 840 BC and by IRSL to 2320 ± 890 BC (figure 6.1.6). These ages overlap by 96% of the IRSL age range, indicating good agreement between dates. The lower age limit of the luminescence ages are however 300 years (TL) and 130 years (IRSL) younger than the calibrated C-14 age range. This difference may be accounted for by local variations in the dates of deposition of the peat and clay units on which the C-14 chronology is based. Possible erosion of interfaces may also be important although there is no stratigraphic evidence for this. The differences between C-14 and luminescence ages, however are not so great when comparisons are made of age ranges rather than dates themselves. Error in the luminescence ages are 38% due to uncertainties in water content.

SLG3 is a sandy layer within the clays of SLG2 and SLG4. The samples was dated by IRSL to 2940 ± 1170 BC. The TL signal was saturated and so could not be dated. This is an example of the

Figure 6.1.5 Hazendonk age comparison

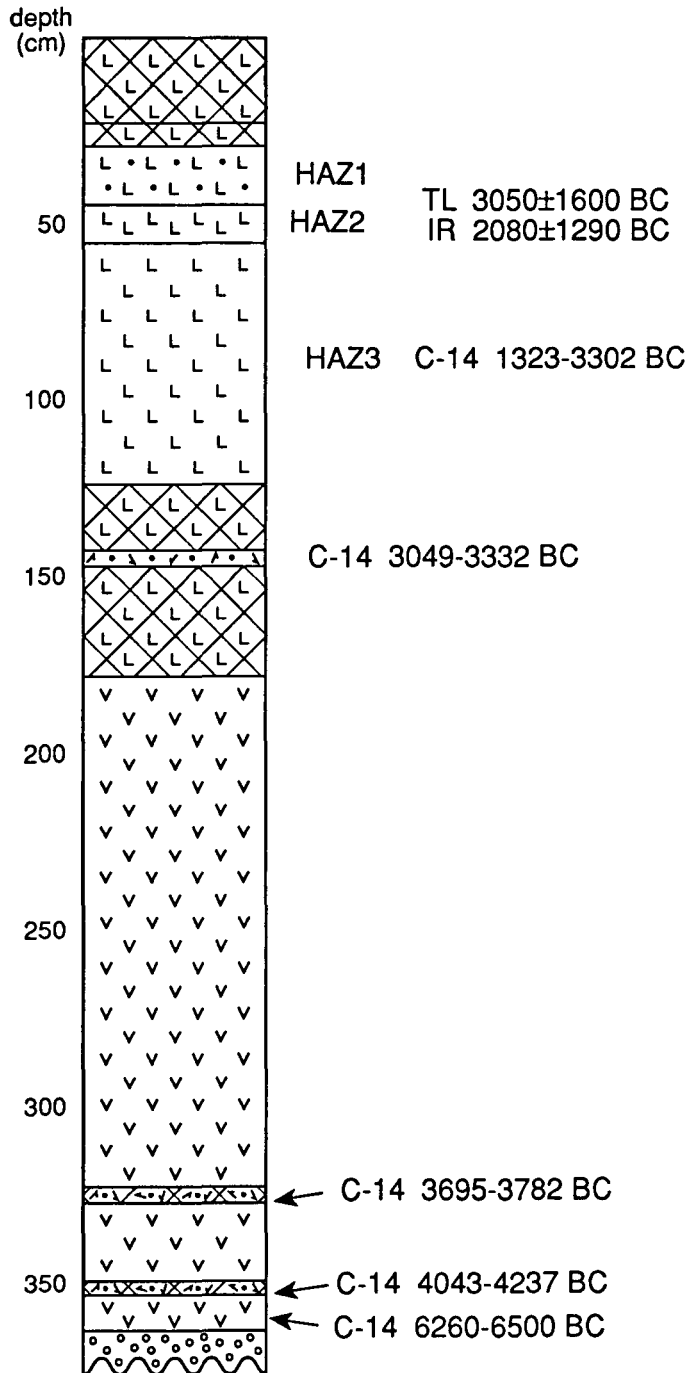
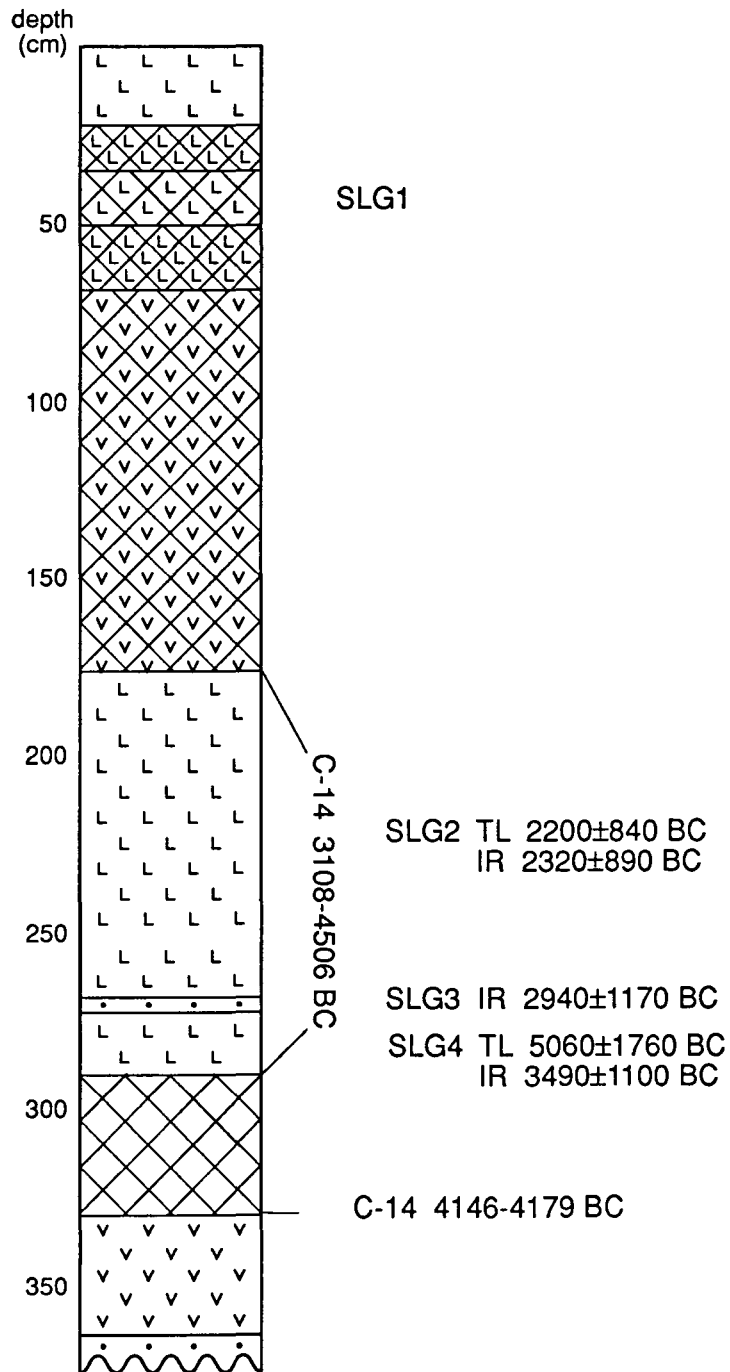


Figure 6.1.6 Slingeland age comparisons



importance of optical techniques for use in waterlain sediments where bleaching may be incomplete for the less sensitive TL signal. The IRSL signal was dated using the additive technique, and the comparison between additive and regeneration EDs demonstrates that the IRSL signal was fully bleached at deposition, despite the TL signal not having been bleached. The error in the IRSL age is 40%, again due to the water content uncertainties. The IRSL date, however, is younger than the C-14 determined range for the deposit by 400 years. The older age limits overlap by 770 years (33% of the IRSL range). The age ranges are in some agreement therefore, even though the actual dates differ.

SLG4 is a sample very similar in physical characteristics to SLG2. It was dated by TL to 5060 ± 1760 BC and by IRSL to 3490 ± 1100 BC. The overlap in age ranges is 59%, indicating good agreement between dates. However, the IRSL age is 1570 years younger than the mean TL age and falls within the C-14 age range where the TL age range does not. The age range of the TL date, however, does overlap the C-14 range by 30% (1070 years) and therefore is in some agreement with the C-14 age, but less so than for the IRSL date. The errors in the TL and IRSL ages were 35% and 31% respectively.

6.2 DISCUSSION

Seventeen out of 27 samples were dated successfully, of which only two (WH1 and 2) differed significantly from the predicted age range based on radiocarbon. Agreement between IRSL and TL ages was good with varying degrees of overlap in the respective age ranges. The main factor affecting accuracy of the dates was the uncertainty relating to past water content history.

The comparisons between luminescence techniques and radiocarbon dating was based on age ranges rather than mean ages. For the purposes of this study such a basis for comparison was considered more appropriate, particularly where different techniques based on different materials are under consideration. The calibrated C-14 dates are given as age ranges from the calibration programme. It is important to include the error limits in considering a date, and this is better done using the age range for comparison. The comparison between techniques based on age ranges also allows the degree of overlap in the age ranges to be assessed.

6.2.1 TL versus IRSL versus C-14

The samples demonstrate good agreement between TL and IRSL ages. Figures 6.2.1, 6.2.2 and 6.2.3 illustrate the close agreement obtained between TL and IRSL ages and C-14 age ranges. The correlation coefficients for the plot of TL against IRSL was 0.977, indicating a very high degree of correlation between the two luminescence techniques. This is important as they are based on

Figure 6.2.1 Plot of IRSL ages against TL ages where data is available, demonstrating good correlation between the ages.

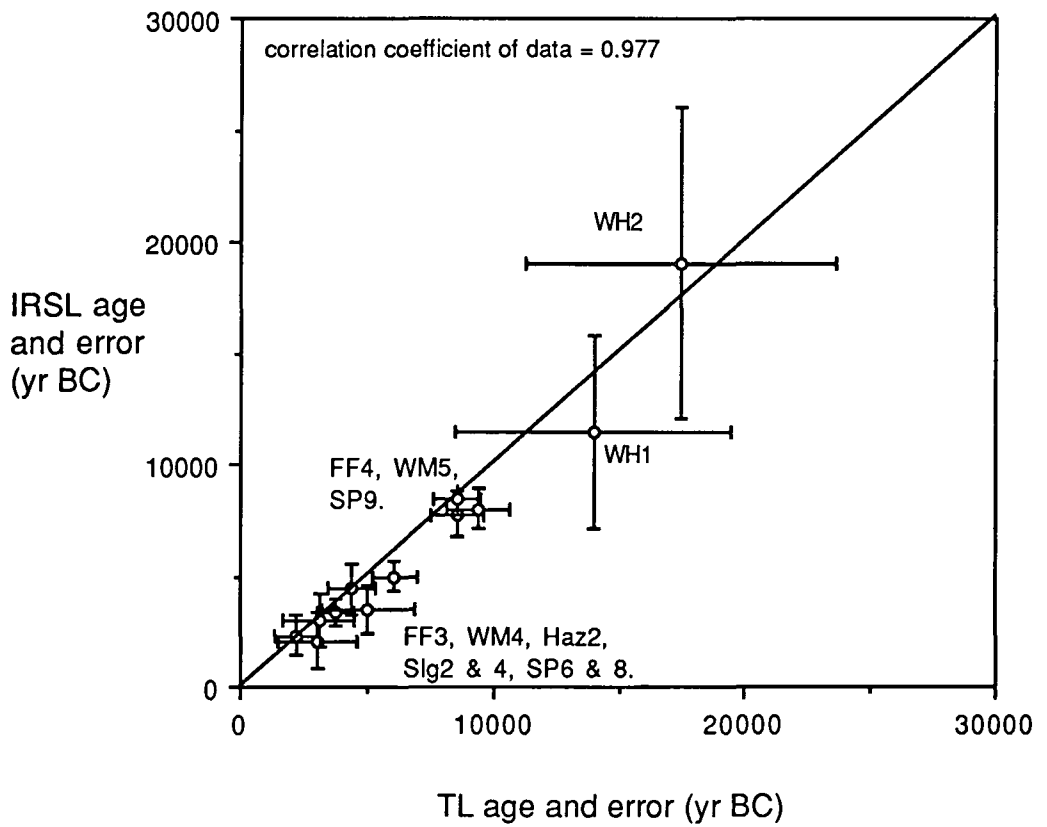


Figure 6.2.2 Correlation between calibrated C-14 and TL dates, where direct comparative data is available.

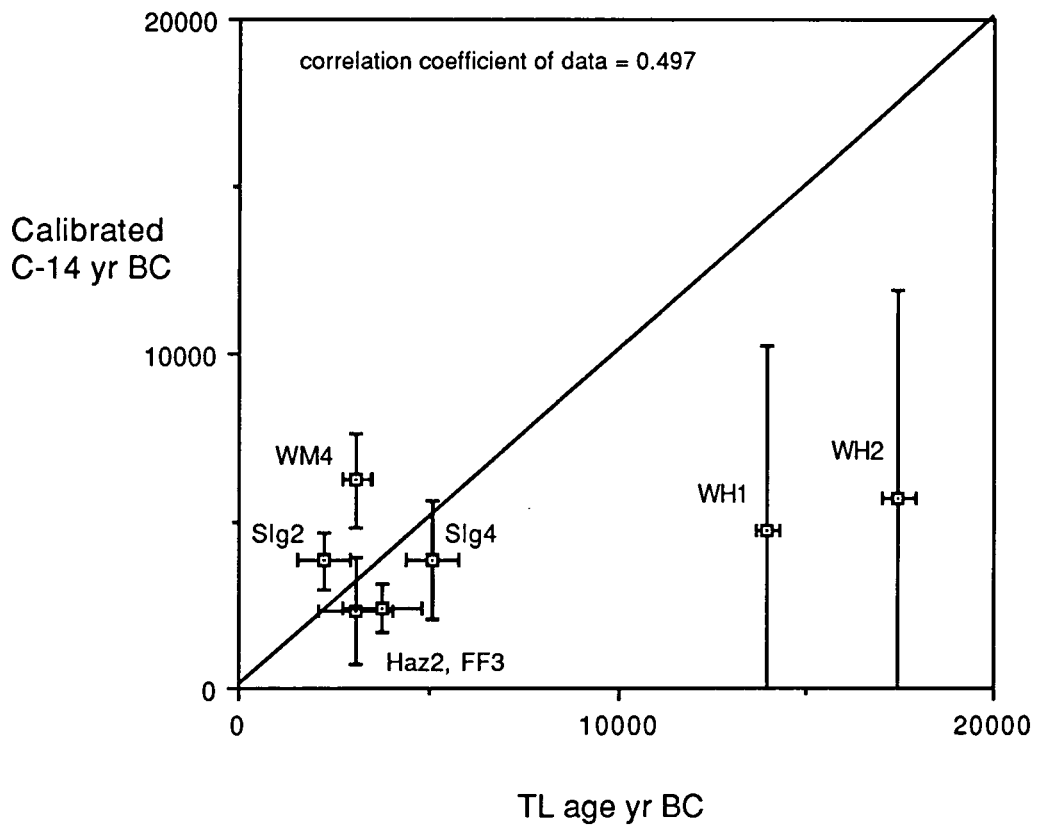
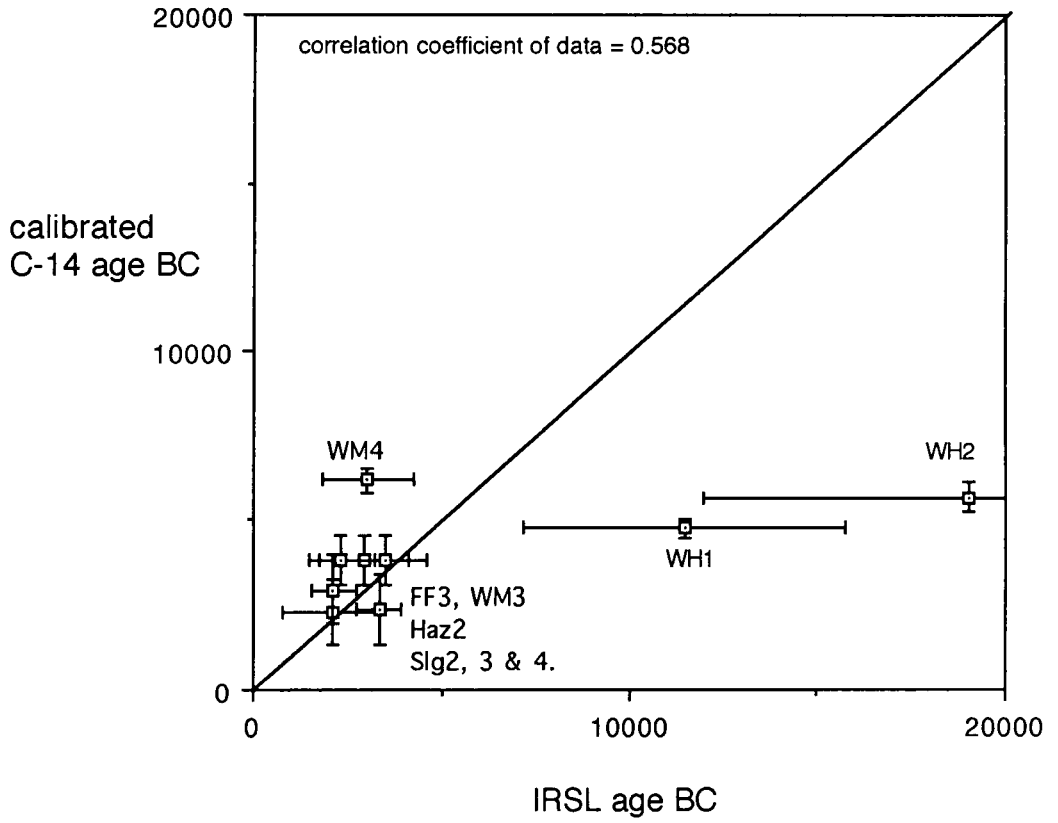


Figure 6.2.3 IRSL ages plotted against calibrated C-14 ages, where data is available



different physical principles so direct comparison between TL and optical techniques has been questioned. The data here indicate that the techniques appear to be comparable. The correlation between TL and C-14 and IRSL and C-14 is less close ($r=0.497$ and $r=0.568$ respectively). However, the trend in the data is largely that of agreement. The problems in the comparison of different dating techniques based on different material is discussed below.

Both luminescence techniques therefore have been shown to be appropriate for dating primarily waterlain sediments of Holocene age. The differences between TL and IRSL ages for individual samples are generally relatively small. The proportion of overlap in the age ranges for these techniques ranges from 25-100%. For the degree of accuracy of the mean ages this may be considered to indicate that the techniques are in overall good agreement. The TL dates are generally slightly older but this effect is not of great importance here.

It is however, worth noting that in other studies of comparisons between TL and OSL/IRSL ages the TL ED's are generally older than the optical ED's (Li and Aitken, 1989; Duller, 1992). Li and Aitken (1989) attribute this difference to bleaching of the optical signal during sampling, incomplete bleaching of the TL signal at deposition or lack of stability of the OSL signal. The last of these possibilities is unlikely for sediments in this study. The optical signal showed no signs of instability in dated samples. The problem of incomplete bleaching of the TL signal may be difficult to detect. However, in many samples studied here, the difference between TL and IRSL ages was negligible. This indicates that in using a total bleach technique for determination of the residual level, the TL signal must have been fully bleached at deposition of the ages would not be in such close agreement. It is possible that this problem could account for differences in ages for example in the case of WM4.

The possibility of bleaching of the sensitive optical signal during sampling and treatments is a problem which is difficult to identify. The samples were taken under sealed conditions during coring and no exposure to white light occurred. Within the laboratory, exposure to the red light conditions was kept to a minimum. In only two samples the overlap in age ranges was less than 50% (TL and IRSL for FF4 and the IRSL coarse and fine grain ages for WM5). This demonstrates that differences between the techniques was of minor importance for samples in this study.

Duller (1992) compared the TL and IRSL EDs of K-feldspars from dune sands and found no significant differences although the regeneration EDs were consistently higher, but within the error limits of 10%. Duller does, however, point out that this agreement between EDs does not imply that the EDs themselves are correct. For samples in this study, however, the agreement of the ages with each other and with independent chronologies suggests that the EDs are correct, and that any differences in ages falls largely within the error limits of the ages.

There are however, a few cases where this is not so. For example, the IRSL ages of the coarse and fine grain fractions of WM5 differed to the extent that only 14% of the age ranges for these dates overlapped. This may be due to differences in the bleaching of coarse and fine grain fractions arising from different conditions of transport and deposition. The coarse grain fraction may have been carried under deeper water conditions or otherwise exposed less to the bleaching source. In this case, laboratory overbleaching to a negligible residual level may have occurred resulting in a higher ED. However, the length and conditions of exposure to laboratory bleaching sources for the fine and coarse grained material were identical. It may be that the coarser fractions have a different degree of sensitivity to optical bleaching, such that the fine grain fraction bleached faster both in the natural and laboratory conditions and under IR stimulation.

Differences between C-14 and luminescence ages are generally easier to explain. For WM4, the TL and IRSL ages are in very close agreement (100% overlap) but both ages are younger than the C-14 age range by a minimum of 1324 years. The luminescence dating samples are from a sandy deposit representing the minerogenic remnants of an ancient soil and the radiocarbon measurements are based on charcoal and wood from hearths stratified within the deposit.

A number of explanations may be evoked to account for this difference. The radiocarbon dates may in part be based on old wood which was burnt on the hearth, thus making the radiocarbon ages older than the real age of the hearth. The luminescence ages may reflect a later period of exposure to sunlight which occurred during erosion of the soil material leaving the sandy lag deposit in the channel.

The luminescence samples were taken from the middle of the deposit, at a level enclosed by the radiocarbon chronology. However, local differences in erosion and exposure of the soil material may have resulted in variation in bleaching of the sediment both laterally and vertically. The samples were taken from the same stratum in which the hearths were dated, but not at the time when the hearths were excavated. This illustrates an important problem in dating material from archaeological sites where samples are not taken from the site at the time of excavation. Local variations in the sediment sequence and in its depositional history can result in such differences illustrated by WM4 and the Hazendonk sample where the ages of the clay deposits are based on cores and dates which may not exactly match the sequence from other, nearby cores.

The case of Hartlepool Bay stands out as another example of the problems of comparison of ages based on different techniques and materials. The luminescence ages for this site are in close agreement (with overlaps in the age ranges of 94% and 95%) but the ages are much older than predicted based on the C-14 chronology. The difference is between 14435 and 12835 years. For

WH1 it is likely that the age of the minerogenic deposit is related to a previous bleaching event to that of its present context. However, if the sediment had been partially bleached during deposition in its present context, the use of the additive and regeneration techniques based on a total bleach may have been inappropriate.

The sensitivity of the luminescence signals to optical bleaching under filtered light was such that the IRSL signal bleached to negligible levels within a very short space of time (c.15 mins.) The TL signal was bleached down to the residual level within 2 hours. Therefore if limited exposure occurred before burial, it would be expected that the IRSL signal would be more completely bleached and hence give rise to a lower ED than for the partially unbleached TL signal. In both samples, the agreement between IRSL and TL is so close that this case seems unlikely. It is probable that the sample was fully bleached at a time indicated by the luminescence date, which was not the depositional event in the present context.

Sample WH2 consists of the minerogenic remnant of a mesolithic soil, Artefacts from this soil have been dated by radiocarbon to 8100 BP (uncalibrated date; see section 2.3). The luminescence ages indicate an age for the sediment predating this. The sediment may contain material eroded from the soils and the underlying weathered boulder clay. The close agreement between IRSL and TL ages argues against bleaching of only the IRSL signal at deposition. However, the radiocarbon dating of stratified artefacts is problematic as the origin of the material and the point in time at which it became incorporated in the sediment is often unknown. Therefore this does not provide a tight comparative chronology for this sediment, even if it could be calibrated.

The luminescence ages for WH1 and 2 need to be accepted as correct dates for the last exposure of these samples to sunlight. That this may not represent the event during which deposition in the present sequence occurred. This again stresses the difficulties in 'proving' the viability of one technique by comparison with a chronology based on another. Merely because the dates do not comply with expectation, is no basis on which to reject them. They need to be accepted with the same confidence as dates which do happen to fit into existing chronologies, as the method and criteria for age and error evaluation and criteria for acceptance are the same for all samples.

The Stubb Place test site is an excellent example of the potential of luminescence dating for sedimentary sequences of Holocene age. This sequence has no existing chronology, but this has been provided by luminescence dating. The ages determined by TL and IRSL have produced a stratigraphically consistent chronology where the two techniques agree where they have been applied to the same sample. Therefore, the establishment of an absolute chronology for previously undated material demonstrates the viability of the technique.

6.2.2 Accuracy of luminescence dates

The errors in luminescence age determination are divided between random and systematic errors (see 5.2.5). The greatest source of uncertainty is that relating to the evaluation of past water contents. This is a significant problem for samples which are uncompacted and which lie in the upper part of sediment sequences and are therefore exposed to greater variations in seasonal water contents.

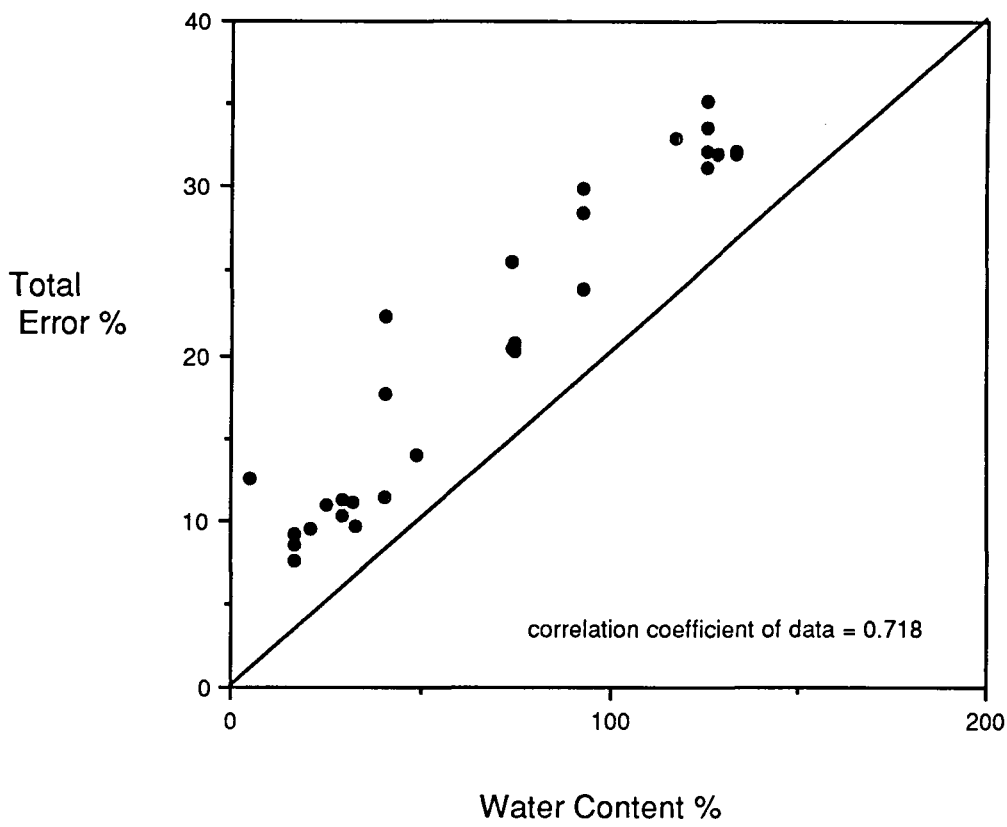
Figure 6.2.4 shows the close relationship between the water content of the sample and the overall error. However, it should be stressed that it is the uncertainty in the water content variation which is the source of error, not the water content itself. In these samples, samples with higher water contents were often those nearer the surface and subject to greater uncertainties. This is also demonstrated by Stubb Place where the overall error falls systematically with depth, and at the same time the random error component becomes relatively more important as the error associated with water content is reduced. This primarily a result of compaction of the lower lying sedimentary units and of a reduction in the effects of water table fluctuations on the water content.

The errors in the dates range from 11.2% to 52.4% of the TL age and 9.4% to 73.8% of the IRSL age. In most of these cases, samples with errors greater than 20% (19 out of 30 dates) this is primarily due to the water content uncertainties described above. This therefore is the greatest obstacle to increasing the accuracy of the luminescence ages particularly for waterlain material. However, even for the dates with error limits of greater than 50% (4 dates) the luminescence date has provided an absolute date for that sediment even if the accuracy is severely affected by water content related errors. This is important where sediments may not be dateable by any other technique.

Other sources of error, such as errors in calibration of sources, measurements and ED evaluation are less important. The correlation coefficient of the fit of the additive growth data to a weighted linear regression curve for all samples dated was >0.84 . Samples with correlation coefficients >0.9 demonstrated a lower uncertainty in ED evaluation due to the improved fit of the data. However, no samples were dated which demonstrated a poor fit of the data to the regression curve.

Finally, an observation concerning the a-value of the samples. The a-value is a measure of the relative efficiencies of alpha-to-beta radiation (see chapter 5 and table 6.1). The causes of differences in a-values between TL and optical techniques has not yet been explained. The definition of what constitutes an 'acceptable' a-value for a sample has not been determined by luminescence workers. For dates in this study the TL a-values were slightly higher than the IRSL values, but the significance of this is not yet known. Other workers, such as Questiaux (1989) observed similar trends but these were not explained. There is not consistent relationship between

Figure 6.2.4 Total error versus water content for all samples



a-value and technique, mineralogy or grain-size but this is not necessarily to be expected as the relative efficiencies of alpha and beta radiation and the a-value is based on physical processes operating within the crystals which are not wholly related to characteristics of the mineral grains. It is however, an area worthy of further investigation.

6.3 Conclusions

The application of luminescence dating has been demonstrated to have been successful for waterlain and archaeological sediments of Holocene age. Both IRSL and TL techniques have proved to be suitable for such applications. In all cases agreement between different luminescence techniques was good which suggests that the use of TL and optical techniques could be used in conjunction in order to increase the confidence that can be placed on the results if this is thought necessary. This agreement is important as it demonstrates that the techniques are dating the same event to similar degrees of accuracy despite the fact that each technique has a different physical basis (see section 5.2).

Agreements between C-14 and luminescence age ranges is generally good, except in the case of Hartlepool Bay and to a lesser extent WM4. The differences in the age ranges for these cases is explained on sedimentological grounds by differences in the type of material and event that the different techniques are based on. The luminescence dates which do not agree with the C-14 chronology should not be dismissed as 'wrong' because they are evaluated in the same way as those dates which do match the C-14 chronology. It is important, however, to identify the types of event and sedimentological processes which may affect the bleaching of luminescence signals. It is also important to assess how appropriate for comparison are the C-14 dates on which the established chronology is based. In the case of WH2, where the C-14 age is based on an antler incorporated in the sediment, ^{these are} problems relating to the derivation of the antler and the length of time elapsed between shedding and incorporation in the ancient soil at that position. In this case, the luminescence date may be more reliable than the C-14 date for the deposit.

The success of the Stubb Place test site has shown that both TL and IRSL techniques can provide a stratigraphically consistent chronology for undated sediments. In this case IRSL provided a greater number of dates and is likely to be a more suitable technique for waterlain sediments.

The water content is the greatest obstacle to accuracy in luminescence dates. This is largely unavoidable where samples are derived from unconsolidated sediments which are affected by significant fluctuations in water content. This uncertainty is reduced for compacted sediments which are not exposed to such variations, and is demonstrated by the systematic reduction in the error of the Stubb Place samples with depth.

The advantages of IRSL over TL lie in the fact that it is more sensitive to sunlight bleaching, so under conditions of attenuated sunlight such as underwater, the minerals are more likely to be bleached in terms of their optical signal than their TL signal. For samples in this study, however, saturation of the signal occurred for both TL and IRSL signals (HAZ3, SP5, 7). IRSL dating of the upper Stubb Place samples (SP2, 3 and 4) was by IRSL only as the TL signal was shown to be unstable. The IRSL signal also bleached down to negligible residual levels, and therefore problems with charge transfer caused by use of inappropriate bleaching sources in the laboratory can be easily detected. Such effects may not be detected in the case of TL.

Both IRSL and TL techniques have been shown to be viable and potentially very important methods of establishing absolute chronologies. The techniques are applicable to a wide range of sedimentary material which may not be dateable by other methods such as radiocarbon. Luminescence dating is an absolute technique so is not affected by problems such as the calibration of radiocarbon dates. The age range is from approximately 0 to around 200 000 years, completely overlapping the radiocarbon age range.

CHAPTER 7 SIGNIFICANCE OF CHEMICAL WEATHERING OF FELDSPARS AND IRSL

In the analyses of the relationships between luminescence dating and sediment characteristics of samples in this study, several trends emerge. These trends form the basis of the grouping of samples into three categories which are discussed below. The relationships between sediment and luminescence characteristics are primarily connected with chemical weathering of the feldspar grains. The processes of feldspar weathering are discussed below. An experiment was conducted to test the observed relationships between weathering and luminescence characteristics, and the implications for dating are discussed.

7.1 Relationships between luminescence and sedimentology

Three types of sample could be recognised, which are discussed individually below, and outlined in table 7.2.1 as groups 1, 2 and 3. These groups form the basis of conclusions relating to the relationships between luminescence and sedimentology.

TABLE 7.2.1 Summary of characteristics of designated groups of samples.

Characteristic	Group1	Group2	Group3
Appearance of mineral grains	Clean faces, no adherent flakes unweathered	clean faces some adherent flakes some weathering	abundant adherent flakes severely weathered
Dominant clay minerals	Kaolinite	kaolinite/illite	illite/montmorillonite
Mixed layer clays	Rare	some present	abundant
Stratigraphic position	deep/middle	deep/middle	surface
Luminescence intensity	high (IRSL Signal:noise = <4.0 for low signal samples)	high or moderate	low
Growth characteristic	linear ($r > 0.8$)	linear ($r > 0.8$)	erratic ($R < 0.8$)
Fading	none	none	severe

7.1.1 GROUP 1.

These comprise all those samples which were dated by either technique. These nine samples were FF4, WM4, WM5, WH1, WH2, SLG3, SP6, SP8 and SP9. These samples also possessed certain sedimentological characteristics; the feldspar and quartz grains were unweathered, in a good state of preservation, and grains were clearly defined (figure 7.1.1). There were only small amounts of clay coatings adhering to the grain surfaces, and a low occurrence of mixed-layer clays. The identified clay minerals were dominated by kaolinite, which is a 1:1 clay mineral with a low cation exchange capacity (CEC) and the stable end-product of K-feldspar breakdown.

7.1.2 GROUP 2.

This group included samples which had been dated, but which contained mineral grains in a partial state of degradation. The samples were FF3, WM3, HAZ2, SLG2, SLG4, SP2, SP3 and SP4. The grains, primarily quartz and feldspar, had some of the characteristics of weathered material such as etch pits and delineation of cleavage planes. There was a higher proportion of adhering clay flakes forming discontinuous coatings on some grains. The clay minerals were again dominated by kaolinite, but with a higher proportion of illite in several samples. Illite is a transitional product of weathering. There was a low abundance of mixed-layer clays.

The grains in some samples had been exposed to a weathering environment at some point in their history, but in their present environment, the continuous process has been interrupted by prevailing equilibrium conditions. Depositional structures such as fine laminations were well preserved in some of these samples in contrast to the samples from the subsequent group. This equilibrium situation could arise from a reduced water percolation rate, which would result from fine-grained material being closely packed or slightly consolidated. Reduction in water flow restricts the primary agent of chemical weathering.

7.1.3 GROUP 3.

These samples were characterised by those which could not be dated for reasons other than saturation of the luminescence signal. The samples were FF1, FF2, WM1, WM2, HAZ1, HAZ3, SLG1, SP1, SP5, SP7. These were affected by fading, weak signals and changes in sensitivity. These samples contained a high proportion of severely degraded feldspar. The quartz, being more



Figure 7.1.1 SEM of sample WM5, an example of clean grains, unaffected by chemical weathering or clay coating. (x500; WD 7 mm; 1 cm = 15 μ m)

resistant, was less affected. However, the quartz signal is not stimulated by IRSL and is less sensitive to attenuated sunlight bleaching, so it is a less suitable mineral in these circumstances.

The clay minerals were dominated by illite, smectite and montmorillonite groups. The former are 2:1 expanding lattice clays with higher CECs than kaolinite. They are more unstable in weathering environments, and easily altered. They are transitional products of feldspar weathering. Illites form when only partial removal of potassium in solution has occurred (see Chapter 3).

There was a high abundance of flaky clay coatings, forming discontinuous coverings of the grains. They may comprise a significant proportion of the mixed-layer clays, and are difficult to remove by sonication. The flakes form from alteration of the feldspar surface. The grains themselves were heavily etched and pitted. This is shown for sample FF2 in figure 7.1.2.

Stratigraphically these samples were in most cases those nearer the surface than those from groups 1 and 2. The distribution of organic matter, and soil-type features suggest active pedogenic processes in the B soil horizons, or those affected by free percolation of ground waters. This relationship between weathering processes, environment and luminescence is explored more fully below.

7.1.4 Significance of categories

The importance of the identification of the three groups of samples given above lies in the fact that it underlines the underlying cause of the failure to date a proportion of the samples in this study. The groups demonstrated a close connection between the physical appearance of mineral grains, the clay mineral content of the samples and the success of the luminescence dating. Samples which could not be dated are derived from strata which are undergoing active pedogenesis and feldspar weathering. Samples which at some time in the past had been exposed to chemical attack, but in their present context are no longer undergoing chemical alteration, were dated to a similar degree of accuracy as those samples showing no signs of alteration.

This distinction between 'active' and 'interrupted' weathering is significant and may have an important bearing on the identification of 'dateable' samples in the field. This may save significant amounts of laboratory measurement time, and aid the selection of potentially the most suitable samples for dating. However, it is also important to explain why the action of chemical weathering should affect feldspars in this way as it is highly relevant in terms of the intensity of luminescence signals and the stability of the trapped charge which gives rise to the emissions used for dating.

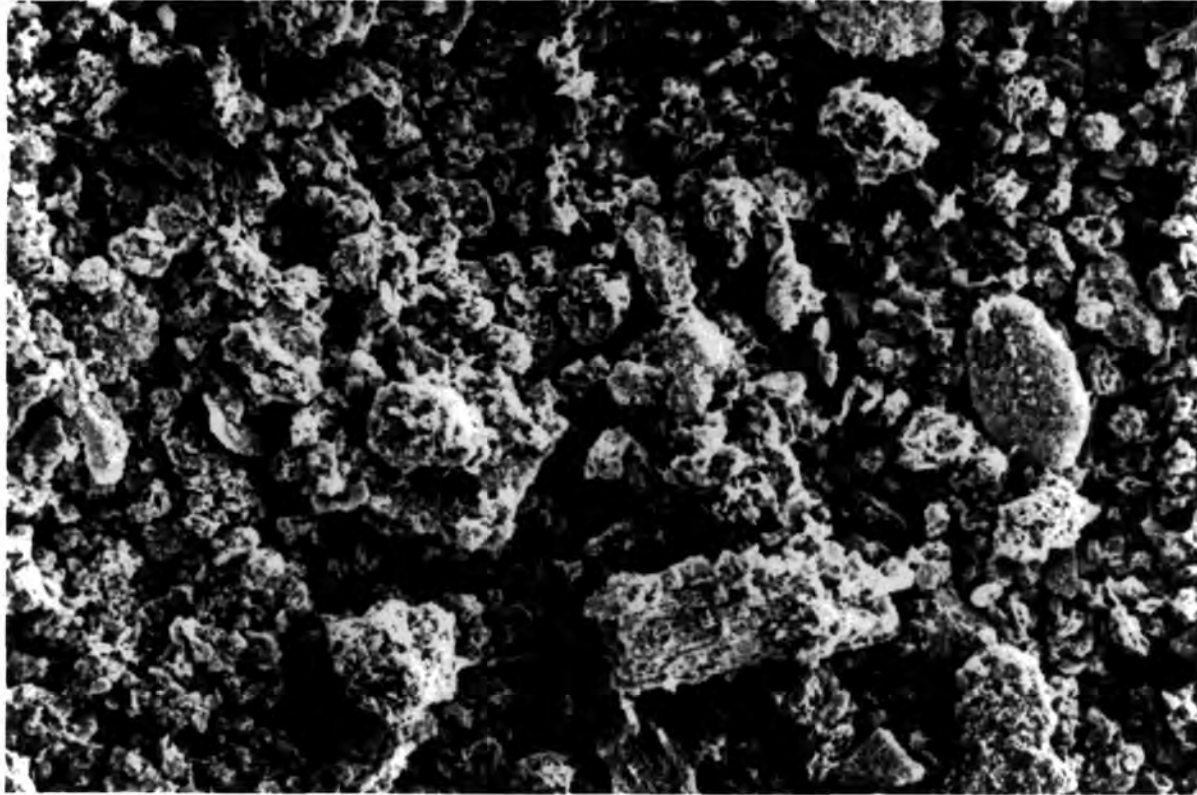


Figure 7.1.2 SEM of sample FF2, an example of weathered grains showing the characteristic 'woolly' appearance of grains caused by erosion of the surface and clay mineral formation. (x500; WD 7 mm; 1 cm = 15 μ m)

7.2 Structure of feldspars

Feldspar minerals are constructed of SiO_2 tetrahedra in which all the oxygen atoms are shared, forming a stable structure. The incorporation of cations can only occur by replacement of Si by Al in proportions of one in four up to a maximum of one in two atoms. A number of feldspar groups exist based on their cation content. The alkali feldspar group included the potassium feldspars (KAlSi_3O_8) which are important minerals for dating. Examples of potassium feldspars include sanidine, microcline and orthoclase, which all differ in their crystal form. Plagioclase feldspars include the sodium ($\text{NaAlSi}_3\text{O}_8$) and calcium ($\text{CaAl}_2\text{Si}_2\text{O}_8$) feldspars which are known as albite and anorthite respectively. The group contains a number of variations based on the relative proportions of albite and anorthite.

The optical properties of feldspars are variable and each type is associated with different luminescence emission wavelengths, intensities and stabilities. The sodium and potassium feldspars are the most important for dating (see chapter 5). All feldspars possess good cleavage parallel to their basal plane which is important with respect to the weathering of these minerals.

7.3 Weathering of feldspars

Weathering of feldspars is of significance to this project as the feldspars are the minerals most widely used for luminescence dating, particularly in the case of IRSL. Some detailed consideration of the weathering of feldspars is therefore relevant to this study, because chemical or physical alteration of the grains may affect their stability with respect to trapped charge, as well as the size and mineralogy of grains available for dating.

The weathering of feldspars proceeds by ion-exchange and dissolution. Removal of soluble cations and replacement with ions of lower valency within the Si-O_2 lattice alters the chemical composition and nature of the defects in which trapped charge may be held. The clay minerals formed depend on the rate of change and the available ions. Orthoclase breaks down into illite or muscovite and releases soluble silica. Illite is ill-defined chemically (Blatt, 1982; 29) but has slightly less potassium than muscovite. Both minerals are further altered to kaolinite. Kaolinite is the end-product of feldspar alteration, and has a low cation-exchange capacity, being chemically stable.

If the type of clay minerals present can be identified, the cation-exchange capacity of the sediment can be estimated. In conditions of chemical disequilibrium this gives an indication of the sediments' propensity for change. An example of the chemical transformation of albite with the formation of kaolinite is given below:



Two mechanisms are thought to explain the rate and form of the dissolution process. Correns and von Engelhart (1938) introduced the concept of a protective surface layer as the system which regulates the rate of dissolution. This is supported by studies such as those of Wollast (1967) and Helgeson (1971). The formation of a layer depleted in Si and cations, and which thickens with time was thought to be the factor causing the fall off in the rate of dissolution with time, and linear increase in released elements. It also accounted for the greater quantity of Si and cations such as Na, K and Ca in solution, compared to Al, relative to the composition of the parent material and has yet to be observed in the natural state (Berner and Holdren, 1977, 1979; Holdren and Berner, 1979).

An alternative theory explaining the results of Petrovic (1976) and of Lagache (1965, 1976) is that there is no coating or that it is not a protective one. Petrovic concludes that the coating of precipitate, if formed, does not limit the diffusion rate through it. Berner and Holdren (1979) support this idea as an explanation for the observed parabolic rate of dissolution with time, the lack of uniform coatings on grains, and the ease with which much of the coating can be removed by soneration in an ultra-sonic bath. If it does occur, the coating may take the form of amorphous alumina material, thereby accounting for the relative paucity of Al in solutions. XPS (X-ray photoelectron spectroscopy) analysis indicated that the surfaces of grains without apparent coatings were not significantly different in composition compared to the inner grain. The clay coatings, however, were of very different composition to the feldspar, but similar to coatings deposited on quartz grains. This may be explained by selective translocation of material by percolating waters. Finally, the coatings were seen to crack on drying, indicating a permeable nature, which could not therefore serve as a barrier to diffusion (Berner and Holdren, 1979). Such coatings are illustrated by sample WM1 in figures 4.2.5, 4.2.6 and 4.2.7.

Further investigations of the altered layer on the surface of weathered feldspars (Casey et al. 1989a) demonstrate that an amorphous, Si and H enriched coating, depleted in Al, Ca and Na, forms in environments of pH < 4.0. An increase in pH is marked by an increase in H in the layer. However, this does not penetrate beyond the outer few units of feldspar (Casey et al 1989b). The thickness of the altered layer depends on the pH of the reactant (Muir et al, 1989, 1990) with the thickness increasing in proportion to pH. Feldspar type is also relevant, and the thickness of the layer increases from a few 100's Å to many 100's Å in the order albite < oligoclase < labradorite < bytownite. This emphasises the central role of hydrolysis in the initial weathering process.

Microscopic evidence of dissolution is provided by the development of highlighted twinning, such as distinctive cross-hatching on microcline. Later evidence includes the formation of prismatic etch pits and cracks along dislocations and defects (figures 7.3.1 and 7.3.2), or 'sites of excess energy' (Berner and Holdren, 1979). These pits enlarge and coalesce, forming a honey-comb like structure,

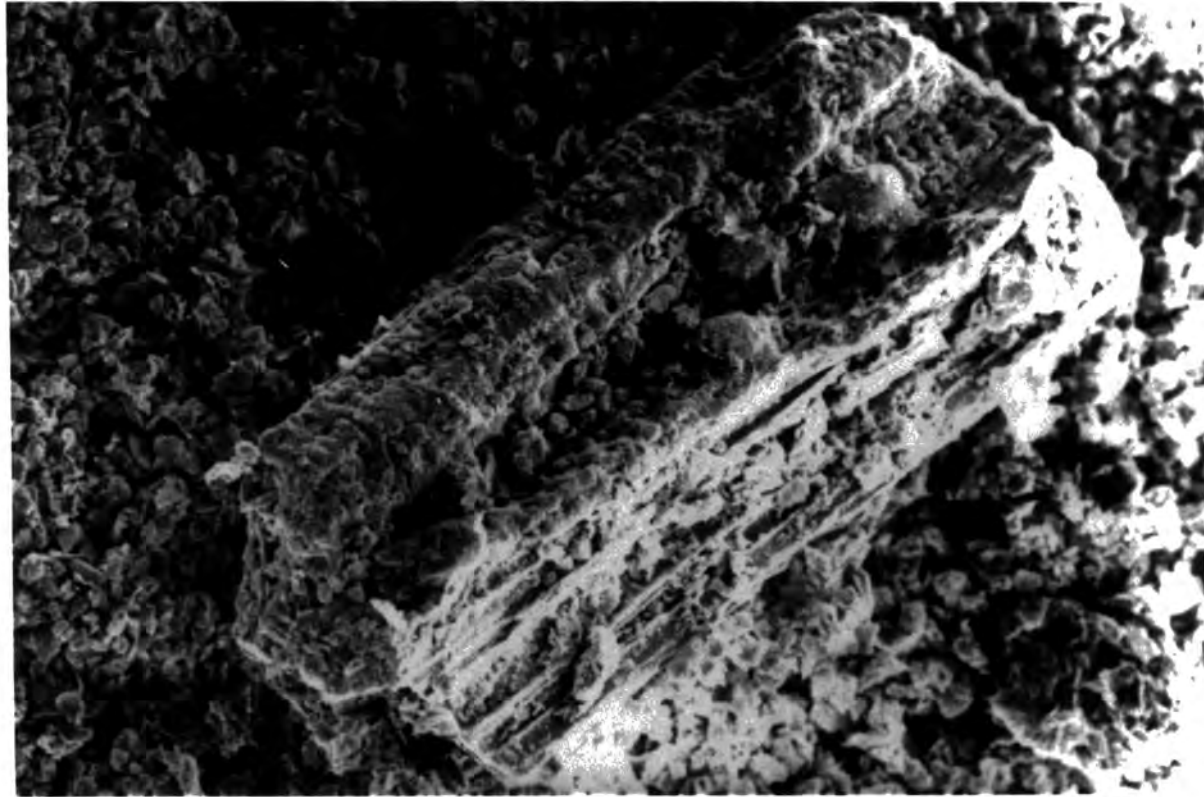


Figure 7.3.1 Mineral grains from sample FF2 demonstrating etching of cleavage planes by chemical weathering. (x500; WD 6 mm; 1 cm = 15 μ m)



Figure 7.3.2 Mineral grains from sample FF2 demonstrating formation of etch pits by chemical weathering. These will eventually coalesce and fragment the grain. (x2000; WD 6 mm; 1 cm = 3 μ m)

which is easily fragmented into finer feldspar grains. Laboratory simulation of etching in 5%HF and 1%H₂SO₄ have replicated this sequence of weathering indicators and the appearance of eroded grains (Berner and Holdren,1979). Lundstrom (1970) observed similar forms on oligoclase.

Plagioclases (Na-K feldspars) were found to be more susceptible to weathering than sodic feldspars in the same weathering environment, and oligoclase weathers faster than microcline. James et al (1981) state that 'regardless of climate, detrital plagioclase.... is generally 15-20% more altered than potassium feldspar ". This affirms the work of Berner and Holdren (1979). In acidic soils (pH 2.5), the weathering was enhanced and aluminium was not deposited. This is common in soil 'A' horizons where organic acid complexes increase the mobility of Al. The effect of aqueous cations in solution is to reduce the thickness of the altered layer on the surface of grains, possibly due to competition between the cations and hydrogen for active surface sites (Muir and Nesbitt, 1991).

The implications for luminescence dating of material which has been subject to weathering may be very significant. First, it is the sites of excess energy, eg. defects and dislocations, twinning planes and cleavage fractures and other zones of weakness, which are initially selectively exploited (Berner and Holdren, 1979; Holdren and Speyer, 1985, 1987) As the defects are also potential sites for trapping the electric charge which gives rise to the luminescence signal, weathering may affect the ability of the sample to retain trapped charge. Secondly, the coalescence of etch pits breaks up larger grains into smaller fragments which may be too small to be suitable for luminescence dating. Thirdly, the substitution of cations at defect sites, along with the dissolution of the crystal, is likely to significantly change the composition of the grain, and therefore reduces its suitability and stability as a crystal for use in dating.

7.4 The Weathering Experiment

A fine-grained, feldspar-dominated sample (WM4) from Group 1 was subjected to artificial weathering following Wollast's (1967) procedure. The 6-11 µm fraction of the sample was separated by sedimentation. Buffer solutions of pH 6.0 and pH 8.0 (composition of buffers were made up as described in Wollast, 1967) were made up in a polythene bottle to 1 litre. Fifty grams of the sample were added to one litre of buffer. In addition, a control sample was made with 50 g of sample in de-ionized water (pH 7.0). These were kept in a water bath at 20°C for 6 weeks. They were covered to prevent optical bleaching under the red light conditions of the laboratory and were agitated frequently.

Subsamples of c. 50 ml were abstracted at 10 day intervals from each bottle. Six discs were prepared from each subsample using standard preparation techniques and settling onto abraded aluminium discs in acetone. The remainder of the dried sample was used for XRD analysis (using a

Co_x tube and orientated samples). The surfaces of the prepared discs were examined by a Jeol-840 SEM. Discs were gold coated and examined at magnifications of up to x10 000, at a working distance of 6 - 7 mm.

TL and IRSL measurements (3 discs for each) were made of the natural signal before weathering using a Risø automated system. For TL a Corning 7-51 filter and a heat rate of 10°C/sec were used, and for IRSL, 880 nm diodes and an exposure time of 160 seconds. The three discs from each subsample per batch were normalised before measurement using a 1 second IR exposure. The natural signals, and mineralogy were compared to the characteristics of the original material, and the control sample.

7.4.1 Results.

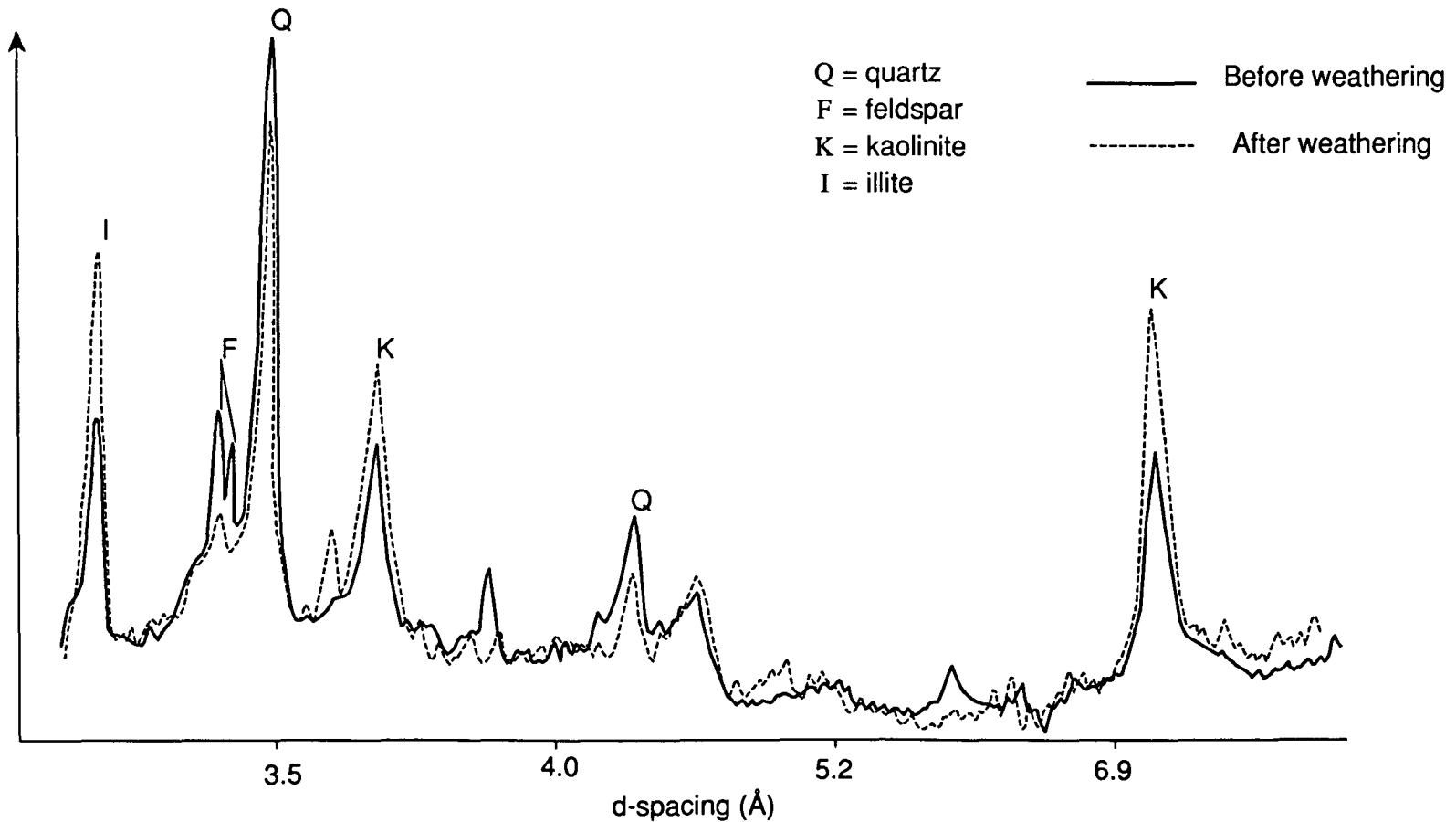
The XRD analysis showed a significant change in the proportions of the identified minerals. There was a fall in the amount of feldspar and increase in the amount of clays, which were dominated by mixed-layer forms. This is shown in figure 7.4.1. The XRD proportions are calculated as the peak areas for identified mineral peaks, and expressed as percentages of total identified minerals. The changes observed were similar for both acid and alkaline buffers, and no significant change was observed in the control.

Under SEM analysis, the grains of the control remained clearly defined, without significant abundance of clay flakes. In the pH buffers, however, after 40 days, the grains exhibited some of the characteristic etch pits associated with weathering. The development of flaky clay coatings associated with mineral breakdown was also observed. The change between the original material and that in a buffer after 40 days is shown in figures 7.4.2 and 7.4.3.

The initial intensity of the natural IRSL signal fell dramatically with duration of exposure in the buffered samples, but not with the control (figure 7.4.4). The control therefore indicates that this reduction is not due to external effects, such as bleaching under laboratory light. This reduction reached levels as low as 27% of the original signal from initial intensities of 1065 counts to levels of 187 counts over the first 2 seconds. These levels are typical of those samples in Group 3.

The natural TL signal was measured, and seen to suffer less reduction than the IRSL signal, but a significant change in the 280°C peak shape was observed, both for acid and alkaline buffers (figure 7.4.5). The flattening out of the peak indicates that some charge transfer is taking place, which may result from changes in the surface distribution of luminescence centres associated with weathering (Baillif, pers. comm.). This may also be a cause of the signal loss.

Figure 7.4.1. Effect of pH buffers on mineralogy; XRD analysis. The changes in mineralogy are similar for both acid and alkaline buffers; reduction in proportion of feldspar, and increase in clays, particularly illite. The control remains relatively unchanged.



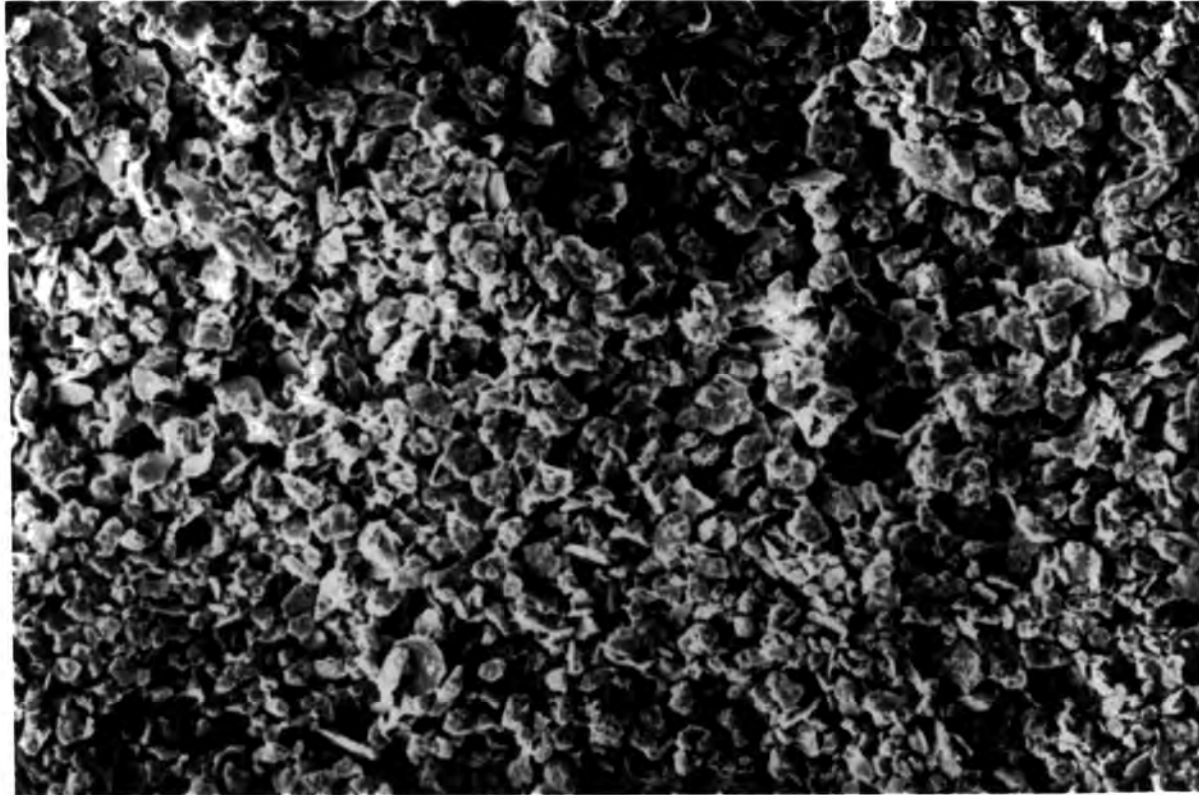


Figure 7.4.2 SEM of sample WM4 before weathering. Note the clarity of the grains and absence of abundant clay minerals. (x500; WD 7 mm; 1 cm = 15 μ m)



Figure 7.4.3 SEM of sample WM4 after 40 days laboratory weathering at pH 6.0. The mineral grains have taken on the 'woolly' weathered appearance similar to that in figure 7.1.2. (x500; WD 7 mm; 1 cm = 15 μ m)

Figure 7.4.4 Reduction in IRSL intensity after weathering

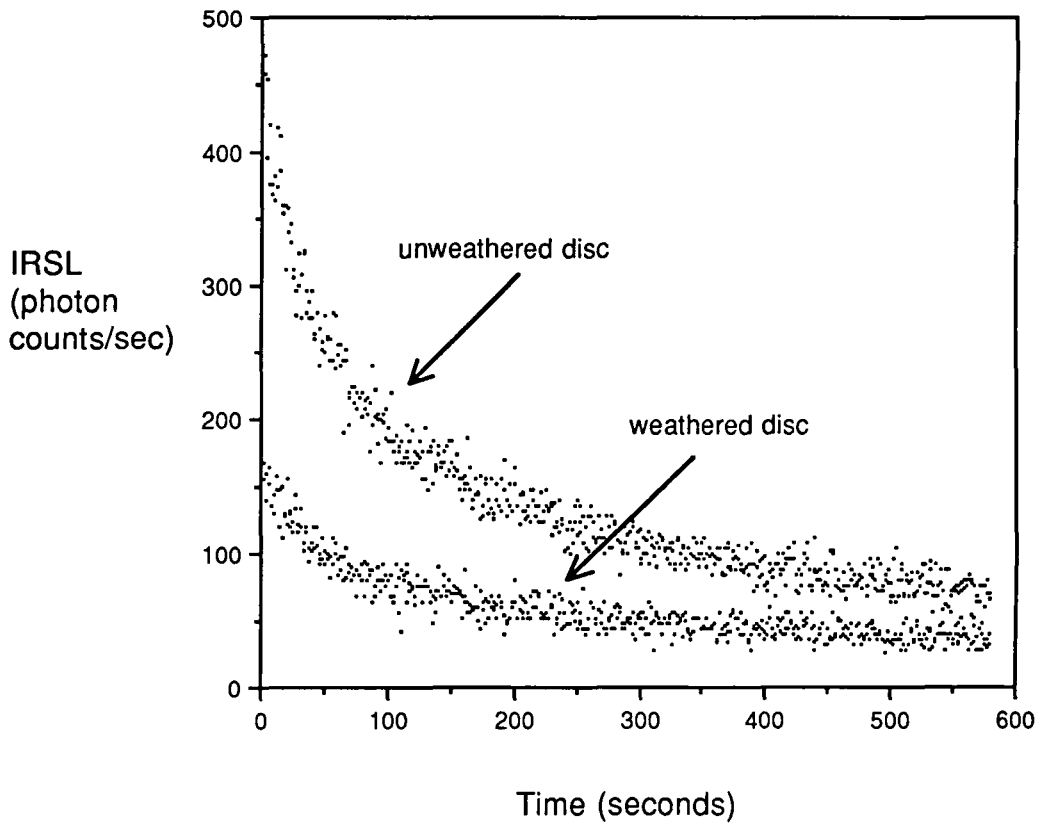
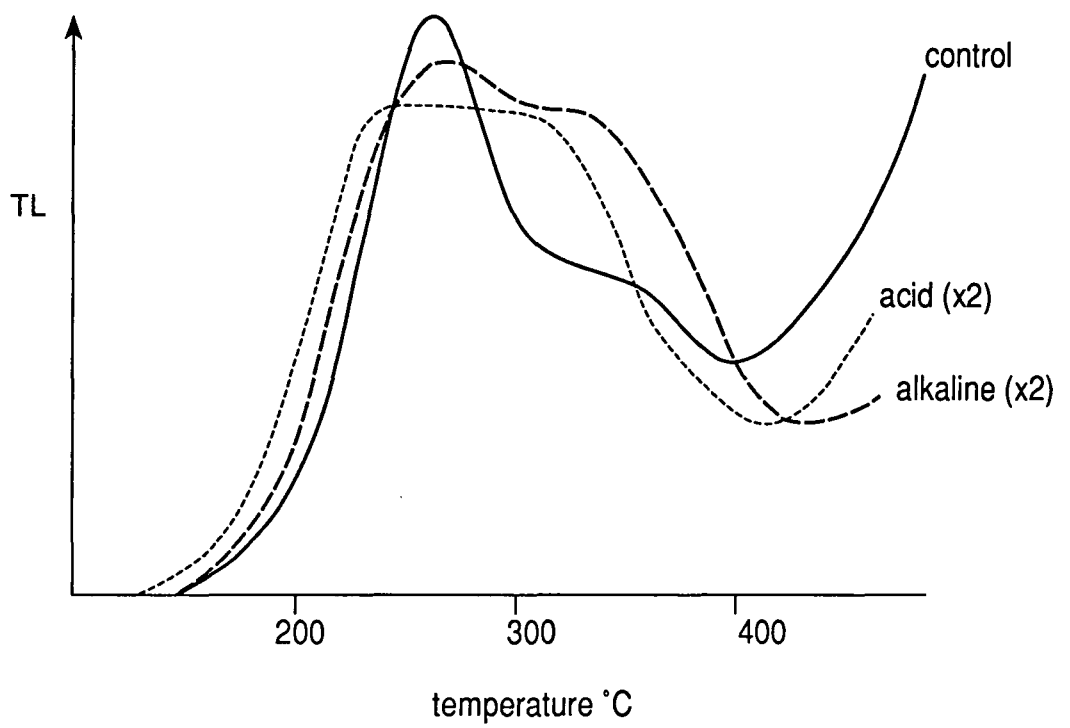


Figure 7.4.5. Changes in the shape of the 280°C TL peak after 40 days in the buffer solutions. The control was unchanged from the original sample (not shown). The acid and alkaline buffers have been scaled up by x2 to account for the loss of signal intensity.



Another significant observation was the onset of fading of the sample (figure 7.4.6), which had previously shown no sign of instability. The control continued to remain stable (101 ± 0.6 over six months at 10°C storage), but the IRSL signal of the buffered samples faded significantly, losing up to 45% of the signal intensity. This fading component was not removed by the preheating treatment, similar to those samples in Group 3 which faded. The TL signal also faded by similar proportions.

7.4.2 Conclusions.

Chemical weathering selectively exploits the defects in feldspar crystals, and causes a loss of signal, and the onset of instability, manifest as fading and changes in the structure of the TL peak.

After 40 days exposure of a selected Group1 sample to buffers of pH 6.0 and 8.0, the sample acquired the mineralogical and luminescence characteristics of a sample from Group 3. The control sample in de-ionized water remained unchanged, and thus retained the characteristics of the original material.

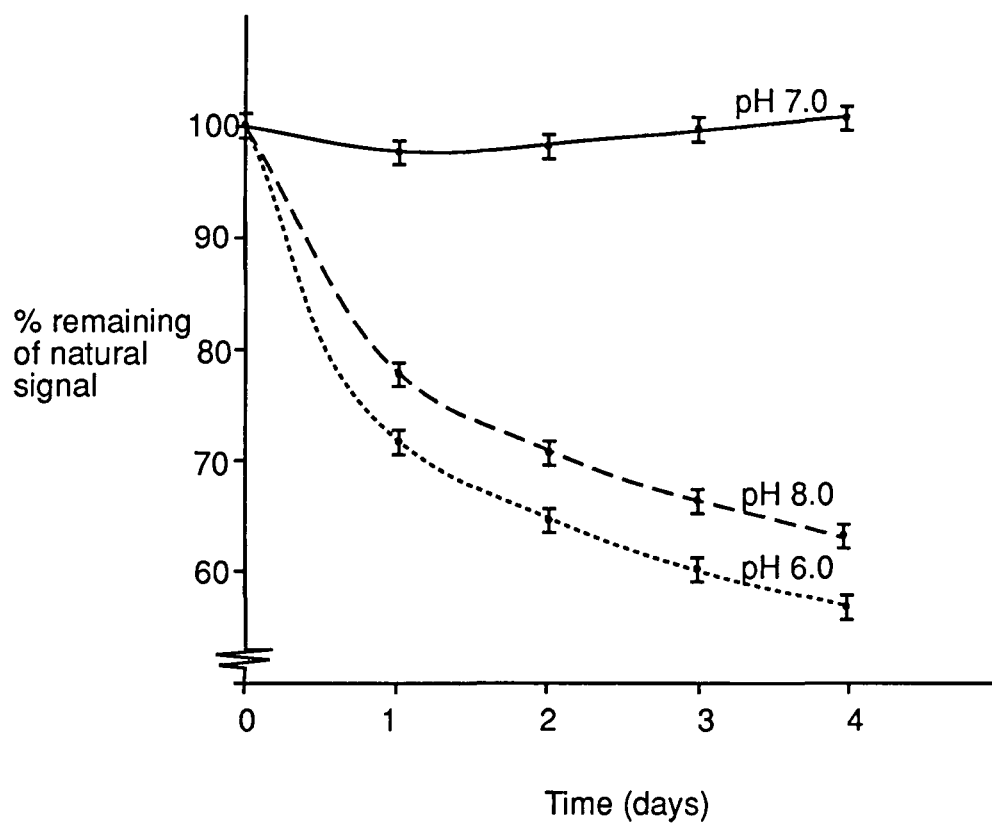
Artificial weathering, by inducing disequilibrium between solution and sample has been observed to cause a number of changes. Mineralogically, the indicators of active weathering develop, ie. the accumulation of mixed-layer clays and the etching of feldspar grains. With respect to the luminescence signal, a significant loss in intensity is observed, together with the onset of fading.

The observed correlation between weathering indicators and poor luminescence signals has been confirmed in this study, in that the same correlation has been induced by active weathering as observed in Group 3 samples, as opposed to a stable-state of grains in equilibrium with their present environment as demonstrated by Group 2 samples.

7.4.3 Implications for Dating.

With respect to dating sediments, the identification of actively weathering environments is important, especially with respect to feldspars which are more susceptible to weathering than, for example, quartz. Detailed stratigraphic analyses, such as the examination of preserved microstructures, can indicate that weathering is active. The microscopic examination of individual grains for evidence of degradation and formation of weathering-related clay coatings (as opposed to those resulting from the translocation of fines within a profile)^{is} in support of the stratigraphic analysis. This is a useful indicator of the state of the mineral grains in terms of processes operating within the profile.

Figure 7.4.6 Loss of IRSL initial signal intensity due to fading after laboratory weathering (see text for details).



In the case of sediments classified as Group 2 in this study, the grains may have been affected by weathering, but the sedimentary structures such as fine laminations have been preserved in the sedimentary section. This indicates that leaching and mixing of minerals associated with active weathering has not occurred.

Other indicators of active weathering are in the clay mineralogy and the presence of mixed-layer clays. Clays dominated by kaolinite have a low CEC, and thus remain more stable in active weathering environments. Clays dominated by mixed-layer or expanding lattice types such as illite and montmorillonite are less stable, and more easily affected by cation exchange.

It is the combination of these characteristics that is most useful, rather than elements taken individually. It is the active weathering environment which appears to affect the dating potential of sediments; a stable environment containing either weathered or unweathered grains is not, in these samples, necessarily a cause for concern.

For sediments from archaeological sites, the identification of weathered horizons may be difficult. Anthropogenic activity can affect the chemical stability of minerals in a number of ways. Trampling and the incorporation of organic material derived from human occupation may increase the rates of weathering of minerals, as the presence of organic acids can increase the rate of dissolution of feldspars. Activity associated with construction of ditches or buildings can lead to exposure of strata to pedogenesis.

However, archaeological material can also be useful in the identification of ancient landsurfaces and buried soils. For example, at Williamson's Moss and Hartlepool Bay the minerogenic remnants of Mesolithic land surfaces were identified by the presence of artefacts and charcoal. Thus archaeological material in these cases can identify strata which may have been affected by pedogenesis in the past. If the strata are in equilibrium in their present context, such samples fall into the Group 2 category and may be dateable by luminescence.

It is therefore important that careful selection of samples is made, and consideration given to their past weathering history as indicated by their stratigraphic and archaeological contexts, and their sedimentological contexts. Identification of weathered samples which may be a problem in terms of dating can further be made by tests on the stability and the intensity of the luminescence emissions. This can be done, and Group 3 type samples eliminated before extensive laboratory measurement procedures have been carried out. It is important, however, that the evidence from sedimentological and luminescence analyses are used in conjunction, particularly at this early stage in the identification of the causes of problems of stability and intensity of IRSL signals. This ^{experiment is} however, an important step in this direction.

CHAPTER 8 SUMMARY AND CONCLUSIONS

The study which has been presented in the foregoing chapters has demonstrated the viability of luminescence dating techniques for Holocene sediments. This is particularly important in the case of the new IRSL technique which has only recently been established as a potential method of sediment dating. It has also established the importance of sedimentary analysis in identifying the environment of deposition and post-depositional changes affecting sedimentary strata selected for dating.

The application of detailed sedimentary analysis, particularly SEM examination of the samples is a new departure in the field of luminescence and has been shown to be of significant value in the identification of samples which are likely to be problematic in terms of their luminescence behaviour. For example, the relationship between chemical weathering and characteristics of the luminescence signals has been identified and tested in a laboratory experiment. This experiment demonstrated that active chemical weathering of feldspars has a significant effect on the stability and intensity of the luminescence signals used for dating, and also explains the failure to date a number of samples in this study.

This chapter summarises the work that has been undertaken and the conclusions that have been drawn. Subsequent sections assess the justification of the luminescence methodology adopted in this study, the importance of the sedimentary analyses and of the weathering experiment and finally, the significance of the work for archaeological and Quaternary dating studies.

8.1 Summary of work undertaken

An interdisciplinary approach was adopted to investigate the potential of luminescence dating techniques for waterlain sediments of Holocene age. The approach combined detailed sedimentological analysis of selected samples in conjunction with TL and IRSL dating. This was done in order to assess the environment of deposition and post-depositional changes affecting the samples and which may affect the luminescence signals of the samples. The selection of sites was based on a number of criteria including the availability of environmental reconstruction data and an independent chronology based on C-14, archaeology and stratigraphy.

The sites selected were Flag Fen, Cambridgeshire; Williamson's Moss and Stubb Place, Cumbria; Hartlepool Bay, Cleveland and Hazendonk and Slingeland in the River-dune district of the Western Netherlands. All these sites, ^(except Stubb Place) had an independent chronology based on C-14 and archaeology. They were also lowlying areas which had been substantially affected by sea-level changes during the

Holocene and which added important information relating to the environment of deposition of the sedimentary units.

The Quaternary history and archaeology of each site were discussed, with particular reference to material relating to the existing chronology of the sites. The radiocarbon dates used for chronological control were all calibrated according to a standard calibration curve, described in Chapter 1. The sedimentary sequences sampled were described and the minerogenic strata sampled for sedimentary and luminescence analysis.

The sedimentological investigations of the samples involved the analysis of the minerogenic and elemental composition by XRD and XRF techniques, particle size distribution, water and organic content and physical examination of grains under SEM. The same samples were dated by TL and IRSL techniques. The luminescence characteristics of the sediments were required to meet several criteria in order to be acceptable for dating. These included stability of the signal, linear growth characteristics and optical signal intensities of at least four times the background levels.

The investigation of laboratory bleaching of the luminescence signals is an important aspect of dating waterlain material. The use of an appropriate bleaching source is vital, in order to avoid the effects of transfer of charge and resultant higher residual levels. This effect was noted in IRSL samples which bleached down to an unexpected residual under sunlight. This residual was not observed after bleaching with filtered white light. The filter cuts out the shorter wavelengths responsible for charge transfer. The residual of TL samples was reduced after filtered light bleaching. The importance of this lies in the fact that under water, sunlight is attenuated by depth, turbulence and suspended sediment. The filtered bleaching light source more closely resembled these conditions than sunlight bleaching. This technique was used for all sediments and has produced ages consistent with each other and with the C-14 chronology.

The dating of the samples was very successful, with 17 out of 27 samples being dated. Three samples which were rejected were saturated with respect to the luminescence signal, and the remainder were affected by instability (fading) and low signal intensities. The ages evaluated by TL and IRSL were in close agreement between techniques and with the independent C-14 chronologies. The agreement between the luminescence techniques was very good ($r=0.977$). Agreement between C-14 and luminescence techniques was less close ($r=0.568$ for IRSL and $r=0.497$ for TL). In three cases where the luminescence techniques were more disparate, the difference is attributed to sedimentological processes in which the signals were not bleached at deposition in the present context, eg. for the coarse grain fraction of a sediment where the IRSL ages of different grain size fractions differed (WM4), or for the bulk sediment where the luminescence ages did not agree with C-14 (WH1, 2).

These ages however, should be accepted as absolute dates of the last exposure of the minerals in that deposit to light, even if they do not fit into the existing chronology. This illustrates the problems associated with comparative chronologies based on different materials and events. In the comparisons discussed in Chapter 6 the age ranges of the dates were compared which is likely to be more appropriate than comparing dates of specific materials within deposits, particularly where these materials differ in their contexts.

The relationships between sedimentological and luminescence characteristics revealed several trends. The samples could be categorised into three groups based on these characteristics. Group 1 comprised nine samples which were dated by one or both luminescence techniques and in which the sediment grains were unaffected by weathering and the clay minerals formed discrete particles rather than coatings. Group 2 comprised eight samples which were dated by one or both techniques but differed from Group 1 samples in their sedimentological characteristics. These samples exhibited some indications that the grains had been weathered but the clay minerals did not form coatings on the grains and the preservation of sedimentary structures in the stratum indicated that the sediments were not undergoing pedogenesis or weathering in their present contexts.

Group 3 samples, of which there were 10, were not dated. These failed the criteria established for the acceptance of samples for dating. They were affected by substantial fading of the signal and low signal intensities. The grains tended to be heavily weathered and clay mineral coatings were abundant, together with mixed layer clay minerals. These samples tended to be located in the upper parts of the sediment sequences and were undergoing active pedogenesis at the time of sampling.

The relationship between weathering of grains and failure to date samples was explored further and tested by an experiment in which a Group 1 sample was exposed to artificial weathering and the changes in luminescence characteristics observed. This sample took on the characteristics of the Group 3 samples, with etching of the grains, abundant clay minerals, inducement of fading and reduction in signal intensities. This is an aspect of sedimentological analysis and luminescence dating which has not been investigated before. It represents an important step forward both in the explanation for why certain samples could not be dated in this study, and on the effects on the luminescence sensitivity and efficiency of samples exposed to physical and chemical alteration.

Overall, luminescence has proved to be a suitable and viable technique for Holocene sediments and that sedimentological analysis has an important role to play in the identification of suitable samples and in the explanation of differences in age determinations between techniques.

8.2 Justification of the luminescence methodology

The novelty of the IRSL technique has meant that a number of procedures adopted during measurements of samples in this study have had to be based on other optical dating work, and on assumptions of similarity between the source and behaviour of TL and IRSL luminescence emissions. The techniques used here are based on those of other workers (cited in the text) examining similar sedimentary material to that studied here; ie. polymineralic fine grain material, dominated by feldspar emissions.

First, the type of sediment examined in this study was primarily silt rich waterlain sediments. Work by Berger (1988, 1990) recommends that silt-rich sediment should be avoided in dating samples. This is drawn from his work in which clay-rich sediments were more successfully dated than silt-rich sediments. This was attributed to problems in the zeroing of silt sized material and in sensitivity changes and reproducibility of the signal. However, in this study many of the sediment samples were silt-rich and these were dated successfully. The problems affecting rejected samples were related to characteristics other than grain size.

Secondly, the method of ED evaluation used in this study was that of the total bleach and regeneration method for determining the level of the TL residual, and the additive technique for ED evaluation. This was justified on the basis that the samples were young (<10 000 years) and that the effects of the onset of saturation were not expected. The dating of waterlain material is often thought to be affected by partial bleaching of the signal. This was overcome by the development of the 'partial-bleach' technique of ED evaluation (see section 5.2.5). This technique is recommended by workers such as Berger (1988, 1990) for TL dating of waterlain material.

Samples were successfully dated using filtered bleaching and total bleaching of the signal. This is likely to be appropriate for IRSL signals which bleach to negligible residual levels within very short exposure times. This can then be used to compare the success of dating the same sediments by TL using the same conditions to determine the level of the unbleachable residual. For samples in this study, very close agreement was obtained using this method for both IRSL and TL signals. This indicates that the use of the total bleach technique for waterlain sediments is appropriate in these cases, provided that a suitable source of laboratory bleaching light is used.

8.3 Role of sedimentary analysis analysis in luminescence dating

The sedimentary techniques adopted in this study examined the mineralogy, elemental composition, water and organic contents of the samples and physical appearance under SEM

examination. These analyses have been shown to be a key aspect in luminescence dating studies for several reasons.

First, the identification of the conditions under which sedimentary deposits were laid down is important with respect to the bleaching of the mineral grains. In some waterlain sediments, bleaching may have been incomplete due to attenuation of sunlight by water depth, turbulence or suspended sediment load. These conditions may be difficult to recognise in individual sedimentary units but indicators of the environment of deposition may be available, such as diatoms and the particle size distribution of the sediment.

Secondly, the effects of post-depositional change are relevant to luminescence dating in three main ways. The effects of compaction of sediments are primarily related to changes in the water content history of the sediment. The variation in water content within a deposit throughout the burial history of the samples is a major source of error in the age. Compaction reduces both the total water content and the uncertainty in its variation. This can be determined from some sedimentary units by their physical nature and particle size distribution - eg. between a compact and a loosely packed clay or a silt with sand. The particle size distribution can also identify sediments which are more likely to be relatively compact at deposition, such as clays and silty clays laid down under slow running water. Such sediments are laid down in a compact state, as is the case for the clay deposits in the Western Netherlands.

Thirdly, the effects of pedogenesis are also important as this can result in significant changes in the mineral grains. The formation of clay coatings due to percolation or weathering of grains may reduce the potential effects of sunlight exposure in minerals re-exposed at the surface. Bioturbation can result in some pockets of sediment which has been bleached at a later date than the bulk of the sediment, and therefore is 'younger' in luminescence age. The bleaching of soils is discussed in Chapter 3, particularly with reference to the uncertainty in bleaching of the mineral grains.

Closely related to pedogenesis are the effects of weathering. The weathering of feldspars has been discussed in detail in Chapter 7. The relationship between sediments which have been weathered and cannot be dated due to disruption of the stability and intensity of the luminescence signal has been demonstrated in the weathering experiment. This is a very important and novel discovery in the field of luminescence.

The samples could be grouped in three categories based on their sedimentological characteristics and luminescence behaviour. Group 1 samples were unweathered and contained few mixed layer clays or clay coatings; these sediments were dated. Group 2 sediments had been weathered but not in their present sedimentary context. These samples were dated and also contained few clay

mineral coatings on quartz and feldspar grains. Group 3 samples were heavily weathered and derived from strata in which weathering was taking place at the time of sampling. These sediments could not be dated due to low signal intensities and fading of the TL and IRSL signals. This observed relationship was confirmed by experiment.

The recognition of active weathering processes is therefore an important step towards the identification in the field of potential dating samples. The luminescence dating procedure is long and complex, requiring many measurements and repetitions to ensure accuracy. If potentially problematic samples could be identified in the field or by simple sedimentary analysis, much time could be saved in the laboratory. It is necessary, however, to extend the experiments given in Chapter 7 both in the type of sediment investigated and by varying the conditions under which weathering was induced.

The extensive use of SEM analysis of the samples dated in this study is a novel combination of techniques and has been of key importance in the categorisation of the samples into the three groups mentioned above. Such examination of dating samples needs to be increased and applied to a wider variety of deposits. It should also be more widely used in dating laboratories as a supplementary technique to those associated with dating. SEM examination not only reveals the physical (and inferred chemical) state of the grains being dated, but also reveals the form and distribution of clay minerals within the sediment. An abundance of clay minerals, and presence of coatings which may survive the treatments given during preparation of dating samples can cause reduction in intensity of emissions from grains. This has been discussed in chapter 3. Its importance in terms of dating is relatively little known, but it likely to be more significant in waterlain and pedogenic samples which are clay-rich, compared to coarser grain sizes and sediments such as sand dunes.

Archaeological material represented within the sediment sequences is important in a number of ways. It can provide a useful additional comparative chronology for the sample contexts, particularly where it is stratified with the sequences. However, this can give rise to problems where the luminescence and C-14 chronologies (the latter being based on archaeological material) do not entirely agree as in the case of WM4. However, even here, the archaeological material gives an approximate age range, as distinct from that provided by the C-14 dates, into which the luminescence ages fit. This is important where C-14 dates are based on artefacts which are 'imported' or incorporated into the sediment and hence may give an incorrect age range for the deposition or formation of the sedimentary unit, as in the case of WH2.

Archaeological evidence in a stratum may also take the form of trampling of ancient surfaces and incorporation of 'foreign' material. This material may be younger than the bulk sediment as it may

have been bleached at a later date. The recognition of such horizons is important in terms of sample selection, as the most representative portion of the stratum should be used for dating, in order to avoid incorporation of material affected in such a way. Trampling has a similar effect to compaction in that it reduces the water content of the sediment. Archaeological horizons are often associated with the remains of ancient soils. The problems of dating some soil material has been discussed above, and the archaeological material may aid the identification of these horizons. This may help to explain any luminescence behaviour which is unexpected during sample measurement.

8.4 Implications of this study for archaeological and Quaternary studies.

The use of TL and IRSL techniques for dating Holocene sediments has been shown to be appropriate in this study. The techniques have produced stratigraphically consistent chronologies for sediment sequences which included waterlain sediments and buried soil horizons. The importance of the establishment of luminescence techniques for dating sediments arise from a number of advantages and applications that luminescence has over, for example, the most commonly used technique of radiocarbon dating.

Luminescence is an absolute dating technique and so does not experience the problems of calibration common in C-14 dating. The techniques are widely applicable to a very wide range of inorganic sedimentary material which is not suitable for C-14 dating, and over a longer timespan, currently 0-200 000 years.

The basic requirement of samples for luminescence dating is that they have been exposed to light before burial, and that the trapped charge which accumulates within the crystal is stable during the timespans and under the burial conditions of the sediment. Exposure occurs during the transport and deposition of most terrestrial sedimentary deposits and in cases where bleaching of the TL signal is incomplete, the optical signal can be used as this is more sensitive to even attenuated sources of light. The IRSL signal primarily stimulates the signal of feldspars. These minerals are almost ubiquitous in sedimentary deposits, so there are few instances where IRSL could not potentially be used to date sediments.

The advantages of the IRSL signal over the TL signal are that it is more sensitive to optical bleaching and that it bleaches down to a negligible residual level. This last characteristic can be important in the dating of waterlain material concerning the choice of suitable laboratory bleaching source. This can then be applied to the TL signal of the same sediment.

The comparisons between IRSL and TL dates have been very close in samples studied here. However the techniques have a different physical basis and have different strengths and

weaknesses. The weaknesses of TL lie in problems of high residual levels in young sediments. IRSL has a greater tendency towards instability than TL. However, TL signals can be equally unstable but there is less uncertainty in the laboratory determination of the IRSL residual. This indicates that IRSL is potentially more widely applicable in the case of waterlain material. However, both techniques have contributed positively to the establishment of absolute chronologies for the sites investigated.

The overall advantage of both techniques is the great variety of sediments to which they can be applied. This is potentially very important for archaeological sites. For example, provided careful selection of samples is made, different elements of site formation can be dated. Not only can the burnt inorganic material present in a hearth be dated, but also the sediment lying above and below it. This would give an age for the formation of the landsurface, the date of human activity and the date when the hearth was buried. This is likely to represent a more detailed and reliable chronology for such samples than only dating the charcoal from the hearth itself.

Luminescence dating can also be of great importance during the periods of significant flatness in the radiocarbon calibration curves, such as the last millennium BC. Different C-14 ages in this region may represent the same calibrated age range. The application of luminescence dating to material of this age may resolve potential dilemmas in selection of the 'correct' C-14 date.

At present, the main problem associated with the accuracy of luminescence ages is that of water content. For aeolian material error limits of around 10% are common for luminescence dates. For compact sediments with low uncertainties in the water content variation, such as SP8 and 9 and WM5, the error limits are equal to these. Therefore, in the future luminescence dating has the potential to rival or surpass the accuracy of radio-carbon dating, on a wider range of material and over greater timespans.

Sample selection is a vital part of successful dating. Consideration must be given to the context of the sediments with respect to the dose-rate of the sample. This can be closely monitored by on-site dosimetry provided that the sample contexts are accessible. The gamma dose-rate component which is significant in sediments, can be considered to be unaffected by the activities of adjacent strata for a distance of 30 cm from the sample. The contribution from adjacent strata can, however be assessed by measurement of activities of these strata and use of computer programmes to evaluate the relative contributions.

The strata from which samples are taken needs to be examined carefully to assess the degree of disturbance and post-depositional change to which the samples have been exposed. The degree of disturbance may be considerable on archaeological sites with complex stratification. However, this

need not be a problem so long as the sequence is examined with a view to assessing the points given above. All samples are potentially suitable for luminescence dating, and it is only by extending the 'repertoire' of applications that the limitations of the technique can be established. It is also significant that many of the fundamental problems of luminescence dating, such as bleaching, stability and water content are sample-driven, and it is only by assessing individual samples that any can be ruled out for dating.

8.5 The future of luminescence dating

In the future luminescence dating is likely to become a more important and widely used suite of techniques. This is due to its wide applicability and age range. The new optical dating techniques such as IRSL have been shown to be highly suitable for waterlain material. The work undertaken here has demonstrated the potential of the technique and has also given important insights to further developments of the techniques.

The importance of sedimentary analysis has been discussed and this needs to be more widely applied within luminescence dating studies. There is much to be derived from simple examination and analytical procedures which is of relevance to luminescence dating. The main areas in which this should be developed is in the extension of studies relating to the weathering of feldspars. The experiments performed here need further replication. They also need to be applied to different types of feldspar and to different minerals such as quartz in order to clarify and extend the explanations for certain luminescence characteristics put forward in these initial studies. This is a very novel aspect of luminescence studies and worthy of attention in the future.

The problems associated with bleaching of waterlain sediments and the different environments in which the techniques can be applied have been an area of investigation for luminescence workers for some time (see discussion on bleaching in chapter 3). However, certain aspects of the sedimentary environment have up to now been dismissed. These aspects include the uncertainties in water content variation. This is a major problem in refining the accuracy of techniques. In this work it has been shown that in most cases the water content uncertainty is related to compaction and depth of sedimentary deposits. This aspect needs to be taken further and methods developed of reducing the uncertainty in water content variation. This may lie in sedimentological analysis and methodology rather than in luminescence methodology. This reinforces the potential of increased interaction between sedimentologists and physicists towards the refinement of luminescence.

Finally, the comparison of C-14 and luminescence ages as a basis of establishing the latter as viable dating techniques needs to be examined. There are relatively few instances where great care has been taken to ensure the viability of the C-14 chronology, particularly with regard to calibration of the

dates. This is likely to become ever more important as the accuracy of luminescence increases and therefore the importance of the difference between an uncalibrated and a calibrated radiocarbon date used as a comparison will become more important. Even in the comparative work by Pye and Johnson (1988) the comparative C-14 chronology is based on uncalibrated dates. This raises the issue, discussed above, of the viability of such comparisons between different techniques. This too, is an aspect worthy of future discussion.

Luminescence dating, however should be considered as a valuable source of absolute chronology, of wide applicability and of an age range which extends beyond radiocarbon, and which is being extended further back as new development in the technique are made. The techniques have been shown to be valid for archaeological sediments of Holocene age and it only remains for this potential to be taken up by the archaeological community for TL, and more particularly IRSL, to become the most important absolute dating techniques of the future.

BIBLIOGRAPHY

- Aitken, M J (1985) *Thermoluminescence Dating* Academic Press, London.
- Aitken, M J and Aldred, J C (1972) The assessment of error limits in thermoluminescent dating
Archaeometry 14(2), 257-267.
- Aitken, M J and Xie, J (1992) Optical dating using infra-red diodes: young samples *Quaternary Science Reviews* 11, 147-152.
- Aitken, M J; Smith, B W and Rhodes, E J (1989) Optical dating - recapitulation on recuperation
Synopses from a workshop on the Long and Short range limits in luminescence, Oxford Res. Lab Arch. & Hist. Art, Oxford, Occ. paper 9.
- Akber, R A and Prescott, J A (1985) TL in some feldspars - early results from the study of spectra
Nuclear Tracks and Radiation Meas. 10, 575-580.
- Andrews, J T; King, C A M and Stuiver, M (1973) Holocene sea-level changes of the Cumbrian coast, NW England: eustatic and glacio-isostatic movements *Geologie en Mijnbouw* 52(1), 1-12.
- Bailliff, I K (1976) The use of phototransfer for the anomalous fading of thermoluminescence *Nature* 264, 531-533.
- Bailliff, I K (1980) A beta irradiator for use in TL dating *Ancient TL* 10, 12-14.
- Bailliff, I K (1982) Beta TLD apparatus for small samples *PACT J* 6, 72-75.
- Bailliff, I K and Younger, E J (1988) Computer controlled TL apparatus *Nuclear Tracks and Radiation Meas.* 14, 171-176.
- Bailliff, I K and Poolton, N R J (1991) Studies of charge transfer mechanisms in feldspars *Nuclear Tracks and Radiation Meas.* 18, 111-118.
- Bailliff, I K; Bowman, S G E; Mobbs, S F and Aitken, M J (1977) The phototransfer technique and its use in thermoluminescence dating *J. Electrostatics* 3, 269-280.

- Balescu, S and Lamothe, M (1992) The blue emission of alkali-feldspar coarse grains and its potential for overcoming TL age under-estimations *Quaternary Science Reviews* 11, 45-52.
- Barden, L (1968) Primary and Secondary consolidation of clay and peat *Géotechnique* 18, 1-24.
- Barker, H and Mackey, J (1961) British Museum Natural Radiocarbon measurements III *Radiocarbon* 3, 39-45.
- Barker, J A (1981) *Dictionary of Soil Mechanics and Foundation Engineering* Construction Press, London.
- Bartley, D D; Chambers, C and Hart-Jones, B (1976) The vegetational history of parts of S and E Durham *New Phytologist* 77, 437-468.
- Bates, R L and Jackson, J A (1980) *Glossary of Geology* American Geological Institute.
- Bennett, P C (1991) Quartz dissolution in organic-rich aqueous solutions *Geochimica et Cosmochimica Acta* 55, 1781-1797.
- Berger, G W (1984) Thermoluminescence dating studies of glacial silts from Ontario *Can. J. Earth Science* 21, 1393-1399.
- Berger, G W (1985a) TL dating of rapidly deposited silts from South Central British Columbia *Can. J. Earth Science* 22, 704-710.
- Berger, G W (1985b) TL dating applied to a thin winter varve of the late-glacial South Thompson silt, South-Central British Columbia *Can. J Earth Science*, 22,1736-1739.
- Berger, G W (1988) Dating Quaternary sediments by luminescence *Geol. Soc. America Special Paper* 227, 13-50.
- Berger, G W (1990) Effectiveness of natural zeroing of the thermoluminescence in sediments *J. Geophysical Research* 95, 12375-12397.
- Berger, G W and Huntley, D J (1982) Thermoluminescence dating of terrigenous sediments *PACT J* 6, 495-504.

- Berger, G W; Huntley, D J and Stipp, J J (1984) Thermoluminescence studies on a C-14 dated marine core *Can. J. Earth Science* 21, 1145-1150.
- Berner, R A and Holdren, G R (1977) Mechanism of feldspar weathering: Some observational evidence *Geology* 5, 369-372.
- Berner, R A and Holdren, G R (1979) Mechanism of feldspar weathering: II Observations of feldspars from soils *Geochemica et Cosmochimica Acta* 43, 1175-1186.
- Birks, H J B (1982) Mid-Flandrian forest history of Roudsea Wood NNR, Cumbria *New Phytologist* 90, 339-354.
- Blatt, H (1982) *Sedimentary Petrology* Freeman, San Francisco.
- Bluszcz, A (1988) Thermoluminescence sensitivity changes of mineral grains after optical bleaching *Quaternary Science Reviews* 7, 321-324.
- Bonsall, C (1981) The coastal factor in the Mesolithic settlement of NW England; in: *Mesolithikum i n Europa. 2nd. internationales symposium, Potsdam, April 1978.* Bericht, Berlin.
- Bonsall, C; Sutherland, D G; Tipping, R M and Cherry, J (1986) The Eskmeals project 1981-85: an interim report *Northern Archaeology* 7, 3-30.
- Bonsall, C; Sutherland, D G; Tipping, R M and Cherry, J (1989) The Eskmeals project: late Mesolithic settlement and environment in NW England; in: *The Mesolithic in Europe* ed. Bonsall,C; John Donald Publ.Ltd. Edinburgh, 175-205.
- Bøtter-Jensen, L (1988) The automated Risø TL dating reader system *Nuclear Tracks and Radiation Meas.* 14, 63-72.
- Bøtter-Jensen, L and Mejdahl, V (1984) Microcomputer controlled reader system for archaeological and geological TL dating *Rad. Prot. Dosim.* 6, 193-6.
- Bøtter-Jensen, L; Ditlefsen, C and Mejdahl, V (1991) Combined OSL (Infra-red) and TL studies of feldspars *Nuclear Tracks and Radiation Meas.* 18, 257-263.
- Bowall, L; Frean, R; McGeogh, K J; Rendell, H M and Townsend, P D (1990) Sensitivity changes in the TL of quartz and feldspar after bleaching *Cryst. Latt. Def. & Amorph. Mat.* 16, 37-43.

- Bowman, S G E (1976) Thermoluminescent dating: the evaluation of radiation dosage
Unpublished D. Phil thesis Faculty of Physical Sciences, Oxford
- Brady, N C (1990) *The nature and properties of soils* Maxwell Macmillan, New York.
- British Standards Institution (1975) Methods of testing soils for civil engineering purposes *British Standards Inst. HMSO 1377.*
- Carroll, D (1970) X-ray identification of clay minerals *Geol. Soc. America Special Paper 126.*
- Casey, W H; Westrich, H R; Arnold, G W and Banfield, J F (1989b) The surface chemistry of dissolving labradorite feldspar *Geochimica et Cosmochimica Acta 53*, 821-832.
- Casey, W H; Westrich, H R; Massis, T; Banfield, J F and Arnold, G W (1989a) The surface of labradorite feldspar after acid hydrolysis *Chemical Geology 78*, 205-218.
- Catt, J A (1979) Soils and Quaternary Geology *J Soil Science 30*, 607-647.
- Chen, R and Kirsh, Y (1981) *Analysis of thermally stimulated processes* Pergamon Press, New York.
- Chen, R; Huntley, D J and Berger, G W (1983) Analysis of thermoluminescence data dominated by second-order kinetics *Physica Status Solidi A 79*, 251-261.
- Cherry, J (1969) Early Neolithic sites at Eskmeals *Trans. Cumb. Westmorland Antiq. Arch. Soc.* 69, 40-53.
- Cherry, J (1982) Sea Cliff erosion at Drigg, Cumbria: evidence of prehistoric habitation. *Trans. Cumb. and Westmorland. Antiq. and Arch. Soc.* 82, 1-6.
- Cherry, J and Cherry, P J (1983) Prehistoric habitation sites in W Cumberland; Part 1; The St Bees area and north to the Solway *Trans. Cumb. Westmorland Antiq. Arch. Soc.* 83, 1-14.
- Cherry, J and Cherry, P J (1984) Prehistoric habitation sites in W Cumberland; Part 2; The Nethertown and Seascale areas *Trans. Cumb. Westmorland Antiq. Arch. Soc.* 84, 1-17.

- Cherry, J and Cherry, P J (1985) Prehistoric habitation sites in W Cumberland; Part 3; The Drigg and Ravenglass areas *Trans. Cumb. Westmorland Antiq. Arch. Soc.* 85, 1-10.
- Cherry, J and Cherry, P J (1986) Prehistoric habitation sites in W Cumberland; Part 4; The Eskmeals area *Trans. Cumb. Westmorland Antiq. Arch. Soc.* 86, 1-17.
- Cherry, J and Cherry, P J (1987) Prehistoric habitation sites in W Cumberland; Part 5; The Eskmeals to Haverigg area *Trans. Cumb. Westmorland Antiq. Arch. Soc.* 87, 1-10.
- Clark, J G D (1972) *Star Carr; a case in bioarchaeology* Addeson-Wesley, Reading, Mass.
- Clark, J G D and Godwin, H (1962) The Neolithic in the Cambridgeshire Fens *Antiquity* 36, 10-23.
- Clark, P A and Templar, R H (1988) Dating thermoluminescence samples which exhibit anomalous fading *Quaternary Science Reviews* 7, 139-142.
- Coles, J and Coles, B (1986) *The Sweet track to Glastonbury* Thames and Hudson, London.
- Coope, G R and Pennington, W (1977) The Windermere Interstadial of the Late Devensian *Philosophical Transactions of the Royal Society, Series B* 280, 337-340.
- Correns, C W and von Engelhart, W (1938) Neue Untersuchungen über die Verwitterung der Kalifeldspates *Chem. Erde* 12, 1-22.
- Crowther, D; French, C and Pryor, F (1985) Approaching the Fens the flexible way; in: *Archaeology from the Ploughsoil* ed. Haselgrove, C; Millett, M and Smith, I; University of Sheffield, 59-76.
- Culver, S J; Bull, P A; Campbell, S; Shakesby, R A and Whalley, W B (1983) Environmental discrimination based on quartz grain surface textures: a statistical investigation *Sedimentology* 30, 129-136.
- Debenham, N C (1985) The use of UV emissions in TL dating of sediments *Nuclear Tracks and Radiation Meas.* 10, 717-724.
- Debenham, N C and Walton, A J (1983) TL properties of some wind-blown sediments *PACT J* 9, 531-538.
- Degens, E T (1975) *Geochemistry of sediments: a brief survey* Prentice-Hall.

- Desai, V S and Aitken, M J (1974) Radon escape from pottery: effect of wetness *Archaeometry* 16, 95-97.
- Dijkmans, J W A and Wintle, A G (1989) Fractional bleaching of potassium feldspars from sediments and its role in equivalent dose determination *Ancient TL* 7(1), 5-10.
- Dijkmans, J W; Wintle, A G and Mejdahl, V (1988) Some thermoluminescence properties and dating of eolian sands from the Netherlands *Quaternary Science Reviews* 7, 349-356.
- Ditlefsen, C (1992) Bleaching of K-feldspar in turbid-water suspensions: a comparison of photo- and thermoluminescence signals *Quaternary Science Reviews* 11, 33-38.
- Duller, G A T (1992) Comparison of equivalent doses determined by thermoluminescence and infrared stimulated luminescence for dune sands in New Zealand *Quaternary Science Reviews* 11, 39-44.
- Ervanne, H ; Jungner, H and Räsänen, M (1992) Dating of fluvial sediments from the Amazon lowland in Peru *Quaternary Science Reviews* 11, 71-74.
- Fairchild, I J (1983) Chemical control of cathodoluminescence of natural dolomites and calcites: new data and review *Sedimentology* 30, 579-583.
- Fairchild, I; Hendry, G; Quest, M and Tucker, M (1988) Chemical Analysis of sedimentary rocks; in: *Techniques in Sedimentology* ed. Tucker, M; Blackwell. 274-354.
- Fleming, S J (1979) *Thermoluminescence techniques in Archaeology* Clarendon Press, Oxford.
- Forman, S L (1988) The solar resetting of TL of sediments in a glacially-dominated fiord environment: geochronologic implications *Arctic Alpine Res.* 20(2), 243-253.
- Forman, S L and Ennis, G (1992) Limitations of thermoluminescence to date waterlain sediments from glacial fiord environments of Western Spitsbergen, Svalbard. *Quaternary Science Reviews* 7, 61-70.
- Forman, S L; Jackson, M E; McCalpin, J and Maat, P (1988) The potential of using thermoluminescence to date buried soils developed on colluvial and fluvial sediments from

- Utah and Colorado, USA: some preliminary results *Quaternary Science Reviews* 7, 287-294.
- French, C A I (1988a) Aspects of the buried prehistoric soils in the lower Welland valley and fen margin north of Peterborough, Cambridgeshire; in: *Man-made soils* ed. Groenman-van-Waateringe, W and Robinson, M; British Archaeological Reports, International Series 410.
- French, C A I (1988b) Further aspects of the buried prehistoric soils in the Fen margin NE of Peterborough, Cambs; in: *The exploitation of Wetlands* ed. French, C and Murphy, P; British Archaeological Reports, British Series 186, 193-211.
- French, C A I (1992) Flag Fen to Fengate; a summary of soil and sediment analysis *Antiquity* 66 (251), 458-461.
- Gale, S J (1985) The late and post-glacial environmental history of the South Cumbrian massif and its surrounding lowland; in: *The geomorphology of NW England* ed. Johnson, R H; Manchester University Press, 282-298.
- Gallois, R W (1979) Geological investigations for the Wash Water Storage scheme *Report of the Institute of Geological Sciences, No. 78/19*.
- Gaunt, G D and Tooley, M J (1974) Evidence for Flandrian sea-level changes in the Humber estuary and adjacent areas *Bull. Geol. Survey GB* 48, 25-41.
- Gemmell, A M D (1988) Zeroing of the TL signal in sediments undergoing fluvio-glacial transport - an example from Austerdalen, W Norway *Quaternary Science Reviews* 7, 339-345.
- Gillott, J E (1990) *Clay in Engineering Geology* Elsevier, Amsterdam.
- Godfrey-Smith, D I; Huntley, D J and Chen, W-H (1988) Optical dating studies of quartz and feldspar sediment extracts *Quaternary Science Reviews* 7, 373-380.
- Godwin, H (1978) *Fenland: its ancient past and uncertain future* Cambridge University Press.
- Godwin, H and Vishnu-Mittre (1975) Studies of the post-glacial history of British vegetation XVI: Flandrian deposits of the Fenland Margin at Holme Fen and Whittlesey Mere, Hunts. *Phil. Trans. Roy. Soc B* 270, 561-604.

- Grün, R; Packman, S C and Pye, K (199) Problems involved in the TL dating of Danish coversands using K-feldspar *Synopses from a workshop on the Long and Short range limits in luminescence, Oxford Res. Lab Arch. & Hist. Art, Oxford, Occ. paper 9.*
- Hageman, Ir B P (1969) Development of the Western part of the Netherlands during the Holocene. *Geologie en Mijnbouw* 48(4), 373-388.
- Hall, D (1987) The Fenland Project 2: Fenland landscapes and settlement between Peterborough and March *East Anglian Archaeology* 35.
- Hardy, R G and Tucker, M E (1988) X-ray powder diffraction of sediments; in: *Techniques in Sedimentology* ed. Tucker, M; Blackwell. 191-228.
- Helgeson, H C (1971) Kinetics of mass transfer among silicates in aqueous solutions *Geochemica et Cosmochimica Acta* 35, 421-429.
- Holdren, G R and Berner, R A (1979) Mechanism of feldspar weathering: I Experimental study *Geochemica et Cosmochimica Acta* 43, 1161-1171.
- Holdren, G R and Speyer, P M (1985) Reaction rate-surface area relationships during the early stages of weathering, I: Initial observations *Geochemica et Cosmochimica Acta* 49, 675-681.
- Holdren, G R and Speyer, P M (1987) Reaction rate-surface area relationships during the early stages of weathering, II: Data on eight additional feldspars *Geochemica et Cosmochimica Acta* 51, 2311-2318.
- Horton, A (1989) Geology of the Peterborough District *British Geological Survey, HMSO.*
- Huddart, D and Tooley, M J eds. (1972) *The Cumberland Lowland Handbook* Quaternary Research Association.
- Huddart, D; Tooley, M J and Carter, P A (1977) The coasts of NW England; in: *The Quaternary history of the Irish Sea* ed. Kidson, C and Tooley, M J, Geol. J. Special Issue 7, Liverpool.
- Huntley, D J and Johnson, H P (1976) Thermoluminescence as a potential means of dating siliceous ocean sediments *Can. J Earth Science* 13, 593-596.

- Huntley, D J; Godfrey-Smith, S D and Thewalt, M W (1985) Optical dating of sediments *Nature* 313, 105-107.
- Huntley, D J; Godfrey-Smith, D I; Thewalt, M W and Berger, G W (1988) Thermoluminescence spectra of some minerals relevant to thermoluminescence dating *J. Luminescence* 39, 123-136.
- Huntley, D J; Godfrey-Smith, D I and Haskell, E H (1991) Light-induced emission spectra from some quartz and feldspars *Nuclear Tracks and Radiation Meas.* 18, 127-130.
- Hütt, G and Jaek, I (1989a) Infra-red stimulated photoluminescence dating of sediments *Ancient TL* 7(2), 48-51.
- Hütt, G and Jaek, I (1989b) Infra-red photoluminescence (PL) dating of sediments: modified physical model, equipment and some dating results *Synopses from a workshop on the Long and Short range limits in luminescence, Oxford* Res. Lab Arch. & Hist. Art, Oxford, Occ. paper 9.
- Hütt, G and Jungner, H (1992) Optical and TL dating on glaciofluvial sediments *Quaternary Science Reviews* 11, 161-163.
- Hütt, G; Jaek, I and Tchonka, J (1988) Optical dating: K-feldspar optical response stimulation spectrum *Quaternary Science Reviews* 7, 381-386.
- Johnson, W J and Meade, R H (1990) Chemical weathering of fluvial sediments during alluvial storage: the Macuapanim Island point Bar, Solimoes River, Brazil *J. Sedimentary Petrology* 60, 820-826.
- James, W C; Mack, G H and Suttner, L J (1981) Relative alteration of microcline and sodic plagioclases in semi-arid and humid climates *J Sedimentary Petrology* 51, 151-164.
- Jelgersma, S (1961) Holocene sea-level changes in the Netherlands *Meded. Geol. Sticht. serie C* 7, 1-100.
- Jelgersma, S (1966) Sea-level changes during the last 10 000 years; in: *World climate 8000-0 BC. Proceedings Int. Symposium, London.* ed. Sawyer, J S, Royal Met. Soc., London, 54-69.

- Jelgersma, S; de Jong, J; Zagwijn, W H and Van Regteren Altena, J F (1970) The coastal dunes of the Western Netherlands: geology, vegetation history and archaeology. *Meded. Rijks Geol. Dienst. NS* 21, 93-167.
- Jenkins, R and de Vries, J L (1970) *Practical X-ray spectrometry* Macmillan, London.
- Jungner, H (1989) Results from a comparison of UV and sunlight bleaching of feldspar and quartz *Quaternary Science Reviews* 7, 331-333.
- Jungner, H and Huntley, D J (1991) Emission spectra of some potassium feldspars under 633 nm stimulation *Nuclear Tracks and Radiation Meas.* 18, 125-126.
- Kemp, R A (1985) The Valley Farm Soil in Southern England; in: *Soils and Quaternary Landscape Evolution*, ed. Boardman, J; Wiley. 176-186.
- Kidson, C and Tooley, M J (1977) *The Quaternary History of the Irish Sea* Geol. J Special Issue, Seel House Press, Liverpool.
- Kitis, G and Charalambous (1991) Relative thermoluminescence response of alpha to beta radiation as a function of irradiation temperature *Nuclear Tracks and Radiation Meas.* 18, 95-99.
- Kronberg, C (1983) Preliminary results of age determinations by TL of interglacial and interstadial sediments *PACT J* 9, 595-605.
- Krumbein, W C (1942) Physical and chemical changes in sediments after deposition *J Sedimentary Petrology* 12(3), 111-117.
- Lagache, M (1965) Contributions à l'étude de l'altération des feldspaths dans l'eau entre 100 et 200 °C, sous diverses pressions de CO₂ et applications à la synthèse des minéraux argillaux *Bull. Soc. French Mineralogists and Crystallographers* 88, 223-253.
- Lamothe, M (1984) Apparent thermoluminescence ages of St Pierre sediments at Pierreville, Quebec and the problem of anomalous fading *Can. J. Earth Science* 21, 1406-1409.
- Lamothe, M (1988) Dating till using thermoluminescence *Quaternary Science Reviews* 7, 273-276.

- Lamothe, M and Huntley, D J (1988) Thermoluminescence dating of Late Pleistocene sediments, St Lawrence Lowland, E Canada *Géographie Physique et Quaternaire* 42, 33-44.
- Li, S-H (1991a) Removal of the unstable signal in optical dating of K-feldspars *Ancient TL* 9(2) 26-29.
- Li, S-H (1991b) A cautionary note: apparent sensitivity changes resulting from curve-fitting *Ancient TL* 9(2), 12-13.
- Li, S-H and Aitken, M J (1989) How far back can we go with the optical dating of feldspar? *Synopses from a workshop on the Long and Short range limits in luminescence, Oxford Res. Lab Arch. & Hist. Art, Oxford, Occ. paper 9.*
- Li, S-H and Wintle, A G (1991) Sensitivity changes of luminescence signals from colluvial sediments after different bleaching processes *Ancient TL* 9(3), 50-53.
- Louwe Kooijmans, L P (1974) The Rhine/Meuse delta *Analecta Praehistorica Leidensia* 7.
- Louwe Kooijmans, L P (1976) Local developments in a borderland: a survey of the Neolithic at the Lower Rhine *Oudheidkundige Mededelingen uit het Rijksmuseum van Oudeiden te Leiden* LVII, 227-297.
- Louwe Kooijmans, L P (1987) Neolithic settlement and subsistence in the wetlands of the Rhine/Meuse delta of the Netherlands; in: *European wetlands in Prehistory* ed. Coles, J M and Lawson, A J; Clarendon Press, Oxford, 227-251.
- Løvborg, L and Kirkegaard, P (1974) Response of 3"x3" NaI (TI) detector to terrestrial gamma radiation *Nuclear Instruments and methods* 121, 239-251.
- Lundqvist, J and Mejdahl, V (1987) Thermoluminescence dating of eolian sediments in Central Sweden *Geologiska Forengensi Stockholm Förhandlingar* 109, 147-158.
- Lundström, I (1970) Etch patterns and albite twinning in two plagioclases *Arkive Min. Geol.* 5, 63-71.
- Lundström, U and Ohman, L-O (1991) Dissolution of feldspar in the presence of natural, organic solutes *J Soil Science* 41 359-369.

- Manheim, F T (1970) The diffusion of ions in unconsolidated sediments *Earth & Planetary Science Letters* 9, 307-309.
- Marshall, D J (1989) *Cathodoluminescence of Geological Materials* Unwin-Hyman, Boston.
- McGrail, S and Switsur, R (1975) Early British boats and their chronology *Int. J. Nautical Archaeology and Underwater Exploration* 4(2), 191-200.
- Meade, R H (1966) Factors influencing the early stages of the compaction of clays and sands - review *J. Sedimentary Petrology* 36, 1085-1101.
- Mejdahl, V (1988a) The plateau method for dating partially bleached sediments by thermoluminescence *Quaternary Science Reviews* 7, 347-348.
- Mejdahl, V (1988b) Long term stability of the TL signal in alkali feldspars *Quaternary Science Reviews* 7, 357-360.
- Morozov, G V (1968) The relative dating of Quaternary Ukraine sediments by the thermoluminescence method *8th Int. Quat. As. Congress, Paris*; U.S. Geol. Survey 167.
- Moseley, F and Walker, D (1952) Some aspects of the Quaternary period in N Lancs. *Naturalist Hull*, April-June, 41-54.
- Muir, I J and Nesbitt, H W (1991) Effect of aqueous solutions on the dissolution of labradorite feldspar *Geochimica et Cosmochimica Acta* 55, 3181-3189.
- Muir, I J; Bancroft, G B and Nesbitt, H W (1989) Characterisation of altered labradorite surfaces by SIMS and XPS *Geochimica et Cosmochimica Acta* 54, 1235-1241.
- Muir, I J; Bancroft, G M; Shotyky, W and Nesbitt, H W (1990) A SIMS and XPS study of dissolving plagioclase *Geochimica et Cosmochimica Acta* 54, 2247-2256.
- Nahon, D B (1991) *Introduction to the petrology of soils and chemical weathering* Wiley Interscience.
- Nanson, G C and Young, R W (1987) Comparison of Thermoluminescence and Radiocarbon age-determinations from Late-Plaeistocene alluvial deposits near Sydney, Australia *Quaternary Research* 7, 263-269.

- Nanson, G C; Price, D M; Short, S A; Young, R W and Jones, B G (1991) Comparative Uranium-Thorium and Thermoluminescence dating of weathered Quaternary alluvium in the tropics of Northern Australia *Quaternary Research* 35, 347-366.
- Neve, J (1992) An interim report on the dendrochronology of Flag Fen and Fengate *Antiquity* 66 (251), 270-275.
- Packman, S C and Grün, R (1989) TL dating of loess samples from Achenheim *Synopses from a workshop on the Long and Short range limits in luminescence, Oxford Res. Lab Arch. & Hist. Art, Oxford, Occ. paper 9.*
- Parish, R (1992) IRSL and Feldspar Weathering *Research Papers in Geography* 2, University of Sussex.
- Parks, D A and Rendell, H M (1992) Thermoluminescence dating and geochemistry of loessic deposits in southeast England *Journal Quaternary Science* 7, 99-107.
- Pennington, W (1970) Vegetation history in the NW of England: a regional synthesis; in: Walker, D and West R G eds. *Studies in the Vegetational history of the British Isles* Cambridge University Press, 41-79.
- Pennington, W (1975) The effect of Neolithic man on the environment of NW England: the use of absolute pollen diagrams; in: *The effect of man on the landscape; the Highland zone* ed. Evans, J G; Limbrey, S and Cleere, H; Council for British Archaeology Research Report 11, 74-85.
- Pethick, J (1984) *An Introduction to Coastal Geomorphology* London, Arnold.
- Petrović, R (1976) Rate control in feldspar dissolution. II The protective effect of precipitates *Geochemica et Cosmochimica Acta* 40, 509-522.
- Pons, L J; Jelgersma, S; Wiggers, A J and de Jong, J D (1963) Evolution of the Netherlands coastal area during the Holocene *Verhandlingen van het koninklijk Nederlandsch Geologisch-Mijnbouw-kundig Genootschap* 21(2) 197-208.
- Poolton, N R J and Bailiff, I K (1989) The use of LEDs as an excitation source for photoluminescence dating of sediments *Ancient TL* 7(1), 18-20.

- Potter, T W (1981) The Roman occupation of the central Fenland *Britannia* 12, 79-133.
- Proszynska-Bordas, H (1988) TL dating of loess and fossil soils from the last interglacial-glacial cycle *Nuclear Tracks and Radiation Meas.* 10; 737-742.
- Proszynska-Bordas, H; Stanska-Proszynska, W and Proszynski, M (1988) TL dating of partially bleached sediments by the regeneration method *Quaternary Science Reviews* 7, 365-371.
- Pryor, F (1992) Discussion: the Fengate-Northey landscape *Antiquity* 66 (251), 518-531.
- Pryor, F and French, C (1985) The Fenland Project 1; the Lower Welland Valley survey *East Anglian Archaeology* 27.
- Pryor, F; French, C and Taylor, M (1986) Flag Fen, Fengate, Peterborough 1: discovery, reconnaissance and initial excavation 9182-82. *Proceedings Prehistoric Society* 52, 1-24.
- Pye, K and Johnson, R (1988) Stratigraphy, geochemistry and thermoluminescence ages of Lower Mississippi valley loess *Earth Surface Processes and Landforms* 13, 103-124.
- Questiaux, D G (1991) Optical dating of loess: comparison between different grain-size fractions for infra-red and green excitation wavelengths *Nuclear Tracks and Radiaton Meas.* 18,133-139.
- Reineck, H-E and Singh, I B (1980) *Depositional Sedimentary Environments* Springer-Verlag, Berlin.
- Rendell, H M (1983) Problems in the estimations of past water-content history of loess *PACT J* 9, 523-530.
- Rendell, H M (1985) The precision of water-content estimation in thermoluminescence dating of loess from N Pakistan *Nuclear Tracks and Radiation Meas.* 10, 763-768.
- Rendell, H M and Townsend, P D (1988) Thermoluminescence dating of a 10m loess section in Pakistan *Quaternary Science Reviews* 7, 251-256.
- Rendell, H M; Gamble, I J A and Townsend, P D (1983) Thermoluminescence dating of loess from the Potwar Plateau, N Pakistan *PACT J* 9, 555-562.

- Rendell, H M; Jones, F H and Townsend, P D (1989) Zero-setting in modern beach and dune sand environments *Synopses from a workshop on the Long and Short range limits in luminescence, Oxford Res. Lab Arch. & Hist. Art, Oxford, Occ. paper 9.*
- Rendell, H M; Mann, S J and Townsend, P D (1989) Spectral measurements of loess TL *Nuclear Tracks & Radiation Meas.* 14, 63-72.
- Rhodes, E J (1990) *Optical dating of quartz from feldspars* Unpublished D.Phil thesis, Oxford.
- Robertson, G B; Prescott, J R and Hutton, J T (1991) Bleaching of the thermoluminescence of feldspars by sunlight *Nuclear Tracks and Radiation Meas.* 18, 101-107.
- Rose, J A; Allen, P; Whiteman, C A W and Owen, N (1985) The early Anglian Barham soil of East Anglia; in: *Soils and Quaternary Landscape Evolution*, ed. Boardman, J; Wiley. 197-230.
- Ruppert, L F (1987) Application of CL of quartz and feldspar to sedimentary petrology *Scanning Microscopy* 1, 63-72.
- Salway, P (1970) The Roman Fenland; in: *The Fenland in Roman times* ed. C W Phillips, Royal Geographical Society Research Series 5, 1-21.
- Shennan, I (1985a) Flandrian sea-level changes in the Fenland 1: geographical setting and evidence of relative sea-level changes *Journal Quaternary Science* 1(2), 119-154.
- Shennan, I (1985b) Flandrian sea-level changes in the Fenland 2: tendencies of sea-level movement, altitudinal changes and local and regional factors *Journal Quaternary Science* 1(2), 155-179.
- Shennan, I; Tooley, M J; Davies, M J and Haggart, B A (1983) Analysis and interpretation of Holocene sea-level data *Nature* 302, 404.
- Singhvi, A K; Sharma, Y P and Agrawal, D P (1982) Thermoluminescence dating of dune sands in Rajasthan, India *Nature* 295, 313-315.
- Skempton, A W (1970) The consolidation of clay by gravitational compaction *Quart. J Geol. Soc. London* 125, 373-412.

- Skertchly, S J B (1877) *The Geology of the Fenland. Memoirs Geol. Survey UK*, London, HMSO.
- Spooner, N A and Questiaux, D G (1989) Optical dating - Achenheim beyond the Eemian, using green and infra-red stimulation wavelengths *Synopses from a workshop on the Long and Short range limits in luminescence, Oxford Res. Lab Arch. & Hist. Art, Oxford, Occ. paper 9*.
- Spooner, N A and Franks, M (1990) Some characteristics of infra-red emitting diodes relevant to luminescence dating *Ancient TL* 8(3), 16-19.
- Stokes, S (1992) Optical dating of young (modern) sediments using quartz: results from a selection of depositional environments *Quaternary Science Reviews* 11, 153-160.
- Stemme, H E (1989) Thermoluminescence dating of the podostratigraphy of the Quaternary period in NW Germany *Geoderma* 45, 185-195.
- Strickertsson, K (1985) The thermoluminescence dating of potassium feldspar - glow curve characteristics and initial rise measurements *Nuclear Tracks and Radiation Meas.* 10, 613-617.
- Strickertsson, K (1989) Trap spectra and mean life activity for potassium feldspar from Nordic bedrock and Scottish vitrified forts *Synopses from a workshop on the Long and Short range limits in luminescence, Oxford Res. Lab Arch. & Hist. Art, Oxford, Occ. paper 9*.
- Tooley, M J (1978a) *Sea-level Changes in North-west England during the Flandrian Stage* Clarendon Press, Oxford.
- Tooley, M J (1978b) The history of Hartlepool Bay *Int. J. Nautical Archaeology and Underwater Exploration* 7, 71-75.
- Tooley, M J (1982) Sea-level changes in northern England *Proc. Geol. Association* 93, 43-51.
- Tooley, M J (1984) Raised and buried beaches on the Durham coast *Institute British Geographers, Durham Meeting, 1984; excursion guide*.
- Tooley, M J (1988) The intertidal peats of Hartlepool Bay *Field Guide for SERC short course on TL dating, January 1988, Durham*.

- Tooley, M J (1990) The chronology of coastal dune development in the UK *Catena Supplement* 18, 81-88.
- Tooley, M J; Powers, R and Mellars, P A (in press) A Neolithic skeleton from Hartlepool Bay: provenance, environment, osteology and archaeology.
- Trechmann, C T (1936) Mesolithic flints from the submerged forest at West Hartlepool *Proc. Prehist. Soc.* 11, 161-168.
- Trechmann, C T (1947) The submerged forest beds of the Durham coast *Proc. Yorks. Geol. Soc.* 27, 23-32.
- Troels-Smith, J (1955) Karakterisering af Løse jordarter (Characterisation of Unconsolidated sediments) *Danm. Geol. Unders.* IV.
- Van de Plassche, O (1980) Compaction and other sources of error in obtaining sea-level data: some results and consequences *Eiszeitalt und Gegenwart* 30, 171-181.
- Van der Woude, J D (1983) Holocene palaeoenvironmental evolution of a perimarine fluvial area *Analecta Praehistorica Leidensia* 16.
- Van der Woude, J D (1985) Two mid-Holocene millennia of swamp forest in the Rhine/Meuse deltaic plain *Boreas* 14, 267-272.
- Verbraek, A; Kok, H and van Meerkerk, M (1974) The genesis and age of the river dunes (donken) in the Alblasserwaard *Meded. Rijks Geol. Dienst. NS* 25(1), 1-8.
- Visocekas, R; Ceva, T; Marti, C; Lefauchaux, F and Robert, M C (1976) Tunnelling processes in the afterglow of calcite *Physica Status Solidi A* 35, 315-327.
- Walker, D (1966) The late Quaternary history of the Cumberland lowland *Phil. Trans. Roy. Soc. B* 251, 1-210.
- Wheeler, G C W S (1988) Optically stimulated phosphorescence and optically transferred TL as a tool for dating *Quaternary Science Reviews* 7, 407-410.
- Wintle, A G (1973) Anomalous fading of the thermoluminescence in mineral samples *Nature* 245, 143-144.

- Wintle, A G (1974) *Factors determining the thermoluminescence of chronologically significant materials* Unpublished D.Phil thesis, Oxford.
- Wintle, A G (1978) Stability of the TL signal in fine-grains from loess *Nuclear Tracks and Radiation Meas.* 10, 725-730.
- Wintle, A G (1980) The dating of ocean sediments *Can. J. Earth Science* 17, 348-360.
- Wintle, A G (1982) Thermoluminescence properties of some fine-grain minerals in loess *Soil Science* 134, 164-170.
- Wintle, A G (1985) Sensitization of the TL signal by exposure to light *Ancient TL* 3, 17-21.
- Wintle, A G (1989) Limits from Loess *Synopses from a workshop on the Long and Short range limits in luminescence, Oxford* Res. Lab. Arch & Art Hist, Occ. Paper 9.
- Wintle, A G and Catt, J A (1985a) Thermoluminescence dating of the Dimlington Stadial deposits in Eastern England *Boreas* 14, 231-234.
- Wintle, A G and Catt, J A (1985b) Thermoluminescence dating of soils developed in late Devensian loess at Pegwell Bay, Kent *J Soil Science* 36, 293-298.
- Wintle, A G and Huntley, D J (1980) TL dating of ocean sediments *Can. J Earth Science* 17, 348-360.
- Wintle, A G and Huntley, D J (1982) Thermoluminescence dating of sediments *Quaternary Science Reviews* 1, 31-53.
- Wintle, A G and Packman, S C (1988) Thermoluminescence ages for 3 sections in Hungary *Quaternary Science Reviews* 7, 515-520.
- Wollast, R (1967) Kinetics of the alteration of K-feldspar in buffered solutions at low temperatures *Geochemica et Cosmochimica Acta* 31, 635-648.
- Zhou, L P and Wintle, A G (1989) Under estimations of regeneration EDs in Chinese loess *Synopses from a workshop on the Long and Short range limits in luminescence, Oxford* Res. Lab Arch. & Hist. Art, Oxford, Occ. paper 9.

Zimmerman, D (1971) Thermoluminescence dating using fine-grains from pottery *Archaeometry* 13, 29-52.

Zöller, L and Wagner, G A (1989) Strong or partial thermal washing in TL dating of sediments
Synopses from a workshop on the Long and Short range limits in luminescence, Oxford
Res. Lab Arch. & Hist. Art, Oxford, Occ. paper 9.

APPENDIX A Radiocarbon data for all ages cited in the text.

Calibration is to 68% confidence level, using the 'CALIB' programme of the University of Washington Quaternary Isotope Unit, 1987.

Ref.	Lab. No.	C-14 date BP	Cal. BC range	Reference
1	BM2123	2830±20	1100-853	Pryor et al, 1992
2	▲	8480±205	**	Huddart et al, 1977
3	Hv208	6850±60	5749-5640	Walker, 1966
4	Hv207	5875±220	5051-4500	Walker, 1966
5	Hv5228	6870±95	5820-5640	Tooley, 1978b
6	Hv4713	5385±280	4510-3827	Tooley, 1978b
7	Y2606	6200±140	5315-4945	Andrews et al, 1973
8	Y2600	6720±100	5694-5500	Andrews et al, 1973
9	UB905	3780±55	2307-2138	Cherry, 1982
10	UB906	4135±55	2878-2611‡	Cherry, 1982
11	Y2597	2120±100	362-40	Tooley, 1990
12	Y2387	3630±160	2273-1772‡	Tooley, 1990
13	Hv5214	1795±240	50BC-AD530	Tooley, 1990
14	Hv4708	1370±85	AD688-606	Tooley, 1990
15	Y2598	1210±100	AD680-953	Andrews et al, 1973
16	Gak1929	1530±80	AD420-622	Andrews et al, 1973
17	Hv5227	6320±85	5345-5227‡	Huddart et al, 1977a
18	SRR8658	5640±50	4530-4407	Bonsall et al, 1986
19	SRR2659	4395±70	3260-2919	Bonsall et al, 1986
20	SRR2660	3612±70	2126-1889	Bonsall et al, 1986
21	SRR3060	2825±90	1121-898	Bonsall et al, 1986
22	SRR3061	3580±100	2123-1777	Bonsall et al, 1986
23	SRR3062	3310±70	1685-1518	Bonsall et al, 1986
24	SRR3063	1810±70	AD118-322	Bonsall et al, 1986
25	SRR3064	1460±70	AD543-652	Bonsall et al, 1986
26	Q1356	7380±370	6570-5844‡	Bonsall et al, 1986
27	BM1216	6750±155	5740-5490	Bonsall et al, 1986
28	UB2568	3665±40	2134-1982‡	Bonsall et al, 1986
29	BM1396	3736±104	2320-1987‡	Bonsall et al, 1986
30	UB2711	4925±165	3950-3526‡	Bonsall et al, 1986
31	UB2544	6015±75	5049-4809‡	Bonsall et al, 1986
32	UB2545	5650±50	4574-4460‡	Bonsall et al, 1986
33	UB2544	5555±40	4461-4355‡	Bonsall et al, 1986
34	UB2712	5520±85	4462-4336‡	Bonsall et al, 1986
35	UB2713	5500±70	4455-4335‡	Bonsall et al, 1986
36	Hv4712	5285±120	4328-3990‡	Tooley, 1978b
37	Hv3459	5240±170	4331-3820‡	Tooley, 1978b
38	BM90	8100±180	7064*	Barker and Mackey, 1961
39	BM80	8700±180	**	Barker and Mackey, 1961
40	Hv5217	5315±80	4315-4006‡	Tooley et al, in press.
41	Hv5220	4640±60	3631-3380	Tooley et al, in press.
42	SRR102	5465±80	4364-4241	Bartley et al, 1976
43	SRR476	5235±70	4222-3990‡	Bartley et al, 1976
44	Q2661	5975±120	5052-4770‡	Tooley, 1984
45	Q2662	5530±90	4466-4337	Tooley, 1984
46	Q2660	6180±100	5240-4949	Tooley, 1984
47	Q2663	4945±50	3785-3695	Tooley, 1984
48	Q2664	4770±50	3637-3387	Tooley, 1984
49	GrN6212	3630±35	2111-1949	Louwe Kooijmans, 1976
50	GrN6213	4480±40	3332-3044	Louwe Kooijmans, 1976
51	GrN6214	4935±40	3782-3695	Louwe Kooijmans, 1976

52	GrN6215	5320±40	4237-4043‡	Louwe Kooijmans, 1976
53	GrN8382	6720±70	5646-5539	van der Woude, 1983
54	GrN8383	7370±100	6381-6100	van der Woude, 1983
55	GrN8351	2420±70	5474-5245	van der Woude, 1983
56	GrN8303	6520±100	5540-5340	van der Woude, 1983
57	GrN7864	6060±80	5198-4863‡	van der Woude, 1983
58	GrN8380	6500±90	5490-5340‡	van der Woude, 1983
59	GrN8932	4570±75	3374-3108	van der Woude, 1983
60	GrN8379	5590±70	4506-4357	van der Woude, 1983
61	GrN7862	3340±80	1740-1523	van der Woude, 1983
62	GrN8377	4370±120	3302-2900	van der Woude, 1983
63	GrN5173	5320±40	4181-4149	Louwe Kooijmans, 1976
64	GrN5179	5165±40	4000-3962	Verbruggen, pers.comm
65	GrN8935	5290±45	4179-4146	Verbruggen, pers.comm

* denotes calibrated age without error, as the date was at the limits of the range of the calibration programme

** denotes age not calibrated, as it was beyond the range of the calibration programme

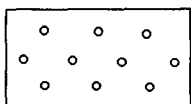
‡ denotes a mean age determined from more than one calibrated date; in these cases the mean date of three or five is given here

🍏 This date is cited in the reference given (page 139) but no laboratory number is given here or in associated references in the text.

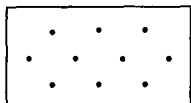
Appendix B Key to stratigraphic diagrams

TABLE B) Key to stratigraphic diagrams (Chs. 2,4,and 6)

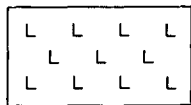
(after Troels-Smith, 1955)



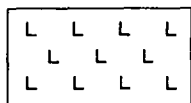
coarse sand (Gs)



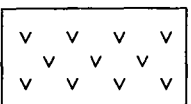
Medium/fine sand (Ga)



silt (Ag)



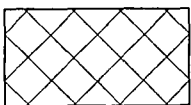
clay (As)



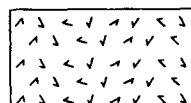
peat (TI)



substantia humosa (Sh)

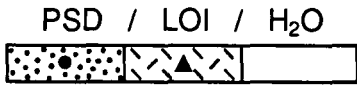


Limus humosus (Ld)

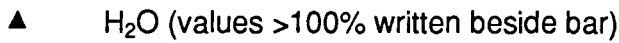


charcoal (anth)

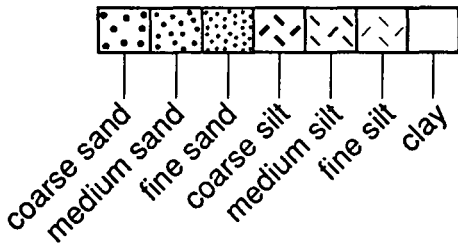
Table B.2 Key to sedimentological analyses for Chapter 4.



PSD = particle size distribution
 LOI = loss on ignition
 H₂O = water content
 all as 0 – 100%



Sample PSD

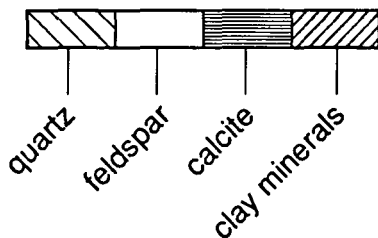


PSD of sample taken for dating

NB
 coarse sand = coarse grain fraction
 medium/fine silt = fine-grain fraction
 for dating

○ FF 1 = location of dating samples

Silt mineralogy



top bar = coarse silt
 middle bar = medium silt
 bottom bar = fine silt

Table C1 Dosimetry data for all samples

	α_0/α_1^*	ratio α_0/α_1^*	Mean β TLD	Potassium % \pm 0.05	fractional doses (%)			
					alpha	beta	gamma	cosmic
FF1								
FF2	8.84/12.31	1.39	1.76 \pm 0.5	1.8				
FF3	8.71/11.01	1.26	1.32 \pm 0.7	1.55	35	36	23	4
FF4	8.75/9.37	1.07	1.66 \pm 0.1	1.34	45	24	24	5
	8.91/9.24	1.04	0.89 \pm 0.2	0.6				
WM1								
WM2	12.1/12.37	1.02	2.69 \pm 0.2	2.82				
WM3	9.84/10.01	1.02	2.97 \pm 0.3	2.96	27	43	25	3
WM4	10.91/11.4	1.04	2.73 \pm 0.2	2.96	19	43	30	7
WM5	9.42/9.52	1.01	1.76 \pm 0.1	1.84	24	41	28	5
	7.25/7.86	1.08	1.26 \pm 0.1	1.18				
HAZ1								
HAZ2	9.53/9.91	1.04	3.33 \pm 0.2	1.55	11	55	27	5
HAZ3	14.39/15.4	1.07	3.46 \pm 0.1	2.0				
	14.56/15.09	1.04	3.25 \pm 0.1	2.73				
SLG1								
SLG2	11.86/12.05	1.02	2.64 \pm 0.1	2.42	36	39	21	3
SLG3	12.01/12.61	1.05	2.97 \pm 0.2	2.68	34	39	21	4
SLG4	11.33/11.82	1.04	2.53 \pm 0.3	1.87	25	44	25	4
	11.34/11.78	1.04	2.67 \pm 0.1	2.63				
WH1								
WH2	12.6/12.7	1.01	3.38 \pm 0.2	3.47	29	42	23	4
	12.46/13.25	1.06	2.72 \pm 0.3	2.4	50	28	17	3
SP1								
SP2	11.06/12.34	1.12	3.2 \pm 0.3	3.08				5
SP3	8.85/9.24	1.04	2.79 \pm 0.1	2.57	19	50	24	6
SP4	8.62/9.31	1.08	2.61 \pm 0.2	2.61	21	48	24	7
SP5	12.05/12.63	1.05	1.13 \pm 0.2	1.88	29	27	36	
SP6	4.81/5.47	1.14	1.02 \pm 0.1	3.49				
SP7	9.99/10.96	1.1	2.62 \pm 0.4	3.07	28	43	24	3
SP8	12.51/13.32	1.06	3.76 \pm 0.3	3.31				
SP9	12.47/13.04	1.05	3.24 \pm 0.1	2.56	26	47	23	2
	12.39/13.13	1.06	3.57 \pm 0.3	2.47	15	56	25	3

* α_0/α_1 denote sealed and unsealed alpha counts in cts/ksec/42mm diameter screen

Table C.2 Measurement data for all samples

	Correlation coefficient*	Stability °C‡	Bleach residual %	TL plateau °C	IRSL signal:noise ratio	IRSL initial signal (cts in 1st sec.)
Dur90TL.FF1		68±3		none	-	-
Dur90IR.FF1		72±4		-	3.1	334
Dur90TL.FF2		43±4		none	-	-
Dur90IR.FF2		51±6		-	2.8	299
Dur90TL.FF3	0.85	100±5	9.1	325-375	-	-
Dur90IR.FF3	0.87	101±2	0.03	-	6.3	682
Dur90TL.FF4	0.88	100±3	7.0	325-375	-	-
Dur90IR.FF4	0.84	100±3	0.04	-	7.3	786
Dur90TL.WM1		96±6		none	-	-
Dur90IR.WM1		98±4		-	3.0	329
Dur90TL.WM2		94±3		none	-	-
Dur90IR.WM2		101±1		-	1.6	177
Dur90TL.WM3		100±5	6.5	325-350	-	-
Dur90IR.WM3	0.21	100±4	0.08	-	9.1	984
Dur90TL.WM4	0.91	101±3	5.7	325-375	-	-
Dur90IR.WM4	0.95	100±3	0.01	-	32.6	3525
Dur90TL.WM5	0.90	100±2	10.0	325-400	-	-
Dur90IR.WM5	0.88	101±1	0.01	-	19.25	2079
Dur90IR.WM5*	0.89	101±4	0.06	-	16.5	1783
Dur90TL.HAZ1		36±9		none	-	-
Dur90IR.HAZ1		40±8		-	1.4	156
Dur90TL.HAZ2	0.93	100±5	16/25	325-375	-	-
Dur90IR.HAZ2	0.87	103±2	0.01	-	4.4	476
Dur90TL.HAZ3		101±4		325-350	-	-
Dur90IR.HAZ3		100±3		-	10.9	1186
Dur90TL.SLG1	0.85	101±2		none	-	-
Dur90IR.SLG1	0.88	102±4		-	1.9	206
Dur90TL.SLG2	0.3	100±2	5.8	325-400	-	-
Dur90IR.SLG2	0.80	101±5	0.08	-	4.7	508
Dur90TL.SLG3	0.91	103±5	4.75	325-400	-	-
Dur90IR.SLG3	0.87	101±1	0.03	-	6.2	669
Dur90TL.SLG4	0.93	100±4	8.3	325-400	-	-
Dur90IR.SLG4	0.95	102±2	0.01	-	7.1	764
Dur90TL.WH1	0.97	104±2	6.7	325-400	-	-
Dur90IR.WH1	0.97	101±3	0.06	-	34.2	3695
Dur90TL.WH2	0.98	101±3	4.6	325-400	-	-
Dur90IR.WH2	0.97	99±2	0.06	-	34.4	3718
Dur90TL.SP1		88±3		none	-	-
Dur90IR.SP1		101±1		-	3.6	394
Dur90TL.SP2		99±1	7.3	none	-	-
Dur90IR.SP2	0.93	102±3	0.01	-	5.6	605
Dur90TL.SP3		100±2	8.3	325-350	-	-
Dur90IR.SP3	0.89	100±4	0.1	-	7.7	834
Dur90TL.SP4		101±1	7.3	325-380	-	-
Dur90IR.SP4	0.9	100±3	0.06	-	7.3	791
Dur90TL.SP5		100±5	3.9	325-400	-	-
Dur90IR.SP5		102±2	0.04	-	28.4	3072
Dur90TL.SP6	0.91	101±1	6.4	325-400	-	-
Dur90IR.SP6	0.83	100±6	0.07	-	6.4	687
Dur90TL.SP7		100±3	5.6	none	-	-
Dur90IR.SP7		101±3	1.2	-	18.6	2007
Dur90TL.SP8	0.85	100±5	2.8	325-375	-	-
Dur90IR.SP8	0.87	101±1	0.04	-	7.4	801
Dur90TL.SP9	0.89	101±1	3.7	325-380	-	-
Dur90IR.SP9	0.94	100±2	0.03	-	8.8	954

* fit of data to weighted linear regression curve. ‡ at 18°C for 6 months

